Microfiltration Membrane Fouling by Dairy Proteins

Thesis submitted

for the degree of Doctor of Philosophy

at Massey University

New Zealand

by

Allen D Marshall

1994

For Sylvia

Abstract

Microfiltration membrane fouling occurs through the deposition of proteins both on the membrane surface and within the membrane pores. Fouling is complex with both the nature and location of fouling dependent upon the properties of the feed material, the properties of the membrane material and the operating conditions used.

Two aspects of fouling have been investigated, one in which the feed contained proteins considerably larger than the membrane pores (casein micelles) and the other, in which the protein (ß-lactoglobulin) was much smaller than the pores. In this way, it was possible to separately investigate surface layer formation and fouling within the membrane pores.

It has been demonstrated that a casein "gel layer" forms on the membrane surface causing severe fouling during the microfiltration of skim milk on a 0.1 μm polysulphone membrane if the combination of cross-flow velocity and permeate flux leads to a concentration of casein at the membrane wall equal to or higher than that required for "gel layer" formation. Once formed, the gel layer restricts the passage of protein through the membrane and reduces plant throughput.

During the microfiltration of ß-lactoglobulin on a 0.1 μm zirconium oxide membrane, in the presence of calcium and with high fluxes, protein-protein interactions at or near the pore entrance lead to pore narrowing and the eventual retention of protein by the membrane. High localised shear rates at the pore entrance lead to partial unfolding of the protein and calcium appears to form an ion-bridge between exposed negatively charged protein groups leading to aggregation and multi-layer deposition on the membrane pore walls. The removal of calcium or a reduction in the permeate flux prevents severe fouling and greater than 90% transmission of protein can be achieved.

The importance of understanding the properties of the feed material in interpreting and explaining membrane fouling is stressed.

Acknowledgements

First and foremost I wish to thank my supervisors, Peter Munro and Gun Trägårdh, for their encouragement, direction and friendship over the last 3 years.

I also wish to acknowledge the support of the New Zealand Dairy Research Institute for allowing me to study for this degree and for keeping my family housed, clothed and well fed. Thanks also to the Swedish Institute and New Zealand Dairy Research Institute for the financial support of my 11 month stay at the University of Lund. The opportunity to travel and study at a foreign university was greatly appreciated.

Designing and building a new sophisticated piece of equipment is often fraught with difficulty and I am indebted to Andrew Fletcher and Dan Johansson for their skilled input to the design and development of the equipment. Also to Byron McKillop for building the polymer membrane module.

Ideas and concepts rarely come only from a single person and there have been a large number of people who have had input directly, by commenting on my results and reports, and indirectly, by at some time acted as a "sounding board" for me. As a consequence something of their ideas have become my own.

To my friends in Sweden, especially Hans Karlsson, Dan Johansson, Vassilis Gekas, Petr Dejmek, Kenneth Persson, Benoit Dutré and Christian Trägårdh (I hope I have not missed anyone), many thanks for your support during our stay. To Helgot Olsson, many thanks for your expert preparation of the samples for electron microscopy.

To Jean-Loius Maubois and Georges Daufin in Rennes, thanks for your time and interest during my visit and for the many contributions from your lab that have advanced our understanding of membranes.

To my colleagues at the New Zealand Dairy Research Institute; there have been so many who have contributed to my project over the last few years, thank you for your input and encouragement. To Peter Hobman and Rex Humphrey, thank you for encouraging me into attempting a PhD that is now almost finished. Special thanks also to Mark Pritchard and Linda Schollum for constantly allowing me to bug them for comments on what I have planned or written.

Finally, to Sylvia, who allowed me to drag her half way around the world and back again, and without whose constant support, encouragement and love this thesis would never have been attempted.

Now all has been heard;
here is the conclusion of the
matter:
Fear God and keep his
commandments,
for this is the whole duty of man.

Ecclesiastes 12 v13.

Table of Contents

1. The complexity of fouling in microfiltration - an overview of the research performed in this thesis

Membrane fouling reduces plant throughput and membrane selectivity and has been the major reason that has prevented microfiltration (MF) fulfilling its potential commercially. In the MF of protein containing solutions, fouling is complex, with the deposition of protein occurring both on the membrane surface and within the membrane pores. The nature and location of protein deposition is dependent upon the operating conditions and feed material used and it is the interaction between fouling and the operating conditions that has led to conflicting views on the principal fouling mechanisms occurring in MF. The purpose of this chapter is three-fold: (1) to give a short overview of the fouling mechanisms that may occur in MF; (2) to present key results from this thesis that are by their nature specific to the experimental conditions used; and (3) to show how these results fit into the larger picture of MF fouling.

1.1. Overview of fouling

A simple model of MF involving two components is illustrated in Fig. 1.1. In this model MF only involves the separation of two components, one of which is completely retained, while the smaller component is free to permeate the membrane. Clearly, the selection of the membrane pore size is critical because, if either of the components is of a similar size to the membrane pores, severe fouling occurs because of pore plugging. In real life, feed solutions often contain a large number of components and unfortunately, there is often a considerable range of component sizes. The problem is made worse by the wide pore size distribution typically found with MF membranes. Both these facts limit the "fineness" of the separation achievable with MF. Membranes with a more clearly defined pore size and a narrow pore size distribution, are needed to improve the selectivity of MF membranes.

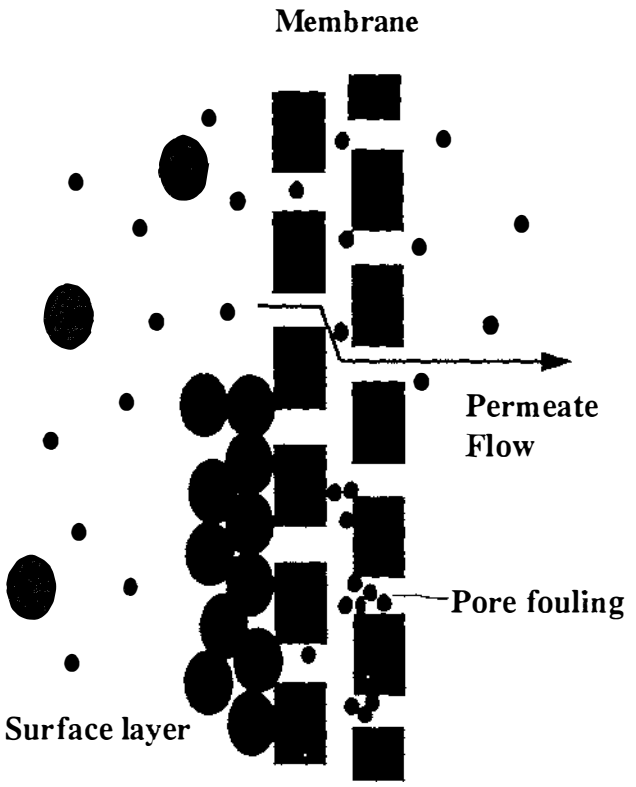

Figure 1.1. Graphical representation of the MF process and the possible locations of fouling.

So, the first way that the membrane can foul is by having components of a similar size or only slightly smaller than the pores as this leads to pore plugging. This problem is exacerbated if the smaller components are aggregated (Kelly *et al.*, 1993). Clearly, pretreatments to the feed prior to MF must ensure that aggregation of the smaller proteins is kept to a minimum in order to prevent pore plugging.

With clean feeds (*i.e.* no aggregation) that do not cause pore plugging (*i.e.* the pore size is sufficiently removed from the size of all of the components) then conceptually, there are two further mechanisms by which the membrane may foul. Firstly, the larger component, that is retained by the membrane, may form a surface or gel layer on the membrane surface. Once formed a surface layer would reduce the permeate flux and potentially restrict the passage of the smaller components through the membrane (Meireles *et al.*, 1991a). Secondly, the smaller component that

permeates the membrane may in some way deposit within the membrane pores and as a consequent restrict the passage of other small components (Bowen & Gan, 1991; Jonsson *et al.*, 1992).

In this thesis, results have been presented from two studies, one of which investigated the formation of a surface layer on the membrane surface during the MF of skim milk, and the second that investigated the deposition of protein within the membrane pores during the MF of ß-lactoglobulin. All of the trials were performed on a computer-controlled cross-flow constant-flux membrane rig.

1.2. Surface layer formation

Skim milk was microfiltered through a 0.1 μm polysulphone membrane (GRM0.1PP, Dow Danmark A/S, Nakskov, Denmark) to investigate surface layer formation. The casein micelles were completely retained by the membrane and as such were a useful model of the large component in Fig. 1.1.

Membrane fouling was very dependent upon the permeate flux (Fig. 1.2). With low permeate fluxes (35-52 L/m^2.h), there was a jump in membrane resistance with the introduction of milk to the membrane; thereafter, the resistance remained constant for at least 4 h. If the initial permeate flux was increased to 67 L/m^2.h, severe fouling occurred, with the resistance increasing to greater than 2500 x 10^{10}/m. Most of the fouling deposit was removed by flushing with water (*i.e.* fouling was reversible). Reducing the cross-flow velocity (with constant flux) also caused severe fouling.

The casein concentration at the membrane wall was estimated using the film model (Blatt *et al.*, 1970). High wall concentrations are favoured by high permeate fluxes that increase the flow of casein towards the membrane or low cross-flow velocities that reduce the mass transfer of casein back into the bulk solution. The wall concentration was compared with the fouling resistance after 4 h operation for trials with various combinations of permeate flux and cross-flow velocity (Fig. 1.3).

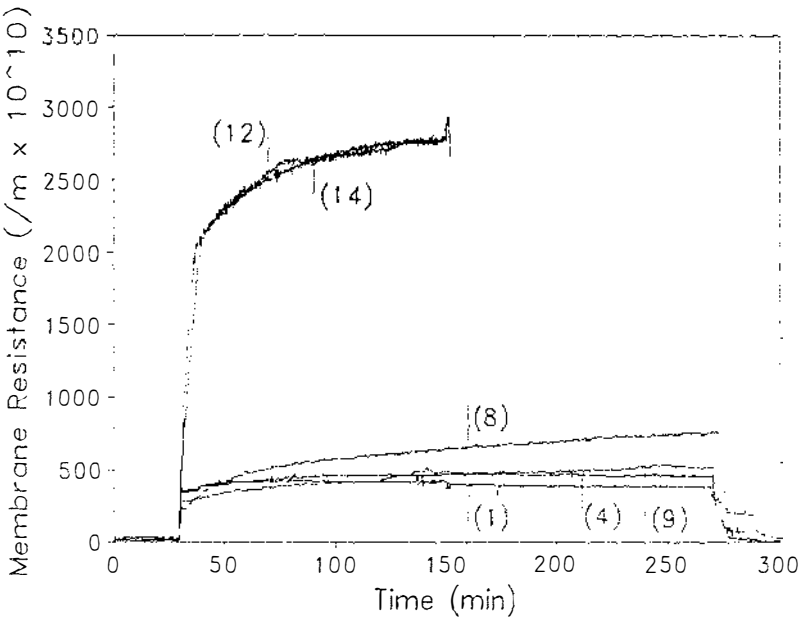

Figure 1.2. The effect of the permeate flux on membrane fouling during the MF of skim milk at 50°C. The numbers on the graph correspond to run numbers: (1) 35 L/m².h; (4, 8, 9) 52 L/m².h; (12, 14) 67 L/m².h.

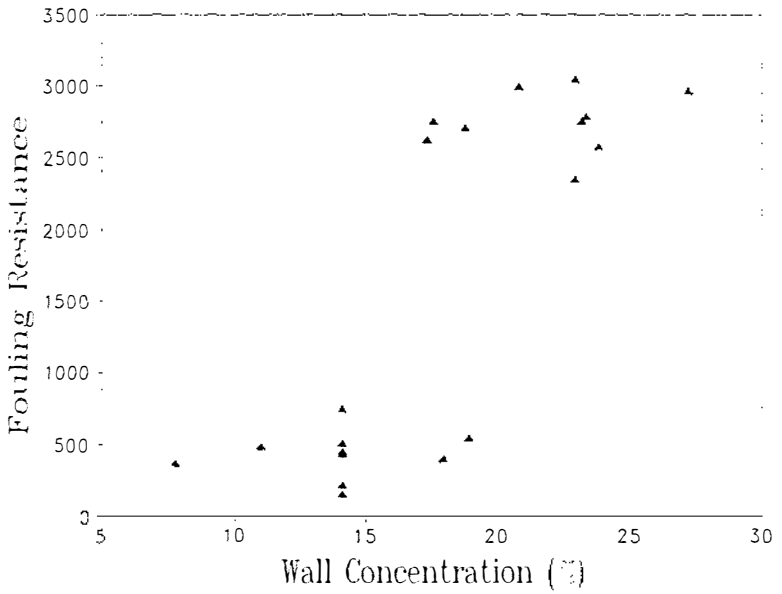

Figure 1.3. Effect of the casein concentration at the membrane wall as estimated by the film model on the final fouling resistance after 4 h MF of skim milk on a GRM0.1PP membrane at 50°C. For trials with severe fouling the resistance has been normalised for the retentate recirculation rate.

With low casein concentrations at the membrane wall, the fouling resistance was low; however, for high casein wall concentrations, severe fouling occurred with a distinct break-point in the behaviour at an estimated casein concentration of around 18% (w/w). The presence of a break-point is evidence that, above a particular wall concentration, a casein "gel layer" forms on the membrane surface. Whether the deposited material is a true gel or some form of viscous layer is not known. The actual casein concentration required for gel layer formation is difficult to estimate using the film model because of difficulties in calculating the mass transfer coefficient. A concentration of 20-25% seems reasonable.

1.3. Deposition of protein within the membrane pores

The MF of a 0.2% ß-lactoglobulin solution through a 50 nm zirconium oxide membrane (S.C.T., Tarbes, France) was investigated. ß-Lactoglobulin was chosen because its size (4-5 nm) is considerably smaller than the membrane pores. The fouling behaviour was highly dependent on the permeate flux and on the concentration of the calcium in the feed (Fig. 1.4). With a high calcium concentration (8 mmol/L) and high permeate fluxes (100+ $L/m^2.h$), severe fouling occurred and the membrane resistance increased from 30 to 800 x $10^{10}/m$. The protein transmission was initially high (90%) but decreased rapidly with increasing fouling to around 10%. Fouling could be prevented either by reducing the permeate flux to 50 $L/m^2.h$ or by reducing the calcium concentration of the feed, preferably to zero. Without severe fouling, the protein transmission remained constant at around 90%. The effect of calcium was not due solely to ionic strength because trials with only sodium chloride and ionic strength greater than that in the calcium trials did not invoke severe fouling. Calcium appeared to play a direct and specific role in severe fouling. The severe fouling was mostly reversible. Furthermore, if, after severe fouling had occurred, a protein solution without calcium was substituted for the feed solution (still leaving the membrane in contact with the protein), the majority of the fouling was removed from the membrane and the protein transmission could be restored to at least 50%.

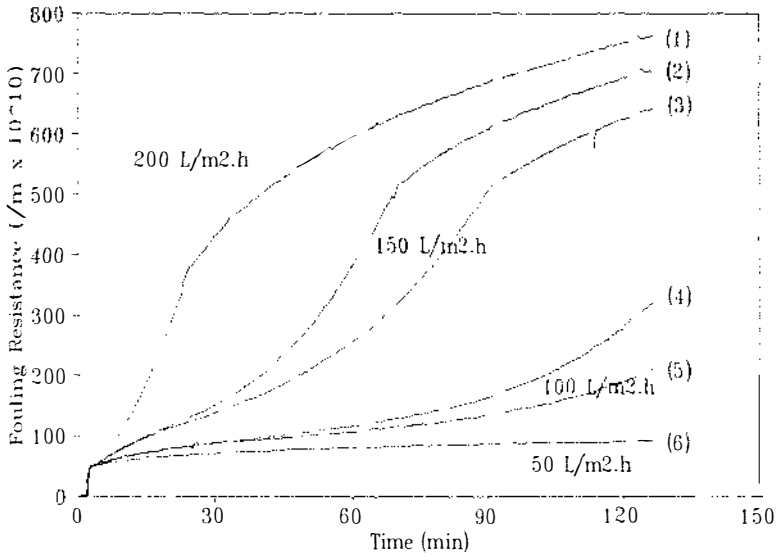

Figure 1.4. Effect of the permeate flux on the fouling resistance during MF of a 0.2% β-lactoglobulin solution in the presence of calcium on a 50 nm membrane. The ionic strength of the solutions was 0.0568 to 0.0577, the calcium content was 8.0-8.5 mmol/L and the pH was 6.2 to 6.4.

The high initial protein transmission suggested that subsequent fouling by the protein was within the membrane pores. The increase in membrane resistance and protein retention was not described by traditional membrane blocking laws (Grace, 1956); however, a modified pore narrowing model was used to demonstrate that protein deposition occurred principally at or near the pore entrance rather than throughout the membrane structure. The question that remained was why calcium and high permeate flows induced severe fouling at the pore entrance.

Calcium has been found to induce the gelation of a pre-heated whey protein isolate at low temperatures (Barbut & Foegeding, 1993) and is generally acknowledged to play a role in protein aggregation or gelation. In an analogy to this, it appears that calcium forms an ion-bridge between the negatively charged groups of a free protein and those of the protein already adsorbed or bound to the membrane resulting in multi-layer protein deposition. This reaction leads to the narrowing of the pores and eventual retention of protein by the membrane. The deposited protein redissolved or

desorbed if calcium was leached out of the deposit. For calcium-induced protein-protein interactions to occur the protein must be denatured, *i.e.* unfolded or at least distorted so that active binding sites normally hidden are exposed. Proteins can be denatured by high shear rates (Harris *et al.*, 1989). With high fluxes, localized shear rates at the pore entrance are high and it is hypothesized that this induces distortions in the protein structure enabling protein interactions to occur.

1.4. Conclusions

The properties of the feed material directly influence the nature of MF fouling. It has been demonstrated that a casein "gel layer" forms on the membrane surface if the combination of cross-flow velocity and permeate flux leads to a concentration of casein at the membrane wall equal to or higher than the "gel" concentration.

Furthermore, during the MF of ß-lactoglobulin, protein-protein interactions at or near the pore entrance lead to pore narrowing and the eventual retention of protein by the membrane. High localised shear rates at the pore entrance lead to partial unfolding of the protein and calcium appears to form an ion-bridge between exposed negatively charged protein groups.

2. Literature review: the effect of protein fouling in microfiltration and ultrafiltration on permeate flux, protein retention and selectivity

Of making many books there is no end, and much study wearies the body. (Ecclesiastes 12 v12b)

2.1. Introduction

The ultrafiltration (UF) and microfiltration (MF) of protein solutions is characterised by a progressive decline in flux with time (Fig. 2.1).

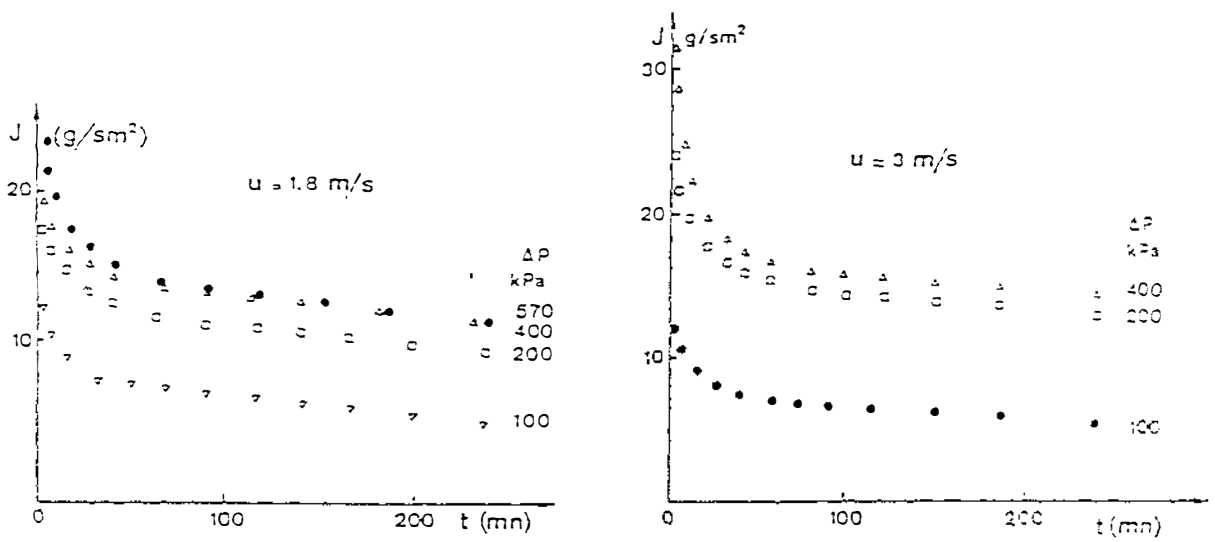

Figure 2.1. Ultrafiltration of sweet cheese whey on a Carbosep M4 membrane (Aimar *et al.*, 1988).

Flux decline in UF has been described in the following ways. Howell and Velicangil (1980) considered that the initial flux drop in UF of cheese whey was due to local convective deposition of protein molecules close to or in the pores, a process complete in less than a second. Flux then continues to drop due to the adsorption of

a protein monolayer at the membrane surface, followed by a much slower decline over a period of hours which was attributed to the reversible polymerisation of protein to gel or chemisorption.

Fane (1983) suggested that fouling occurs in three phases. The first occurs during operation on water and is due either to colloid and bacterial fouling or to membrane compaction. The second phase occurs during the first few seconds or minutes of UF due to the build-up of the concentration polarisation layer. At the end of this phase, the permeate flux should equal the flux predicted by the film model. In the third phase, the flux continues to decline at a slower rate due to membrane fouling.

Aimar *et al.* (1988) for the UF of cheese whey with Carbosep M4 inorganic membranes, found three successive stages in flux decline. Initially, reversible concentration polarisation builds up within the first minute, and then remains constant until the end of the run. This reduces the effective pressure driving force. After this, the flux curves have two distinct features: a sharp decrease during the first hour, followed by a slow decrease over three hours. From a comparison of fouling models they concluded that the sharp decrease in the first hour could be due to either protein adsorption or particle deposition, and that the longer term decline was due to convective deposition of particles.

Hallström *et al.* (1989) described fouling by protein as a three-step process. Firstly there is a rapid deposition on the membrane surface and at the entrances to the pores. This causes a rapid increase in the membrane resistance due to a reduction in the pore size (possibly monolayer adsorption). Further deposition then occurs on top of the first deposited layer, causing a slower rate of increase in the membrane resistance than the initial deposition. And thirdly, eventual bridging of the pore entrances occurs, and a complete surface layer builds up. At this stage the properties of the fouling layer dominate the behaviour. These three stages correspond to a transfer from membrane-controlled separation to fouling-layer-controlled separation.

To summarise, a number of phenomena acting simultaneously reduce the permeate flux. Chronologically it is possible to identify three separate phases of flux decline

(Fig. 2.2). In the first minute the initial rapid drop in flux is due primarily to concentration polarisation. The flux continues to decline, initially rapidly, for up to one hour due to protein deposition. It is likely that deposition is initially monolayer adsorption and that, at least in UF, a complete surface layer builds up. The third phase, a quasi-steady-state period where the flux declines slowly, may be due to further deposition of particles or to consolidation of the fouling layer (Howell & Velicangil, 1980; Turker & Hubble, 1987).

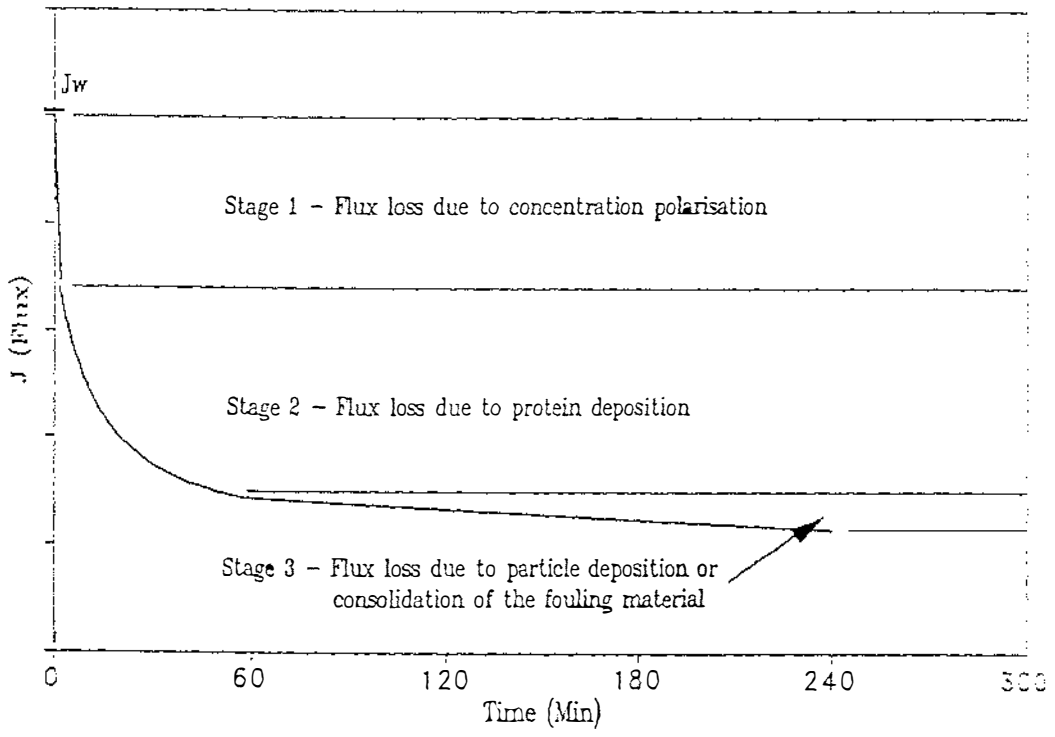

Figure 2.2. Various stages of flux decline.

In addition to the decline in flux, the retention of protein generally increases with time (Fane *et al.*, 1983a; Aimar *et al.*, 1988; Abaticchio *et al.*, 1990; Attia *et al.*, 1991a). This is an advantage in UF applications where a high protein retention is required, but is a disadvantage in some MF applications that require high protein transmission. Some workers have found that the protein retention is high initially, and that it then declines, passing through a minimum before increasing with time.

Aimar *et al.* (1988) suggested that adsorption on the membrane material initially leads to a chromatographic delay that explains the apparent initial high retention.

Various workers have related the increase in protein retention to an increase in membrane resistance (Taddei *et al.*, 1986; Bentham *et al.*, 1988; Hanemaaijer *et al.*, 1988, 1989). Gergen *et al.* (1989) found during the UF of dextrans that the retention curve was shifted to lower molecular weights as the operating time increased. The membrane selectivity also decreased with time due to the increased retention of low molecular weight components (also see Taddei *et al.* (1988)).

A clear distinction must be made between concentration polarisation and membrane fouling. Concentration polarisation is the development of a concentration gradient of the retained components near the membrane (Gekas, 1988). It is a function of the hydrodynamic conditions in the membrane system and is independent of the physical properties of the membrane. The membrane pore size and porosity are not directly affected by concentration polarisation.

Fouling, on the other hand, is the deposition of material on the membrane surface or in its pores, leading to a change in the membrane behaviour. Fouling is the "coupling" of deposited material to the membrane through the intermediate step of concentration polarisation, which first causes an accumulation or increase in concentration on the membrane surface. Fouling must also be distinguished from membrane compaction, which is the compression of the membrane structure under the transmembrane pressure, causing a decrease in membrane permeability (Gekas, 1988).

This review concentrates on protein fouling in UF and MF, although it is recognised that fouling with a biological feed material like milk or whey may also be due to fats, minerals, or bacteria. It is generally accepted that protein adsorption plays an important part in fouling, and that more protein than expected from monolayer adsorption often deposits on the membrane. Different conclusions have, however, been drawn as to whether protein deposition occurs on the front surface of the membrane or within the membrane pores.

With a surface deposit, a dynamic membrane that has a resistance much larger than that of the clean membrane is formed. The dynamic membrane controls membrane behaviour and the intrinsic properties of the membrane are not changed. Typically the increase in membrane resistance is modelled using a resistance-in-series model, and by assuming that the dynamic membrane behaves like a filter cake. The Carmen Kozeny equation is used to calculate its resistance.

Fouling within the membrane structure (pore plugging or pore narrowing) results in a change in the apparent pore size, pore size distribution and pore density of the membrane. It is likely that fouling in the immediate vicinity of the pore entrance dominates this behaviour. Internal membrane fouling is usually modelled by calculating an apparent reduction in pore size using the Hagen Poiseuille equation for capillary flow.

Although proponents of the above models have argued strongly for a specific fouling mechanism, fouling is a complex phenomenon, and it is likely that both surface and internal fouling, to a greater or lesser extent, occur simultaneously. The predominant fouling mechanism is a function of the experimental conditions, and is influenced by the operating conditions, membrane properties and the properties of the feed material.

In this review protein adsorption has been considered in some detail, and the physical evidence in the literature for the formation of a surface layer, internal membrane fouling and fouling at the pore entrance is presented. The effect on the membrane behaviour of the properties of the feed material, the properties of the membrane material and the membrane operating parameters have also been reviewed. Information and conclusions from the review have then been used to consider the effect of the pore size, or the protein to pore size ratio, on the probable fouling mechanisms and subsequent membrane behaviour.

2.2. Protein adsorption or deposition on the membrane

A typical adsorption curve is shown in Fig. 2.3. See Howell *et al.* (1981), Matthiasson (1983), Reihanian *et al.* (1983), Nabetani *et al.* (1987) and Turker & Hubble (1987) for other examples of static adsorption studies.

The term adsorption has often been used to describe all of the protein that accumulates on the membrane. However, adsorption strictly implies an equilibrium process with partitioning of solute between a solution and a surface. Therefore, adsorption refers to molecules that are in direct contact with the membrane, *i.e.* effectively a monolayer or less. Its use in this review has been limited to this definition. The term deposition has been used for all material irreversibly deposited at the surface of the membrane due to convection, protein-protein interactions and adsorption.

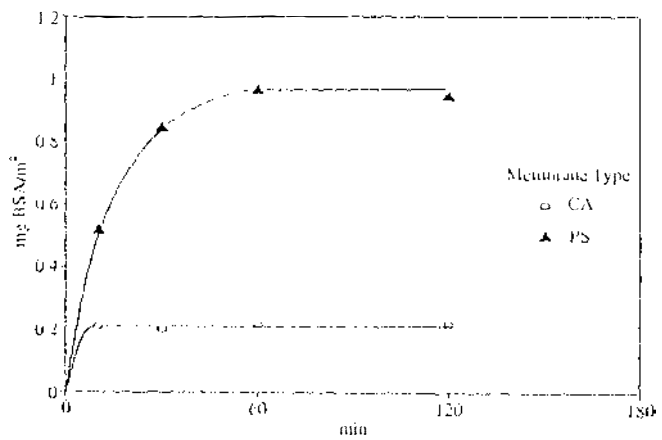

Figure 2.3. The adsorption of bovine serum albumin from a 0.2% solution on ultrafiltration membrane surfaces as a function of time (Matthiasson, 1983).

Protein adsorption is far from simple and is often a highly dynamic phenomenon. The molecules may change orientation and conformation during or after the adsorption, and protein adsorption appears to be mainly irreversible (Lundström, 1985). Larsson (1980) states that protein molecules have low energy barriers against changes in conformation, and formation of an interfacial protein film at the solid/liquid interface is therefore often irreversible.

Proteins may adsorb for a number of reasons. The DLVO theory is based on the superimposition of van der Waals attraction forces on electrostatic repulsion forces (Larsson, 1980). Typically biomolecules and colloidal particles carry a negative charge (Larsson, 1980). The surface charge is successfully reduced by adsorption of counter-ions, and an electrical double layer is formed, the structure of which determines the electrostatic repulsion forces. The dominating component of the attraction forces originates from the polarisability of the electron clouds (London dispersion forces). The energy of interaction is thus the sum of the energy contributions from these attraction and repulsion forces. Typically as two particles approach each other there is a negative region (*i.e.* good for interaction) and as they get closer together there is a high energy barrier that must be overcome for adhesion to occur. This occurs for particles or surfaces with similar charges. Obviously if the molecule and the membrane surface have opposite charges there will be an electrostatic attraction. Hydrophobic forces can also cause protein adsorption. Water molecules form hydrogen bonds, both with themselves and with hydrophilic surfaces. The intrusion of another surface or molecule, particularly if it is hydrophobic, disrupts this ordered structure and is thus energetically unfavourable. A gain in entropy can be obtained if contact with hydrophobic components can be minimised and this gives rise to strongly attractive hydrophobic interactions.

The amount of protein deposited onto the membrane is often greater than that corresponding to a protein monolayer. Le and Howell (1983) concluded that membrane fouling by protein occurs first by physical adsorption, probably in a monolayer, and then further protein build-up takes place via intermolecular disulphide bonding and hydrophobic interactions. Matthiasson (1983) concluded that there are at least two distinct steps in the adsorption process of BSA protein onto UF

membrane surfaces. The hydraulic resistance increases linearly with the amount adsorbed for both the first and second steps, but more rapidly for the first.

Fane *et al.* (1983b) found that the amount of BSA deposited on a UF membrane corresponded to 100-400 layers of protein. Using electron microscopy they observed that the protein layers that initially deposited on the membrane were much more densely packed than those in contact with the moving bulk solution. Chudacek and Fane (1984) showed that BSA forms compressible polarised layers during dead-end UF and suggested that the local void fraction increases with distance from the membrane. Consequently the probability of aggregation is less further from the membrane, and if it occurs the structure will be more open and porous, and be weak and susceptible to erosion.

Turker and Hubble (1987) from studies of BSA deposition on Amicon H1P10-8 hollow fibre membranes suggested that fouling initially occurs due to Langmuir (monolayer) adsorption which modifies the membrane surface properties. Reversible kinetic deposition due to convection follows and pressure-driven compaction of the membrane-associated protein leads to changes in flow resistance and porosity. Possible chemical interactions and protein denaturation lead to aging and further time-dependent changes in flux.

Bowen and Hughes (1990) investigated the deposition of BSA on aluminium oxide MF membranes. They suggested that deposition occurs in two phases. The first phase of rapid deposition is the result of monolayer adsorption onto the membrane surface and is very strongly bound. It can be described by a Langmuir-type isotherm. The second less rapid phase is the building-up of relatively weakly bound multi-layers of protein better described by the adsorption isotherm of Brunauer, Emmett and Teller (BET). The total amount of protein adsorbed increases if the permeate flow increases perhaps, they suggested, due to increased collisions within the pores resulting in greater interaction. Turker and Hubble (1987) and Bowen and Hughes (1990) showed that convective deposition significantly elevates the steady-state level of membrane-associated protein.

Fane *et al.* (1983b) concluded that deposition under UF conditions is not analogous to a Langmuir-type equilibrium process. Rather the initial rate of deposition is strongly linked to the initial rate of accumulation of solute molecules at the membrane surface. Suki *et al.* (1984) discussed similar data and suggested that it is more appropriate to consider the deposition process as starting with the initial accumulation of polarised solute which then provides a "reservoir" of molecules which gradually become fixed due to slow aggregation and flocculation. Matthiasson (1984) showed that the adsorption rate increases with increasing concentration when the membrane is exposed (statically) to BSA solution. These results suggested that the adsorption rate is limited by the movement, in this case by diffusion, of solute to the surface rather than by some kind of energy barrier.

Bowen and Gan (1991) found that the amount of protein adsorbed onto an Anopore membrane corresponds closely to the amount of protein calculated as occupying a single closely packed monolayer. However, the loss of permeability due to monolayer adsorption is substantially less than the loss of permeability during the filtration of protein solutions. Therefore the loss of permeability cannot be explained solely in terms of equilibrium adsorption of the protein onto the pore walls. Neither is it due to rejection and accumulation of protein at the front face of the membrane. A possible explanation is that the shear occurring due to flow through the micropores results in some changes in the protein structure which lead to a further mechanism of protein deposition.

Maximum deposition generally occurs around the protein isoelectric point (IEP) (Fane *et al.*, 1983c; Reihanian *et al.*, 1983; Bowen & Hughes, 1990; Clark *et al.*, 1991). McDonogh *et al.* (1990) studied the deposition characteristics of BSA under cross-flow conditions *in situ* by using ^{125}I-labelled albumin and measuring the signal directly over a flow cell. By varying the conditions they were able to distinguish between protein tightly bound to the membrane (not removed by flushing or mechanically wiping), protein loosely bound to the membrane (removed by scrubbing) and that dynamically bound or in the concentration polarisation layer (removed by flushing). At the IEP the largest amount of protein is associated with the membrane, in both dynamic and weak association, and also the flux is lowest.

The strong association is, however, smaller. Well away from the IEP there is least dynamic and weakly held protein, but more that is strongly associated. The flux is nearly constant with pH above the IEP. They also showed that the increase in deposition at the IEP is greater when the concentration of the BSA was increased.

To summarise, in almost all instances protein adsorption occurs on the membrane surface. This layer is tightly bound and can be removed only by cleaning. Upon the application of transmembrane pressure, further protein deposits on the membrane due to convection. This deposit, consisting of many protein multi-layers, is not as strongly bound as the protein adsorbed directly to the membrane. The degree of protein deposition is affected by both the membrane and the state of the protein. Increasing the charge on the protein, by adjustment of the pH away from the IEP, results in greater protein adsorption but, overall, less deposition of protein due to a reduction in the protein that is loosely bound. In MF, increased deposition within the membrane pores may be due to increased collisions (Bowen & Hughes, 1990) or some form of shear-induced denaturation (Bowen & Gan, 1991; Jonsson *et al.*, 1992).

2.3. Evidence for proposed fouling mechanisms

2.3.1. Formation of a dynamic membrane (surface layer or filter cake) on the front face of the membrane

Lim *et al.* (1971) during reverse osmosis (RO) of cottage cheese whey found that protein formed a gel-like deposit on the membrane surface that resisted removal by fluid shear. Glover and Brooker (1974) showed during the RO of milk that a 30 μm layer was deposited on the membrane. They identified this layer as being predominantly protein (casein), the density of which increased with proximity to the membrane (also see Chudacek & Fane (1984)). Lee and Merson (1975) ultrafiltered (PM10) and dead-end filtered (0.4 μm Nuclepore membrane) different whey protein solutions. ß-Lactoglobulin and BSA formed protein sheets on the surface of the membrane, especially near the entrance to the pores, whereas γ-globulin formed granules. The granules appeared to be roughly spherical bodies of irregular sizes

randomly agglomerated. With higher concentrations of γ-globulin, the granules stacked into layers. The texture of the deposits did not hinder permeation as drastically as the complete sheet that occurred with BSA and ß-lactoglobulin. Lee and Merson (1976) considered the UF of cottage cheese whey and concluded that large components (microorganisms, γ-globulin and protein polymers or complexes) bind together to form lattice-like structures on the surface of the membrane. The spaces in the lattice network are then filled with the smaller proteins which are trapped to form a second "protein membrane".

Kim *et al.* (1992) used a high resolution field emission scanning electron microscope (FESEM) to view membranes that had been used to filter 0.1% BSA for various times. Two different fouling mechanisms were observed. With PTHK (Millipore) and PM30 membranes, protein granules grew on the membrane surface until they merged into a protein cake, blocking the pores. With MPS (Memtec), ANO (Anotec), PC (Nuclepore) and XM300 membranes, protein aggregates, which seemed to grow in number and size as the filtration progressed, formed on the surface. Aggregates were found on the MPS membrane with a transmembrane pressure of 100 kPa but not at 50 kPa. They concluded that aggregates were formed when the initial permeate flux was high due to rapid supersaturation of protein molecules at the pore entrances.

Attia *et al.* (1991a) showed that, in the processing of skim milk on a 0.2 μm aluminium oxide membrane, a dense layer of casein built up on the surface of the membrane within the first 10 minutes. There was no evidence of casein penetrating the membrane. Vetier *et al.* (1986), in static studies with skim milk on a 0.2 μm aluminium oxide membrane, found that there was little or shallow fouling within the membrane due to casein micelles, but a considerable amount of surface deposit (20 μm). Fat globules were also present after processing whole milk. In dynamic studies the deposit on the membrane was less than 5 μm thick, was similar in nature, but appeared to be more strongly adsorbed than in the static study (Vetier *et al.*, 1988). Vetier *et al.* (1988) found that the surface deposit contained all of the initial protein constituents in milk. This deposit was removed from the membrane by ultrasound in two stages. Deposit from the first removal stage (deposit that was farthest from the membrane) had a protein composition that was close to that of normal milk. On the

other hand, the second removal stage (deposit that was closest to the membrane) was richer in serum proteins and the overall serum protein content of the deposit increased with time, revealing progressive internal plugging of the micellar casein deposit (also see Lee & Merson (1976) and Baker *et al.* (1985)). The α-lactalbumin and β-lactoglobulin levels in the deposit were similar to that of milk whereas there were higher levels of BSA. This increased BSA content was considered to be due either to higher retention or to slower re-diffusion into the milk because of BSA's larger size. The calcium and phosphate content of the deposit was high, suggesting that there was also some precipitation of calcium phosphate within the micelle layer.

To summarise, a number of workers have physically observed a dynamic membrane, consisting mostly of protein, on RO and UF membranes, and during the MF (0.2 μm) of milk. In the latter case the dynamic membrane consists of casein micelles whose size is of the same order as the pores. The nature of the layer depends on the type of protein present, and can be influenced by the hydrodynamic conditions. With multi-component solutions there is some evidence that smaller components deposit within a protein lattice formed from the larger components (Lee & Merson, 1976; Vetier *et al.*, 1988) and that the protein layer compacts with time (Howell & Velicangil, 1980; Turker & Hubble, 1987).

2.3.2. Fouling within the membrane structure

In some UF studies, in addition to the formation of a surface layer, protein has been identified within the membrane structure. Labbe *et al.* (1990) used infrared and X-ray photoelectron spectroscopy to evaluate fouling during UF of various whey types on a Carbosep M4 membrane (20 kD). They found that proteins were the major foulants, especially at the membrane surface but also to a lesser extent within the membrane structure. Only above pH 6.9 was evidence of apatite structures seen supplementary to protein adsorption. Sheldon *et al.* (1991) using a combination of staining methods in transmission electron microscopy (TEM) found that BSA accumulated not only at the membrane surface but also within the bulk of 10 kD polysulphone and regenerated cellulose membranes. On the other hand, Kim *et al.* (1992) found that, although massive protein deposition was observed on the surface

of the membrane (100-200 monolayers), no protein was observed within the membrane structure. However, their calculation of pore radius change (using the Hagen Poiseuille equation) revealed that only one or two layers of protein inside pores would be necessary to explain the experimental flux decline, *i.e.* levels of protein that cannot be detected using FESEM.

Protein deposits have also been identified within the membrane structure in MF. With a 0.8 μm membrane, Attia *et al.* (1991b) showed that casein both formed a layer on the surface of the membrane and penetrated the membrane structure to deposit within the pores (in contrast to their results on a 0.2 μm membrane (Attia *et al.*, 1991a)). With acidified milk, particles were identified within the membrane at pH 5.6 but not at pH 4.4, suggesting that the particle size of the precipitated casein was larger than the pore structure of the fouled membrane. Pusch and Walch (1982) showed electron micrographs of the top surface of a 3 μm Nuclepore membrane after filtration of latex/styrene particles. Even though the styrene particles were only one-tenth of the pore diameter, they interacted with the pore walls of the membrane, thus forming agglomerates that finally blocked the pores.

A number of authors have considered the adsorption of protein within the membrane pores. Hanemaaijer *et al.* (1989) found that the amount of protein adsorbed onto a non-porous polysulphone surface was 100-400 times less than the amount adsorbed onto a membrane, which suggests that the protein adsorbs within the membrane structure. Using different saccharides to determine membrane retentions, they showed that the increase in retention and membrane resistance after protein fouling was greatest with the tightest membrane, supporting the view that adsorption occurs internally, given that the percentage reduction in pore size increases as the pore size decreases. Further evidence of adsorption within the membrane pores is given by Nakao *et al.* (1988), Bowen & Gan (1991) and Dejmek & Nilsson (1989).

Robertson and Zydney (1990) considered the static adsorption of BSA onto PES NOVA and OMEGA (Filtron) membranes of various pore sizes. The amount of adsorbed protein increased from 50 kD membranes to 300 kD membranes, but decreased again for 1 MD membranes. There was no measurable protein adsorbed

in the active membrane layer (skin) of the 50 kD membrane, only about half a monolayer in the skin of the 100 kD membrane and approximately a monolayer in the skin of the 300 kD and 1 MD membranes. The amount of protein adsorbed to the 1 MD membrane was less than that on the 300 kD membrane because the total surface area of the membrane decreases as the membrane pore size increases. With the 50 and 100 kD membranes, the size of the BSA molecule is such that pore blocking can occur and this will prevent protein from reaching some of the internal pore structure. Analysis of the permeability data suggests that the pore diameter of the 1 MD membrane was reduced by 6 nm which loosely corresponds to the thickness of a protein monolayer. The "apparent" reduction in pore diameter reduced as the membrane pore size decreased.

Interpretive studies based on permeate flux and component retention behaviour have been performed. Bowen and Gan (1991) found during MF of 0.01% BSA through 0.2 μm membranes that stirring the cell had very little effect on the flux behaviour. In contrast, if a BSA solution was filtered through a UF membrane in the same cell and conditions, the membrane flux doubled with stirring. In UF both concentration polarisation and deposition on the front face of the membrane are important. The absence of any effect of stirring in the present case of MF is strong evidence that there is no accumulation of BSA molecules at the front face of the membrane; in other words, that there is no concentration polarisation. It is also very unlikely that the filtration characteristics of the membrane are modified by deposition of material on the front face of the membrane.

Zeman (1983) proposed that the increase in retention during filtration of polyethylene oxides (Carbowax) and dextrans on HFK-100 membranes (Abcor) was a result of a reduction in the pore size due to adsorption on the pore walls. Theoretically, he estimated the pore size from water flux data and the Hagen Poiseuille equation and using this data and the Ferry equation he found good agreement between theoretical and experimental retentions. The pore size reduction increased as the size of the dextrans increased, in keeping with the proposed model.

Matsumoto *et al.* (1988) compared the resistances due to internal and surface layer fouling with ovalbumin and ceramic membranes. With low velocities (laminar) and with the 0.2 μm and to a lesser extent the 0.8 μm membrane, surface layer fouling dominated. With larger pore sizes (1.5, 3 μm) pore plugging appeared to be the predominant fouling mechanism. With high velocities for all four membranes, pore plugging was predominant.

In summary, there is evidence that protein deposits within the membrane pores as well as on the surface. In UF the amount of protein deposited within the membrane pores is small compared with that on the membrane surface. However, in MF there is greater deposition within the pores, and internal fouling appears to dominate with large pores. The fouling mechanism is affected by operating parameters such as the cross-flow velocity and protein concentration.

2.3.3. Fouling at the pore entrance

Protein deposition is likely to be accentuated in the immediate vicinity of the pore entrance due to the higher local permeate flows. A number of papers have considered the effect on the permeate flux of deposited material on the membrane surface near the pore entrance. Le and Howell (1984) suggested the so-called limiting flux model, where some pores may become blocked and others unblocked in a dynamic fashion. While a pore is blocked it is non-permeating and thus deposited protein is not held on the membrane by hydrodynamic forces; while a pore is unblocked, it tends to pass a flux close to that of the pure solvent and can "recapture" protein molecules.

Weldring and van't Riet (1988) exposed UF membranes to adsorption with sodium carboxymethyl cellulose. After flushing of the adsorbed membrane, which was then assumed to be covered by a monolayer of molecules, they found that the hydrodynamic resistance was influenced by transmembrane pressure and shear rate. They hypothesised that the freely movable parts of the adsorbed macromolecules can block and unblock the pore entrances in a partly reversible way. In other words, under conditions of low shear or high flux the carboxymethyl cellulose tails "lie down" on the membrane over the pores.

Devereux and Hoare (1986) found that the membrane resistance decreased as the size of the particles increased when processing soy protein precipitate suspensions at the IEP. They suggested that a particle polarisation model together with consideration of membrane pore obstruction can explain this trend. It is assumed that there is a coherent layer near the membrane surface consisting of particles that are closely packed. The porosity of this layer, repeated over several layers, is too great to cause any significant resistance to flow itself. However, particles immediately adjacent to the membrane surface can obstruct membrane pores and cause a reduction in the permeate flux. If the precipitate particles are considered as spherical, the number of pores obstructed decreases with increasing particle diameter due to the increase in distance between adjacent particles.

Visvanathan and Ben Aim (1989) considered that, in the early stages of filtration, colloids can be deposited on the membrane surface in between the pores, and thus accumulate. Later, these aggregates of colloids can form bridges over the pore openings, resulting in partial blocking of the pores, a smaller pore structure available to subsequent colloids and particle retention. This bridging of aggregated colloids leads to the eventual formation of a film of colloids on the membrane surface.

Elbers and Brink (1990) found that the hydraulic resistance of poly(vinylmethylether)-coated membranes was very dependent upon the clean membrane pore size. With tight membranes (6 kD, 20 kD) the coating caused a large increase in membrane resistance, but not with a 50 kD membrane. They hypothesised that poly(vinylmethylether) shields the pore entrances of the smaller membranes but does not cover the larger pores of the 50 kD membrane.

In summary, the deposition of material on the surface of the membrane must in some way obstruct the pore entrances. The loss of effective membrane porosity is dependent upon the size of the depositing molecules and the pore size. In a resistance-in-series model, the addition of a term to describe the resistance to flow at the membrane/surface layer interface may be appropriate, especially if the porosity of the surface layer is greater than that of the membrane. The concept of molecules blocking and unblocking pores or sometimes lying down over the pore entrance is

unlikely to describe the behaviour of protein at the membrane surface, as protein adsorption is largely irreversible (Larsson, 1980).

2.4. The effect of the feed properties

2.4.1. Concentration

Increasing the feed concentration during UF generally results in a decrease in the permeate flux. In many cases the flux reduces with the logarithm of concentration as predicted by concentration polarisation theory (Kessler, 1981; Cheryan, 1986). Scott (1988) showed that at high velocities increasing concentration did not reduce the flux much, whereas at low velocities increasing concentration reduced the permeate flux, again in keeping with polarisation theory.

However, with high concentrations the linear relationship between the flux and the logarithm of the concentration does not necessarily hold. Tutunjian (1984) found when processing cells (*E. coli*) at high concentration that the rate of flux decline was faster than the expected linear relationship. On the other hand, Sun and Ouyang (1988) and Le *et al.* (1984) found permeate fluxes higher than expected with high feed concentrations, and in some cases the permeate flux has been found to increase at high concentration (Pritchard, 1990).

Where surface fouling predominates, increasing concentration increases the total membrane resistance (Sun & Ouyang, 1988; Taddei *et al.*, 1988; Daufin *et al.*, 1991). However, Daufin *et al.* (1991) and Sun and Ouyang (1988) found that the irreversible fouling remained reasonably constant, whereas reversible fouling (fouling that was removed by water flushing) increased with concentration. This suggests that membrane fouling does not increase but that the decrease in flux is due solely to concentration polarisation. In addition, retentions do not generally vary with increasing concentration in spite of the decrease in permeate flux, suggesting that the 'actual' membrane resistance has not changed (Bennasar *et al.*, 1982; Matsumoto *et al.*, 1988; Taddei *et al.*, 1988).

On the other hand, where internal fouling was predominant increasing the concentration resulted in more rapid loss of permeate flux with time (Bowen & Gan, 1991). This may be due to the increased exposure of the membrane to solute with increasing concentration.

Concentration affects the fouling mechanism that occurs. Clark *et al.* (1991) with Membralox membranes and BSA found, at low concentrations (0.1 g/L), that the retention of BSA decreased as the pore size increased. However, at concentrations above 1 g/L, the retention was high (approximately 0.98) for all three membranes and was independent of the pressure, velocity, concentration and pore size. Grace (1956) suggested in dead-end filtration of suspensions containing more than 1% total solids, that the pores block in the first few seconds and a continuous cake covers the surface of the filter and that, with dilute suspensions, the particles penetrate into the membrane and are trapped within the membrane. Both these results suggest that a filter cake or dynamic membrane is more likely to form at high concentration.

To sum up, increasing concentration generally results in a decrease in the permeate flux and has little effect on the membrane retention characteristics, except where the component size changes with concentration (Olson *et al.*, 1977; de Balmann & Nobrega, 1989). Where surface fouling occurs, increasing concentration has little effect on irreversible membrane fouling but causes an increase in reversible fouling. When internal membrane fouling dominates, increasing concentration increases the rate of membrane fouling. At high concentrations, cake or surface fouling is likely to dominate.

2.4.2. pH and ionic strength

The pH affects the amount of protein deposited on the membrane and the permeate flux in UF. Muller *et al.* (1973) and Hayes *et al.* (1974) during UF of hydrochloric acid casein whey, and Fane *et al.* (1983a) with BSA, showed that the permeate flux has a minimum at pH 4.5-5. The decrease in flux around the protein IEP is generally attributed to increased adsorption or deposition of protein (Fane *et al.*, 1983c; Reihanian *et al.*, 1983; Bowen & Hughes, 1990; Clark *et al.*, 1991). In contrast

Matthiasson (1983), in static adsorption studies with polysulphone and cellulose acetate membranes in an unstirred cell, found that adsorption increased with decreasing pH. Maximum adsorption was at pH 3. The level of protein deposited during Matthiasson's study was 1-2 orders of magnitude smaller than that seen in dynamic studies like those of Fane *et al.* (1983c), and the difference in behaviour may be due to the balance between strongly and weakly adsorbed protein (McDonogh *et al.*, 1990). With aluminium oxide membranes Bowen and Hughes (1990) found that adsorption decreased rapidly below pH 4 (the IEP of the membrane) when both the membrane and the BSA had a similar charge.

Alterations in the ionic strength have been shown to affect the amount of protein deposited and the permeate flux (Muller *et al.*, 1973; Hayes *et al.*, 1974; Turker & Hubble, 1987; Clark *et al.*, 1991). Fane *et al.* (1983c) found that, during stirred cell UF of 0.1% BSA with retentive PM30 and GR61PP polysulphone membranes, the effect of the addition of salt on the permeate flux varied with pH. They suggested that the behaviour shown in Fig. 2.4 was due to changes in the porosity of the deposited protein. At the IEP the protein molecule is in its most compact state and has no net charge, and this would provide the least permeable deposited layer. In the presence of ions at this pH, anion binding leads to an increase in the size of the protein. Away from the IEP the BSA molecule acquires significant net charge and enlarges due to electrostatic repulsion. These effects would give a more permeable deposited layer and should give a higher flux. Added salts tend to reverse the effect by shielding charges, causing molecular contraction and thereby decreasing permeability.

The effect of pH and ionic strength on the retention of protein has also been investigated. Fane *et al.* (1883a) found that the retention of BSA went through a shallow minimum at pH 5 both in the absence and in the presence of salts. Hanemaaijer (1985) found a slight decrease in the retention of protein as the pH was decreased from 6.5 to 5.5. However, when studying β-lactoglobulin Hanemaaijer *et al.* (1988, 1989) found that maximum retention occurred at around pH 4 which corresponded to the point of maximum protein deposition. Renner and Abd El-Salam (1991) presented data that showed that the permeability of β-lactoglobulin and α-lactalbumin during UF of whole milk increased as NaCl was added to the milk.

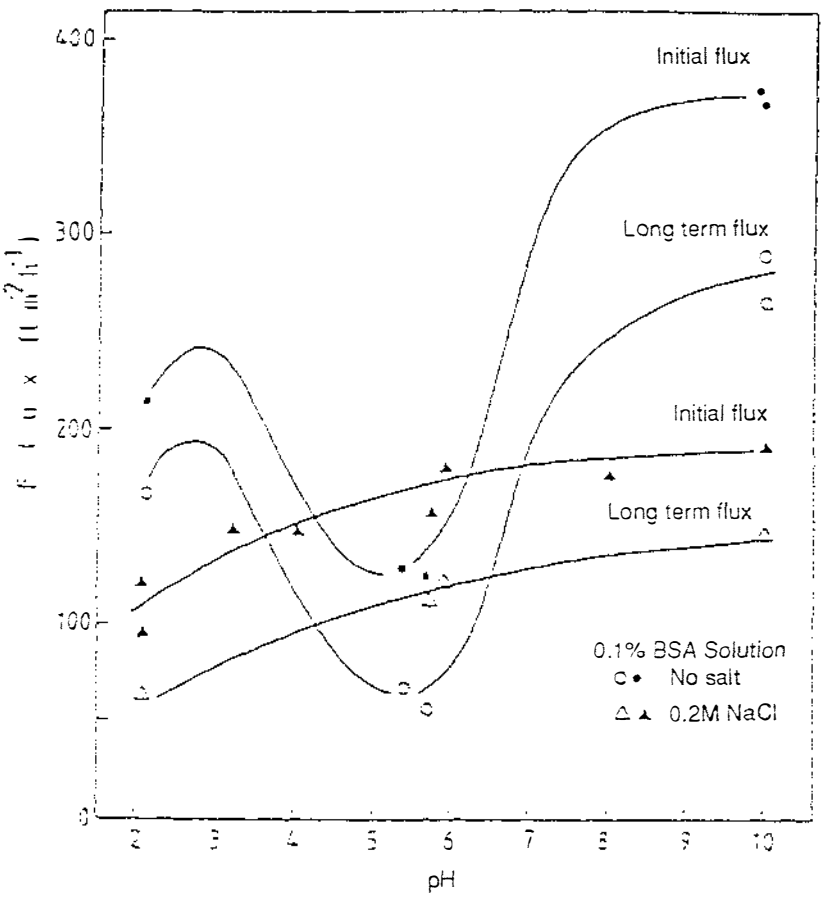

Figure 2.4. The effect of pH on flux for 0.1% bovine serum albumin, with and without NaCl present (PM30, 100 kPa) (Fane *et al.*, 1983c).

The difference in charge between the membrane and protein has been used to explain permeate flux behaviour. Nyström and Lindström (1988), found that, during the removal of chlorolignin from waste water using negatively charged GR61PP and GS61PP membranes the flux increased with increasing pH - matching an increase in the negative charge of the chlorolignin. Also see Heinemann *et al.* (1988). Nyström (1989) ultrafiltered ovalbumin through GR61PP and GS61PP membranes. The permeate flux was lowest at the IEP, where the net charge on the protein is zero. At pH 8, where both protein and membrane are negative, the flux was high. At low pH

values (3-4), where the protein is positively charged, the flux was also high. The GS61PP membrane is negatively charged at this pH and, the increase in flux compared to the flux at the IEP, cannot be explained by protein-membrane electrostatic interactions alone. It appears that the charge on the protein, rather than the difference in charge between the membrane and the protein, determines the degree of deposition. When the protein is charged the solubility (protein stability) increases and the affinity for the membrane material decreases. Where the membrane charge is opposite to that of the protein, initial adsorption may result in a thin modified layer of charged protein on the membrane surface that then repels further deposition (Nyström, 1989).

The effect of pH on the permeate flux depends on the nature of the protein. Attia *et al.* (1988) investigated the effect of acidifying milk on the performance of a Ceraver 0.2 μm aluminium oxide membrane. Acidification from pH 5.9 to 5.6 resulted in a significant decrease in permeate flux. pH adjustment from 5.4 to 4.6 resulted in higher initial fluxes but a rapid decrease in flux to less than the permeate flux seen with normal milk. Initial fluxes increased as the pH was decreased in this range. In a separate paper Attia *et al.* (1991a) used electron microscopy to determine the nature of membrane fouling. At pH 6.0 to 5.6 they observed a tendency for the micelles to combine but retain their individual shape. The fouling structure became increasingly compact with minimum pore space at pH 5.6. At pH 5.45 to 5.2 a different more open structure was apparent, with the casein forming chains linked together. Below pH 5.2 the deposit consisted of more or less individually clumped particles (consisting of demineralised casein micelles) which formed an increasingly open structure.

The level of calcium in the whey or protein solution has been implicated in the reduction in permeate flux. Hayes *et al.* (1974) noted that addition of calcium to cheese whey reduced the flux at pH 6.2. Patocka and Jelen (1987) found that all pretreatments of cottage cheese whey resulting in the elimination of free calcium increased the permeate flux. Daufin *et al.* (1989) investigated UF of a defatted whey protein concentrate solution at pH 5.6 and 6.9. Although the permeate flux at pH 6.9 was initially higher, it decreased to less than the flux at pH 5.6. The authors

attributed this to increased protein fouling on the surface of the membrane and to increased calcium phosphate fouling both on the surface and within the membrane structure. There is a change in the form of phosphate from sodium hydrogen phosphate to hydroxyapatite, an insoluble precipitate at pH 6.9. Labbe *et al.* (1990) found that, when the pH was raised from 5.6 to 6.9 during UF of whey on zirconium oxide membranes, a calcium phosphate precipitation phenomenon was observed supplementary to a sodium phosphate adsorption at lower pH values. Vetier *et al.* (1988) performed trials with milks of various calcium contents. Increased calcium resulted in increased fouling due to calcium phosphate precipitation. Increasing or decreasing the soluble calcium content also increased or decreased the fouling due to total nitrogen components, suggesting that the most important role of the calcium and phosphate salts present in the soluble phase of milk is to act as "cement" between micelles and alumina and between the micelles themselves.

To summarise, proteins are complex molecules and their aggregation or interaction with the membrane surface, which is influenced by the pH and ionic strength, is not clearly understood. The three most common explanations for the observed membrane behaviour with pH and ionic strength are: that changes in protein conformation and stability affect the tendency of the protein to deposit on the membrane; that changes in the protein's effective size alter the porosity of the dynamic membrane; that changes in the charge difference between the protein and the membrane surface affect protein adsorption or deposition. It is likely that all three explanations have some validity, the contribution from each varying depending upon the protein type, conformation and pretreatments, and the type of membrane material used. Obviously any major change in protein structure such as that with casein as the pH is lowered affects the nature of protein deposition on the membrane. Also, the levels of calcium and phosphate have been directly implicated with membrane fouling due to the formation of insoluble calcium salts and as possible catalysts or bridging agents in the deposition of protein on the membrane. For a more detailed discussion of the effects of salts on fouling the reader is referred to Marshall & Daufin (1994).

2.4.3. Prefiltration and the removal of aggregates

It has been demonstrated that the permeate flux in UF can be improved by prior filtration or clarification of the feed material (Lee & Merson, 1976; Tanny *et al.*, 1982; Merin *et al.*, 1983). Fluxes also increase if whey has been defatted by the process described by Maubois *et al.* (1987). Also see Rinn *et al.* (1990) and Daufin *et al.* (1991).

Kelly *et al.* (1993) found that the MF fluxes (0.16 μm, Filtron) of BSA solutions were dependent upon the technique used to manufacture the BSA. By prefiltering (100 kD), the flux of a BSA fraction that fouled badly could be vastly improved. Using scanning electron microscopy they demonstrated that the badly fouled membranes were coated with a heavy protein layer and large protein aggregates whereas after MF of prefiltered feed material the membrane was essentially free of protein deposit. Using gel filtration they correlated the increased rate of membrane fouling with an increase in the number of large molecular weight compounds in the feed. They suggested that the differences in fouling rates were due to the deposition of aggregates on the membrane and that aggregates may act as "seeds" for the formation of further protein deposits. Aggregates may also block the larger membrane pores, causing a disproportionate loss of membrane area and permeate flux (Fane *et al.*, 1981; Munari *et al.*, 1987; Persson *et al.*, 1993).

In summary, the removal of large molecular weight compounds, by prefiltration or other means, results in an improvement in the permeate flux in both UF and MF. Protein aggregates may potentially block the larger membrane pores, resulting in a disproportionate loss of flux, and may act as seeds or catalysts for the formation of a protein fouling layer on the membrane surface.

2.4.4. Component interactions

The presence of a larger component in the solution can increase the retention of smaller components. Blatt *et al.* (1970) found that the rejection of human serum albumin ultrafiltered through XM-100 membranes was approximately zero in the

absence of γ-globulin. However, its retention rapidly increased as γ-globulin was added to the solution. The higher the concentration of γ-globulin, the higher was the retention of human serum albumin. Bottino *et al.* (1984) ultrafiltered a mixture of 3 kD and 35 kD polyethylene glycol (PEG) molecules and found that the flux and retention behaviour matched that of a pure solution of 35 kD PEG. Porter (1988) suggested that, when the solution to be ultrafiltered contains two or more solutes, the retention of the smaller of the two solutes may be increased dramatically. If the larger molecule is retained by the membrane in sufficient concentration, it may form a secondary membrane that can be more retentive than the primary membrane. He showed that the retentions of ovalbumin, chymotrypsinogen and cytochrome C are increased when 1% albumin is added to the solution. The effect is most dramatic for the smallest component, cytochrome C, where the retention increases from <5 to about 70%.

Gergen *et al.* (1987), when characterising UF membranes by dextran challenge, found that the shape of the retention curve was affected by the composition of the dextran mixture. High molecular weight fractions caused increased retention of smaller molecules. Tam and Tremblay (1991) calculated molecular weight cut-off (MWCO) curves by performing experiments with a mixture of five PEG components, initially all at once, and by combining the data from experiments with the five individual PEGs. They showed that the apparent MWCO curve of a PTGC Millipore 10 kD membrane shifted towards a higher retention when a mixture was used. They suggested that differential solute lag within the pore is the most likely reason for the shift observed in sieving curves. Large molecules travelling through the narrow, tortuous, confines of the porous membrane matrix are slowed down by friction with the pore wall and hinder the transport of smaller molecules. The result is a decrease in the net flow of both solute and solvent across the membrane. In an extreme case, differential solute lag becomes pore blockage. To support this view they showed that the flux of four- and five-component mixtures were very similar to the flux of the largest component in the mixture.

Papamichael and Kula (1987) considered the retention of PEG in the presence of BSA. Retention initially increased from 0.3 in pure solution to 0.58 with 0.2% BSA.

Thereafter, with increasing BSA concentration the retention decreased to a stable value of 0.18 with a BSA concentration above 4%. The mechanism for this behaviour is not clear. They suggested that the reduction in retention may be due to a reduction in the size of the PEG. PEG is known to carry a large cocoon of water molecules, which would be reduced in the presence of proteins due to competition for water. The initial increase in retention may be due to protein fouling or interference from the slower moving BSA molecules.

Wahlgren and Arnebrant (1989) considered the adsorption of fatty-acid-free and "native" BSA onto polysulphone. The amount adsorbed for the fatty-acid-free BSA was slightly higher than that for the native BSA. They suggested that the stability of proteins may be affected by the presence of polar lipids. Relative flux reductions for modified DDS GR61PP membranes were 66% for fatty-acid-free BSA and 39% for native BSA.

In summary, the presence of larger molecules cause a steric hinderance to the passage of smaller molecules through the membrane. This may occur because the larger component forms a dynamic membrane that has a smaller porosity than the original membrane, or because of interactions within the membrane pores. In some cases, specific component interactions in the feed solution may also affect the retention of different components.

2.5. The effect of the membrane material

A number of workers have attempted to change the nature of the membrane surface by precoating the membrane prior to filtration (Fane *et al.*, 1985; Bauser *et al.*, 1986; Kim *et al.*, 1987, 1989; Brink & Romijn, 1990; Chen *et al.*, 1992) in an attempt to improve performance by changing the membrane hydrophobicity, charge or surface properties.

2.5.1. Hydrophobicity

Reihanian *et al.* (1983) studied the static adsorption of BSA onto various membranes and found that the hydrophobic membranes (XM200, XM50 and PM30) declined in permeability with increasing concentration of protein. In contrast, the permeability of the highly hydrophilic cellulosic YM30 and poly-ion complex UM10 membranes showed no loss of hydraulic permeability on contact with BSA solution, which indicates that there is no significant BSA adsorption. Further evidence that hydrophilic membranes adsorb less protein can be found in Matthiasson (1983), Hanemaaijer *et al.* (1989) and Oh *et al.* (1989). Complementing these findings from protein adsorption studies, higher permeate fluxes have often been achieved when the membrane surface is more hydrophilic (Fane *et al.*, 1985; Fane & Fell, 1987; Aimar *et al.*, 1988; Hanemaaijer *et al.*, 1988, 1989; Stengaard, 1988). Furthermore, membrane fouling is often less severe (Gekas & Hallström, 1990).

In spite of the above results from experimental studies, commercial hydrophilic polymer MF membranes do not foul less than hydrophobic types (van der Horst & Hanemaaijer, 1990), indicating, that hydrophobicity is not the only factor involved in membrane fouling.

Rolchigo *et al.* (1989) considered the behaviour of a protein solution (horse heart myoglobin, BSA and horse spleen ferritin) with two membranes: a 100 kD Ultrafilic (Membrex, hydrophilic, contact angle 4°) and a 100 kD unmodified Ultrafilic precursor (contact angle 46°). Apart from hydrophobicity, the membranes were considered to have similar properties. Permeate fluxes were similar for both membranes in a cross-flow system, but in a Membrex rotary system with a large Taylor number, the permeate flux of the hydrophilic membrane approached 90% of the water flux and was much higher than that of the hydrophobic membrane. Protein transmissions of myoglobin and BSA were higher with the hydrophilic membrane in both operating systems, but the difference between the two membranes was more marked in the rotary system. With the cross-flow system, the effect of concentration polarisation dominates the effect of membrane material on membrane fouling. With the rotary system, where concentration polarisation can be minimised, the hydrophilic membrane is superior with respect to flux.

The hydrophobic nature of the membrane surface can also influence the nature of the deposited protein. Sheldon *et al.* (1991) considered the adsorption of BSA onto 10 kD polysulphone and regenerated cellulose membranes using various TEM techniques. From flux data they showed that approximately three times the amount of protein adsorbed onto the polysulphone membrane, and that the specific resistance (hydrodynamic resistance per unit weight of protein adsorbed) of the polysulphone membrane was also higher. The nature of the BSA molecule was examined by freeze fracture and deep-etching techniques. In solution, the BSA molecules appeared to be more or less globular, consistent with the accepted molecular size. Protein at the surface of the regenerated cellulose membranes had a similar appearance. Examination of replicas of protein-fouled polysulphone membranes, however, did not reveal particles of the dimensions of native BSA molecules within the protein layer. Instead the protein molecules were long and filamentous. It appears that the tertiary protein structure of the globular protein had, in some way, been disrupted and distorted by interaction between the BSA and polysulphone. Because, in normal circumstances, the outer layer of a BSA molecule is hydrophilic, it appeared that the hydrophobic surface of the polysulphone membranes had caused the molecule to unfold and expose its hydrophobic sites.

In summary, proteins generally adsorb less to hydrophilic membranes than to hydrophobic membranes, and there is the potential for permeate flux improvement. However, where concentration polarisation and total protein deposition are high, the effect of hydrophobicity is masked by the effects of concentration polarisation. The work of Sheldon *et al.* (1991) suggests that the increase in protein adsorption on hydrophobic membranes may be due to increased protein denaturation at the surface of the membrane.

2.5.2. Charge effects

The charges on a membrane are strongly dependent upon the membrane material, the pH and the ionic strength of the feed solution. For example, polysulphone PM10 and Dynel XM-300 membranes carry negative charges at pH 2-10. On the other hand, cellulosic YC-05 membranes carry positive charges at a pH below 9 and negative

charges at a pH above 9 (Lee & Hong, 1988). Generally, higher permeate fluxes are obtained if a membrane of similar charge to the protein is used (Casiraghi & Peri, 1983; Heinemann *et al.* 1988; Nyström & Lindström, 1988; Nyström, 1989; Brink & Romijn, 1990)(see previous discussion in Section 2.4.2 on pH and ionic strength for further details).

The charges on the membrane have also been used to enhance the separation of similar sized proteins. Nakao *et al.* (1988) considered the transmission of myoglobin and cytochrome C (of similar sizes) through positively and negatively charged polysulphone membranes (with large pores). Rejection of proteins of the same charge as the membrane (both negative and positive) was high, whereas rejection of proteins at their IEP was low, despite a reduction in pore size due to increased deposition at the IEP. Separation of protein could be enhanced when UF was performed at a pH where one protein had a zero net charge (its IEP) and the other protein had the same charge as the membrane. With a negatively charged membrane at pH 9.2, cytochrome C freely permeated the membrane whereas myoglobin was retained (about 60%). Reducing the operating pressure reduced the permeate flux, and the retention of myoglobin increased to around 80-90%, probably due to a reduction in concentration polarisation.

In summary, operation with a membrane of similar charge to the protein can enhance the permeate flux if concentration polarisation is minimised. With membranes of a large pore size, greater protein selectivity may be possible.

2.5.3. Surface rugosity or roughness

Larsson (1980) stated that the adhesion of surface-active molecules onto a surface results in a reduction in surface free energy and with a low energy surface the adhesive strength is generally weak. Any increase in surface roughness increases the surface free energy, which in turn could be expected to increase the adhesiveness.

Although an increase in surface rugosity or roughness may increase the likelihood of protein adsorption (Fane *et al.*, 1985; Kim *et al.*, 1987, 1989), it can also affect

the nature of the dynamic membrane. Le *et al.* (1984) found during enzyme separation from cell debris by 0.45 μm MF membranes (Domnick Hunter) that the protein transmissions were higher when the membrane was placed open-side up (OPU) rather than with the tight side of the membrane (TSU) in contact with the retentate. Permeate fluxes were similar. These results demonstrate that the surface properties of the membrane can affect the nature of the polarisation layer and that the characteristics of the dynamic membrane are largely determined by the primary pore structure of the polymeric membrane itself. With the TSU membrane, a dynamic cake may form on the membrane surface, whereas, with the OSU membrane, the dynamic membrane is established within the pores themselves and so enables it to reflect the asymmetric nature of the support membrane (Le *et al.*, 1984).

Shoji *et al.* (1988) investigated the performance of dynamic membranes formed with water-soluble proteins in waste water from surimi production. The effect of the pore size of the ceramic porous support was investigated. As the pore size increased it took longer for the dynamic membrane to form - perhaps due to having to "fill" and bridge the pores. However, after formation the permeate flux was not affected by the pore size of the support membrane suggesting that the flux was totally controlled by the dynamic membrane. However, the MWCO decreased as the pore size decreased, suggesting that the dynamic membrane was "better" formed with a tighter porous support.

In summary, although increasing surface roughness may increase the tendency for protein to adsorb, the "completeness" of the dynamic membrane is reduced. In an extreme, with a "reverse" asymmetric membrane, the dynamic membrane forms within the pores and the structure of the deposits is compromised by the proximity of the pore walls.

2.5.4. Porosity and pore size distribution

Typical UF membranes have relatively low surface porosities and a wide distribution of pore sizes (Fane & Fell, 1987; Kim *et al.*, 1990), whereas, commercial MF

membranes have a higher porosity, but also have a wide distribution of pore sizes (Persson *et al.*, 1993). This is not surprising considering that some commercially available MF membranes are depth filters that have been adapted for cross-flow operation.

Suki *et al.* (1984) showed with different polysulphone membranes that the ranking of protein deposition matched the ranking of the heterogeneous nature of the membrane surface. The largest deposition occurred with membranes of the lowest porosity or highest heterogeneity. They suggested that the more heterogeneous the membrane surface, the higher the local velocity normal to the surface, and that this effect, applied on a local scale around individual pores, results in higher local concentration polarisation and more rapid initial deposition. Also see Fane *et al.* (1985). Fane *et al.* (1981) considered the behaviour of two UF membranes, of differing initial porosity (L=low initial water flux; H=high initial water flux), laid one on top of the other. Highest flux with a γ-globulin feed was obtained with an H/L combination (with the H membrane closest to the feed); the flux was higher than that for the L membrane alone even though the overall resistance to flow was higher.

The effect of the pore size distribution on the permeate flux can be appreciated when the balance of flow through different membrane pore sizes is considered. Using the Hagen Poiseuille equation for a single capillary Fane *et al.* (1981) showed with UF membranes that the solvent flow is strongly biased to the larger pores, with 50% of the flow through 20-25% of the pores. Munari *et al.* (1987) found with a PC-300 membrane that approximately 70% of the permeate flows through the largest 10% of the pores. Also see Persson *et al.* (1993) for more examples of MF membranes. The overall membrane flux is, therefore, very sensitive to the population of large pores. Their loss through plugging or obstruction by large components or aggregates results in a disproportionately high loss in the permeate flux (Kelly *et al.*, 1993).

Membrane selectivity is also affected by the pore size distribution, where a wide variation in pore size results in poorer selectivity than for an ideal membrane (Jonsson, 1985).

Fouling can change the pore size distribution of a membrane. Fontyn *et al.* (1989) measured the pore size distribution before and after a DDS GR61PP membrane had been fouled with polypropylene glycol (PPG). The numbers of small and large pores in the fouled membrane decreased significantly whereas there were more middle-sized pores. The total number of accessible pores dropped by a factor of 10. The average pore size of the membrane actually increased. The authors concluded that the smaller pores were completely blocked by the PPG whereas the pore diameter of the larger pores was reduced by adsorption of PPG onto the pore surfaces.

The balance between the pore size and the pore density must also be considered. Piot *et al.* (1984) considered the performance of two different Rhone Poulenc membranes. The more porous membrane, as demonstrated by higher initial protein transmission, fouled more rapidly, and the permeate flux decreased to below that of the tighter membrane. The protein transmission of the more open membrane decreased, but the tighter membrane still had lower protein transmission in spite of having a higher flux. Attia *et al.* (1991b) while processing skim milk on aluminium oxide membranes (0.2 and 0.8 μm) showed that the retention of total nitrogen was slightly lower with the 0.8 μm membrane (96.6-97.7%) than with the 0.2 μm membrane (99.5-99.7%) even though the permeate flux was lower for the 0.8 μm membrane. Gatenholm *et al.* (1988a) using a 100 kD UF membrane and a 0.2 μm MF membrane found that the protein retention after processing of a fermentation broth (*Escherichia coli*) was 25% for MF and 90% for UF even though the MF membrane had a lower final flux. It seems that, although increased membrane fouling results in lower permeate fluxes for the more open membranes and changes in retention are generally more severe as the pore size increases, the retention characteristics of the membrane are still dominated to a certain extent by the clean membrane pore size. One reasonable explanation is that with the larger membrane some large pores remain permeable, allowing a lower membrane retention, but the number of open pores is much reduced, and is less than that of the tighter membrane, resulting in a lower solvent flux.

In summary, most UF and MF membranes have a wide pore size distribution. The flow through the largest pores dominates the total permeate flow, and, as a

consequence, the permeate flux is very sensitive to fouling or plugging of the larger pores by, for example, protein aggregates. Membrane selectivity is poor with membranes of a wide pore size distribution. Membrane fouling changes the pore size distribution and pore density of the membrane. Thus, the permeate flow, component retentions and membrane selectivity change as the membrane fouls with time.

2.5.5. Pore size

This section summarises the behaviour of membranes with different pore sizes, and the fouling mechanisms are discussed in Section 2.7.

There are numerous examples where increasing the pore size, and hence reducing the intrinsic membrane resistance, actually results in increased membrane fouling and in some cases poorer permeate fluxes. Devereux and Hoare (1986) when processing isoelectric soy protein precipitate suspensions found that the flux decline of a 0.2 μm MF membrane was greater than that of a PM50 UF membrane. Attia *et al.* (1988, 1991b) while processing skim milk on aluminium oxide MF membranes found higher permeate fluxes with a 0.2 μm membrane than a 0.8 μm membrane. Gatenholm *et al.* (1988a) using a 100 kD UF membrane and a 0.2 μm MF membrane found with a fermentation broth (*E. coli*) that the flux decline was much greater with the MF membrane, and final MF fluxes were less than those of the UF membrane. Gatenholm *et al.* (1988b) while processing an *E. coli* fermentation broth with a range of UF and MF membranes showed that the final steady-state product flux was proportional to the initial membrane resistance, *i.e.* the tighter the initial membrane, the higher was the final flux. Also see Kim *et al.* (1992) and Nobrega *et al.* (1989). Scott (1988) considered the performance of various Millipore membranes on Minitan and Pelican systems while removing yeast cells from apple cider broths. Fluxes increased with increasing pore size; however, flux decline was greatest as the pore size increased. Chmiel and McDonough (1989) showed that the flux decline during the MF (IRIS 6501) of beer (still containing yeast) was higher than that during the UF (IRIS 3065) of beer. In the application of MF to cell recovery and washing, cell debris removal and cell recycling, it is generally found that UF membranes of a high cut-off value (greater than 100 kD) give better flux results than MF membranes in the long term (Defrise & Gekas, 1988).

Fane *et al.* (1983a) when comparing the behaviours of a UF membrane (PM30) with BSA and lysozyme found that the permeate flux was initially higher with lysozyme. However, the flux declined steeply and the final steady-state flux was lower than that of the totally retained BSA. The retention of lysozyme initially decreased with time, probably due to the losses to protein adsorption, and then increased to about 45%. This result shows that the important variable is actually the protein to pore size ratio, a ratio that can be altered by changing the size of either the protein or the pore size.

In a number of cases an optimum pore size with respect to permeate flux has been identified, below which the resistance of the membrane itself and the formation of a surface fouling layer reduce the permeate flux, and above which the increased rate of membrane fouling due to deposition within the pores causes lower longer term fluxes. Le *et al.* (1984) during the concentration of *Erwinia carotovora* cells by MF with Acroflux modules found that the flux increased with increasing pore size from 0.2 to 0.45 μm, but then decreased from 0.45 to 0.6 μm. Piot *et al.* (1984) considered the performance of Nuclepore membranes (0.01, 0.03, 0.05, 0.08, 0.1 μm) with cheese whey in an Amicon Cell. Fluxes increased until the 0.08 μm membrane, after which the flux declined. In addition, they found that retention was lowest for the 0.05 μm membrane, increasing as the pore size both decreased and increased. Matsumoto *et al.* (1988) processed ovalbumin through 0.2, 0.8, 1.5 and 3 μm ceramic membranes. The effect of the pore size interacted with the velocity. At low velocities, the limiting flux was similar for all four membranes. However, at high velocity, the limiting flux was highest with the 0.8 μm membrane.

Meireles *et al.* (1991a) considered the performance of a range of polysulphone (Techsep) membranes with BSA, ovalbumin and α-lactalbumin. After 1 minute the protein retentions were 100, 85 and 20% for 10, 40 and 100 kD membranes respectively. However, protein retentions for the three membranes at steady-state were 100, 100 and 98%. Changes in protein retention by fouling are more severe as the membrane pore size increases.

To summarise, numerous examples show that membrane fouling is more severe with increasing pore size. There appears to be an optimum pore size, below which the

membrane resistance restricts permeate flow and above which severe membrane fouling reduces the flux. Increases in membrane retention are generally more severe as the pore size increases. There is one paper that shows that protein transmission can pass through a maximum in a similar way to the permeate flux.

2.5.6. Membrane consistency

One difficulty encountered in the evaluation of different polymer membranes is the variation seen in the pore size and pore size distribution of supposedly identical membranes. Fane *et al.* (1983a) found considerable difference in the process fluxes of different batches of new XM100A membranes when processing BSA even though the initial water fluxes were similar. Analysis of the water fluxes following processing suggested that the lower water flux membranes had adsorbed more protein than their counterparts, a conclusion that was backed up by the protein retention data. Furthermore Nilsson (1989) found that there was a ten-fold difference in the water flux of small sections of GR61PP membranes cut from the same membrane sheet.

Greater membrane consistency and a tighter pore size distribution are required, if difficult separations are to be achieved with membranes. This is especially so in MF, where retention and selectivity are dependent upon the primary membrane structure, rather than the dynamic membrane.

2.6. The effect of the processing variables

2.6.1. Transmembrane pressure

Taddei *et al.* (1986, 1988) found during UF of cheese whey with an M4 Carbosep membrane that increasing the transmembrane pressure (from 1 to 4 bar) increased the permeate flux but also increased membrane fouling. Increasing the pressure further to 5.7 bar did not result in further increases in the permeate flux. For a range of concentrations, higher pressures and lower velocities resulted in increased resistance. Aimar *et al.* (1988) showed that the initial permeate flux decline with

cheese whey was larger as the pressure was increased. Furthermore, increasing the transmembrane pressure resulted in higher retentions for α-lactalbumin and β-lactoglobulin. Nakanishi and Kessler (1985) found that reducing the transmembrane pressure during UF considerably increased the rate of removal of the deposited layer during rinsing, even though the transmembrane pressure had little effect on the flux during UF.

In MF, Attia *et al.* (1988) with a Ceraver 0.2 μm aluminium oxide membrane found in the pressure range 3-7 bar that the permeate flux was highest at 5 bar. With a 0.8 μm membrane Attia *et al.* (1991b) considered pressures of 3, 5 and 7 bar. After 5 minutes the permeate flux was highest at 5 bar, then 3 bar then 7 bar. After 1 hour the flux was highest with a pressure of 3 bar. Bentham *et al.* (1988) processed a soy protein solution containing precipitate and soluble protein with a 0.2 μm membrane. They found that increasing the pressure from 0.41 to 0.97 bar in the middle of a run caused an instantaneous increase (approximately 100%) in flux and an increase in protein transmission. However, the flux and protein transmission declined rapidly, so that, after less than 15 minutes, they were less than the transmission and flux obtained at the lower pressure. Bowen and Gan (1991) processing BSA with 0.2 μm Anopore capillary membranes found that increasing the transmembrane pressure (0.14, 0.34, 0.69 and 1.38 bar) increased the initial permeate flux but also increased the rate of flux decline. The final permeate fluxes were fairly similar. Piot *et al.* (1986) considered the separation of raw whole milk with a 1.8 μm Ceraver membrane. The rate of flux decline decreased and the average permeate rates increased as the transmembrane pressure was reduced from 10 to 0.8 to 0.65 bar.

Hodgson and Fane (1991) considered the performance of various MF membranes with a fermentation broth of *Streptococcus lactis* cheese starter. Increasing the transmembrane pressure in the range 0.5-2 bar caused a decrease in final flux for the 0.2 μm Ceramesh membrane. With a 0.02 μm Anapore membrane the maximum flux was at 1 bar pressure. These results, together with the results of Attia *et al.* (1988, 1991b), show the interaction between the transmembrane pressure and the pore size. The optimum transmembrane pressure, with respect to maximising the permeate flux, decreases as the pore size increases. Increasing the transmembrane pressure also

resulted in lower water flux recovery after water flushing, suggesting that more severe fouling had occurred.

Defrise and Gekas (1988), in reviewing the application of MF to cell recovery and washing, cell debris removal and cell recycling, concluded that increasing the transmembrane pressure caused the flux to increase initially but that it later accelerated flux decay. Kroner *et al.* (1987) and Kroner and Nissinen (1988) investigated the separation of cell debris from enzymes (10% suspension of disrupted *Candida boidinii*) and found that enzyme transmission decreased rapidly with increasing transmembrane pressure.

Attia *et al.* (1988, 1991b) found that increasing the transmembrane pressure increased the protein retention. Gekas and Hallström (1990) investigated the retention of 0.1% BSA by a 0.2 μm Nylon 66 MF membrane over 5 hours operation at 0.1 (0.05 m/s) and 0.7 (5 m/s) bar. Protein retention increased with time at a lower rate and to a lower final retention coefficient at the lower pressure. Kim *et al.* (1992) used an MPS (Memtec, 100 kD) membrane and found that retention increased rapidly at 1 bar to around 70% after 40 minutes. At 0.5 bar the retention remained constant for 20 minutes before increasing more slowly to around 35%. Capannelli *et al.* (1983) found that the retention of BSA, immunoglobulin and bovine myoglobin was stable with time and that the permeate flux was reasonably stable with time, at low concentration (0.1%) and at low pressures (0.15 bar) through a modified PVDF UF membrane.

Forman *et al.* (1990) while processing *E. coli* lysate by MF found that the retention of the soluble protein increased sharply as the permeate flux and hence the transmembrane pressure increased (pressures less than 1 bar). Other workers (quoted in Forman *et al.* (1990)) have found with lysates that the soluble protein retention decreases as the permeate flux is increased at transmembrane pressures above 2.45 bar. These results suggest that protein retention may pass through a maximum. At very low pressures the retention is low, and at high pressures increased concentration polarisation results in decreased retention. Jonsson (1986) and Jonsson and Christensen (1986) showed that the observed retentions of various sized 0.1% PEG

and dextran solutions go through a maximum as the permeate flux is increased, at which point the increase in true retention is balanced by the increase in concentration polarisation. The decrease in retention of 20 kD PEG is such that at high fluxes its observed retention is less than that of 6 kD PEG. Selectivity is greatest at low fluxes.

To summarise the above findings, increasing the transmembrane pressure in the low pressure range (<4 bar) initially results in an increase in permeate flux but also an increase in the fouling rate. Initially, membrane retention can decrease due to increased concentration polarisation, but, after more time, in UF the increased rate of fouling results in an increase in the final component retention. In UF there is an overall increase in permeate throughput.

In MF the increase in fouling rate is much higher, and in some cases the permeate flux can decline to less than the flux at lower pressure. Membrane retention increases with the increase in membrane fouling and appears to remain constant only at very low pressures and low concentrations. To maximise the permeate flux there is an optimum pressure, below which the driving force is too low and above which increased fouling causes a large reduction in flux. The optimum pressure decreases with increasing membrane pore size.

2.6.2. Cross-flow velocity and turbulence promoters

Increasing the cross-flow velocity generally results in an improvement in permeate flux in both UF (Blatt *et al.*, 1970; Kessler, 1981; Nakanishi & Kessler, 1985; Aimar *et al.*, 1988) and MF (Bennasar *et al.*, 1982; Maubois *et al.*, 1987; Attia *et al.*, 1988, 1991b). Taddei *et al.* (1986) found that the membrane resistance was reduced when the velocity was increased, suggesting that increasing the velocity reduces membrane fouling as well as the polarisation layer. Nakanishi and Kessler (1985) considered the rinsing behaviour of a UF membrane (Kalle CA-30, 30 kD) that had been fouled with skim milk. With rinsing, the relative flux (compared with the original water flux) increased quickly, then flattened out and appeared to asymptotically approach a final value after 60 minutes. Increasing the velocity increased both the flux during UF and the recovery of flux during rinsing, suggesting

reduced fouling. When velocity was low during UF and high during rinsing, the relative flux after rinsing increased, but not to the same extent as when both velocities were high.

Further evidence that the cross-flow velocity reduces membrane fouling can be found from the retention data. In a number of cases (Maubois *et al.*, 1987; Shoji *et al.*, 1988; Taddei *et al.*, 1988; Hodgson & Fane, 1991) protein retention has been found to decrease with increasing velocity, contrary to the result expected from concentration polarisation theory. This is evidence that membrane fouling decreases and the effective pore size increases with increasing velocity.

In all the above cases the retention of protein was high and surface fouling was predominant. However, where internal fouling rather than surface fouling occurs the cross-flow velocity has limited effect (Bowen & Gan, 1991). This suggests that the effect of the cross-flow velocity on membrane fouling is connected to concentration polarisation and supports the concept that protein deposition can be linked to the rate of accumulation of protein at the membrane surface (Fane *et al.*, 1983c; Matthiasson, 1984; Suki *et al.*, 1984).

Pulsing has been found to improve the permeate flux but does not remove the problem of flux decline (Wyatt *et al.*, 1987; Chmiel & McDonough, 1989). Finnigan and Howell (1989) showed that the permeate flux increased when baffles were incorporated in a tubular membrane system. Additional improvement in flux was seen when pulsed flow was used. The use of corrugated or dimpled membranes has also been found to improve the permeate flux (Wyatt *et al.*, 1987; van der Waal & Racz, 1987, 1988). In summary, various means of creating greater turbulence at the membrane surface generally result in an improvement in mass transfer and a higher membrane flux.

There are some situations where a high cross-flow velocity is not beneficial. Devereux and Hoare (1986) when processing isoelectric soy protein precipitate suspensions found that greater pore obstruction occurred at high shear rates due to break-up of precipitate aggregates by higher pump speeds. Bearing in mind the

conclusions from the section on transmembrane pressure, with large pore membranes increasing cross-flow velocity may improve the permeate flux to such an extent that the membrane fouls internally (Bennasar, 1982). This problem is avoided by the use of a system where the transmembrane pressure has been "decoupled" from the cross-flow velocity (*e.g.* rotary systems (Kroner *et al.*, 1989; Kroner & Nissinen, 1988)).

2.6.3. Backflushing

The use of backflushing has met with varied results. Bhattacharyya *et al.* (1979) suggested that the flux drop can be minimised with short term membrane depressurization during UF of oil-detergent-water systems. van Gassel and Ripperger (1985) showed that the long term permeate flux during MF of wine could be almost doubled by the use of 2 second backflushes every 2 minutes. With whey, Bauser *et al.* (1986) found that a flux improvement of 50% could be obtained by generating a transmembrane pressure pulse, by varying the pressure applied to the permeate side of the membrane. However, Piot *et al.* (1986) while processing raw whole milk with a 1.8 μm Ceraver membrane found that backflushing the membrane by closing the permeate valve (effectively only backflushing the low pressure end of the membrane) resulted in an immediate improvement in the permeate flux, but the improvement was very short-lived with the permeate flux returning to the original flux almost immediately. van der Horst and Hanemaaijer (1990) found that backflushing had no effect on the permeate flux obtained from various MF membranes used for the removal of fat from whey.

If the accumulation of particles takes place on the surface of the membrane rather than in the pores, there is a good chance that the particles can be removed by intermittent backflush pulses that blow the particulates off the surface (Porter, 1988). However, it seems that backflushing is not effective where protein is strongly adsorbed or bound onto the membrane surface.

2.6.4. Temperature

Increasing the temperature generally increases the permeate flux due to the dual effect of lowering the permeate viscosity, which assists flow rate, and of increasing diffusivity, which assists dispersion of the polarised layer in both UF and MF (Piot *et al.*, 1984; Scott, 1988; Attia *et al.*, 1988, 1991b).

The retention of protein can decrease with increasing temperature (Piot *et al.*, 1984; Attia *et al.*, 1988, 1991b). However, Piot *et al.* (1984) suggested that the reduction in protein retention may be due to increased concentration polarisation as a result of higher membrane fluxes rather than to a reduction in membrane fouling. Vetier *et al.* (1988) used scanning electron microscopy to investigate the effect of temperature (20 and 50°C) with raw whole milk. They showed that increasing the temperature reduced the viscosity of the milk, which resulted in a considerable fall in the thickness of the surface cake/polarisation layer. The permeate flux increased and the total nitrogen retention decreased due to the passage of the serum proteins through the membrane.

Piot *et al.* (1984) and van Boxtel *et al.* (1991) both found with cheese whey that the rate of flux decline was higher as the temperature was increased. Piot *et al.* (1984) suggested that the increased fouling rate is due to the precipitation of calcium phosphate. Vetier *et al.* (1988) also saw a distinct increase in calcium and phosphate fouling with skim milk at 50°C compared with 20°C. They suggested that this occurs due to the increased solvent flow and, to a lesser extent, by the movement of the phosphocalcic equilibrium in the milk from the soluble phase to the colloidal phase when the temperature is increased.

Prior heat treatments of the feed material can also have a beneficial effect on flux. Hayes *et al.* (1974) found that short heat treatments (80-85°C for 15 seconds) of cheese whey improved the permeate flux in UF. They suggested that the heat treatment causes complex formation between casein components and β-lactoglobulin and that these aggregates do not foul the membrane to the same extent. On the other hand, Meireles *et al.* (1991b) investigated the denaturation of BSA during UF on a

100 kD polysulphone (IRIS, Techsep) membrane. BSA denaturation, as measured by solution turbidity, increased exponentially with time when the solution was ultrafiltered at temperatures greater than 8°C. Below this temperature there was no increase in turbidity with time. At 30°C the turbidity doubled in about 40 minutes. Studies of the solution by size exclusion HPLC and laser light scattering confirmed that polymers and large species, probably protein aggregates were now present in solution. The permeate flux at 22°C, while initially higher than at 8°C, fell below the flux at 8°C after 1 hour processing and continued to decline. These results suggest that increasing the temperature can result in protein denaturation and aggregation and that fouling is more severe when a solution contains denatured proteins.

To sum up, increasing the temperature generally results in an increase in the permeate flux. Fouling on the membrane surface may be reduced due to the increase in protein diffusivity and a lessening of concentration polarisation. On the other hand, the removal of the surface layer may lead to greater internal fouling. In solutions where protein denaturation or precipitation of calcium phosphate is likely the rate of fouling may increase, resulting in a final flux lower than that at a lower temperature.

2.7. Fouling mechanisms and the influence of the membrane pore size

The influence of the pore size on membrane fouling is most clearly seen from a comparison between UF and MF behaviour. Typically the pores in UF membranes are less than 15 nm (Capannelli *et al.*, 1983; Meireles *et al.*, 1991a; Tweddle *et al.*, 1992), and therefore, given that proteins like BSA and ß-lactoglobulin are about 5-15 nm in size, UF can be considered as a process where the protein is of a similar size to the pores. The typical pore size of an MF membrane is around 200 nm, hence BSA and ß-lactoglobulin are 15-30 times smaller than the pore size. Thus MF could equally be defined as a membrane operation where the protein is significantly smaller than the average pore size of the membrane.

Given these definitions, it could be expected that most protein will be retained on the surface of a UF membrane, the protein forming a surface layer or dynamic membrane. Whereas, protein should permeate an MF membrane and fouling should be confined to deposition on the pore walls. However, in MF, fouling is far more severe that might be expected, causing a rapid reduction in the permeate flux and an increase in protein retention. In badly fouled membranes the loss of effective pore area or pore numbers can result in permeate fluxes that are less than those seen in UF (Piot *et al.*, 1984; Defrise & Gekas, 1988; Gateholm *et al.*, 1988a, 1988b; Attia *et al.*, 1988, 1991b). MF behaviour will be considered later in the discussion.

In UF, the general consensus is that a dynamic membrane (gel layer, filter cake, surface layer) does form on the membrane surface (Howell & Velicangil, 1980; Aimar *et al.*, 1988; Hallström *et al.*, 1989). A small amount of protein does deposit within the membrane structure (Labbe *et al.*, 1990; Sheldon *et al.*, 1991), possibly in the small percentage of large pores (*i.e.* pores more typically found in MF). The density of the dynamic membrane increases with proximity to the membrane surface (Glover & Brooker, 1974; Fane *et al.*, 1983b; Matthiasson, 1983; Chudecek & Fane, 1984) and may be localised around the pore entrances (Kim *et al.*, 1992). The evenness of the protein layer can be disrupted by large membrane pores that are not completely covered (Suki *et al.*, 1984; Meireles *et al.*, 1991a) or by changes in the roughness of the membrane surface.

The resistance of the dynamic membrane is generally much larger than that of the actual membrane, and as a consequence, the permeate flow is controlled by the dynamic membrane. The effect of the dynamic membrane on protein retention depends on the membrane pore size. Meireles *et al.* (1991a) obtained dextran retention curves for a range of polysulphone membranes (Techsep) before and after fouling with BSA. The retention curve and the pore size distribution for the 10 kD membrane did not change. However, with the 40 and 100 kD membranes the retention curves shifted to higher retentions and the pore size distribution shifted to smaller pores. They proposed that the membrane retains its own selectivity if the "apparent" pore size of the deposit (on the membrane surface) is larger than that of the membrane. Otherwise, the deposit enforces its own selectivity. A deposit made up of a single type of molecule seems to have 100% retention for this molecule.

The properties and "apparent" pore size of the dynamic membrane are affected by:

- the type and state of the proteins that are present (Lee & Merson, 1976);
- changes in the apparent physical size of the protein due to changes in pH or ionic strength (Fane *et al.*, 1983c; Nyström, 1989);
- increased compaction or thickness of the dynamic layer due to increasing transmembrane pressure (Porter, 1988; Shoji *et al.*, 1988; Mochizuki *et al.*, 1990);
- the increase in concentration due to increased polarisation with reduced cross-flow velocity or increased pressure may result in greater aggregation or precipitation at the membrane surface (Chudecek & Fane, 1984);
- the membrane material (Kim *et al.*, 1992), membrane hydrophobicity (Fane *et al.*, 1985; Fane & Fell, 1987; Stengaard, 1988; Hallström *et al.*, 1989) and membrane porosity or heterogeneity (Suki *et al.*, 1984).

Although, it is observed that a dynamic membrane forms on the membrane surface, attempts to model this mathematically have their limitations. Typically, based upon filtration theory, the Carmen Kozeny equation is used to describe the resistance of the deposited layer, which is then considered to be in series with the resistance of the membrane. Proteins are large and complex molecules. They may change orientation and conformation during or after interactions with either the membrane surface or other protein molecules (Lundström, 1985). It is therefore simplistic to expect a layer of deposited protein to behave in the manner of a packed bed of inert particles and, one must therefore question the suitability of the Carmen Kozeny equation to describe the resistance of a protein layer. Furthermore, there are several assumptions made in applying the Carmen Kozeny equation to UF systems that are not always true: that the deposited layer is of even thickness and density; that the deposited layer is not affected by the properties of the membrane; that the intrinsic properties of the membrane do not change.

Kim *et al.* (1993) considered the filtration of very dilute silver colloids with 30, 100, 300 kD and 0.22 μm membranes. The silver colloids were about 8.3 ± 2.6 nm in size. Fouling was highest with the 100 and 300 kD membranes and least with the 0.22 μm membrane. These data suggest a natural progression in fouling as the pore

size increases. With a small pore size (30 kD) the silver particles form a cake on the membrane surface, as expected; retention is high and the flux stabilises at a constant level below that of the pure water flux. With membranes that are partially permeable, *i.e.* the pore size is just larger that the size of the foulant, in this case the 100 and 300 kD membranes, severe fouling occurs due to fouling within the membrane pores. These results fit with the comments of Porter (1988) who stated; "membranes are inherently susceptible to internal plugging or fouling by particles or solute molecules whose dimensions lie within the pore size distribution of the membrane. Fouling will be most pronounced with solutes whose dimensions lie in the lower third of the pore-size distribution, since these will have the least difficulty in entering the structure but the greatest likelihood of lodging in pore constrictions". With a very large pore like those of the 0.22 μm membrane, the retention of silver colloids is low and the small increase in resistance is probably due to the deposition of silver particles on the pore walls.

However, different behaviour is observed with a protein solution. Jonsson *et al.* (1992) compared the contributions to membrane fouling of protein adsorption and pore plugging for membranes of different pore sizes. He compared the reduction in water flux after static and convective exposure of the membrane to a dilute BSA solution. With a GR61PP polysulphone membrane (20 kD) adsorption had a major role in membrane fouling. The additional reduction in flux due to convection was small and may have been due to additional deposition of protein on the front face of the membrane rather than pore plugging. With 0.2 and 1 μm polysulphone membranes static exposure of the membrane to BSA (*i.e.* adsorption) caused a very small drop in permeate flux. However, upon application of low pressures (0.1-0.5 bar) and permeate flow very severe fouling occurred, showing that pore plugging dominated fouling with these membranes. Interestingly, the majority of the water flux could be recovered by water flushing and scrubbing the front face of the membrane. This indicates that, in spite of the large pores, the majority of the fouling occurred on the front face of the membrane. This conclusion was supported by scanning electron microscope photographs. After static exposure small amounts of adsorbed protein were observed on the front face of the MF membranes. With convection a protein layer formed on the membrane surface regardless of the pore size. It seems

with protein, or at least with BSA, that molecules of around 10 nm can successfully plug an MF membrane with 200 nm pores. Pore plugging reduces the apparent pore size of the membrane leading to the formation of a surface layer, as in the case of a UF membrane. It would be interesting to repeat these experiments with different types of protein to see if the behaviour is specific to BSA.

Some larger pores were still visible with the 1 μm membrane and it seems reasonable that if the pore size is greatly increased the effect of pore plugging on membrane flux will become insignificant. Therefore it seems with BSA that, as the membrane pore size is increased, the range of pore sizes where plugging occurs is extended beyond that found with less interactive molecules. Several theories have been suggested to explain this behaviour.

As the permeate flow is biased towards the larger pores, with up to 90% of the flow passing through the largest 10% of the pores (Persson *et al.*, 1993), any increase in the number of protein aggregates that block the larger pores results in severe membrane fouling (Kelly *et al.*, 1993) and, in support of this hypothesis, it has been shown that prefiltration improves the permeate fluxes seen in UF and MF (Lee & Merson, 1976; Merin *et al.*, 1983; Le *et al.*, 1984; Kelly *et al.*, 1993). Kelly *et al.* (1993) also suggested that the protein aggregates on the surface of the MF membrane act as catalysts or seeds for the further formation of a surface layer on the membrane. The aggregate content of the feed may change because of: prior processing (Kelly *et al.*, 1993); an increase in temperature (Meireles *et al.*, 1991b); any treatment that increases protein denaturation, for example, the presence of air in the membrane system that can cause denaturation at the air/liquid interface (Matthiasson, 1983); changes in pH and ionic strength. Whereas in UF changes in ionic strength or pH that increase the size of the protein result in an increase in the permeate flux the opposite can be inferred for MF, as an increase in the size of the protein increases the tendency of the protein to plug the membrane pores.

Proteins can adsorb to the exposed membrane surfaces within the pore structure. Polysulphone, a hydrophobic material, has been shown to affect the tertiary structure of BSA upon adsorption, whereas regenerated cellulose, a hydrophilic material does

not (Sheldon *et al.*, 1991). This change in conformation may affect protein-protein interactions and hence, further protein deposition within the membrane pores.

Numerous workers have shown that the rate of membrane fouling in MF increases as the transmembrane pressure or permeate flux is increased (Bentham *et al.*, 1988; Defrise & Gekas, 1988; Attia *et al.*, 1991b; Hodgson & Fane, 1991). Both the pore narrowing and pore plugging models show that the fouling rate is a function of the volume of product processed, thus increasing as the transmembrane pressure increases. Increasing the permeate flow will also increase the probability of larger particles or aggregates entering the membrane structure due to the higher convective flow overcoming the drag force of the cross-flow velocity on the particle (de Balmann *et al.*, 1990).

However, the increased volume of solute permeating the membrane cannot explain all of the behaviour seen. The protein appears "more likely to deposit" as the permeate flow is increased. If protein deposition is linked to the rate of accumulation of protein inside the pores then deposition kinetics may be faster with higher fluxes (Fane *et al.*, 1983c; Matthiasson, 1984; Suki *et al.*, 1984). Also, Lundström (1980) found that the final amount of protein adsorbed onto a surface, increased with faster exposure of the surface to protein. Therefore, it seems reasonable that increasing the rate of exposure of the membrane surface to adsorbing proteins will increase the final amount of protein adsorbed and, will result in a lower final flux and higher retention.

It has also been suggested that increasing the permeate flow increases the shear forces within the pore, resulting in some deformation or denaturation of the protein (Bowen & Gan, 1991; Jonsson *et al.*, 1992). However, it must be noted that there is considerable debate as to whether shear forces can cause protein denaturation. Increased fouling may be due to the action of shear in the presence of the pore walls and prior adsorbed layers of protein or, to protein aggregation within the close confines of the pores as a result of increased protein collisions due to the higher permeate flow (Bowen & Hughes, 1990).

To summarise, in UF a protein layer or dynamic membrane forms on the membrane surface and dominates the subsequent behaviour of the membrane. The structure of the protein layer is affected by: the protein type and changes in pH or ionic strength that affect the apparent size of the protein; hydrodynamic conditions that increase concentration polarisation; the properties of the membrane. The mathematical model (Carmen Kozeny) generally used to calculate the resistance of the dynamic membrane is not appropriate for a protein layer.

In MF as the pore size increases, at least with silver particles, fouling moves from a surface layer phenomenon, through internal membrane fouling (pore plugging) to pore narrowing as would be expected from steric effects. However, with protein (BSA), as the membrane pore size is increased, the range of pore sizes where plugging occurs is extended beyond that found with less interactive molecules. Extensive pore plugging results in permeate fluxes sometimes lower than those observed in UF, and changes in the pore size distribution and pore density affect membrane retention. The reason for the increase in membrane fouling with protein solutions is not clear. There have been several hypotheses:

- the presence of aggregates in the feed (larger than the membrane pore size) causing increased pore plugging;
- interactions of the protein and the membrane material within the pore structure leading to a change in protein conformation and further deposition of protein;
- increasing permeate flow rates resulting in greater deposition of protein, due either to the increased exposure of the membrane to protein or, to the high shear rates in the membrane pores causing changes in protein conformation and hence, increased aggregation and interaction with the membrane.

3. Membrane theory

3.1. Concentration polarisation

In RO and UF, the permeate flux increases less than linearly with the transmembrane pressure, and is always smaller than the pure water flux. At high transmembrane pressure, the permeate flux is no longer significantly affected by increases in pressure; it levels off to almost constant values. This constant flux is called the "limiting flux" and increases with increasing cross-flow velocity. With constant mass transfer conditions, only the feed concentration is an important variable and a linear relationship between the logarithm of the feed concentration and the limiting flux is often obtained (Blatt *et al.*, 1970). This behaviour is generally considered to be due to the influence of concentration polarisation.

3.1.1. The film model

The model most often used to describe concentration polarisation is the film model, which is based upon the equation of continuity for solute. The model assumes that the concentration boundary layer resides within a thin laminar film at the membrane surface and that all mass transfer takes place by diffusion perpendicular to the membrane.

A steady-state mass balance gives:

$$JC_b - \frac{D.dC}{dx} - JC_p = 0 \qquad (3.1)$$

where **D** is the diffusivity of the retained solute. The first term represents the convective movement of solute towards the membrane due to the permeate flux and the second term represents the diffusion of solute back into the bulk solution. The third term describes the loss of solute to the permeate.

By integrating over the boundary layer thickness and substituting a mass transfer coefficient (**k**), as the boundary layer thickness is unknown, the following equation for the permeate flux can be derived:

$$J = k.\ln\frac{C_w - C_p}{C_b - C_p} \qquad (3.2)$$

where C_w, C_b and C_p are the solute concentrations at the membrane wall, in the bulk solution and in the permeate respectively.

The mass transfer coefficient is usually estimated by analogy from convective heat-transfer correlations. For turbulent flow conditions, the most popular correlations used are those based on the Chilton-Colburn and Deissler analogies (Gekas & Hallström, 1987). Deriving **k** from the Chilton-Colburn equation leads to the following equation:

$$k = 0.023.(\frac{\rho}{\mu})^{0.47}.D^{0.67}.\frac{u^{0.8}}{d^{0.2}} \qquad (3.3)$$

where ρ is the permeate density and **d** is the retentate channel diameter. Under turbulent conditions, the flow velocity (**u**) has the most influence on the mass transfer coefficient and offers the most potential for minimising polarisation. Increasing the diffusion coefficient (**D**) or reducing the viscosity (μ) by increasing the temperature will also increase the mass transfer coefficient.

The film model has been found to predict the performance of protein UF reasonably well. However, when applied to the MF of small particles, permeate fluxes are predicted to be as much as two orders of magnitude lower than experimentally observed. The predicted fluxes are too low because the value of the diffusion coefficient, which is inversely proportional to the particle radius, is quite low and understates the movement of particles away from the membrane. This discrepancy between the film model and experimental results is commonly known as the "flux paradox for colloidal suspensions" (Romero & Davis, 1988). Alternative models, such as shear-induced diffusion and lateral migration, have been proposed to describe the transport of particles away from the membrane. Romero & Davis (1988) consider this issue in more detail and review the various models that have been proposed to explain this behaviour.

3.1.2. Gel layer and osmotic pressure models

Various models have been proposed to explain why the build-up in solute concentration at the membrane wall affects membrane behaviour. The two most commonly used are the gel model and the osmotic pressure model.

In the gel model, gel formation on the membrane occurs when the concentration at the membrane wall reaches a limiting concentration (C_g) when further concentration cannot take place because of the impermeability of the polarised macromolecular layer to other macromolecules (Michaels, 1968; Blatt *et al.*, 1970). The gel layer acts as a hydraulic barrier in series with the membrane, reducing the permeate flux until the point is reached at which the reduced convective forward transport of the solute is balanced by diffusive back-transport of solute from the concentrated gel layer into the bulk solution. Any increase in transmembrane pressure would simply result in the build up of a thicker or denser cake of retained species with no influence on flux.

Experimental results where the permeate flux becomes independent of the transmembrane pressure lend support to the gel model. However, various researchers have questioned its validity as the gel concentration (as calculated by extrapolation of the flux/ln(concentration) graph to zero flux) has been found to vary with bulk concentration and cross-flow velocity, in contrast to the prediction of the gel model (Nakao *et al.*, 1979). Furthermore, solutions of the gel concentration display considerable fluidity and are below the solubility limit of the solute (Nakao *et al.*, 1979; Isaacson *et al.*, 1980; Jonsson, 1984).

The effect of the osmotic pressure can be described as follows. The presence of solute molecules in a solution lowers its chemical potential relative to that of the pure solvent. As a consequence, the chemical potential of the retentate is less than that of the permeate. At equilibrium, a positive osmotic pressure must be applied to the retentate in order to match its chemical potential to that of the permeate. A transmembrane pressure greater than the osmotic pressure is required for solvent to flow from the retentate to the permeate and the consequence of the osmotic pressure

difference across the membrane is a reduction in the effective transmembrane pressure driving force.

In an ideal dilute solution, the osmotic pressure ($\Delta\Pi$) is expressed by the van't Hoff equation:

$$\Delta\Pi = \frac{C.R_g.T}{M} \qquad (3.4)$$

where **C** is the component concentration, $\mathbf{R_g}$ is the gas constant and **M** is the molecular weight of the component. According to this equation, the smaller the component the greater is its contribution to the osmotic pressure of the liquid. Thus, in milk, the greatest contribution to the osmotic pressure comes from the lactose and minerals.

In skim milk or whey, the osmotic pressure is around 7 bar, a pressure that must be exceeded in RO before permeate will flow. For milk or whey concentrated by RO or evaporation to 25% total solids, the osmotic pressure is 27-35 bar (Glover, 1985; Cheryan, 1986). Thus, in RO, where the lactose and minerals are retained in the retentate, the osmotic pressure limits both the permeate flux and the maximum concentration achievable.

In UF, only the larger components (*i.e.* proteins) contribute to the osmotic pressure and, according to the van't Hoff equation, the osmotic pressure should be small. However, several authors have pointed out that the osmotic pressure of protein containing solutions increases exponentially rather than linearly with concentration. Thus, when protein is concentrated near the membrane surface, the osmotic pressures may be comparable with typical transmembrane pressures and have a significant impact on flux (Goldsmith, 1971; Vilker *et al.*, 1981; Jonsson, 1984). Jonsson (1984) and Wijmans *et al.* (1984) have also shown that the osmotic pressure model can produce trends similar to those of the gel model.

In summary, both the gel model and the osmotic pressure model are similar mathematically, and both essentially describe the reversible changes in effective

pressure or membrane resistance typically seen in UF. Vilker *et al.* (1984) compared bovine serum albumin (BSA) (67 kD) with bovine fibrinogen (340-400 kD), human low density lipoprotein (3000 kD) and polyethylene oxide (600 kD) by measuring both the permeate flux and osmotic pressures. Only with BSA was the osmotic pressure of a sufficient magnitude to reduce the effective applied pressure during UF. They concluded that the osmotic pressure model could be applied only to solutes with molecular weights less than 100 kD. Wijmans *et al.* (1984) also concluded that, in UF, gel layer limitation is more likely with high molecular weight solutes (>100 kD) whereas osmotic pressure limitation is expected with medium molecular weight solutes (10-100 kD).

3.2. Membrane fouling

3.2.1. Resistance model

When water is filtered through a membrane, the permeate flux (**J**) is proportional to the transmembrane pressure ΔP_{TM} as described by D'Arcy's law:

$$J = \frac{\Delta P_{TM}}{\mu_p . R_m} \qquad (3.5)$$

where R_m is the membrane hydraulic resistance and μ_p is the viscosity of the permeate.

The effect of fouling is generally considered as an addition to the membrane resistance of another resistance (R_f) resulting from the deposition of material both on the membrane surface and in the membrane pores. As discussed previously there has been considerable disagreement over how concentration polarisation reduces the permeate flux. If the view is that there is a resistance to flow through the boundary layer near the membrane then an additional resistance term is added to the bottom line of Equation (3.5). If the osmotic pressure model is accepted then the osmotic pressure is subtracted from the transmembrane pressure in Equation (3.5).

Equation (3.1) can be modified to account for membrane fouling and concentration polarisation (assuming the osmotic pressure model).

$$J = \frac{\Delta P_{TM} - \Delta \Pi}{\mu_p.(R_m + R_f)} \qquad \textbf{(3.6)}$$

$\mathbf{R_f}$ is often broken up into reversible fouling ($\mathbf{R_{rf}}$), that is the fouling removed by flushing with water, and irreversible fouling ($\mathbf{R_{if}}$), that which is only removed by chemical cleaning.

3.2.2. Protein deposition models

A number of researchers have proposed mathematical models that are based on a first order kinetic relationship. Bhattacharyya *et al.* (1979) suggest that the UF fouling mechanism can be compared to scaling problems in heat exchangers (heat flux versus water flux). Probstein *et al.* (1981) considered the kinetics of colloidal fouling of RO membranes. By assuming that the deposition rate is independent of the fouling film thickness and the removal rate is linearly dependent on the film thickness then a first order rate equation for film growth can be written. From trials with BSA and PM30 membranes Suki *et al.* (1984) suggested that the data could be expressed by a first order relationship if it was assumed that the rate of deposition was governed by a deposition potential. Aimar *et al.* (1986) suggested that the concentration of fouling material on the membrane and hence the membrane resistance could be represented by this type of equation.

The basic form of these equations is;

$$\frac{dR_f}{dt} = k_d.(R_f^* - R_f) \qquad \textbf{(3.7)}$$

where $\mathbf{R_f^*}$ is the plateau membrane resistance and $\mathbf{k_d}$ is the rate constant. So,

$$R_f = R_f^*.[1 - e^{-k_d.t}] \qquad \textbf{(3.8)}$$

3.2.3. Cake filtration model

This model is based on conventional filtration theory. It assumes the continual build up of a filter cake on the membrane surface and is usually used in dead-end or unstirred cell filtration. The fouling resistance is proportional to the volume of material processed (**V**):

$$R_f = \alpha_f . \frac{V . C_b}{A_m} \qquad \textbf{(3.9)}$$

where α_f is the specific cake resistance. Substituting this in Equation (3.6) and integrating gives the well known equation for constant pressure filtration.

$$\frac{t}{V} = \frac{R_m . \mu}{\Delta P_e . A_m} + \frac{\alpha_f . C_b . \mu}{2 . A_m^2 . \Delta P_e} . V \qquad \textbf{(3.10)}$$

If this equation applies then a plot of **t/V** versus **V** will be linear. It can also be expressed in terms of the permeate flux (Grace, 1956; Chudacek & Fane, 1984).

$$\frac{1}{J^2} = \frac{1}{J_o^2} + \frac{2 . C_b . \alpha_f . \mu}{\Delta P_e} . t \qquad \textbf{(3.11)}$$

A plot of $\mathbf{1/J^2}$ versus **t** should give a straight line.

The specific cake resistance (α_f) is often estimated from the Carmen-Kozeny equation for packed beds of rigid particles. On the basis that a globular protein can be approximated by a sphere, α_f is given by:

$$\alpha_f = \frac{180 . (1 - \epsilon)^2}{\rho_p . d_p^2 . \epsilon^3} \qquad \textbf{(3.12)}$$

where ϵ is the porosity or void fraction.

The effect of stirring or cross-flow on cake formation has been considered, originally by Kimura & Nakao (1975) and more recently by Chudacek & Fane (1984) and Aimar *et al.* (1988). Assuming that the removal of cake is constant and equal to the

convective solute transport at steady state ($J_{ss}.C_b$) then the fouling resistance can be calculated from;

$$R_f = \alpha_f.C_b.(\frac{V}{A_m} - J_{ss}.t) \qquad (3.13)$$

This resistance equation can then be substituted into Equation (3.6) and integrated as in Equation (3.10) (Aimar *et al.*, 1988). An experimental value of J_{ss} is required to solve the resulting equation.

3.2.4. Blocking laws

The equations that relate the permeate flux or transmembrane pressure to time or permeate volume (**V**) are listed for each of the standard (pore narrowing), intermediate and complete (pore plugging) blocking laws. For an explanation of the blocking mechanisms and derivation of the equations the reader is referred to Grace (1956), Hermia (1982) and Hlavacek & Bouchet (1993). For constant flux (or rate) filtration when the increase in fouling corresponds to an increase in transmembrane pressure, then the fouling resistance can be substituted for the transmembrane pressure in the following equations. For this substitution to be valid the permeate flux, feed concentration and temperature must remain constant.

Pore narrowing model (Standard blocking law)

Equations for constant pressure filtration:

$$\frac{1}{V} = \frac{1}{Q_o.t} + K_s \qquad (3.14)$$

where **V** is the permeate volume and **Q** is the filtration rate. The permeate flux is **Q** divided by the membrane area. K_s is a constant and is given by:

$$K_s = \frac{M_s}{N.\pi.L.r_o^2} \qquad (3.15)$$

where $\mathbf{M_s}$ is the mass of protein deposited per unit volume of permeate, **N** is the number of pores, **r** is the pore radius and **L** is the pore length.

Equation (3.14) predicts a linear relationship between **1/V** and **1/t** from which $\mathbf{K_s}$ can be obtained. **Q** can also be described in terms of time (Bowen & Gan, 1991):

$$Q = \frac{Q_o}{(1 + K_s.Q_o.t)^2} \tag{3.16}$$

Equations for constant rate filtration are:

$$\frac{\Delta P_o}{\Delta P} = (1 - K_s.V)^2 \tag{3.17}$$

$$\frac{\Delta P_o}{\Delta P} = (1 - K_s.Q_o.t)^2 \tag{3.18}$$

Pore plugging model (Complete blocking law)

Equations for constant pressure filtration:

$$K_p.V = Q_o.(1 - e^{-K_p.t}) \tag{3.19}$$

$$Q = Q_o.e^{-K_p.t} \tag{3.20}$$

Equations for constant rate filtration:

$$\frac{\Delta P_o}{\Delta P} = 1 - \frac{K_p.V}{Q_o} \tag{3.21}$$

$$\frac{\Delta P_o}{\Delta P} = 1 - K_p.t \tag{3.22}$$

where $\mathbf{K_p}$ is given by:

$$K_p = \frac{M_p.\pi.r^4.\Delta P}{8.\mu.L} \qquad (3.23)$$

where $\mathbf{M_p}$ is the proportion of the feed material that actually plugs the pores. In other words, $\mathbf{M_p}$ can be considered as a measure of "plugging tendency" for the feed material.

Intermediate blocking law

Equations for constant pressure filtration:

$$K_i.V = \ln (1 + K_i.Q_o.t) \qquad (3.24)$$

$$K_i.t = \frac{1}{Q} - \frac{1}{Q_o} \qquad (3.25)$$

Equations for constant rate filtration:

$$\ln [\frac{\Delta P}{\Delta P_o}] = K_i.V \qquad (3.26)$$

$$\ln [\frac{\Delta P}{\Delta P_o}] = K_i.Q_o.t \qquad (3.27)$$

$\mathbf{K_i}$ is:

$$K_i = \frac{A_i}{A_o} \qquad (3.28)$$

where $\mathbf{A_i}$ is the area of the membrane blocked per unit volume of permeate. $\mathbf{A_o}$ is the original area of the membrane (Hermia, 1982).

3.3. Retention calculations

The difference between the observed retention coefficient (σ) and the true or intrinsic retention coefficient (σ_i) is as follows. The observed retention coefficient is defined as:

$$\sigma = 1 - \frac{C_p}{C_r} \tag{3.29}$$

where C_p and C_r are the component concentration in the permeate and retentate respectively. The true or intrinsic retention coefficient takes account of the increase in the component concentration at the membrane wall and more truly reflects the actual behaviour of the membrane separation. It is defined as;

$$\sigma_i = 1 - \frac{C_p}{C_w} \tag{3.30}$$

where C_w is the component concentration at the membrane wall. C_w cannot be measured directly and must be estimated from concentration polarisation theory.

Using the film model (Equation 3.2) it is possible to derive the following expression for the wall concentration:

$$C_w = \frac{C_b . e^{\frac{J}{k}}}{\sigma_i + (1 - \sigma_i) . e^{\frac{J}{k}}} \tag{3.31}$$

This reduces to the following equation when $\sigma_i = 1$:

$$C_w = C_b . e^{\frac{J}{k}} \tag{3.32}$$

It is also possible to derive the following equation for the observed retention coefficient in terms of the intrinsic retention coefficient (Capannelli *et al.*, 1983):

$$\sigma = \frac{1}{1 + e^{\frac{J}{k}}.(\frac{1}{\sigma_i} - 1)} \tag{3.33}$$

The retention coefficient can also be related to the membrane pore size. Ferry (1936) described the steric rejection of a non-interacting sphere by the following equation:

$$\sigma = [\lambda.(\lambda - 2)]^2 \tag{3.34}$$

where:

$$\lambda = \frac{d_{particle}}{d_{pore}} \tag{3.35}$$

Based on this equation it is possible to relate the apparent pore size of the membrane to the increase in resistance because of fouling and the initial membrane pore size (Zeman, 1983). This model assumes that the fouling material deposits evenly over all internal pore surfaces.

$$\frac{d_{pore}}{d_{pore_o}} = [\frac{R_m}{R_f + R_m}]^{0.25} \tag{3.36}$$

The observed component transmission through the membrane is defined as:

$$T_r = 100 \times \frac{C_p}{C_r} \tag{3.37}$$

The transmission is related to the retention coefficient:

$$\sigma = 1 - \frac{T_r}{100} \tag{3.38}$$

3.4. Miscellaneous calculations

The shear stress at the membrane surface was calculated from:

$$\tau = \frac{d_e}{4} \times \frac{\Delta P_L}{L} \tag{3.39}$$

where $\mathbf{d_e}$ is the equivalent diameter of the channel, $\mathbf{\Delta P_L}$ is the retentate side pressure drop and **L** is the distance between pressure readings. The $\mathbf{\Delta P_L}$ quoted in this paper and used in the shear equation was that measured during the first few minutes of filtration as this is considered as the most critical time for membrane fouling.

The following equation was used to account for variations in the permeate viscosity (**Pa.s**) due to temperature. The equation is based on a regression of the viscosity of water in the range 10 to 60°C. The viscosity of permeate is slightly higher than that of water and does vary slightly with protein content. For the experimental conditions used these differences were considered negligible and for the purposes of calculating the membrane resistance the viscosity was assumed to be the same as that of water.

$$\mu = \frac{2.428 - 0.4788.\ln(T)}{1000} \qquad \textbf{(3.40)}$$

The units of temperature (**T**) are °C.

4. Design and development of a cross-flow/constant-flux membrane rig

4.1. System design

MF fouling has been found to be dependent upon the permeate flux or transmembrane pressure (see Section 2). To investigate this area a membrane rig capable of operation at constant flux rather than the traditional constant pressure was required. To be comparable with larger membrane units, the rig must also operate in cross-flow mode. Unfortunately, operation with cross-flow results in a pressure drop along the length of the module (ΔP_L) and hence, different sections of the membrane (in the same plant) are exposed to differing transmembrane pressures. This situation is best avoided. One option was to design a plant similar to that described by Daufin *et al.* (1993). In this design permeate is recirculated in order to maintain an even transmembrane pressure along the membrane (Sandblom, 1978). However, there are several difficulties with this system which detract from its obvious advantages. Firstly, there is a considerable hold up volume on the permeate side of the membrane resulting in a "buffering" of the permeate solute concentration. When the membrane fouls and the permeate concentration is changing quickly it is impossible to accurately calculate the membrane retention. Secondly, calculation of the transmembrane pressure is difficult as four pressure readings are necessary (inlets and outlets of the retentate and permeate sides) and it is not possible to obtain pressure readings from directly over the membrane surface. Thirdly, there is a problem with cost as essentially the equivalent of two traditional membrane systems are needed. Having therefore rejected the concept of permeate recirculation, it was decided to operate with a short membrane module in order to minimise the pressure differences in the plant.

Operating with very low transmembrane pressures (<10 kPa) is common in MF. Pressures this low could not be achieved in a typical recirculation loop because of pressure losses within the loop. The lowest achievable pressure drop would also be a function of the cross-flow velocity. It was therefore decided to control the transmembrane pressure by changing the permeate side pressure for both constant pressure and constant flux operation. This was achieved with a small pneumatic

control valve on the permeate line. Control of the permeate flow and hence, the permeate side pressure, allowed a partial separation of the effect of the cross-flow velocity and the transmembrane pressure. The effect of changes in the recirculation loop (pressure losses) brought about by changes in the cross-flow velocity were eliminated; however, changing the cross-flow velocity also changed $\mathbf{\Delta P_L}$, changing the range of the transmembrane pressure within the module. This could not be avoided without permeate recirculation.

4.2. Control of important variables

Another requirement of the rig was accurate control of the four major operating parameters; cross-flow velocity (**u**), transmembrane pressure ($\mathbf{\Delta P_{TM}}$), permeate flux (**J**) and temperature (**T**).

4.2.1. Cross-flow velocity

Retentate was pumped through the membrane module using a Johnson OL1 positive displacement lobe pump (Fig. 4.1). The recirculation rate, and hence cross-flow velocity, was controlled by varying the speed of the pump with a frequency controller (PDL Microdrive 3). A computer based control algorithm (PI) was used to supply an external set point to the frequency controller. A variable pot was also installed on the control panel where an additional external set point could be fixed manually. The frequency controller was set to accept the highest frequency (computer or manual). This allowed a minimum pump speed to be set to prevent the pump running backwards if the computer controller became unstable. The retentate pressure (baseline pressure) in the plant was controlled with a manual valve (**V05**).

4.2.2. Constant transmembrane pressure

When a constant transmembrane pressure was required in the plant, the permeate valve (**V04**) was controlled by a PID controller.

Figure 4.1 Flow diagram of the membrane rig.

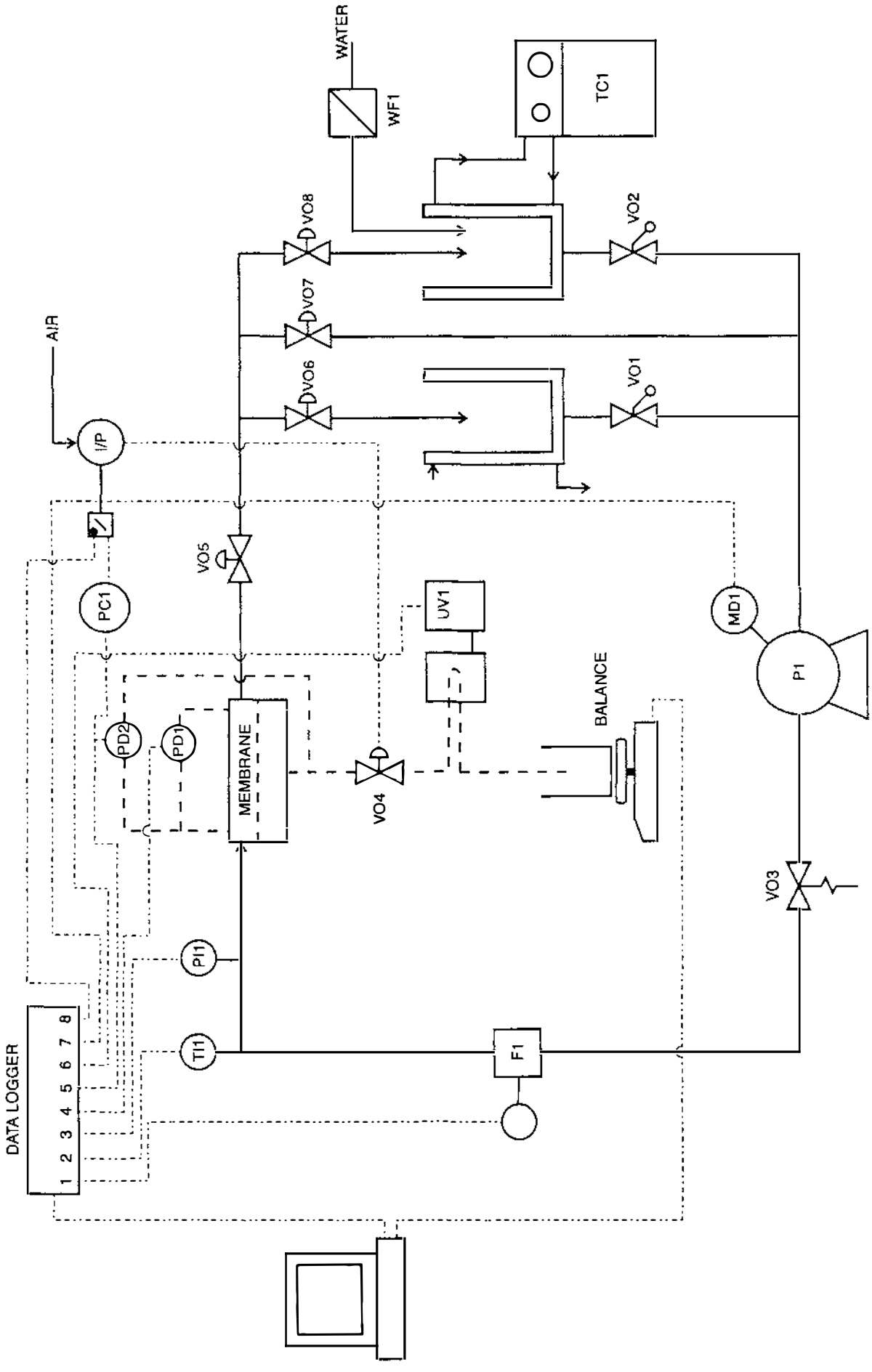

Opening the valve increased the permeate flow and decreased the pressure on the permeate side of the membrane and, as the pressure on the retentate side of the membrane remained constant, increased ΔP_{TM}. A differential pressure transmitter was used to measure ΔP_{TM} and provided feedback for the controller. In the course of a typical run, the controller was required to close the valve as the permeate flow decreased in order to maintain the same pressure on the permeate side of the membrane. This system effectively decoupled the transmembrane pressure from the retentate side pressure removing the disturbances caused by changes in the cross-flow velocity *etc.*

4.2.3. Constant flux

The permeate flow was monitored using an electronic balance. With constant flux operation a PID controller (computer algorithm) compared the measured mass flow (calculated from the average difference in weight recorded over 10 consecutive 2 second intervals - effectively a 20 second filter) to the required set point. In a typical run the controller was required to open the permeate valve as the transmembrane pressure increased with fouling. The balance was very sensitive to external disturbances (*e.g.* bumping or air currents) as the measured differences in weight were small. As a consequence the balance had to be protected by a stainless steel cover.

Constant flux control was difficult with a standard PI algorithm (differential action not used) because the combination of control valve and membrane were non-linear. The permeate valve, in isolation, was reasonably linear. However, when coupled with the membrane (see Fig. 4.2) non-linearity was introduced because, in addition to changes in permeate flow, the pressure drop over the valve also changed. For example, with constant flux operation, an increase in fouling caused an increase in $\Delta P_{membrane}$ and hence, a drop in ΔP_{valve}. The practical consequence of this was that the valve gain decreased as the valve opened, requiring a greater movement in the valve to achieve the same change in the flow. A control algorithm that incorporated gain scheduling was used to ensure that regardless of valve position the permeate flow controller was able to effect a similar change in flow against time.

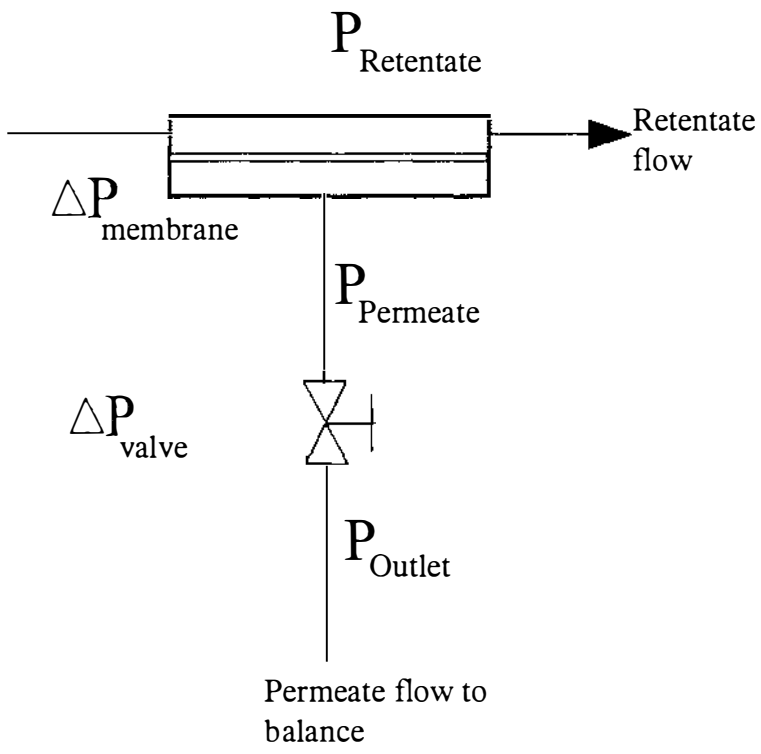

Figure 4.2. Pressure drops over the membrane and permeate control valve.

The modification to the permeate controller algorithm worked well for UF. However, the relationship between the permeate flux, membrane resistance (or transmembrane pressure), valve position and valve gain is a complex one. What was appropriate for low fluxes and UF membranes did not work for the combination of high flux and a low resistance MF membrane. With an MF membrane the pressure drop over the membrane is very small; the majority of the pressure drop is over the permeate valve. Hence, the permeate valve acted as if the membrane did not exist and was reasonably linear. In this case, the gain scheduling caused controller instability when the permeate valve was near fully open. Furthermore, with an MF membrane very small changes in the transmembrane pressure resulted in very large changes in the permeate flux, again contributing to control instability. The problem could not be solved simply by removing the gain scheduling for MF membranes during operation on water, because, as the MF membrane fouled its resistance became typical to that

of a UF membrane; conditions that required gain scheduling! The practical solution implemented was to manually reduce the controller gain and integral action when the MF membrane was operating on water. On the introduction of product the gain and integral action were then increased to ensure the controller was sufficiently reactive to maintain good control. This situation was not ideal and further work is required to optimise this control algorithm.

4.2.4. Temperature

The rig did not have automated temperature control (to be installed in late 1994) during the period of research reported in this thesis. On product, a small amount of heat generated by the pump had to be removed to prevent the temperature of the plant from rising.

Various schemes were tried in order to maintain a constant plant temperature. Cold or hot water was passed though the jacket of the balance tank. However, for removing such small amounts of heat from the system this proved very difficult to control. A much less efficient heat exchanger was required so that the cold water flows were controllable, and dribbling water over the pump housing was found to work reasonably well. This method was used in the trials on milk.

Another approach was to use a waterbath with external recirculation through the balance tank jacket. In this way the temperature of the cooling water could be maintained close to product temperature allowing more accurate control. If the water bath cooling unit was reasonably powerful this system worked well and was an improvement on the pump housing heat exchanger. However, the quantity of heat to be removed from the plant was very small and hence, small changes in ambient conditions upset the balance between heat generation in the plant and heat removed by the exchanger. As a consequence frequent adjustment of the waterbath temperature was required. This system was used in trials at Lund on ß-lactoglobulin. In New Zealand a refrigeration unit was used in place of the waterbath to maintain a product temperature of 25°C.

Designs are currently (June 1994) being considered for automating the temperature control. The most likely design is a waterbath equipped with powerful heating and cooling units controlled from an external set point (ex computer) using the plant temperature for feedback.

4.3. Measurement of variables

A further requirement of the system was the accurate monitoring and recording of all of the process variables. As previously indicated the recirculation flow was monitored using a magnetic flowmeter. This meter required a small conductivity in the process fluid in order to accurately measure the flow-rate. Unfortunately the conductivity of the demineralised water used in all of the trials was lower than the minimum requirements of the meter necessitating the addition of a small quantity of salt (sodium chloride) to all of the process water. Care was also needed when adding salt or cleaning chemicals directly to the balance tank, as the "spike" in the flow reading (the flow meter required a few seconds to adjust to the higher conductivity) upset the flow controller.

Temperature was monitored using a PT100 probe and the baseline pressure monitored using a pressure transmitter located in the recirculation loop prior to the membrane unit. ΔP_{TM} and ΔP_L were monitored with differential pressure transmitters (range 0-248 and 0-50 kPa respectively) connected directly to the membrane module with 3 mm stainless steel tubing. Pressure points were kept as close as possible to the actual inlet and outlet of the membrane to minimise the impact of entrance and exit effects on measurements. In some trials in New Zealand a UV cell placed in the permeate line after the control valve and before the balance was used to monitor the protein transmission through the membrane. All of the data was sent via a data logger to a computer. Data from the balance was sent directly to the computer via a RS232 line.

A computer programme written in Turbo Pascal (Engineering Services Section, New Zealand Dairy Research Institute, Palmerston North, New Zealand) was used to collect and process all of the data. The package also contained the necessary

controller algorithms used to operate the rig. Data from the plant was logged to file from which the data was able to be imputed to a spreadsheet for manipulation.

4.4. Membrane modules

In the trials on skim milk a flat channel module was used in which small pieces of polymer membrane could be mounted. Figs. 4.3 & 4.4 show the module which consisted of two parallel stainless steel plates bolted together with the piece of membrane sandwiched between them. The retentate channel (dimensions: 2 mm deep x 25 mm wide) was machined into the bottom plate (Fig. 4.3). The permeate collection chamber was machined into the top plate (dimensions: 25 mm wide x 125 mm long x 1.6 mm deep; with an exit port to enable the removal of permeate); the dimensions of which effectively determined the membrane area of 3125 mm^2. An O-ring which surrounded the active membrane area, sealed the gap between the two plates and a piece of polypropylene air filter (80 μm pore size) was placed in the permeate chamber to support the membrane. Beyond either end of the active filtering area the membrane was bent away from the retentate flow channel using stainless steel wedges. In this manner it was possible to have the retentate enter and leave the ends of the module without any change in flow direction; entry from the top would require a 90° turn upon entry and exit.

1 mm holes were drilled in the bottom plate directly over the beginning and end of the active membrane area (120 mm apart) to enable measurement of ΔP_{TM} and ΔP_L. The permeate side pressure was measured at the exit point from the module. The pressure transmitters were connected to the membrane module with Swagelock™ fittings and 3 mm stainless steel tube.

In the trials on ß-lactoglobulin a Membralox™ 1T1-70 module (S.C.T., Bazet, France) was modified to fit the existing pipework of the rig. The module containing a tubular ceramic membrane is shown in Fig. 4.5. Pressure taps were inserted in the end fittings of the module and connected with 3 mm tube to the pressure transducers. The end fittings were further modified so that the inlet and outlet tube for the retentate "butted" up to the end of the membrane element (about 1 mm clearance).

Figure 4.3. Photograph of dismantled flat channel membrane module.

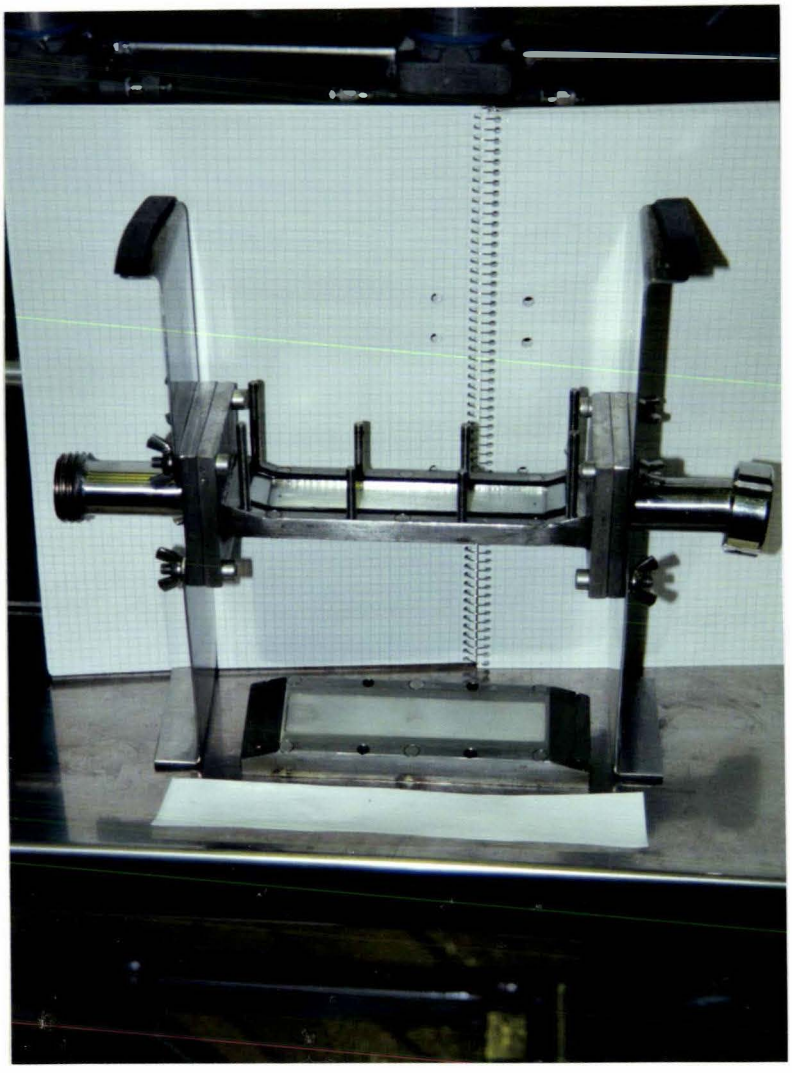

Figure 4.4. Photograph of flat channel membrane module.

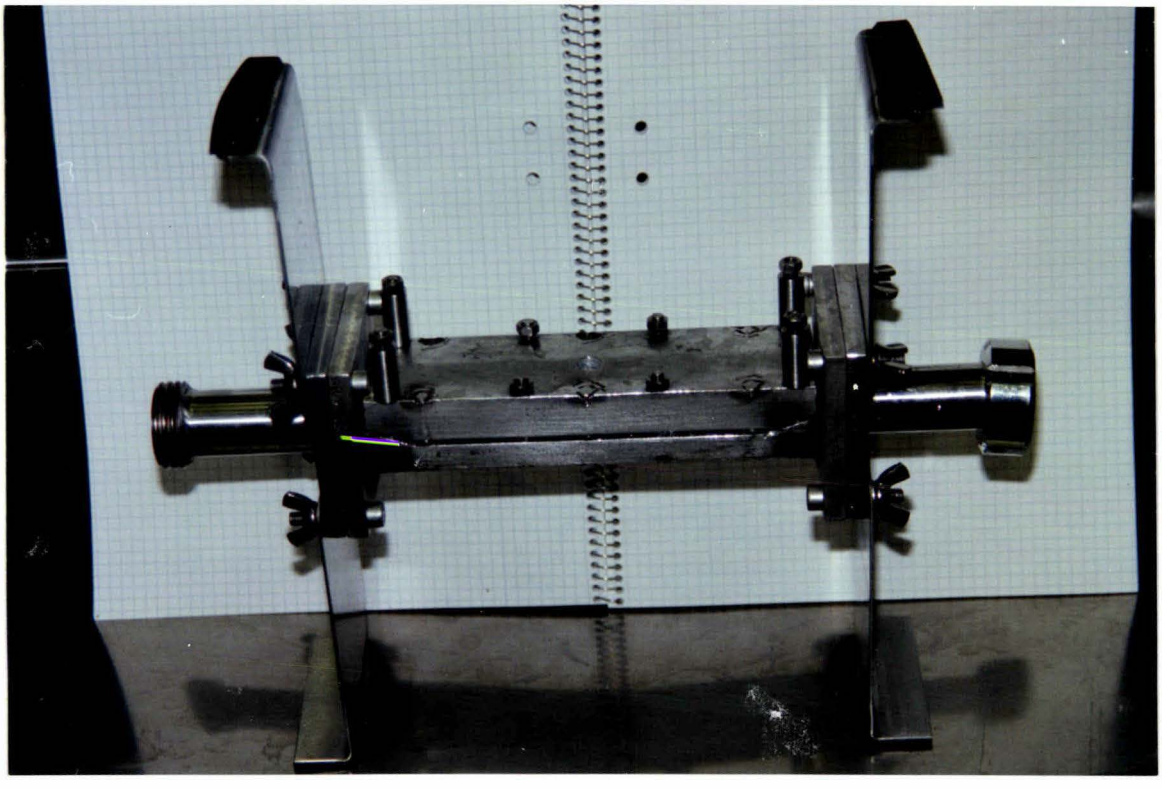

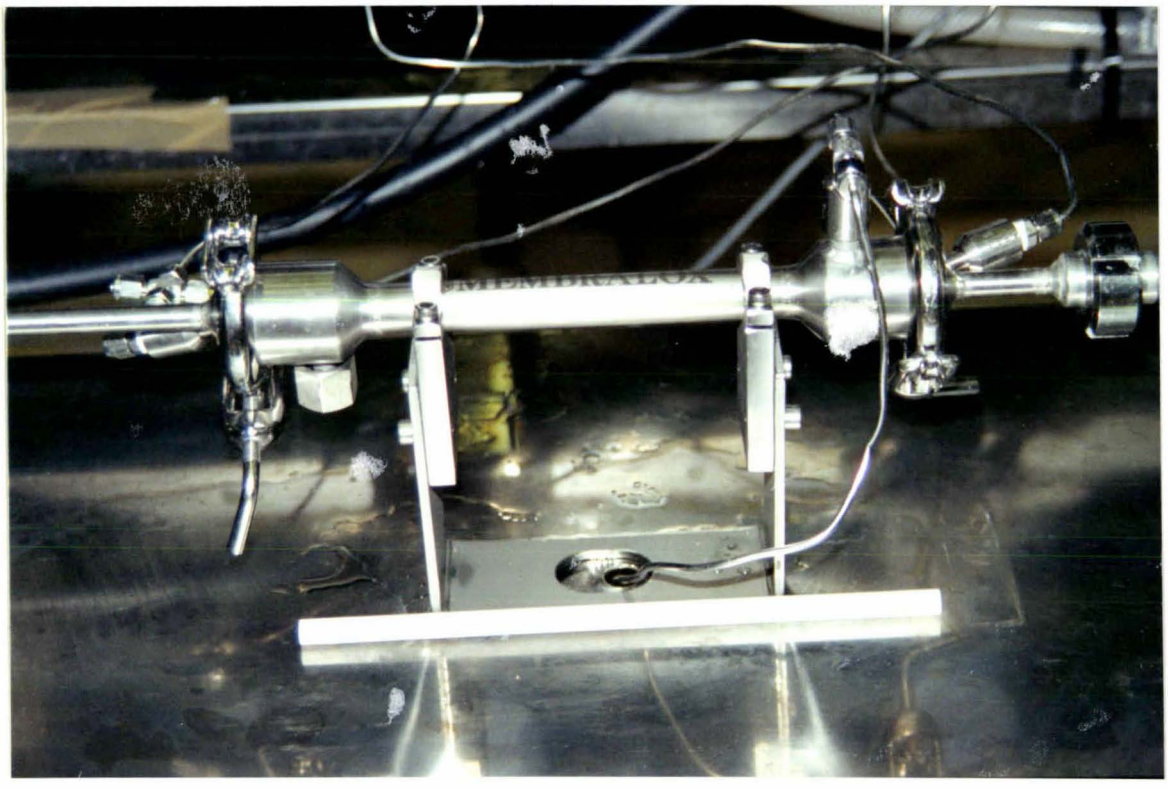

Figure 4.5. Photograph of ceramic membrane module.

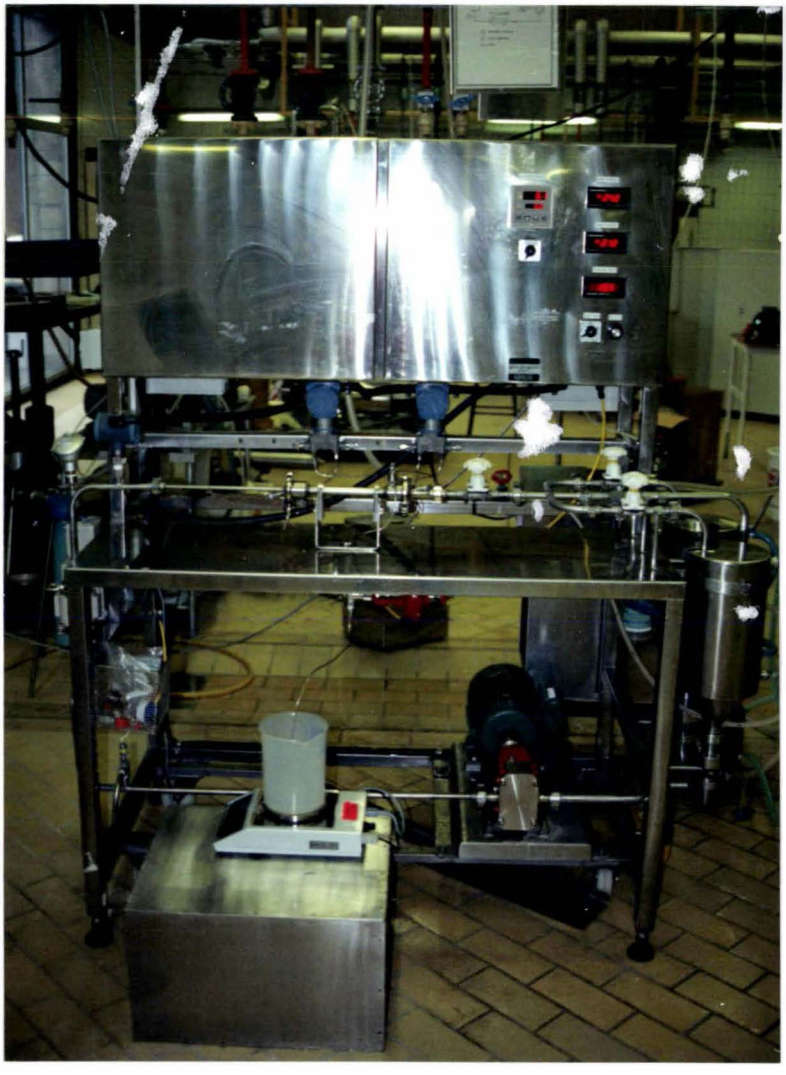

Figure 4.6. Photograph of the membrane rig.

In this way it was hoped to minimise pressure losses at the inlet and outlet to the modules and to have as even flow distribution through the membrane as possible. To further minimise entrance effects the inlet pipe consisted of a 300 mm length of 7 mm tube, the same diameter as the membrane, in contrast to the 15 mm tube used in the remainder of the recirculation loop.

The membranes used with this module were 250 mm long with an internal diameter of 7 mm (quoted by supplier). Measurement with callipers suggested that the internal diameter was 6.8 mm and this diameter was used to calculate the membrane area of 5341 mm^2. Membrane elements supplied by S.C.T. and manufactured from zirconium oxide were used in the trials.

4.5. Plant operation and performance

A photograph of the membrane rig with the ceramic membrane module installed is shown in Fig. 4.6. A full list of all of the components is in Appendix 1.

4.5.1. Start up

Manipulation of the on/off valves **V01** & **V02** and the control valves **V06** and **V08** enabled feed products to be switched without interrupting the flow of liquid over the membrane surface (*e.g.* water to milk). In all of the trials product was immediately recirculated to the feed tank in order to preserve product. This resulted in a 15-20% dilution of the feed material at start up. Although not used in these trials, the first product could have been flushed to drain to remove the water from the plant. A portion of the recirculation flow bypassed both tanks through valve **V07** to reduce flow to the balance tank to minimise foaming and air incorporation in the retentate stream.

ΔP_L was typically 3.5-4.5 kPa. If the average transmembrane pressure dropped below this value a negative transmembrane pressure resulted at the module outlet. With the polymer membrane module this caused the membrane to "ride out" into the retentate stream with the potential to rupture the membrane. Therefore the average

transmembrane pressure was always maintained above 5-6 kPa to ensure this did not occur. With a clean membrane (R_m of 10-20 x 10^{10} /m) operating on water the minimum flux possible was in the range 8-12 g/min. When milk was introduced to the membrane the total membrane resistance increased almost instantaneously to a high level (200 x 10^{10} plus) thus enabling the flux to be reduced to that specified for the experiments (1.8-3.6 g/min) without the transmembrane pressure decreasing below 6 kPa. The time taken for the flux to reduce to the specified flux was typically about 30 seconds. Unfortunately higher fluxes than necessary were unavoidable for the first few seconds of the trial. With the ceramic membrane this was not a problem.

4.5.2. Performance of controllers

The flux was controlled to $\pm 1.1\%$ in the trials on ß-lactoglobulin (Table 4.1 - row 1). The flux tended to be slightly below the set point (see typical deviations from set-point) as the flux declined with fouling. Also, in trials with severe fouling, the 20 s filter on the signal from the balance effectively reduced the response time of the control loop. Control of the transmembrane pressure was excellent to 0.2% of 200 kPa. This control loop was "fast" as it took a signal directly from the differential pressure meter.

The retentate shear, a measure of the cross-flow velocity, was controlled to $\pm 0.8\%$; again good control. Three values are shown for the temperature control. The first is taken from trials on milk at 50°C with the pump housing heat exchanger. The second from trials on ß-lactoglobulin at 25°C at Lund (waterbath) and the third in trials on ß-lactoglobulin in New Zealand (refrigeration unit). In all three cases control to 2% of set point was achieved. The lower overall deviation observed in (2) and (3) reflects the improved control achieved with the waterbath and refrigeration unit.

Overall control of the important process parameters was excellent.

Table 4.1. Control of the permeate flux, transmembrane pressure, retentate recirculation rate, wall shear stress and temperature during trials on skim milk and ß-lactoglobulin.

Parameter	3 x SD	Maximum deviation below SP	Maximum deviation above SP	Typical percent Variation
Flux ($L/m^2.h$)	2.2	4	2	1.1
Transmembrane pressure (kPa)	0.47	1.5	1.3	0.2
Retentate shear (Pa)	0.24	0.3	0.38	0.8
Temperature (°C) (1)	0.9	0.7	0.7	1.8
(2)	0.4	0.5	0.4	1.6
(3)	0.5	0.6	0.3	2

4.6. Specific problems and solutions

4.6.1. Pump failure

Considerable problems were experienced with the pump "seizing". All process water was filtered (5 μm woven water filter) to prevent rust, scale *etc.* getting to the plant but, in spite of this precaution, the pump still seized every two months on average. Problems with seizing are not uncommon with rotary lobe pumps especially with dilute solutions. Even though the pump operated extremely well between failures this type of pump is not recommended for this type of application.

4.6.2. Creasing and rupture of polymer MF membranes

With MF membranes "folding" or "creasing" of the membrane (along the flow path) occurred especially at the low pressure end of the module. During installation the membrane could not be positioned "tightly" in position. Consequently, upon the application of pressure the membrane was forced against the permeate side support material and any excess membrane creased. A small amount of creasing did occur with UF membranes but the problem was far more severe with MF membranes. Two possible reasons for the susceptibility of the MF membranes are: firstly the MF membranes used were softer and thinner than the UF membranes; and secondly, the operating pressures were far lower in MF (< 10 kPa). In an extreme case, with low permeate flows, the negative flow at the module outlet resulted in the MF membrane separating from the support membrane and eventually "blowing out". The variations in pressure seen by the MF membrane (close to zero on water and up to 2 bar on product) may also have caused the membrane to "lift" and "settle" and hence contribute to membrane creasing.

Several changes in installation and start-up procedures were tried in an attempt to eliminate the creasing problem. During installation the membrane was stretched as tightly as possible over the permeate section of the membrane module prior to the two membrane sections being bolted together. At start-up the pump was started with a small pressure head (0.5-1 bar) to provide an initial positive pressure on the membrane and the permeate valve was fully open to ensure that the maximum ΔP_{TM} possible occurred across the membrane. Lower recirculation rates (250-300 L/h) were also used at start up to help reduce ΔP_L and hence, reduce the possibility of negative permeate flows at the module outlet. In addition to these measures, the permeate flow was controlled so that the transmembrane pressure never dropped below 5 kPa at the module outlet. These changes did reduce the problem with creasing but did not eliminate it.

Operation with a ceramic module capable of being backflushed eliminated the problem. Likewise a hollow fibre membrane would probably not have the problem. This type of module should be used if constant flux operation is considered with MF membranes.

4.6.3. Air in the permeate chamber

In early commissioning trials it was noted that the permeate flux and transmembrane pressure did not relate exactly to one another. For example, data from a trial on skim milk using constant flux operation is shown (Fig. 4.7). The permeate flux set point was varied through the trial and at one point a severe disturbance was introduced by changing the baseline pressure. Looking more closely at this point (11.25 on graph) the decrease in baseline pressure resulted in a momentary decrease in transmembrane pressure and permeate flux. The permeate flux was restored to the set point very quickly; however, the transmembrane pressure did not return to its level before the disturbance for about 5 minutes. Similarly when the permeate flow rate set point was increased (see step change at 11.35 h) the permeate flux increased almost immediately; however, the transmembrane pressure again required 5-8 minutes to increase to its expected level.

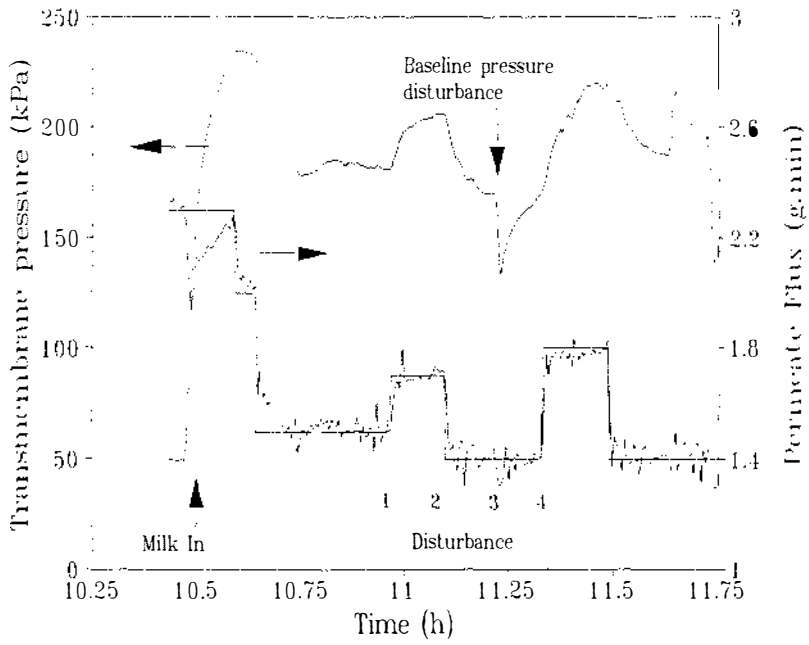

Figure 4.7. Flux and transmembrane pressure data from a commissioning trial (11/12/92) on a GR61PP membrane with skim milk. The straight line for permeate flux is the set point and the variable line is the measured permeate flux.

These results are inconsistent with the normal expectation of flux being proportional to transmembrane pressure (assuming a constant membrane resistance). It is hypothesised that the above effect was because of air in the permeate chamber. Air is compressible and hence, the air volume changed with changes in the permeate side pressure; also changing the liquid volume. The permeate flux measured by the balance is that which passes through the control valve, not through the membrane. Equation (3.5) was used to calculate the theoretical permeate flux through the membrane based on the observed transmembrane pressure. A value for the membrane resistance was chosen so that the calculated flux equalled the measured flux at steady-state points in the run.

A comparison of the theoretical flux and the flow measured by the balance was made, and the difference in permeate volume for each of the disturbances shown in Fig. 4.7 was estimated (Column 2; Table 4.2). The permeate chamber pressure was estimated from the difference in baseline pressure and ΔP_{TM} before the disturbance and after steady state has been reached (Columns 3&4). The difference in these two values corresponds to the change in pressure in the permeate chamber due to the disturbance.

The ideal gas law was assumed and from the percent change in pressure (Column 5) and the mass of water unaccounted for, the volume of air required to account for the difference between the actual and calculated permeate fluxes was estimated (Column 6). Averaging the values for the volume of air gives an air volume of 2.5 cc. This is equivalent to 40% of the volume of the permeate chamber (6.25 cc). This is reasonable given that the membrane module was assembled dry and the permeate initially drawn from the bottom of the chamber. Only a small percentage of the permeate chamber was required for the small flow of permeate and the likelihood of air bubbles remaining in the chamber was high.

Table 4.2. Calculation of the volume of air needed in the permeate chamber to account for the permeate flow discrepancy.

Disturbance	Weight g	Pinit kPa	Pfinal kPa	% difference	Volume of Air/cc
1	0.38	124	106	10	3.8
2	-0.33	107	154	-28	1.2
3	0.57	152	111	19	3.0
4	0.67	109	55	32	2.1

To avoid this problem the permeate chamber must be completely filled with water prior to the trial commencing. This is impossible if the permeate is drawn from the bottom of the module (the original set up for the module). Assembling the membrane module under water (with considerable difficulty) and placing the porous support material under vacuum to remove entrapped air improved the performance of the module but did not solve the problem. However, the problem was solved by running the membrane permeate-side-up, a configuration that was used in all of the trials following this diagnosis. No further problems were encountered with lag in the ΔP_{TM} response.

5. The influence of the permeate flux and cross-flow velocity on membrane fouling during the microfiltration of skim milk

5.1. Introduction

The MF of whole and skim milk has been reported in the literature. Piot *et al.* (1986) found that MF of whole milk with a 1.8 μm membrane could be used to separate the milk fat and skim milk. The transmembrane pressure had a significant effect on fouling with the highest overall permeate flux being achieved with the lowest transmembrane pressure. Malmberg & Holm (1987) reported that a 99.6% reduction in the bacterial count of skim milk could be achieved using a 1.4 μm membrane. In this application only the bacteria and a portion of the fat are retained by the membrane. Hansen (1988), Olesen & Jensen (1989), Trouvé *et al.* (1991) and Madec *et al.* (1992) have further investigated this process that utilises the "Bactocatch" plant (Alfa Laval Filtration Systems, Aarhus, Denmark), the design of which is based on the concept of Sandblom (1978). In this design the permeate is recirculated through the membrane module in the same direction as the retentate resulting in an even transmembrane pressure over the entire membrane module and the ability to operate with very low transmembrane pressures. In the studies on bacterial removal, operation with low transmembrane pressure was crucial to prevent severe fouling of the membrane.

Another process involving the MF of skim milk is the separation of the casein micelles from the whey proteins in order to produce native phosphocaseinate as investigated by Fauquant *et al.* (1988) with a Carbosep M14 membrane (0.14-0.2 μm) and Pierre *et al.* (1992) with a 0.2 μm aluminium oxide membrane (S.C.T.). In this case the casein micelles are retained by the membrane.

Several studies have shown that a layer of casein builds up on the membrane surface during RO, UF and MF of milk. Glover & Brooker (1974) showed during RO that a 30 μm layer was deposited on the membrane. They identified this layer as being predominantly casein, the density of which increased with proximity to the membrane. Bennasar *et al.* (1982) investigated the UF of raw whole milk.

Irrespective of the membrane pore size they found that the low permeate fluxes were because of the presence of a polarisation layer, composed mainly of casein micelles, that formed an efficient prefilter.

Attia *et al.* (1991a) with a 0.2 μm aluminium oxide membrane, showed that a dense layer of casein built up on the surface of the membrane within the first 10 min. There was no evidence of casein penetrating the membrane. Vetier *et al.* (1986), in static studies with a 0.2 μm aluminium oxide membrane, found that there was little or shallow fouling within the membrane due to casein micelles, but a considerable amount of surface deposit (20 μm). Fat globules were also present after processing whole milk. In dynamic studies the deposit on the membrane was less than 5 μm thick and was similar in nature to the static study (Vetier *et al.*, 1988). Vetier *et al.* (1988) found that the surface deposit contained all of the protein constituents of milk. This deposit was removed from the membrane by ultrasound in two stages. Deposit from the first stage (deposit that was farthest from the membrane) had a protein composition that was close to that of normal milk. On the other hand, the second removal stage (closest to the membrane) was richer in serum proteins and the overall serum protein content of the deposit increased with time, revealing progressive internal plugging of the micellar casein deposit (also see Lee & Merson (1976) and Baker *et al.* (1985)).

Regardless of the type of membrane used (RO, UF, MF) a surface layer of predominantly casein has been observed on the membrane surface and thereafter controls the filtration. The exceptions to this are when a very open membrane is used (1.4 μm plus) and the casein retention is close to zero or when the permeate flux or transmembrane pressure is carefully controlled and severe fouling is prevented.

The purpose of this study was to investigate the effect of the permeate flux and cross-flow velocity on fouling during the MF of skim milk on a 0.1 μm polysulphone membrane and to determine the mechanisms by which the surface layer formed on the membrane.

5.2. *Materials and methods*

5.2.1. Feed material and pretreatment

Skim Milk (Mini Mjölk, Skånemejerier, Malmö) was purchased from the local store the morning of each experiment. The milk age from the date of packaging varied from 1-4 days. The skim milk was heated in a jacketed tank to 50°C by passing 50-55°C water through the heating jacket for 20-30 min. The skim milk was held for at least a further 30 min at 50°C (60 min total from the beginning of heating) before filtration was commenced. At start up the skim milk was diluted by approximately 15-20% because of the water in the recirculation loop. This water was demineralised (2-3 $\mu S/cm^2$), but a small quantity of sodium chloride had been added to obtain a satisfactory flowmeter performance (typically 500 $\mu S/cm^2$).

5.2.2. Operating procedures

Two membranes were used in the trials: a GRM0.1PP 0.1μm polysulphone MF membrane; and a GR61PP polysulphone UF membrane. Both membranes were from Dow Danmark A/S (Nakskov, Denmark). After each trial the membrane was cleaned and reused, the cleaning regime successfully restoring the clean membrane resistance. However, if there was a break in the trials of more than one week the membrane was removed and replaced with a new piece of membrane as there was the possibility that the installed membrane had "dried out". The membrane was cleaned with alkali before each trial (1.4% v/v solution of P3 Ultrasil 25 (Henkel), 50°C, at least 30 min). At the completion of the cleaning cycle the plant was flushed with water for at least 7 min (60-70 L, 50°C). The plant continued to operate on water for a further 1 h at 50°C before the introduction of skim milk. Typically, there was a small increase in the membrane resistance with time.

At start up the permeate flux was set to the minimum value possible (8-12 g/min for the MF membrane; the permeate flux set for milk on the UF membrane) in order to maintain a positive pressure over the entire membrane area. When milk was introduced to the membrane by switching from the water balance tank to the tank

containing milk, the MF membrane resistance increased almost instantaneously to a level (200 x 10^{10} /m plus). This enabled the flux to be quickly reduced to that specified for the experiments (1.8-3.6 g/min). The time taken for the flux to reduce to the specified flux was typically about 30 seconds. Unfortunately higher fluxes than necessary were unavoidable for the first few seconds of the trials with the MF membrane.

In all trials milk was introduced in constant flux mode - the transmembrane pressure increasing with membrane fouling. If the transmembrane pressure increased above 200 kPa, operation was switched to constant pressure mode and the transmembrane pressure set to 200 kPa. In 2 experiments the permeate flux was reduced and constant permeate flux operation re-introduced after 2 h operation. The operating temperature in the plant was 50°C.

At the completion of the trial on milk the plant was flushed with 90-100 L of 50°C demineralised water (small amount added NaCl) for at least 10 min. The permeate flux was maintained at the same value as during milk processing. When the permeate controller was in constant pressure operation the flux was allowed to increase back to the initial flux set point on milk, and then operation was switched back to constant flux and this flux maintained until the end of flushing.

After flushing the MF membrane was cleaned in the same manner as prior to the trial commencing. For the UF membrane an additional acid cleaning step of 0.4% Ultrasil 75 (Henkel) for 20 min at 50°C was performed. For the MF membranes as the membrane resistance decreased with cleaning the permeate flux was increased to maintain the required minimum transmembrane pressure.

5.2.3. Protein analysis

In four trials the following samples were taken: raw feed; diluted feed taken after 5 min operation; feed samples after 2 and 4 h; and permeate samples after 1, 2, 3 and 4 h. The total nitrogen content of each sample was determined using a Tecator Kjeltec Auto 1030 Analyser. Duplicates of each sample were analysed.

5.2.4. Scanning electron microscopy

In two trials the membrane was carefully removed from the module after 4 h operation. The module was not flushed prior to membrane removal but was drained. Each membrane was cut into 4 sections (approximately 25 x 25 mm) and placed for 30 seconds in demineralised water (NaCl added, conductivity 500 μS) without stirring before being carefully removed. The pieces of membrane were then freeze dried for at least 48 h, placed in an excavator (vacuum chamber) for a further 48 h, before being cut and mounted. To obtain cross-sections of the membranes the membrane was fractured in liquid nitrogen. The skilled work of Helgot Olsson who prepared the samples for viewing is gratefully acknowledged.

The mounted membranes were coated with 20 nm of gold (spattering process) prior to viewing on a Philips SEM 515 scanning electron microscope at the Electron Microscopy Unit of the University Hospital in Lund (Dr Rolf Odselius; S-221 85 Lund, Sweden).

5.2.5. Experimental design

Preliminary experiments were performed with skim milk on an MFS1 "Bactocatch" pilot plant (Alfa Laval Filtration Systems, Aarhus, Denmark) with a 0.5 μm membrane to investigate the effect of the permeate flux on membrane fouling. These trials demonstrated that severe membrane fouling could be prevented if constant flux operation was used and the permeate flux was carefully controlled at about 35 L/m^2.h. If the permeate flux was increased to 45 L/m^2.h severe fouling occurred. The relationship between severe fouling and the permeate flux was investigated in more detail on the membrane rig described in Section 4.

A series of trials with the MF membrane were performed with varying permeate fluxes and cross-flow velocities (Table 5.1). Trials were also performed where the permeate flux was decreased after 2 h and where the cross-flow velocity was changed during the trial.

Table 5.1. MF trials on skim milk: permeate flux and recirculation rate information.

Run No	Run Time (min)	Flux[1] (g/min)	Flux[1] (L/m^2.h)	Flow rate (L/h)	ΔP_L (kPa)	Shear[3] (Pa)
Comparison of the permeate flux						
1	239	1.8	35	540	4.82	37
4	240	2.7	52	540	3.93	30
8	242	2.7	52	540	3.59	28
9	240	2.7	52	540	3.59	28
3	239	3.14	60	540	3.83	30
10	240	3.15	60	540	3.63	28
12	122	3.47	67	540	3.54	27.3
	118	1.8	35	540		
14	120	3.46	66	540	3.52	27.2
	120	1.8	35	540		
Comparison of cross-flow velocity						
5	185	2.49	48	360	1.85	14
15	240	2.7[2]	52	380	1.82	14
6	241	2.67	51	460	2.72	21
11	125	2.7	52	460	2.76	21
	60	2.7[2]	52	360	1.66	13
	57	[2]		540	3.34	26
16	301	2.7	52	470	2.77	21
4	240	2.7	52	540	3.93	30

Table 5.1 cont. MF trials on skim milk: permeate flux and recirculation rate information.

Run No	Run Time (min)	Flux[1] (g/min)	Flux[1] (L/m^2.h)	Flow rate (L/h)	ΔP_L (kPa)	Shear[3] (Pa)
Comparison of the cross-flow velocity continued						
9	240	2.7	52	540	3.59	28
2	243	2.7	52	540	4.96	38
7	240	2.7	52	650	4.95	38
Trial with immediate flushing after severe fouling						
13	20	3.44	66	540	3.54	27
Trials for analysis of protein transmission and scanning electron microscopy						
24	242	2.7	52	540	5.01	39
25	240	3.7	71	540	4.76	37
26	240	3.5	67	540	4.05	31
27	240	2.7	52	540	4.18	32

Notes on Table 5.1.

(1) Flux values are only for the constant flux period of each trial.
(2) Constant pressure operation occurred almost immediately.
(3) Wall shear stress calculated from ΔP_L from Equation (3.39).

The longitudinal pressure drop (ΔP_L) varied with the transmembrane pressure as the polymer membrane "flapped" up and down and changed the retentate channel height. Typically ΔP_L decreased with time as the membrane fouled and the transmembrane pressure increased. The ΔP_L also varied slightly with membrane history reflecting the previous transmembrane pressure that the membrane had been exposed to. On account of these problems, ΔP_L and the wall shear stress (calculated from ΔP_L; Equation (3.39)) was considered a better measure of the effect of the cross-flow velocity that the actual recirculation rate. The value of ΔP_L used in the shear stress calculation was that measured in the first few minutes of milk filtration as this was considered the most critical time for membrane fouling.

The trials on the MF membrane clearly demonstrated that with careful control of the permeate flux severe membrane fouling could be prevented. Four further trials were performed in which samples of feed and permeate were taken for protein analysis to investigate the effect of severe fouling on protein transmission (trials 24-27). At the completion of two of these trials, one with severe fouling and one with light fouling, the membranes were removed and viewed with a scanning electron microscope (trials 25, 27).

It was of interest to determine whether fouling could also be prevented in ultrafiltration. Seven trials were performed with a UF membrane (Table 5.2).

Table 5.2. UF trials (GR61PP) on skim milk: permeate flux and pressure information.

Run No	Run Time (min)	Time to 200 kPa (min)	Initial Flux[1] (g/min)	ΔP_L (kPa)	Flux at 15 min (g/min)	Flux at 240 min (g/min)	ΔP_{TM} (kPa)
17	240	-	-	3.31	1.7	1.2	200
18	241	10.5	1.43	3.35	1.36	1.02	200
19	240	-	-	3.51	0.34	0.29	20 & 50
20	180	-	-	8.79	0.149	0.18	20 & 35
21	240	-	-	3.36	1.08	0.88	200
22	239	4	1.3[2]	3.52	1.02	0.84	200
23	243	-	-	3.34	0.98	0.83	200

Notes on Table 5.2.

(1) All permeate fluxes are shown in g/min. They can be converted to L/m^2.h by multiplying by 19.2.

(2) The flux set point was 1.3 g/min, however, the actual flux was much lower as the controller could not maintain the set flux because of the extremely rapid increase in the transmembrane pressure.

In trials 17, 21 & 23 an initial transmembrane pressure of 200 kPa was set and the plant operated in constant pressure mode throughout. In trials 18 & 22 a permeate flux of 1.3-1.5 g/min (25-29 L/m^2.h) was set (lowest controllable constant flux) to compare constant pressure control with constant flux control. Even with low initial fluxes fouling was rapid; the transmembrane pressure increased to 200 kPa and constant pressure control was instigated after 4-10.5 min. It was difficult to investigate operation with lower fluxes as, using the balance for measurement of the flow, it was impossible to control the permeate flux below 20 L/m^2.h. Therefore, two trials (19&20) were performed with low transmembrane pressures. In both trials 20 kPa was initially tried, however, control was difficult at this level as the permeate flow was extremely small and consequently the transmembrane pressure was increased to 50 kPa after 10 min and 35 kPa after 8 min in trials 19 and 20 respectively. In trial 20 a permeate flux of 0.036 g/min (0.7 L/m^2.h) was recorded at 20 kPa. This flow was beneath the controllable range for the valve (valve almost closed) and was at the limit of that measurable by the balance.

5.3. Results

5.3.1. MF trials

5.3.1.1. The effect of the permeate flux

With an initial permeate flux of 67 L/m^2.h severe fouling occurred (Fig. 5.1); the transmembrane pressure increased to 200 kPa in about 8 min after which, the run proceeded under constant pressure operation. Reducing the permeate flux to 52 L/m^2.h prevented severe fouling although the membrane resistance still increased to around 500x10^{10} /m (cf. clean membrane resistance of 20x10^{10} /m and a severely fouled membrane of 2500-3000x10^{10} /m). Reducing the permeate flux further to 35 L/m^2.h did not result in a further reduction of the fouling. With a permeate flux of 60 L/m^2.h in one run, run (3), severe fouling occurred while in another, run (10), it was prevented (Fig. 5.2). Reproducibility between duplicates under other operating combinations was reasonably good, leading to the conclusion, that the hydrodynamic conditions in trials (3) and (10) were near a "break-point", above which severe fouling occurred.

In the trials when the initial flux was 66-67 L/m^2.h, after switching to constant pressure control, the permeate flux declined to below that achieved in trials where severe fouling was prevented (52 L/m^2.h) in less than 60 min (Fig. 5.3). Therefore, in a longer trial total throughput would be greater when severe fouling had been prevented.

Once severe fouling had occurred, reducing the flux to 35 L/m^2.h resulted in a reduction in the fouling resistance (Fig. 5.4), initially rapidly, to about one half that with a constant transmembrane pressure of 200 kPa. The resistance did not drop to the resistance obtained when a flux of 35 L/m^2.h was set throughout the run (run 1), indicating that severe fouling was only partially reversible.

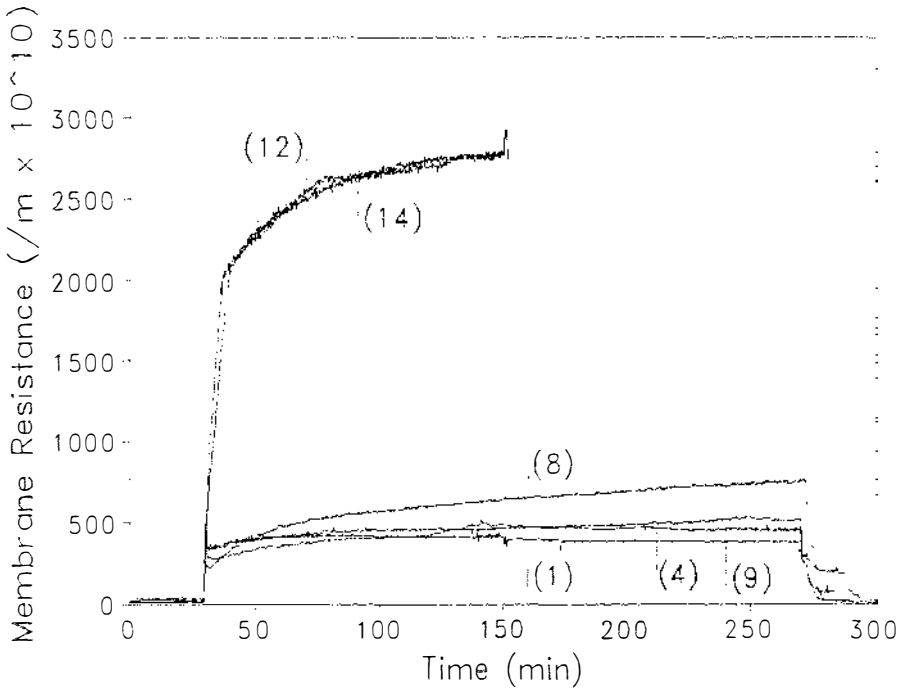

Figure 5.1. The effect of the permeate flux on membrane fouling during the MF of skim milk at 50°C. The numbers on the graph correspond to run numbers: (1) 35 L/m^2.h; (4, 8, 9) 52 L/m^2.h; (12, 14) 67 L/m^2.h.

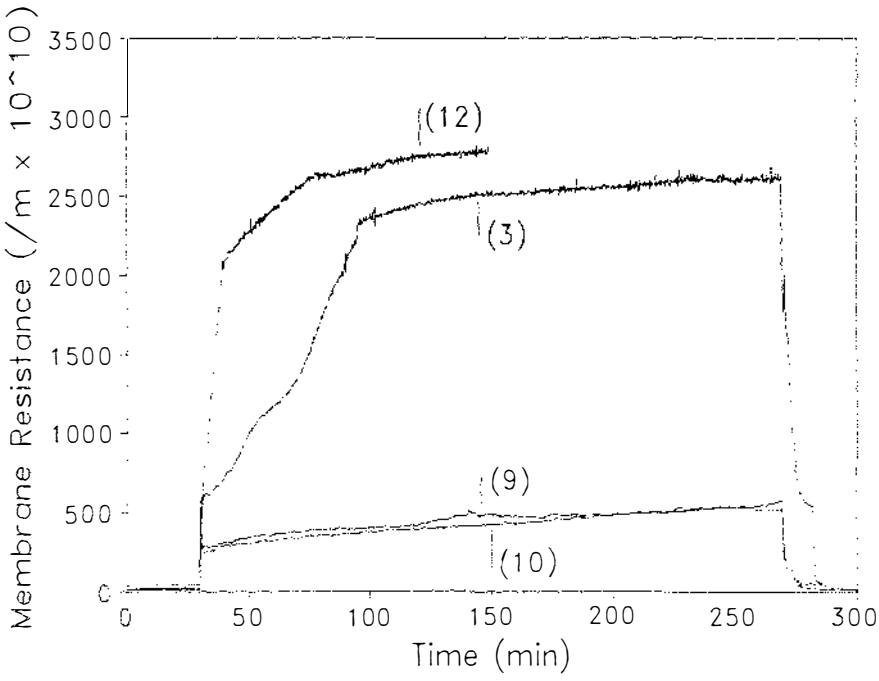

Fig. 5.2. The effect of the permeate flux on membrane fouling during the MF of skim milk at 50°C. The numbers on the graph correspond to run numbers: (9) 52 L/m².h; (3, 10) 60 L/m².h; (12) 67 L/m².h.

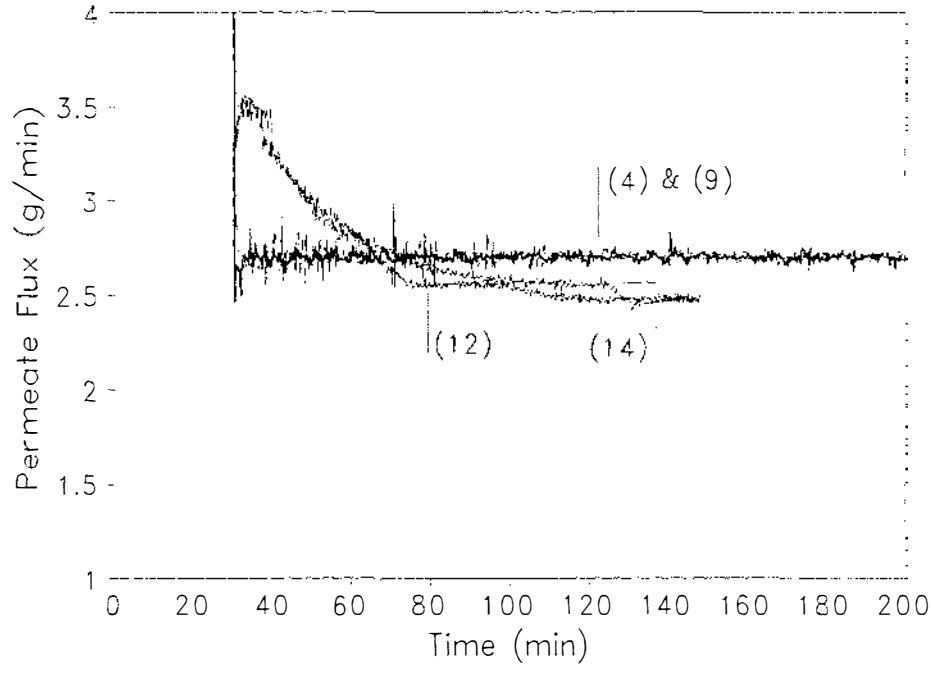

Figure 5.3. The effect of the initial permeate flux on the long term plant throughput: (4, 9) initial permeate flux 52 L/m².h; (12, 14) 67 L/m².h.

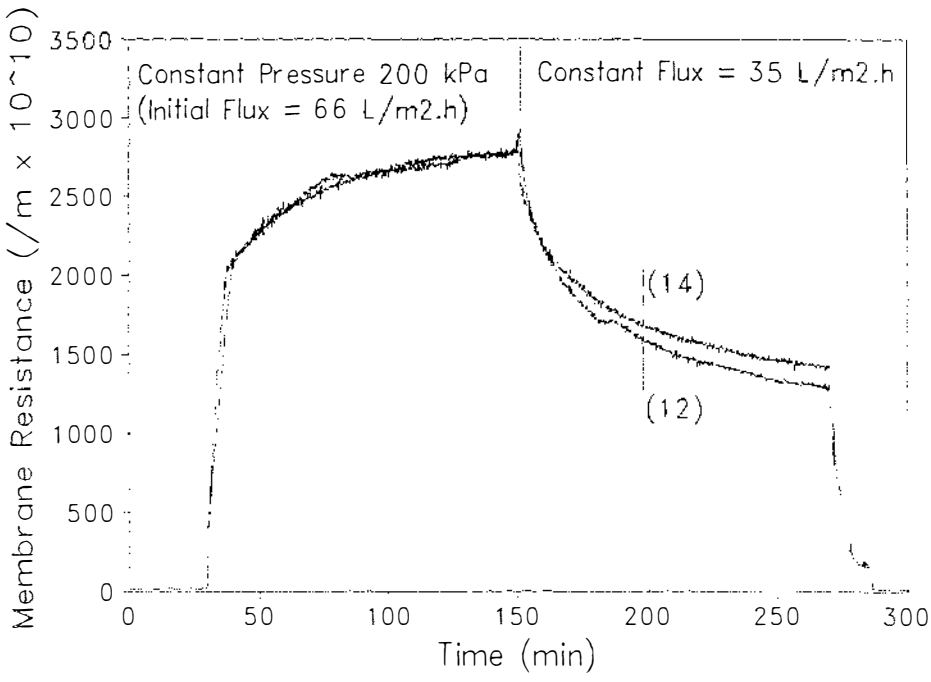

Figure 5.4. The effect of reducing the permeate flux after heavy fouling had occurred: runs (12) & (14). The initial permeate flux was 66-67 L/m^2.h; then constant pressure operation (200 kPa) from 10 min until 2 h operation on milk; then switch to constant flux operation at 35 L/m^2.h. The plant was then flushed with water.

5.3.1.2. The effect of the retentate recirculation rate

Reducing the recirculation flow from 540 L/h (standard conditions, wall shear 27-33 Pa) to 360-380 L/h and hence, reducing the wall shear stress, resulted in severe membrane fouling (Fig. 5.5). Increasing the wall shear stress to 38 Pa either by reducing the channel height (smaller O-ring) or increasing the recirculation rate (runs 2 & 7) did not reduce the fouling resistance below that obtained at a shear stress of 30 Pa. With a shear stress of 21 Pa the onset of fouling was different in each of the 3 trials performed (6, 11, 16), severe fouling being prevented in 1 trial, occurring immediately in the second and occurring after 3-4 h in the third (Fig. 5.6). Similarly to the results with a permeate flux of 60 L/m^2.h and a shear stress of 30 Pa, it appears that a flux of 52 L/m^2.h and a shear stress of 21 Pa is very near the "break point", above which severe fouling occurs.

Reducing the wall shear stress (recirculation rate) during a run resulted in an extremely rapid increase in the membrane resistance (Fig. 5.7). Subsequently, increasing the shear to above that originally resulted in a rapid, but relatively small reduction in the membrane resistance to a level well above that obtained prior to the onset of severe fouling.

In runs when severe fouling occurred, the fouling resistance was inversely related to the membrane shear stress (Fig. 5.8) suggesting that the "thickness" of the fouling layer reduced with increasing cross-flow velocity as has been found by others (*e.g.* Blatt *et al.*, 1970; Kessler, 1981).

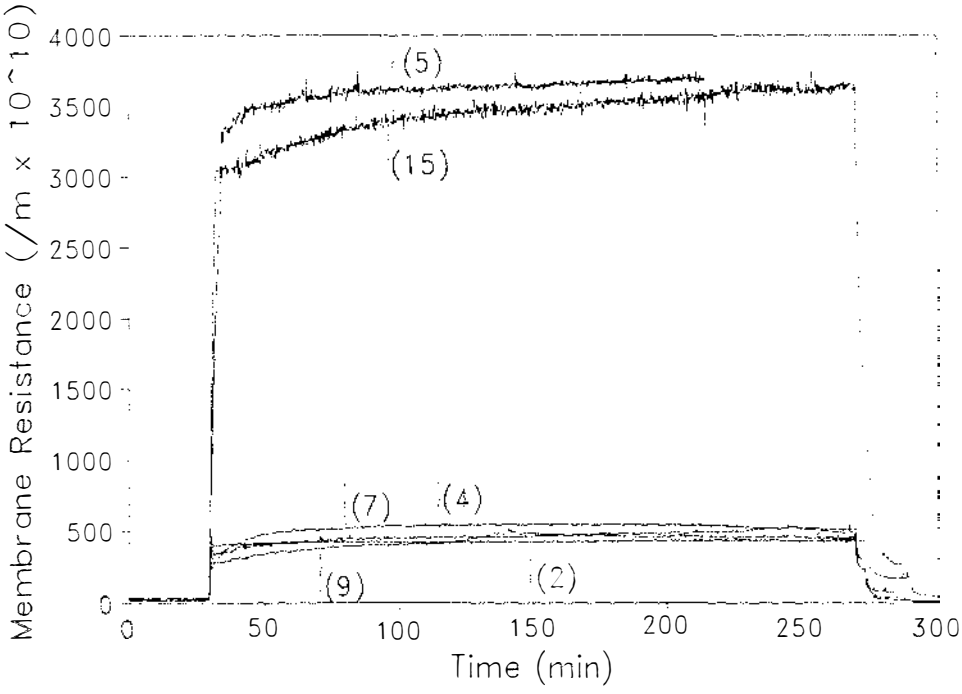

Figure 5.5. The effect of the recirculation rate on membrane fouling during the MF of skim milk at 50°C and with a permeate flux of 52 L/m^2.h. The wall shear stress was 14 Pa in runs (5, 15); 30 Pa (4); 28 Pa (9); 38 Pa (2, 7).

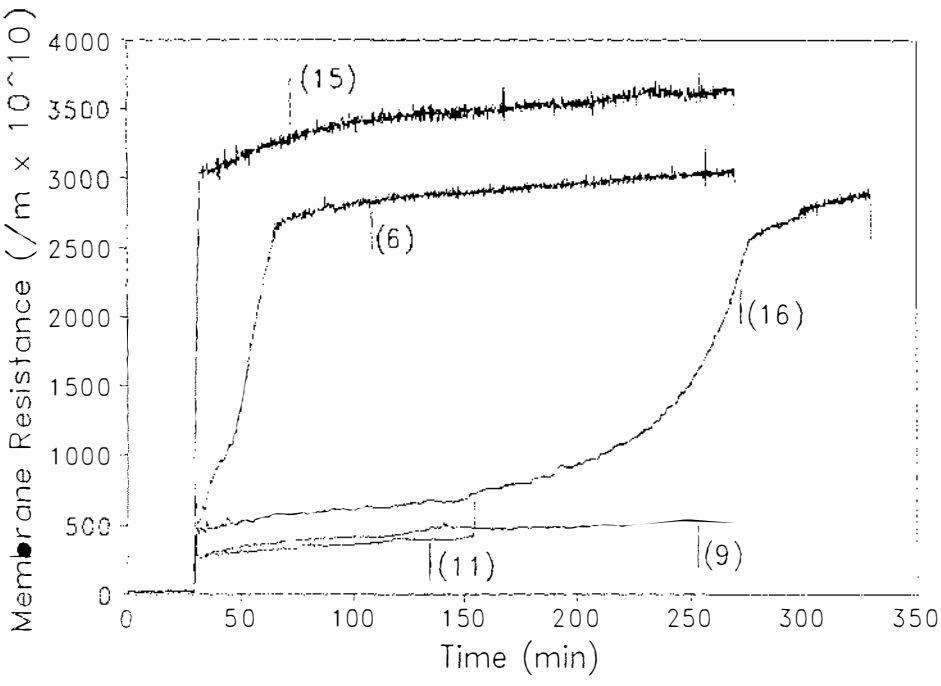

Figure 5.6. The effect of the recirculation rate on membrane fouling during the MF of skim milk at 50°C and with a permeate flux of 52 L/m².h. The wall shear stress was 14 Pa (15); 21 Pa (6, 11, 16); 28 Pa (9).

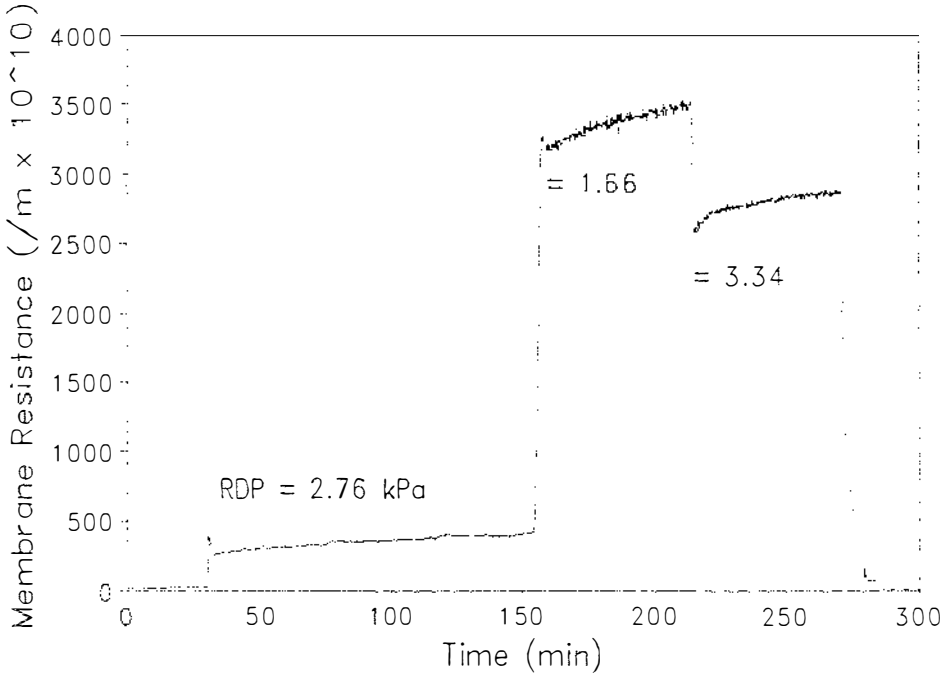

Figure 5.7. The effect of increasing and reducing the recirculation rate during the MF of skim milk at 50°C and an initial permeate flux of 52 L/m².h; run (11). Initial wall shear stress 21 Pa, then 13 Pa, then 26 Pa.

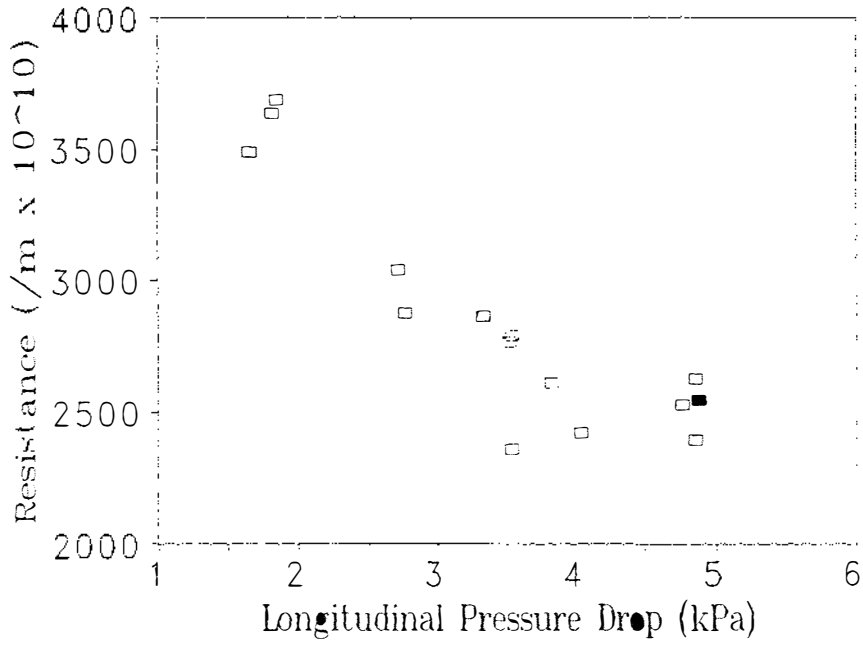

Figure 5.8. The effect of the recirculation rate on the final total resistance when heavy membrane fouling had occurred. Skim milk was microfiltered at 50°C on a GRM0.1PP membrane.

5.3.1.3. Flushing and cleaning of the membrane

The membrane resistances measured throughout each experiment are summarised in Table 5.3. For runs when severe fouling occurred the majority of the resistance due to fouling was reversible; *i.e.* removed during water flushing. The resistance dropped rapidly for the first 2-3 min after the introduction of water to the plant as the milk was displaced. During further flushing (7 min) the effluent from the plant was clear to the human eye although the membrane resistance continued to drop at a slower rate indicating that there was continued erosion of the fouling layer on the membrane. The resistance stabilised after 8-10 min total flushing. Cleaning completely restored the membrane resistance to the same or lower resistance to that initially.

There was a suggestion that irreversible fouling increased from the time severe fouling occurred (Fig. 5.9) perhaps due to increased consolidation of the fouling layer or to increased cross-linking within the fouling layer (Howell & Velicangil, 1980; Turker & Hubble, 1987). In trials when severe fouling was prevented, with the exception of runs 1&2, most of the fouling resistance was restored with water flushing (>90%). The reason for the discrepancy in trials 1 & 2 is not known.

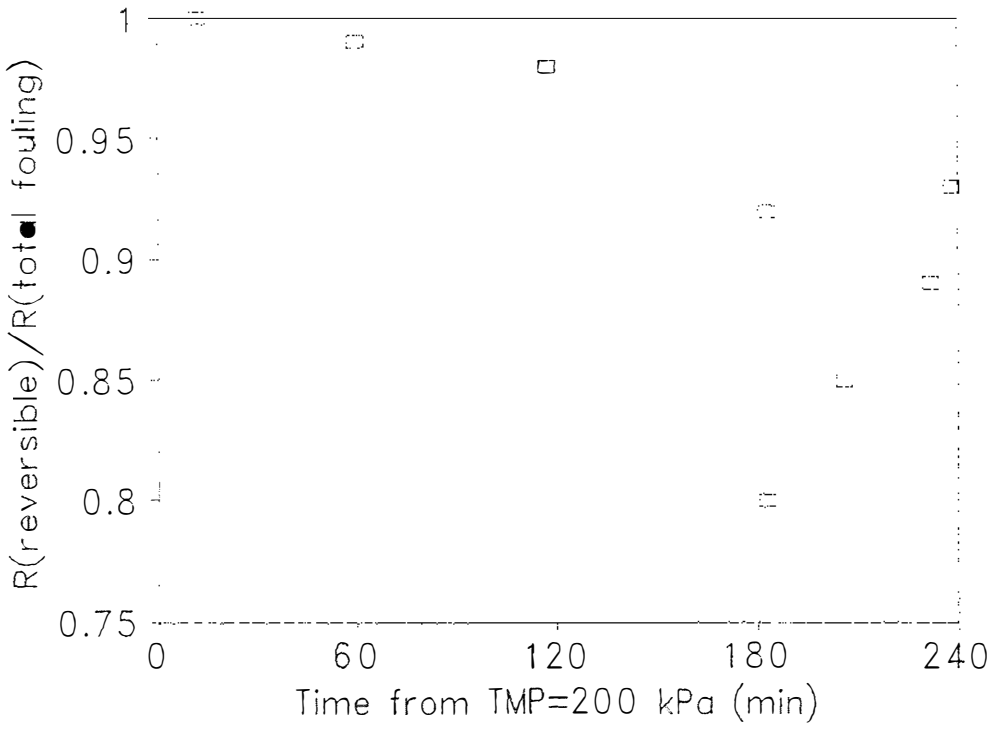

Figure 5.9. The effect of the fouling time (from time when ΔP_{TM} = 200 kPa) on the proportion of the fouling resistance (R_f) that is reversible (*i.e.* removed by flushing).

Table 5.3. MF trials on skim milk: summary of resistance data. All resistances are shown in units of /m x 10^{10}. *e.g.* $R_{membrane}$ for run 1 is 39 x 10^{10}/m.

Run No	Flux[1] L/m².h	Shear[2] (Pa)	$R_{membrane}$	$R_{fouling}$[3]	$R_{irreversible}$	$R_{reversible}$	$\%R_{if}$	$\%R_{rf}$
Comparison of the permeate flux								
1	35	37	39	341	148	193	43	57
4	52	30	31	422	40	383	9	91
8	52	28	14	737	8	729	1	99
9	52	28	8	505	10	494	2	98
3	60	30	40	2573	503	2070	20	80
10	60	28	20	533	25	507	5	95
12	67	27.3	16	2774	-	-	-	-
	35			1290	139	1151	11	89
14	66	27.2	14	2753	-	-	-	-
	35			1432	161	1257	11	89
Comparison of cross-flow velocity								
5	48	14	20	3666	288	3377	8	92
15	52	14	21	3610	245	3365	7	93
6	51	21	15	3026	449	2576	15	85
11	52	21	22	387	-	-	-	-
		13		3463	-	-	-	-
		26		2839	44	2795	2	98
16	52	21	13	2863	40	2823	1	99
4	52	30	31	422	40	383	9	91

Table 5.3 cont. MF trials on skim milk: summary of resistance data. All resistances are shown in units of /m x 10^{10}. *e.g.* $R_{membrane}$ for run 1 is 39 x 10^{10}/m.

Run No	Flux[(1)] L/m².h	Shear[(2)] (Pa)	$R_{membrane}$	$R_{fouling}$[(3)]	$R_{irreversible}$	$R_{reversible}$	$\%R_{if}$	$\%R_{rf}$
Comparison of the cross-flow velocity continued								
9	52	28	8	505	10	494	2	98
2	52	38	31	404	139	265	34	66
7	52	38	11	495	19	465	4	96
Trial with immediate flushing after severe fouling								
13	66	27	21	2332	7	2325	0	100
Trials for analysis of protein transmission and scanning electron microscopy								
24	52	39	25	286	-	-	-	-
25	71	37	14	2508	-	-	-	-
26	67	31	27	2391	-	-	-	-
27	52	32	17	215	-	-	-	-

Notes for Table 5.3.

(1) Flux values are only for the constant flux period of each trial.

(2) Wall shear stress is calculated from Equation (3.39).

(3) $R_{fouling}$ is measured at the end of the run just before water flushing.

5.3.1.4. Protein analysis

The protein concentrations of the 4 raw milk samples analysed were consistent in the range 3.50 to 3.59 (Fig. 5.10). The feed was diluted at start up by the water in the recirculation loop by a factor of 0.82-0.83 giving a "plant feed" protein content of 2.89 to 2.95%. The feed concentration increased through the run as permeate was removed and the retentate concentrated (Fig. 5.10). The protein content (TN x 6.38) of the permeate remained reasonably constant against time although the actual level differed depending upon whether severe fouling occurred or not (Fig. 5.11). With severe fouling a value of 0.22-0.3% was found compared to a value of 0.43-0.49% without severe fouling.

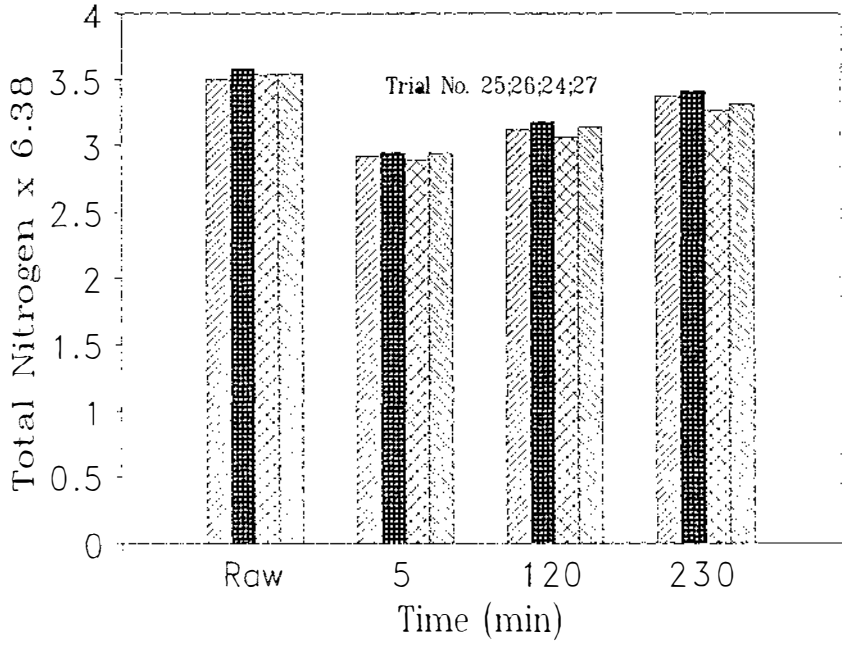

Figure 5.10. Feed protein concentration of skim milk during MF on a GRM0.1PP membrane. The raw sample was taken prior to milk entering the plant.

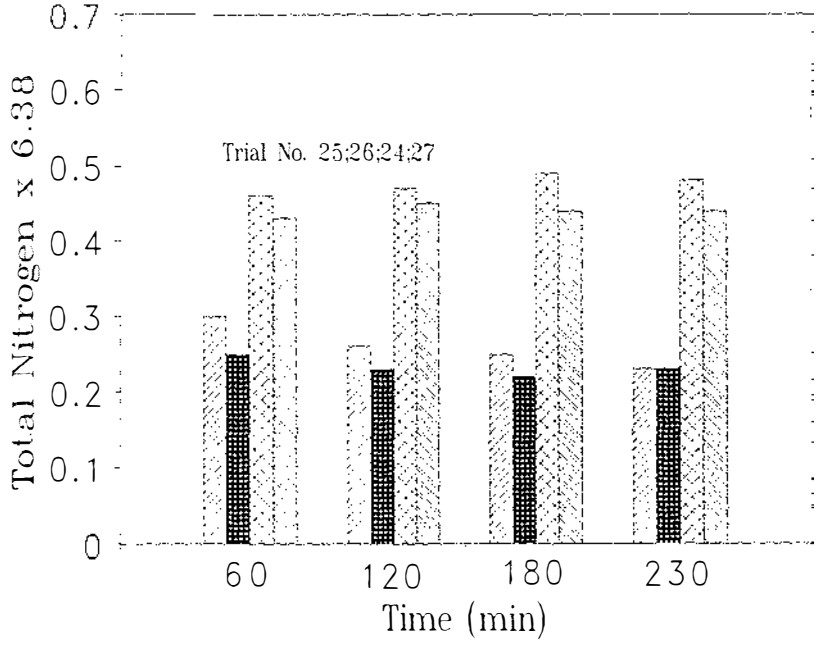

Figure 5.11. Protein concentration of the permeate during the MF of skim milk on a GRM0.1PP membrane. Severe fouling occurred in trials 25 & 26 and light fouling in trials 24 & 27.

If it is assumed that the NPN content of the raw milk is 0.21% (NPN x 6.38) and the casein makes up 83% of TN-NPN then it is possible to estimate the whey protein and casein content of the feed. The casein content of the diluted plant feed (82.5% of the raw milk concentration) was estimated to be about 2.3-2.4%. Then, assuming that the casein is totally retained by the membrane and that the NPN is totally permeable, it is possible to estimate the whey protein content of the permeate and hence, calculate an apparent whey protein retention coefficient. The whey protein retention coefficients are shown in Fig. 5.12. When severe fouling occurred (runs 25 & 26) the whey protein retention coefficients ranged from 0.83-0.9. In the absence of severe fouling the retention coefficients were from 0.39 to 0.50. It is clear that the presence of the heavy fouling layer significantly increased the retention of the whey proteins.

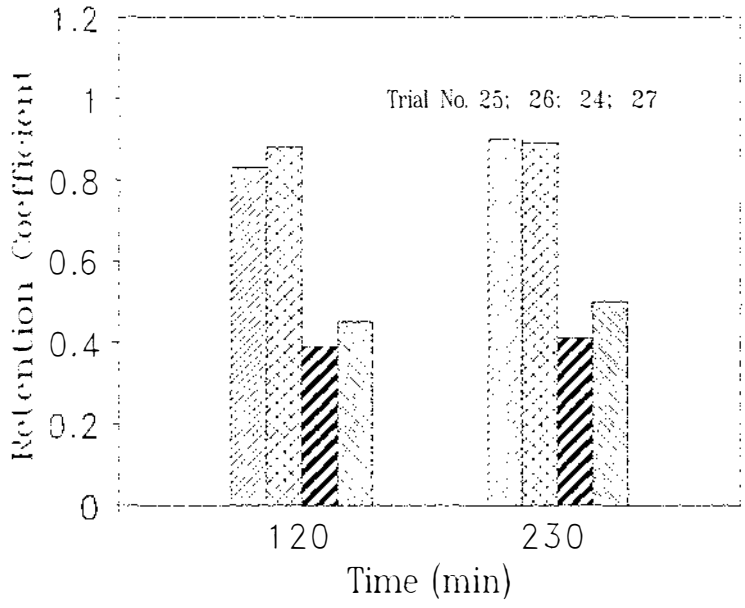

Figure 5.12. Estimated whey protein retention coefficients during the MF of skim milk on a GRM0.1PP membrane. Severe fouling occurred in trials 25 & 26 and light fouling in trials 24 & 27.

5.3.1.5. *Scanning electron microscopy*

An electron micrograph of a clean membrane is shown in Fig. 5.13. The membrane pores are distributed unevenly over the membrane surface and it is clear, at least from observing the pore entrances, that a considerable variation in the pore size exists over the membrane. Figs. 5.14 & 5.15 show a surface view of a severely fouled membrane (trial 25) and a lightly fouled membrane (trial 27) respectively. In both cases the majority of the membrane pores have been obscured by what appears to be a thin surface layer on the membrane surface. In many ways the two membranes (Figs. 5.14 & 5.15) appear similar in spite of the major difference in final fouling resistance. The layer on the heavy fouled membrane is perhaps thicker and there is some evidence of cracks in the layer, probably because of the drying of the fouling deposits in preparation for viewing.

Fig. 5.16 shows a low magnification view of a fractured membrane. The woven backing material was not broken and the fractured membrane was folded so that both fractured pieces could be viewed. A cross-section of a clean membrane gives an impression of the internal structure of the filtering layer (Fig. 5.17). The majority of the membrane is porous with many inter-connecting chambers. Fig. 5.18 shows a cross section of the severely fouled membrane. The majority of the pore structure remains free without apparent deposition and fouling is limited to a thin layer on or near the membrane surface. The thickness of the layer is less than 1 μm.

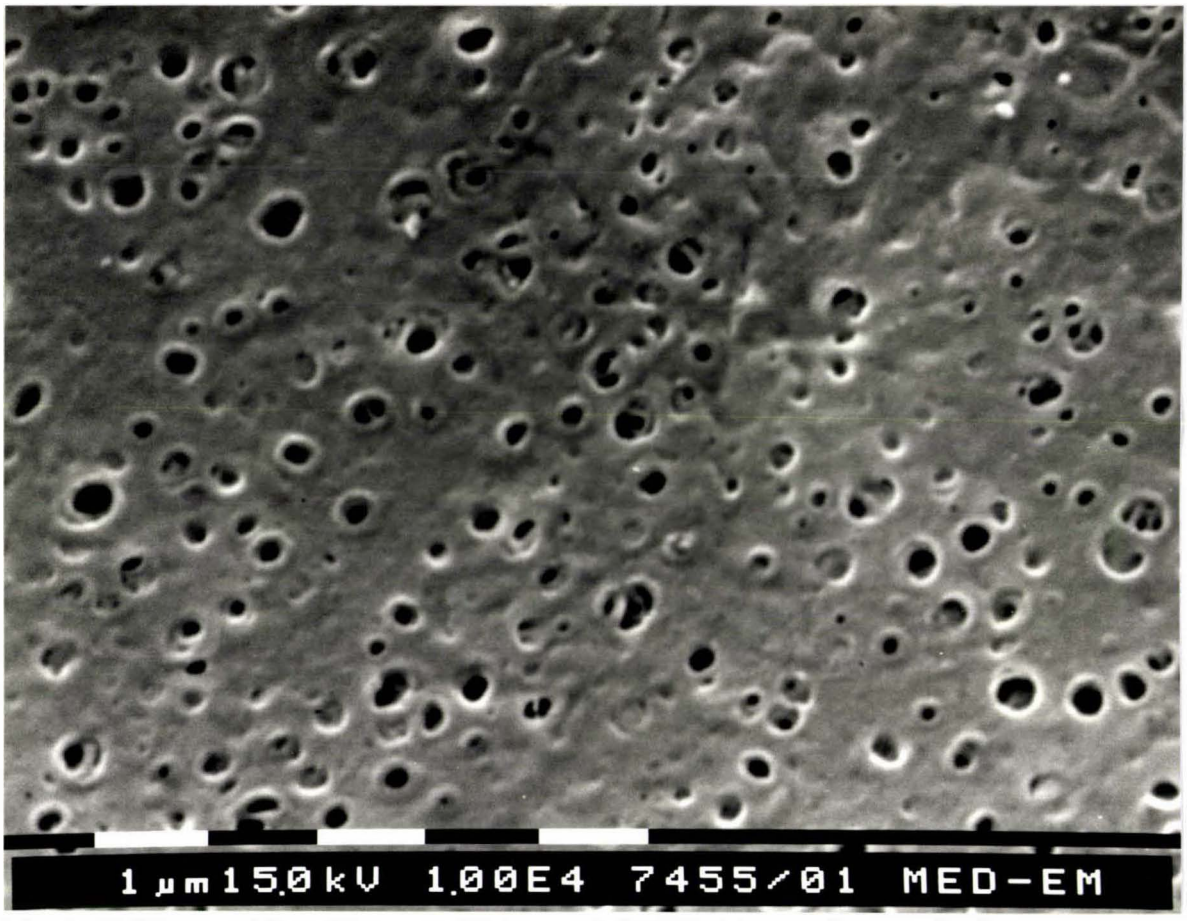

Figure 5.13. Scanning electron micrograph (14,000x magnification) of a clean GRM0.1PP MF membrane.

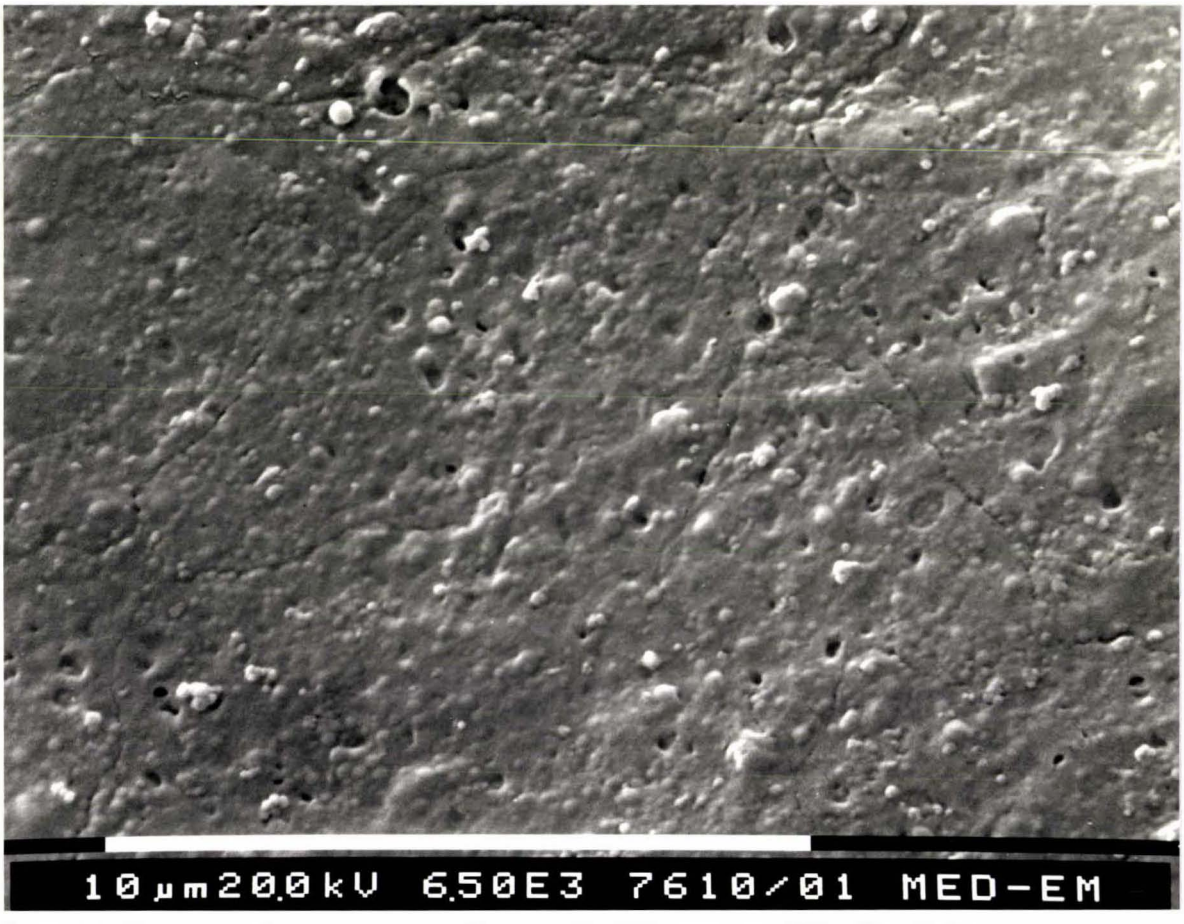

Figure 5.14. Scanning electron micrograph (9,200x magnification) of a severely fouled GRM0.1PP MF membrane. The final membrane resistance prior to removal of the membrane was 2522 x 10^{10} /m (run 25).

Figure 5.15. Scanning electron micrograph (9,200x magnification) of a lightly fouled GRM0.1PP MF membrane. The final membrane resistance prior to removal of the membrane was 232 x 10^{10} /m (run 27).

Figure 5.16. Scanning electron micrograph (140x magnification) of a liquid nitrogen fractured light fouled GRM0.1PP MF membrane.

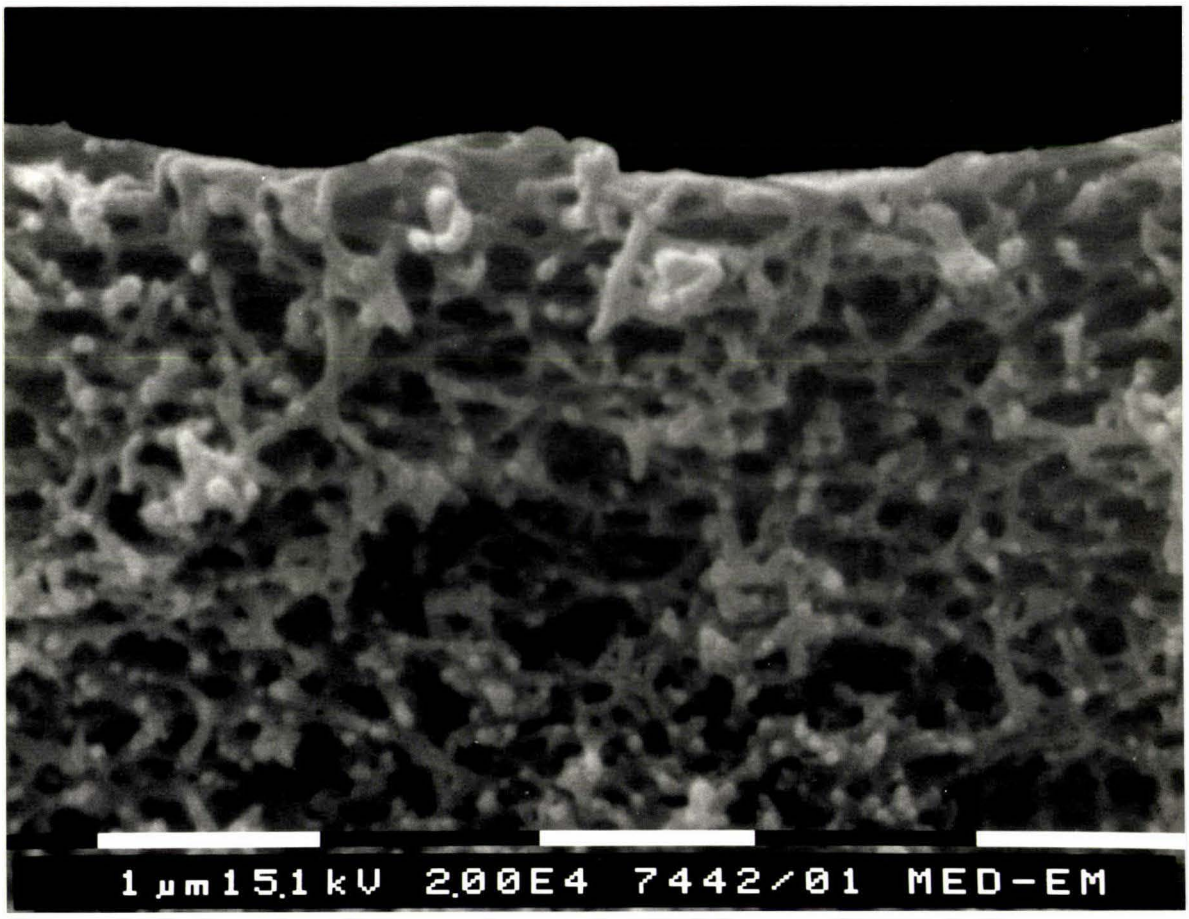

Figure 5.17. Scanning electron micrograph (27,500x magnification) of a cross-section of a clean GRM0.1PP MF membrane.

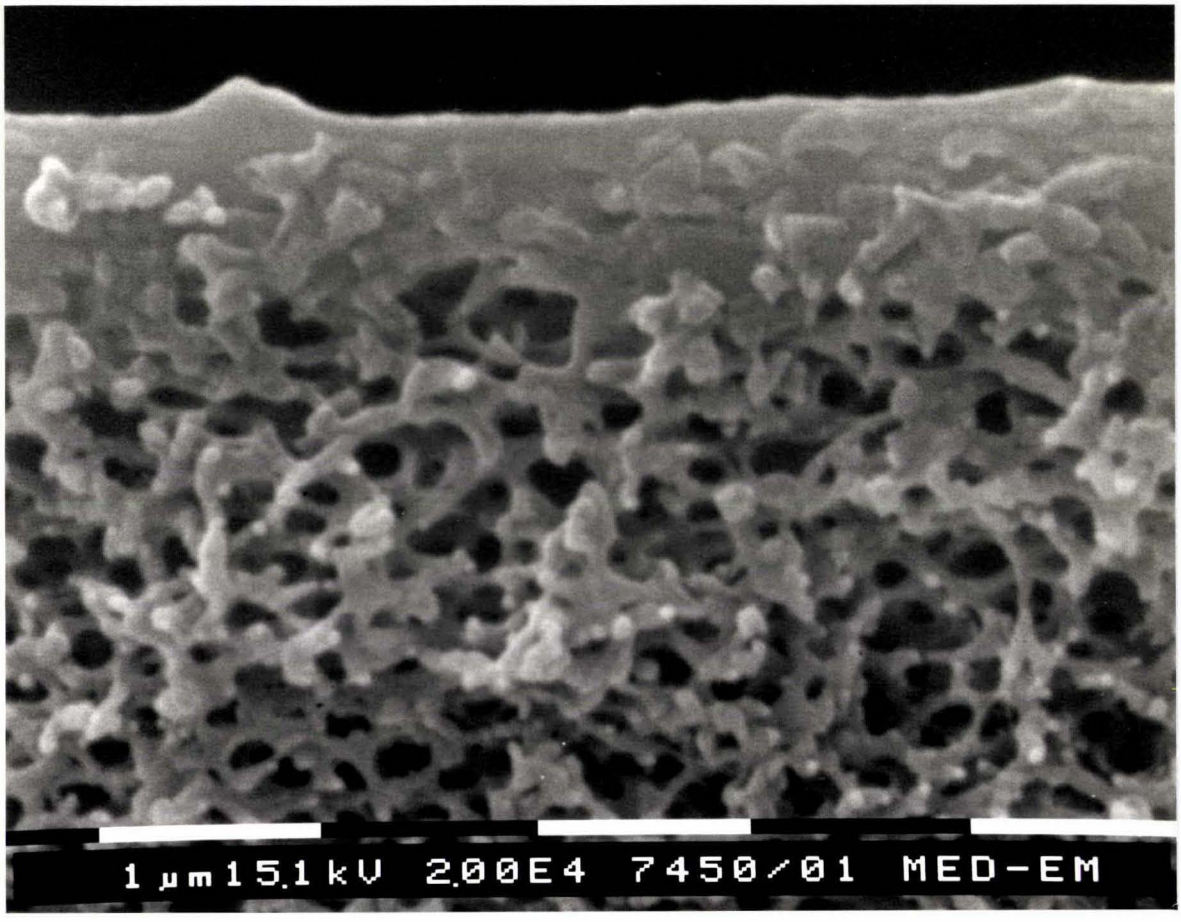

Figure 5.18. Scanning electron micrograph (27,500x magnification) of a cross-section of a severely fouled GRM0.1PP MF membrane. The final membrane resistance prior to removal of the membrane was 2522 x 10^{10} /m (run 25).

5.3.2. *UF trials*

In all seven trials performed severe fouling occurred (Fig. 5.19 and Table 5.4) with the membrane resistance increasing from around 270 to 6000-8000 x 10^{10} /m after 4 h operation. The majority of the increase in resistance occurred in the first 20 min. There was an upward trend in the clean membrane resistance with run number (Table 5.4) indicating that the cleaning regime had not been totally effective in restoring the membrane to its initial resistance. It has been the author's industrial experience that UF membranes take several production/cleaning cycles to "settle down" or condition into steady performance and this may also be responsible for the variations seen in the water flux.

By comparing trials 17, 21 & 23, all of which were operated with a constant transmembrane pressure of 200 kPa it is apparent that the initial variation in water flux also appeared to impact upon fouling as the membrane resistance increased with run number. Also compare trials 18 and 22 for the same effect.

In all of the trials severe fouling occurred. Start-up with a controlled permeate flux of 1.3-1.5 g/min (25-29 L/m^2.h) had no obvious effect on the final fouling resistance (compare trials 21-23), in contrast with the behaviour seen with the MF membrane. In the trials initially with constant flux, constant pressure operation was initiated after only 4-10 min because of rapid initial fouling and thereafter, the membrane was exposed to the same conditions as in the trials when the transmembrane pressure was 200 kPa from the start. It is therefore perhaps better to state that constant flux operation did not appear to affect the initial rate of fouling by the membrane. Furthermore, operation with lowered transmembrane pressures and permeate fluxes did not appear to reduce fouling, although, the rate of increase in fouling in trial 19 did appear to be slower than in the trials at higher transmembrane pressure (Fig. 5.19). Unfortunately, the effect of increased fouling with trial number compromised this comparison.

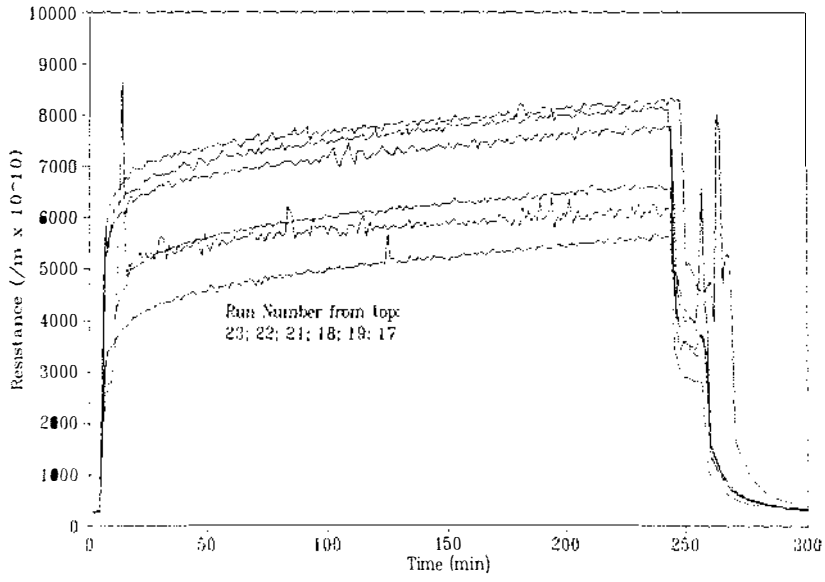

Figure 5.19. Membrane fouling during the UF (GR61PP) of skim milk at 50°C. Details of the operating conditions for each of the runs are given in Table 5.2.

Table 5.4. Summary of resistance data from the UF of skim milk at 50°C on a GR61PP membrane. All resistances are shown in units of /m x 10^{10}.

Run No	$R_{membrane}$	$R_{fouling}$	$R_{reversible}$	$R_{irreversible}$	% R_{rf}	% R_{if}
17	255	5350	2796	2554	52	48
18	267	6286	3244	3042	52	48
19	277	5885	2710	3174	46	54
20	265	6188	2288	3900	37	63
21	305	7494	4108	3387	55	45
22	280	7828	4120	3708	53	47
23	306	7932	3708	4225	47	53

5.4. Discussion

5.4.1. MF fouling

Two different fouling states exist during the MF of skim milk under constant flux operation. With low permeate fluxes and high cross-flow velocities the membrane resistance increased almost instantaneously after the introduction of skim milk from 10-20x10^{10} /m (clean membrane resistance) to 300-400x10^{10} /m. Thereafter, the resistance remained reasonably constant increasing very slowly up to 400-500x10^{10} /m after 4 h operation. The majority of the resistance due to fouling was removed by water flushing.

With higher fluxes or lower cross-flow velocities severe fouling occurred, usually rapidly, with the membrane resistance increasing to 2500-3500x10^{10} /m. After the permeate controller had switched to constant pressure, the resistance increased less rapidly with time. Flushing with water removed 80-99% of the resistance due to fouling, the percentage decreasing with the length of time the fouling layer had been on the membrane.

There appeared to be a "break-point" in the hydrodynamic conditions above which severe fouling occurred. One possibility was that severe fouling occurred if the casein concentration at the membrane wall exceeded the maximum permissible volume fraction of the casein and hence, formed a "gel layer" of some description, as has been suggested for BSA by Blatt *et al.* (1970). At or approaching the maximum concentration the protein may pack into a close packed network and the layer would exhibit an extremely high viscosity. Calculations were performed to explore this possibility.

The membrane wall concentration was estimated using Equation (3.32) as the casein retention was assumed to be 1. The mass transfer coefficient was calculated from Equation (3.3). The diffusion coefficient plays an important part in estimating the mass transfer coefficient. Conflicting data exist in the literature for the diffusivity of casein. For example Horne (1986) measured the diffusivity as 2.4-2.8x10^{-8} cm^2/s

whereas Delaney & Donnelly (1977) found 1.9×10^{-7} cm^2/s - an order of magnitude larger than Horne (1986). Further difficulties exist in estimating the diffusivity as it is generally considered to be dependent upon concentration (de Kruif, 1992) and the literature is in conflict over which boundary layer concentration: C_w, as suggested by Probstein *et al.* (1978); C_b; or an average concentration over the boundary layer (Chiang & Cheryan; 1987), should be used in the calculations.

de Kruif (1992) stated (based on Cichocki & Felderhof (1990)) that the collective diffusion of casein micelles at concentration **C** is equal to:

$$\frac{D_c}{D_0} = 1 + (1.454 - \frac{1.125}{\psi}).\phi \qquad \textbf{(5.1)}$$

where D_0 is the diffusivity calculated from the Stokes-Einstein relationship (Equation (5.2)). ψ is an interaction factor and is assumed to be infinite (valid for hard non-interactive spheres) and ϕ the volume fraction.

$$D_0 = \frac{k_b.T}{6.\pi.\mu_s.r_p} \qquad \textbf{(5.2)}$$

k_b is the Boltzmann constant, **T** is the temperature (K), μ_s is the solvent viscosity and r_p is the particle radius.

In this thesis the diffusivity was calculated from the equations stated by de Kruif (1992). This required an estimation of the casein volume fraction. The volume fraction is the product of the concentration (g/ml) and voluminosity (ml/g). Differing values exist in the literature for the voluminosity. Hallström & Dejmek (1988) found the voluminosity of casein in skim milk ranged from 3.7-5 and was dependent upon the concentration and temperature. Walstra (1979), in a review of the voluminosity of casein micelles, found values from 1.5-7.1 ml/g and indicated that the results were dependent upon temperature and the measurement method. Schmidt & Payens (1976) found voluminosities in the range 1.5-4. In this thesis a voluminosity of 4 was used as this was mid-range for the values reported. The concentration was estimated from the arithmetic mean of the bulk concentration and the concentration corresponding to the maximum volume fraction (ϕ) permissible (*i.e.* the maximum conceivable

concentration in the boundary layer). The maximum volume fraction of equal sized spheres is 0.74 whereas in a system with spheres of different sizes it may be higher. For skim milk concentrates Snoeren *et al.* (1982) calculated $\phi_{max} = 0.79$, the figure that was used in the calculations.

Therefore based on a maximum volume fraction of 0.79 and a voluminosity of 4 the maximum concentration achievable in the boundary layer is 0.2 g/ml or 20%. The feed casein concentration was taken to be 2.4% and the diffusivity was calculated for a concentration of 11.2% (volume fraction of 0.448).

The parameters used in the calculation of the wall concentration for run 8 are summarised in Table 5.5.

Table 5.5. Calculation of casein wall concentration.

Calculation of D_0 (Equation (5.2))					
k_b=	1.38×10^{-23}	J/K			
T=	323.15	K			
μ_s=	0.000544	Pa.s			
r_p=	50	nm	D_0=	8.7×10^{-8}	cm^2/s
Calculation of Diffusion Coefficient (Equation (5.1))					
C=	11.2	%			
Vol=	4	ml/g			
$\Psi \rightarrow$	∞		D_c=	1.44×10^{-7}	cm^2/s
Calculation of Mass Transfer Coefficient (Equation (3.3))					
ρ=	1000	Kg/m^3			
μ=	0.000544	Pa.s			
u=	3	m/s			
d=	3.704	mm	k=	8.12×10^{-6}	m/s
Calculation of Wall Concentration (Equation (3.32))					
C_p=	0 (total retention)				
C_b=	2.4	%			
J=	52	$L/m^2.h$	C_w=	14.1	%

Clearly the wall concentration is highly dependent upon the diffusivity and errors in the estimation of this parameter lead to significant changes in the wall concentration. Furthermore, the film model upon which this calculation is based, assumes brownian diffusion that is perpendicular to the membrane wall. This may or may not be appropriate for large casein micelles. For these reasons such a theoretical analysis is useful in demonstrating the presence of a "break-point" but little can be safely drawn from the actual figures calculated.

The wall concentration increases with permeate flux and decreases with cross-flow velocity. At the beginning of each of the trials performed the casein concentration at the membrane wall was estimated. Fig. 5.20 shows the influence of the initial casein wall concentration on the final membrane resistance after 4 h operation. It is clear that when the wall concentration exceeds 18-20% severe membrane fouling occurred. The variation in total fouling resistance seen in the trials with severe fouling was because of the influence of the retentate recirculation rate (Fig. 5.8). Fig. 5.21 shows the same data as in Fig. 5.20 but with the data from trials with severe fouling normalised with respect to the longitudinal pressure drop (measure of recirculation rate and wall shear stress).

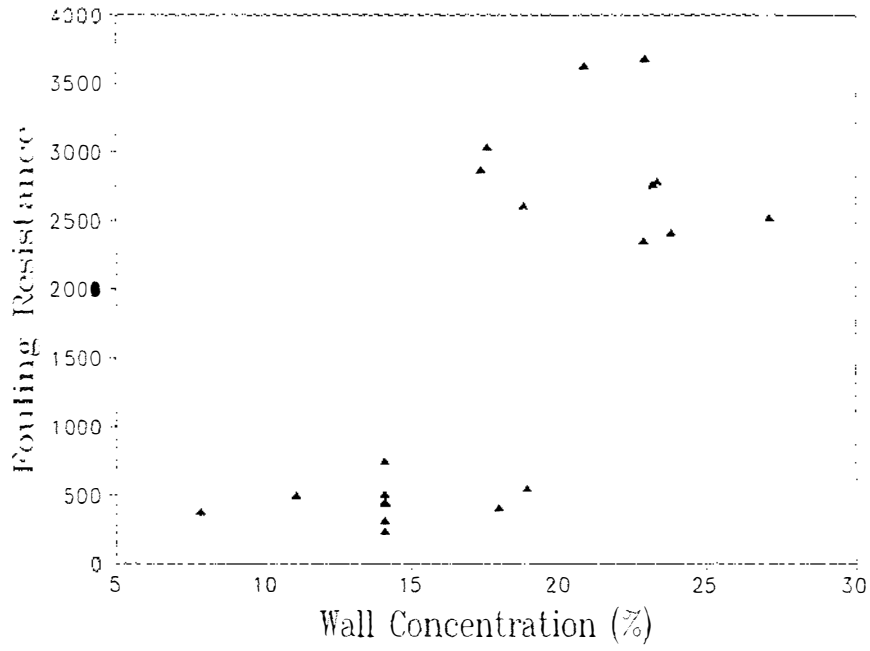

Figure 5.20. Effect of the casein concentration at the membrane wall as estimated by the film model on the final fouling resistance (x10^{10}/m) after 4 h MF of skim milk on a GRM0.1PP membrane at 50°C.

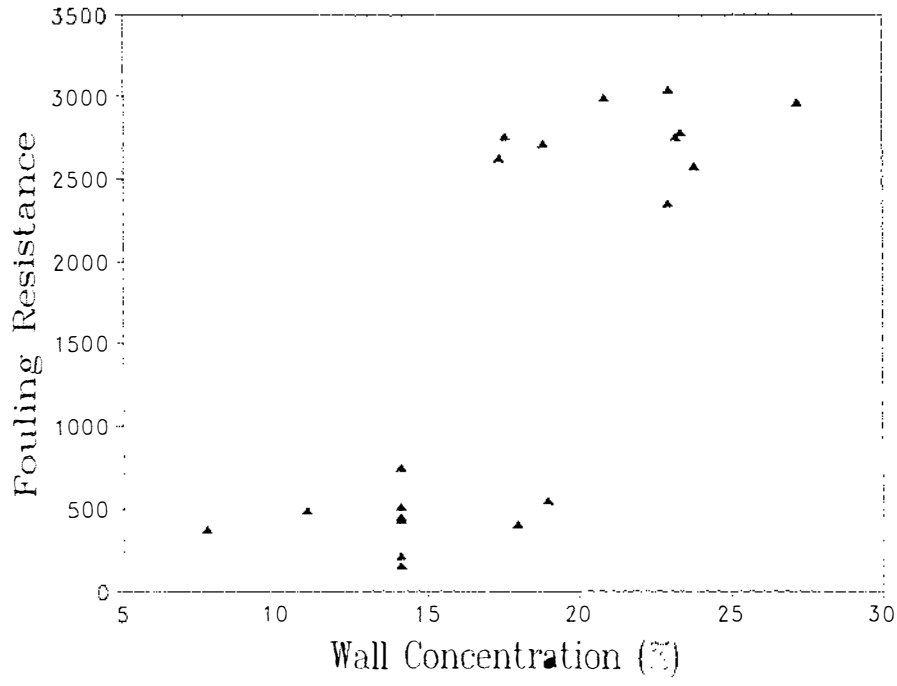

Figure 5.21. Effect of the casein concentration at the membrane wall as estimated by the film model on the final fouling resistance (x10^{10}/m) after 4 h MF of skim milk on a GRM0.1PP membrane at 50°C. For trials with severe fouling the resistance has been normalised for the retentate recirculation rate.

The presence of the break-point in the graph is good evidence that the influence of both the permeate flux and cross-flow velocity can be explained in terms of the wall concentration and the formation of a casein "gel layer"; however, the good agreement between the theoretical maximum concentration of casein (20%) and the observed break-point with wall concentration (18-20%) in Fig. 5.21 is considered fortunate given the assumptions made in the calculations!!!

Whether the casein forms a stationary close-packed structure, a "gel" of some description or a very slow moving viscous layer is open to conjecture. Indeed the concept of a gel layer has been the subject of considerable debate in the literature, both for (*e.g.* Blatt *et al.*, 1970) and against (Nakao *et al.*, 1979; Isaacson *et al.*, 1980; Fane *et al.*, 1981; Jonsson, 1984). Wijmans *et al.* (1984) concluded that in UF gel layer limitation is more likely with high molecular weight solutes (>100 kD),

whereas osmotic pressure limitation is expected when using small-medium size solutes (10-100 kD): also see Vilker *et al.* (1984). Given the size of casein micelles (100 nm, 10^7-10^9 kD) gel formation does not seem unreasonable. In whatever form, the fouling layer creates a resistance to flow through the membrane.

5.4.2. UF and the role of the whey proteins

With the UF membrane severe fouling occurred regardless of the operating conditions used. The fouling resistances were at least twice that seen in the MF trials and only around 50% of the fouling on the UF membrane was removed by flushing (cf. 80-100% for the MF membrane). In trials 18 & 22 the permeate flux was well below that necessary to achieve a wall concentration of 18% and hence, gel formation was unlikely. Therefore, it must be concluded that the membrane fouled by a different mechanism. It is suggested that the fouling was predominantly due to the adsorption and possible multi-layer deposition of the whey proteins on the membrane surface. The casein proteins may also contribute to the formation of a multi-layer.

In MF, monolayer protein adsorption reduces the membrane pore size by approximately two times the diameter of the protein. With a 100 nm membrane this has only a small effect on the membrane resistance (see Section 6). Furthermore, the permeate fluxes used in the trials on milk were less than that necessary for calcium induced protein-protein interactions in the membrane pores (see Section 6). Thus the effect of the casein gel layer appeared to dominate the membrane fouling.

However, in UF, protein adsorption has a major impact on the membrane resistance. With typical pore sizes of less than 10 nm, protein that is adsorbed on or near the pore entrances can cause a significant reduction in the apparent pore size of the membrane with a corresponding large increase in the membrane resistance.

These results suggest that careful control of the permeate flux (to avoid gel formation) is essential to prevent severe fouling in MF and hence maintain a high membrane selectivity, but in UF, constant flux operation has little if any value.

5.4.3. Nature of the casein "gel layer"

Once formed, the gel layer exhibits behaviour similar to that observed by others with skim milk in that the final membrane resistance and the permeate flux are dependent upon the cross-flow velocity (Cheryan & Chiang, 1984). The discontinuities in the resistance versus time curves (most evident in Fig. 5.6) correspond to the changeover from constant flux to constant pressure control. If the required permeate flux is above the "limiting" flux (the flux at which a gel layer forms given a particular combination of cross-flow velocity and transmembrane pressure) then the flux controller increases the transmembrane pressure rapidly in an attempt to increase the flux to a set point that cannot be achieved. In trials 12 & 14 the average permeate flux was only 3.46 g/min compared to the set point of 3.6 g/min. At the point of transfer from constant flux to constant pressure control, the "target" for the controller was reduced to the limiting flux at 200 kPa. Therefore, the increase in the resistance after this point was much slower and was probably due to consolidation of the fouling layer or the slow increase of the bulk casein concentration. There was a suggestion in the data that the initial rate of increase in membrane resistance was proportional to the "overshoot" of the "limiting flux" (compare runs 3 & 12 and 6 & 15 in Figs. 5.2 & 5.6).

After the switch from constant flux to constant pressure control, the theoretical wall concentration drops below that calculated for trials where the casein gel layer did not form (Fig. 5.22). Despite this, there is no reduction in the membrane resistance indicating that once formed the casein gel layer remains on the membrane.

The change in wall concentration in trial 11 is shown in Fig. 5.23. In this trial the recirculation rate was changed during the run (the change in membrane resistance is shown in Fig. 5.7). When the velocity was decreased (t=150 min) the wall concentration increased and the membrane resistance increased rapidly until the switch to constant pressure control. From this point the permeate flux fell and the resistance stabilised to a resistance corresponding to the "limiting flux" conditions. The theoretical wall concentration fell with the decreasing flux to a level below that before the velocity was decreased (Fig. 5.23).

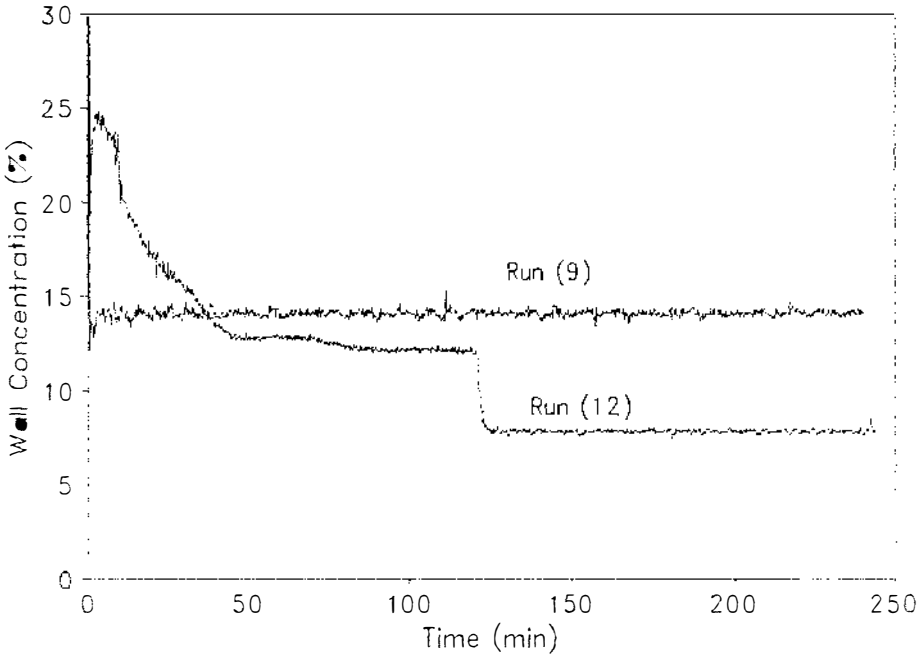

Figure 5.22. Comparison of the calculated casein concentration at the membrane wall in trials 9 & 12. In trial 12 severe fouling occurred followed by a switch to constant pressure control after 10 min. After 120 min the permeate flux was decreased to 35 L/m².h and constant flux control re-initiated. In trial 9 severe fouling was prevented.

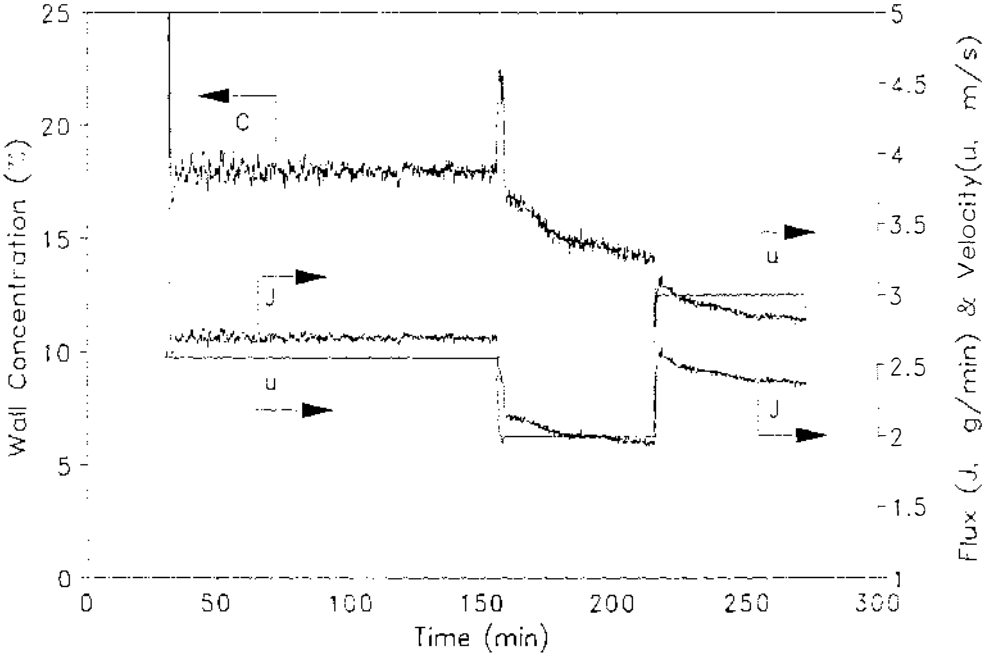

Figure 5.23. The effect of time on the calculated casein concentration at the membrane wall in run 11: skim milk feed; 50°C; initial flux 52 L/m².h. The cross-flow velocity was varied during the trial.

Gel layer formation occurred despite the fact that the wall concentration was only above the critical concentration for 2-3 min. Furthermore, there was no decrease in the membrane resistance once the wall concentration dropped below the critical concentration, indicating that once formed, the gel layer cannot be removed by changes in the hydrodynamic conditions. Increasing the velocity to above that at the beginning of the run reduced the wall concentration further and while there was a small reduction in the membrane resistance the gel layer remained on the membrane.

Changing the flux mid-run did result in a reduction in the membrane resistance (Fig. 5.4) and the wall concentration (Fig. 5.22). In effect, there was a shift down the transmembrane pressure/limiting flux curve to a new point appropriate for 35 $L/m^2.h$, but, the change in flux did not result in the removal of the gel layer.

Interestingly most of the resistance due to the fouling layer is removed by water flushing under the same hydrodynamic conditions as that during operation on milk. This indicates that the gel layer is not strongly bound to the membrane and that the stability of the gel layer, that is not significantly affected by small to medium changes in the hydrodynamic conditions, is affected by the removal of the feed.

One possibility is that if the protein concentration in the feed reduces below a critical point the gel layer is able to "re-solubilise" into the bulk solution. Another possibility is that the calcium or phosphate concentration in the feed is the critical parameter stabilising the gel layer. The similarity of the electron micrographs of the severely fouled and lightly fouled membranes provide further evidence that the gel layer is essentially "dynamic" or a close packed viscous liquid with a yield stress rather than a genuine cross-linked gel.

5.4.4. Nature of membrane fouling when casein "gel layer" formation was prevented

In the trials when fouling was designated as "light" the membrane resistance still increased to around 400-500 x 10^{10}/m. This is about 20 times that of the clean membrane and is of a similar value to that of a clean UF membrane. Most of the increase in resistance occurred in the first few minutes of the trial and the final

resistance level appeared to be independent of the permeate flux and cross-flow velocity. The almost instantaneous increase in resistance after the introduction of milk and the fact that the majority of the fouling was removed by flushing suggested that the resistance was directly related to concentration polarisation behaviour although it is not clear by what mechanism.

The resistance may be because of the osmotic pressure of the proteins, in particular the whey proteins that are partially retained by the membrane (Goldsmith, 1971; Vilker *et al.*, 1981; Jonsson, 1984). The influence of the osmotic pressure may be more important given the relatively low transmembrane pressures (typically 20-40 kPa) used in the experiments. Alternatively, the casein micelles are of a similar size to the membrane pores and the resistance may come from obstruction of the pore entrances by the moving casein micelles, perhaps in a similar way to that suggested by Le & Howell (1984). However, if they stopped completely the membrane resistance and protein retention would be very high.

5.5. Conclusions

In the MF of skim milk on a membrane that is retentive to casein but not to the whey proteins, a casein "gel layer" is formed on the membrane surface if hydrodynamic conditions (permeate flux and cross-flow velocity) are used that cause the wall concentration to exceed a critical concentration. The critical concentration is thought to be equivalent to the maximum volume fraction of the casein. Once formed, the gel layer cannot be removed by relatively small changes in the hydrodynamic conditions even if the wall concentration moves to below the critical level. The gel layer is, however, removed by water flushing.

If the critical concentration is not exceeded at any point through careful start-up procedures and control of the permeate flux, then MF with a much reduced membrane resistance, higher overall throughput and lower whey protein retentions can be achieved.

In MF (0.1 μm pore size) fouling is dominated by the casein gel layer and the adsorption of the whey proteins on to the membrane surface has only a small effect. In contrast, in UF, whey protein adsorption appears to dominate fouling and severe fouling could not be prevented by operation with low permeate fluxes.

Constant flux operation is crucial for preventing severe fouling in MF. However, there appears to be little benefit in UF to operate at constant flux, at least in the pressure ranges considered in this thesis.

6. Fouling of microfiltration membranes by ß-lactoglobulin

6.1. Introduction

The trials with skim milk showed that a large component, retained by the membrane, can form a concentration-induced surface layer on the membrane restricting the passage of smaller proteins through the membrane and causing an increase in the resistance to permeate flow. A study with ß-lactoglobulin was performed in order to investigate whether smaller proteins, freely permeable to the membrane, also caused membrane fouling.

Severe membrane fouling has been reported in MF experiments with bovine serum albumin (BSA) even when the pore size was considerably larger than the protein (Bowen & Hughes, 1990; Bowen & Gan, 1991; Jonsson *et al.*, 1992). One possibility is that the protein is aggregated and therefore not small enough to pass through the membrane pores. Kelly *et al.* (1993) reported that the severity of membrane fouling could be related directly to the number of aggregates in the BSA solution. In this case fouling occurs predominantly on the membrane surface. On the other hand, Bowen & Gan (1991) and Jonsson *et al.* (1992) have suggested that shear within the membrane pores caused the protein to deposit within the membrane, although, by what mechanism is not clear. Bowen & Gan (1993) with yeast alcohol dehydrogenase found that the membrane pore structure influenced fouling and suggested that pores with a "sharp lip" result in more severe fouling because of greater shear at the pore entrance.

The purpose of this study was to investigate the fouling behaviour of ß-lactoglobulin on ceramic MF membranes with pore sizes much larger than the protein. The effect of the permeate flux was believed to be particularly important. Therefore, most trials were performed in a cross-flow rig with constant flux rather than a constant transmembrane pressure.

ß-Lactoglobulin was chosen as the feed material because of its relevance to fouling in the milk and whey system and its relative size compared to the 50 and 100 nm

membranes used in the study. It also allowed the study of the fouling behaviour of another protein apart from BSA. There is an over-dependence on BSA as a model protein in the membrane fouling literature. ß-Lactoglobulin is a typical globular protein and exists as a dimer at room temperature between pH 7.0 and 5.2; the conditions used in most of the trials. Above 40°C, the dimer begins to dissociate to monomers. Octamers may form between pH 5.2 and 3.5, with a maximum number at pH 4.4-4.7 and 0°C. The dimers dissociate to monomers below pH 3.5.

6.2. Materials and methods

6.2.1. Feed material and pretreatment

A 0.25% w/v ß-lactoglobulin solution was prepared by mixing ß-lactoglobulin powder and demineralised water on a magnetic stirrer for at least 30 min. The spray-dried ß-lactoglobulin powder was prepared at the New Zealand Dairy Research Institute (details of manufacturing procedure not available). During spray drying, the powder was split into two samples, hereafter called powder "A" and powder "B". Powder B contained the dryer "sweepings". Powder A was used in most of the experiments.

The composition of the powder was: 14.82% TN; 0.054% NPN; 1.71% ash; 2.95% moisture, and accounted for 99.2% of the powder. The protein content of the powder (TN-NPN x 6.38) was 94.2%. Analysis by gel filtration (TSK3000x column) showed that powder A contained 89% ß-lactoglobulin (94.1% of the protein in the powder was ß-lactoglobulin; Fig. 6.1). The remaining protein was mostly α-lactalbumin. Similar analysis of powder B showed a ß-lactoglobulin content of 83% (of powder) indicating that there had been a small quantity of protein denaturation in this sample (probably because of inclusion of the dryer sweepings).

Sodium chloride (Merck p.a. grade) or calcium dichloride (Merck p.a. grade) were added during the mixing of the protein solution to achieve the required ionic composition of the solution. Following mixing the protein solution was allowed to stand for at least 30 min prior to MF commencing. If it was necessary, the temperature of the solution was adjusted to 25°C by placing the beaker in 40°C water.

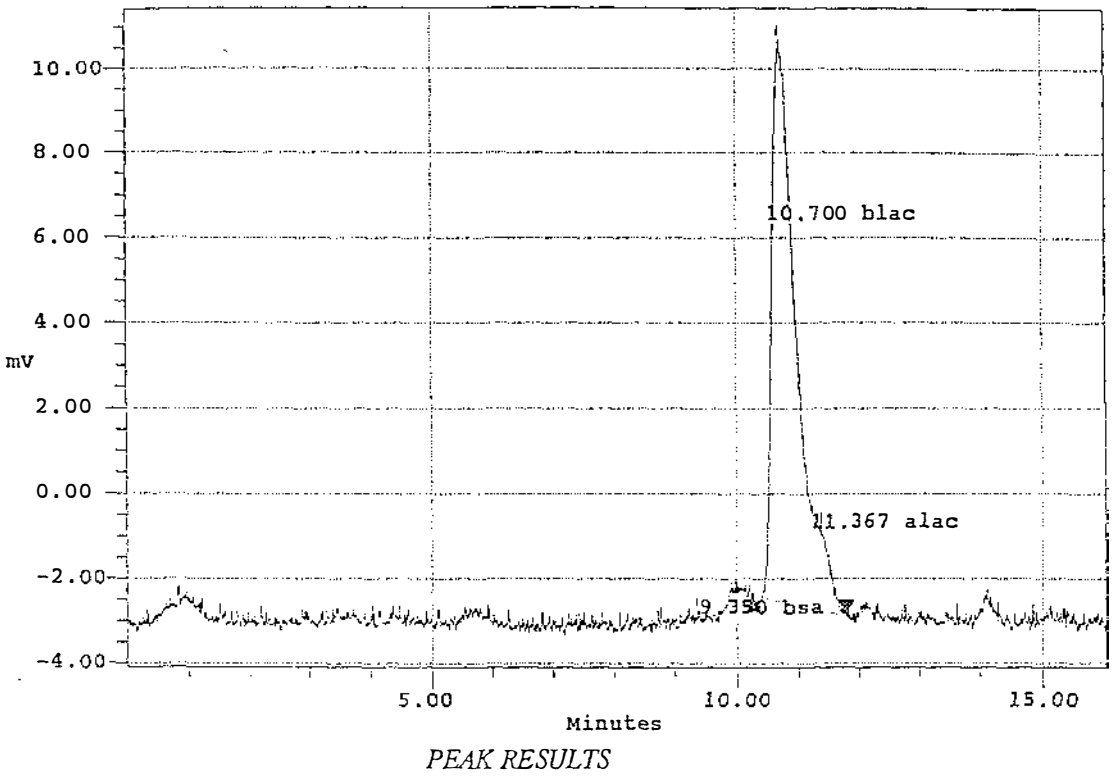

Figure 6.1. Gel filtration chromatograph (TSK 3000 x) of powder A.

6.2.2. Membranes

Three zirconium oxide membranes (S.C.T., Tarbes, France) with nominal pore sizes of 20, 50 and 100 nm were used in the trials. On the morning of each trial the membrane was flushed for 7-10 min with 50°C water and then cleaned with 0.4% HNO_3 for 30 min at 50°C. The membrane was then flushed for 10 min with 25°C water to remove the cleaning chemicals and left recirculating on water (typically with a permeate flux of 110 L/m^2.h) during the preparation of the feed material.

Immediately before the addition of feed to the plant the ionic strength of the water was adjusted by the addition of sodium chloride to that of the feed product (measured by conductivity). Then the clean membrane resistance was assessed by measuring the transmembrane pressure for at least 5 different permeate fluxes (typically 56, 112, 223, 338 & 450 L/m^2.h). A linear regression was performed on these data, giving the slope of the line, and allowing the calculation of the membrane resistance.

6.2.3. Plant operation

At start up the ß-lactoglobulin solution was introduced to the membrane by switching from the water balance tank to the tank containing the feed solution. The water in the recirculation loop was added to the ß-lactoglobulin solution resulting in a 15-20% dilution of the feed material. The ß-lactoglobulin concentration during the trial was typically 0.2% w/v. All of the trials commenced in constant flux mode - the transmembrane pressure increasing with membrane fouling. If the transmembrane pressure increased above 200 kPa, operation switched to constant pressure mode with the transmembrane pressure set to 200 kPa. The temperature in all of the trials was 25°C.

At the completion of the trial on ß-lactoglobulin the membrane was flushed with 90-100 L of 25°C demineralised water (small amount of added NaCl) for 10-14 min. The permeate flux was maintained at the same value as during protein processing. When the permeate controller was in constant pressure mode the flux was allowed to increase back to the initial flux set point on ß-lactoglobulin, and then operation was switched back to constant flux and this flux maintained until the end of flushing.

After flushing, water was circulated for a further period of time (5-30 min) before the water flux was again measured. Following the water flux the membrane was cleaned with a 1.4% solution of Ultrasil 25 for 40-50 min at 50°C.

6.2.4. Measurements and analysis

The conductivity and pH of the feed were measured at regular intervals throughout each trial. Samples of the feed (typically: raw, 5, 60 & 120 min) and permeate (typically 30, 60, 90 & 120 min) were taken in each trial and the protein content of each sample measured by spectrophotometer at 280 nm (DMS 80 UV visible spectrophotometer in Lund and a Beckman DU 7500 in New Zealand). Samples were diluted to ensure that absorbances of less than 1 were obtained. Standard samples of the powder were analysed and the following regression equation used to calculate the protein concentration from the absorbance.

$$C_{protein} = 0.0009 + 0.1051 \times \text{Absorbance} \quad \textbf{(6.1)}$$

In some trials a Pharmacia UV1 cell equipped with an industrial flow cell was installed in the permeate line. The cell was calibrated with data from the spectrophotometer.

6.2.5. Overview of experiments

Experiments were performed first in Lund (Sweden) (25/10/93-26/11/93) and then at the New Zealand Dairy Research Institute (8/2/94-31/3/94). A full list of all of the trials performed, together with a summary of relevant processing information can be found in Appendix 2.

The first trials considered the effect of permeate flux on fouling. Trials were performed on the 100 nm membrane at 50 [runs 3, 9, 11] and 200 L/m^2.h [4, 7]. In addition, preliminary investigations had indicated that the ionic strength of the protein solution had a significant impact on the retention of protein by the membrane. Trials were performed to investigate: ionic strength [runs 1,5]; pH 5.0 compared to approximately 6.5, the pH of the reconstituted powder [2, 6]; and the addition of calcium [8, 10].

The initial results of the trials on the 100 nm membrane showed that the retention of β-lactoglobulin increased if the ionic strength was less than 0.02, although fouling was not significantly increased. As a consequence the ionic strength of all further experiments was increased by the addition of NaCl or $CaCl_2.2H_2O$ to at least 0.045 in order to minimise the effect on ionic strength on retention. Lowering the pH, adding calcium or operating at 200 L/m^2.h all increased membrane fouling, but, the impact of these pretreatments was insufficient to increase protein retention by the membrane. It was therefore decided to move to membranes with a smaller pore size for further experiments.

Initial trials on the 20 nm membrane [12, 13] showed that severe fouling with high protein retentions could not be prevented by reducing the permeate flux, whereas

trials on the 50 nm membrane showed that low protein retentions could be achieved. For an investigation of MF fouling, a membrane with low initial protein retentions is required and therefore, investigations concentrated on the 50 nm membrane. The remaining trials performed in Lund [14-19] investigated the effect of calcium addition and high flux (200 $L/m^2.h$). As with the 100 nm membrane, the addition of calcium or operation at 200 $L/m^2.h$ increased membrane fouling but had little effect on protein retention. However, the combination of these parameters resulted in severe fouling and high protein retention.

All subsequent experiments were performed in New Zealand. The interaction between flux and calcium addition was investigated in more depth; firstly by standardising the calcium content and altering the permeate flux [20-24, 38], and secondly, by altering the calcium content of the feed material at 200 $L/m^2.h$. [25-30, 32]. Experiments were also performed to investigate the effect of the ionic strength above 0.05 [31, 37].

Intuitively, given the relative size of the proteins and pores and the low initial protein retention, it was thought that fouling initially occurred within the membrane pores rather than on the membrane surface. Thus, experiments had concentrated on the influence of the permeate flux on fouling and retention. If fouling is occurring only in the pores, cross-flow velocity should not affect it. Nevertheless, a series of experiments were performed [33-36] in the presence of calcium and at high flux to investigate the effect of varying the cross-flow velocity. Finally, to complete the experiments, the 100 nm membrane was re-installed and two experiments performed at high flux and in the presence of calcium.

6.3. Results

6.3.1. Consistency of feed and membrane preparation

The protein concentration in the initial feed material ranged from 0.230 to 0.257% for powder "A" and from 0.240 to 0.267 for powder "B". Differences in the feed preparation and errors in the dilution and measurement of the samples probably contributed to the differences. With powder "A" there was a slight downward trend in the protein concentration with run date (Fig. 6.2). The powder was observed to be more "clumpy" in later experiments and it is suggested that there was some water uptake by the powder with time leading to slightly lower protein concentrations. The trend was not seen with powder "B" (Fig. 6.3) perhaps due to the limited number of runs performed with this powder.

The plant feed was diluted by water. The dilution ratio ranged from 0.76 to 0.87 with an average of 0.82.

For each pore size one membrane element was used in all of the experiments. The effectiveness of the cleaning regime was assessed from the membrane resistance measured prior to the following trial. For the 100 nm membrane the membrane resistance varied from 10.2 to 12 x 10^{10} /m (Fig. 6.4); for the 50 nm membrane from 29.8 to 35.7 x 10^{10} /m (Fig. 6.5); and from 107.4 to 117.8 x 10^{10} for the 20 nm membrane. The reason for the slightly higher resistances initially observed with the 50 nm membrane upon commencement of trials in New Zealand is not known. It is possible that differences in the water conductivity were responsible (see Section 6.3.4). In any case, variations in the clean water resistances were small and cleaning was therefore considered satisfactory over the entire period of the experiments.

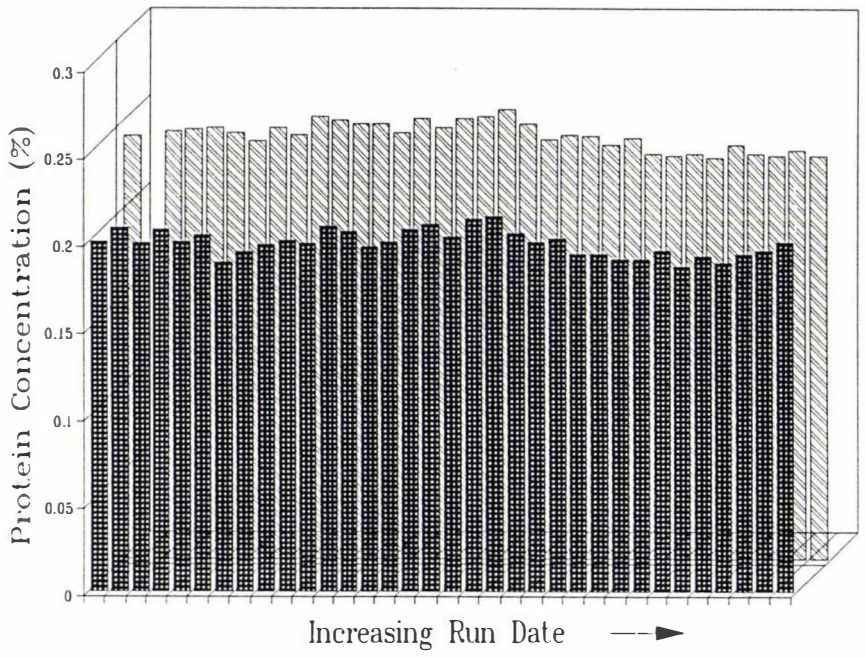

Figure 6.2. Protein concentration (%) in the initial feed (back) and the plant feed averaged from readings at 5, 60, 120 min (front). Trials with ß-lactoglobulin powder "A".

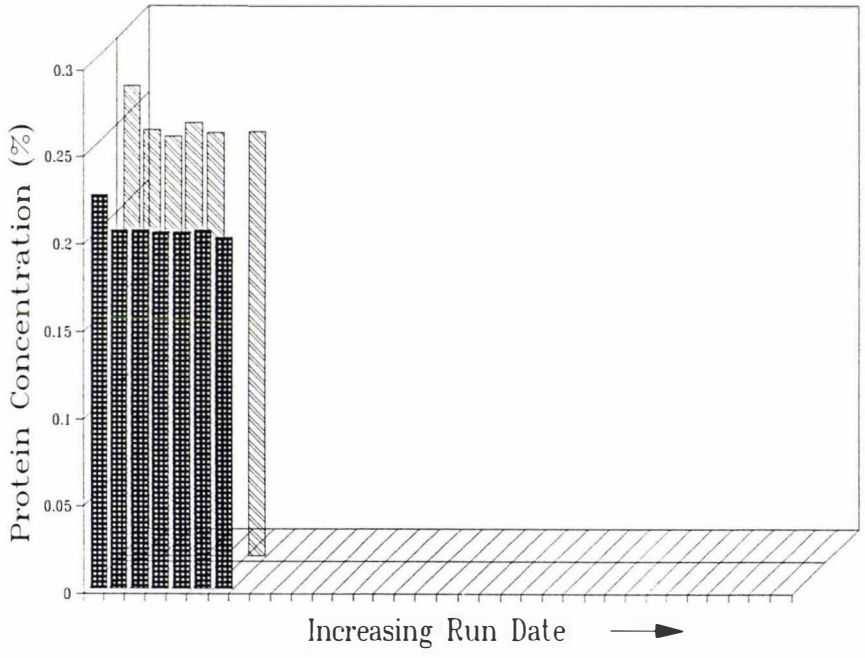

Figure 6.3. Protein concentration (%) in the initial feed (back) and the plant feed averaged from readings at 5, 60, 120 min (front). Trials with ß-lactoglobulin powder "B".

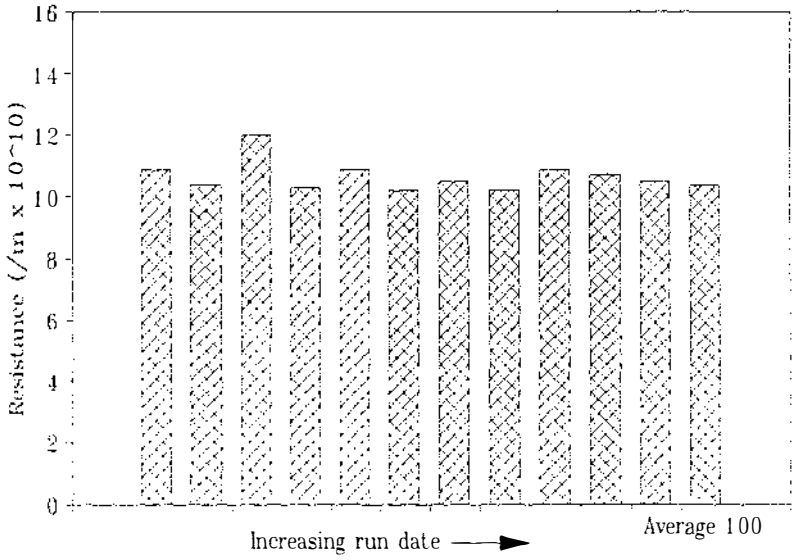

Figure 6.4. Clean membrane resistances in trials on the 100 nm zirconium oxide membrane.

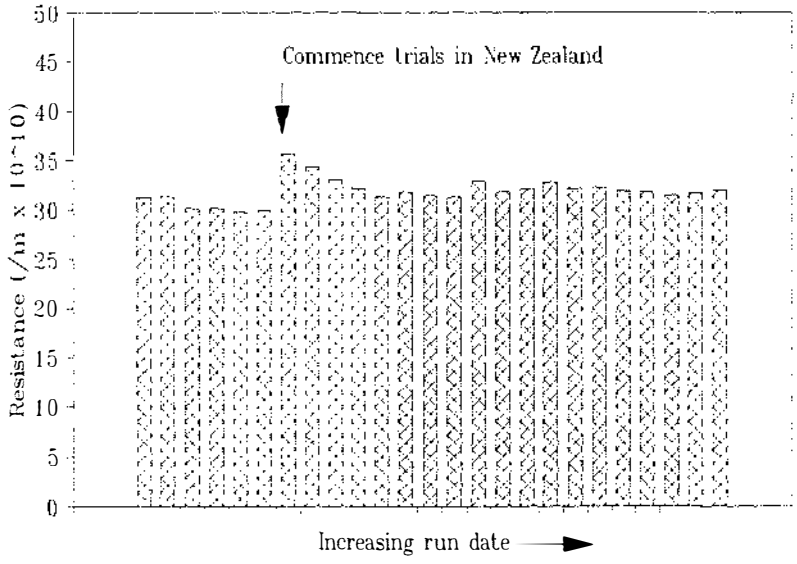

Figure 6.5. Clean membrane resistances in trials on the 50 nm zirconium oxide membrane.

6.3.2. Comparison of powder "A" and powder "B"

Although both powders were dried from the same concentrated material, powder "B" contained the "sweepings" from the dryer. Results from gel chromatography indicated some differences in the state of the proteins between the two powders and therefore a direct comparison of the fouling behaviour of the two powders was necessary if results were to be cross-compared.

With a flux of 50 L/m^2.h, when the increase in membrane resistance was reasonably small and protein transmission was not affected by processing time, there were no differences observed in the behaviour of powder "A" and powder "B" (Figs. 6.6&6.7). Likewise, at 200 L/m^2.h, when severe fouling occurred and the protein transmission was low, no observable differences in behaviour were identified (Figs. 6.8&6.9). On the basis of these comparisons, it was considered acceptable to make direct comparisons between runs with either powder.

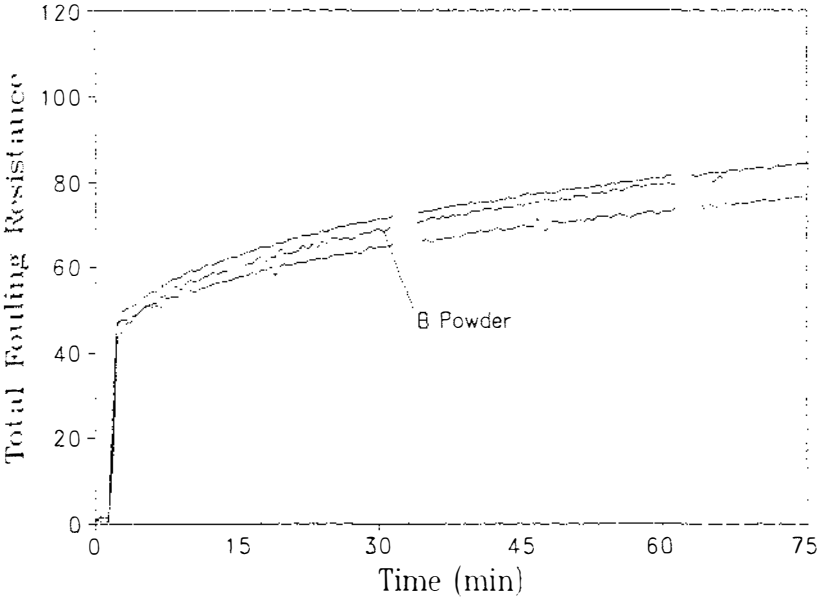

Figure 6.6. Comparison of fouling resistance (/m x 10^{10}) of powder "A" and powder "B" on the 50 nm membrane at 50 L/m^2.h in the presence of calcium (8.04-8.34 mmol/L). The ionic strength of the feeds ranged from 0.0569 to 0.0572 and the pH from 6.15 to 6.36.

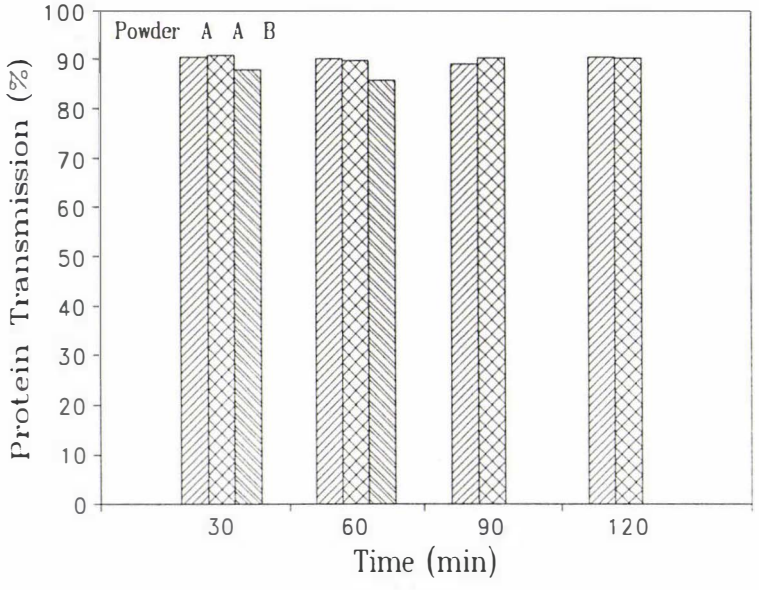

Figure 6.7. Comparison of the protein transmission of powder "A" and powder "B" on the 50 nm membrane at 50 L/m^2.h in the presence of calcium (8.04-8.34 mmol/L). The ionic strength of the feeds ranged from 0.0569 to 0.0572 and the pH from 6.15 to 6.36.

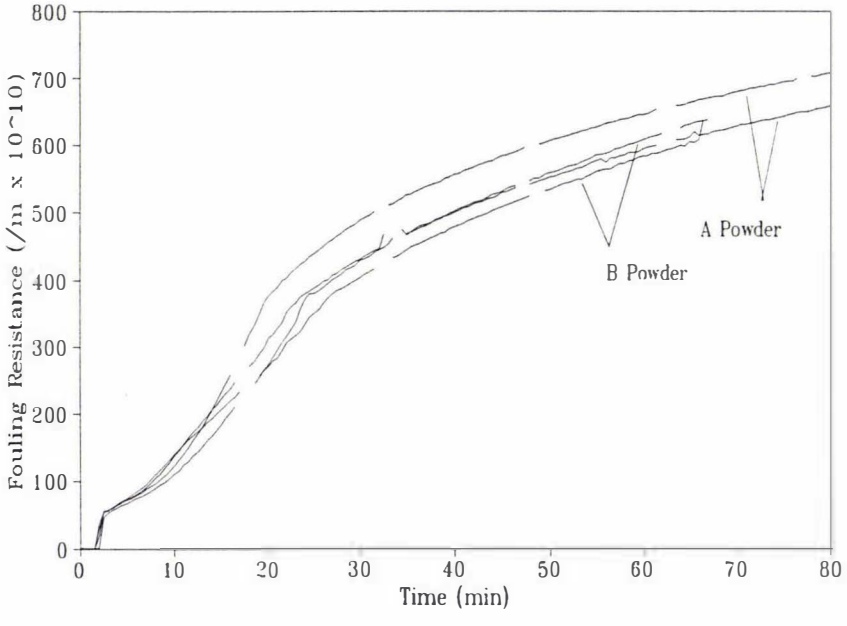

Figure 6.8. Comparison of fouling resistance of powder "A" and powder "B" on the 50 nm membrane at 200 L/m^2.h in the presence of calcium (8.14-8.44 mmol/L). The ionic strength of the feeds ranged from 0.0568 to 0.0575 and the pH from 6.19 to 6.43.

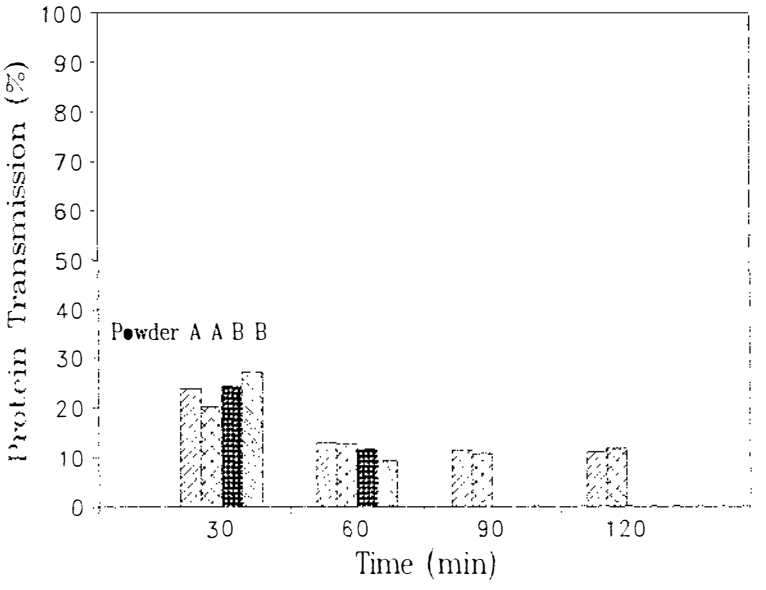

Figure 6.9. Comparison of the protein transmission of powder "A" and powder "B" on the 50 nm membrane at 200 L/m^2.h in the presence of calcium (8.14-8.44 mmol/L). The ionic strength of the feeds ranged from 0.0568 to 0.0575 and the pH from 6.19 to 6.43.

6.3.3. Flushing

An example of the process treatments given after ß-lactoglobulin filtration is shown in Fig. 6.10. The recirculation loop was flushed with 25°C water causing a reduction in ΔP_{TM} and the resistance. The permeate flux remained at the product flux. The flushing time increased in the range 10-15 min with run date as experience showed that fouling deposits continued to be removed with longer flushing. The displacement of feed material from the loop occurred quickly (flushing rate 6-7 L/min, retentate loop hold up volume of 1 L) and the further reduction in resistance was because of the erosion or desorption of the deposited material.

After flushing the plant was left recirculating on water for a period of time prior to the commencement of the water flux measurements. In the trials at Lund (trials 1-19) this period of time was short (5-10 min). However, the resistance continued to

decrease with time because of continued removal of deposits from the membrane (Fig. 6.10) and in the New Zealand trials the time on recirculation was increased to approximately 30 min. The reversible resistances from the trials at Lund may have been underestimated on account of the short recirculation time.

A small amount of NaCl was added to the water used for flushing. The conductivity of the water was not measured regularly, although spot checks indicated a typical conductivity of 0.5-1 mS/cm (ionic strength 0.004-0.008). The ionic strength of the water has been shown to have a small effect on the clean membrane resistance (see Section 6.3.4) and variations in the salt content of the water may have slightly affected the water flux measurement after ß-lactoglobulin filtration. Furthermore, in two or three trials a "slug" of high ionic strength water (ex the second balance tank) was introduced to the flush, and appeared to cause a rapid increase in the removal of fouling from the membrane. Unfortunately, the conductivity of the water was not monitored and the effect cannot be quantified. It does, however, suggest that the ionic environment of the flushing water has an impact on the removal or desorption of material from the membrane.

The effect of variations in flushing time and ionic strength on the removal of deposited material from the membrane does compromise the data obtained from flushing - principally the breakdown of the fouling resistance into reversible and irreversible fouling. As a consequence, these results were only considered as qualitative rather than quantitative. In particular, the results obtained from runs 17 and 19 (the only runs at Lund where severe fouling occurred on the 50 or 100 nm membrane) appear to be suspect. A comparison of the 50 nm membrane results when severe fouling occurred (sufficient to impact on protein transmission) showed that the breakdown of reversible and irreversible fouling for these two runs (Fig. 6.11, first two bars) are out of step with the results from the remaining trials. In the remaining trials on the 50 nm membrane the irreversible resistance was reasonably consistent, despite the wide range of operating conditions and variations in the reversible resistance. It is not believed that the differences seen are because of the particular operating conditions in runs 17 and 19 as reasonably similar conditions (feed pretreatment, permeate flux, final fouling resistance *etc.*) existed in several of the other runs.

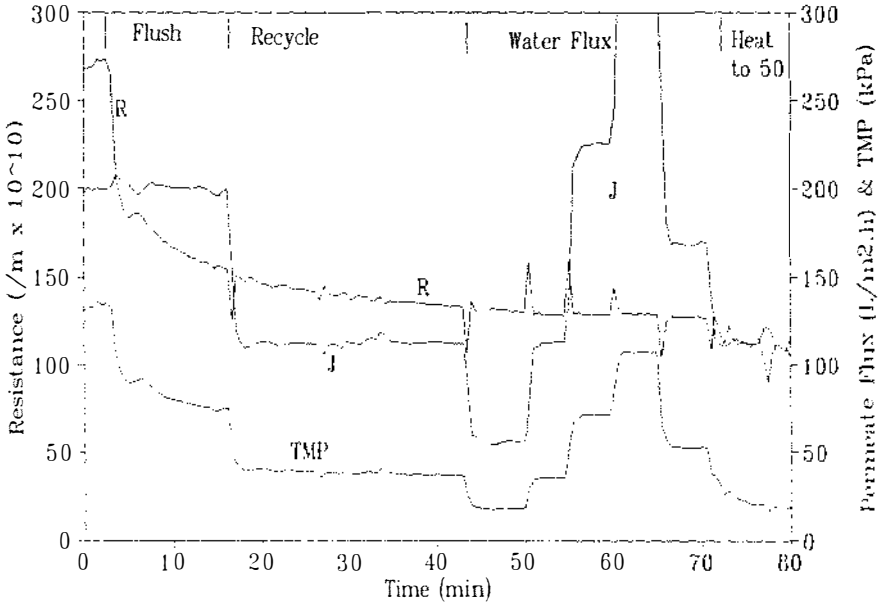

Figure 6.10. Example of process conditions used at the completion of a trial on ß-lactoglobulin. Data from trial 28 (9/3/94) is shown. A description of the various stages is given in the text.

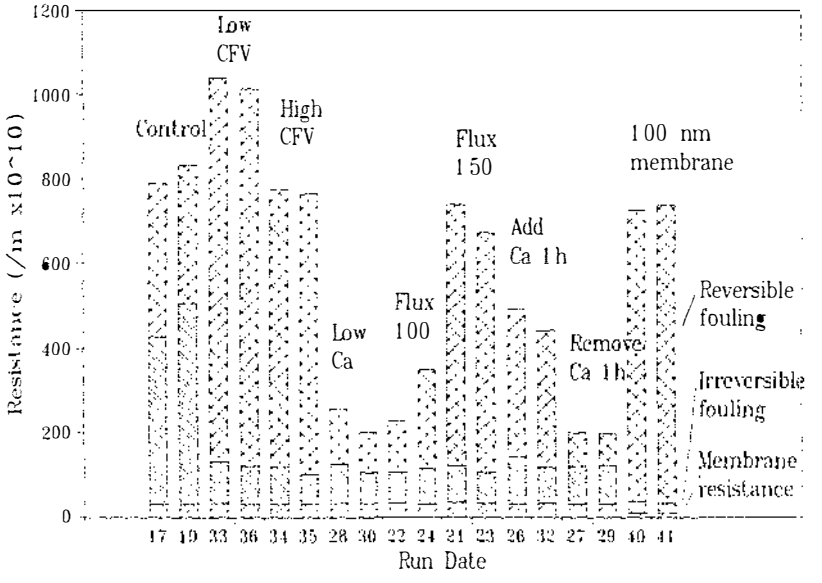

Figure 6.11. A comparison of the reversible and irreversible fouling from all of the trials on the 50 and 100 nm membranes (two bars on the right) when severe fouling occurred.

6.3.4. Effect of ionic strength

Preliminary experiments indicated that the retention of protein by a 100 nm membrane was sometimes high even when fouling was not severe enough to reduce the effective pore size of the membrane. Two experiments were performed with step-wise addition of NaCl in order to investigate the effect of ionic strength on membrane fouling and the retention of protein (Figs. 6.12&6.13). Increasing the ionic strength up to 0.01 resulted in a decrease in membrane resistance (superimposed on a slow increase in fouling with time).

At very low ionic strength the protein transmission was low with up to 70% of the protein retained by the membrane (Fig. 6.14). Above an ionic strength of 0.02 the protein transmission was greater than 90% as would be expected from a membrane of this pore size. In a separate experiment with the 50 nm membrane the effect of ionic strength on the clean membrane resistance was investigated (Fig. 6.15). Below an ionic strength of 0.025 the clean membrane resistance increased from around 31-32 to around 38 x 10^{10} /m. This corresponded to a 15% decrease in resistance which was smaller than the 30-40% decrease in resistance seen with ß-lactoglobulin. With ß-lactoglobulin the drop in membrane resistance with increasing ionic strength also reflected a decrease in protein retention and thus, in addition to the drop in the clean membrane resistance, the drop in resistance may be due to a decrease in the polarisation layer.

Nakao *et al.* (1988) found that the retentions of cytochrome C and myoglobin were affected by the charges on the proteins (changed by pH) and the membrane. Where similar charges existed the retention of the protein was increased. Thus it is possible that electrostatic repulsion of the protein from the pore may be responsible for the increased retention at low ionic strength as has recently been suggested by Saksena & Zydney (1994). At higher ionic strength charge neutralisation of the active groups by the increased salt presence would reduce the electrostatic effects allowing free passage of the protein through the pores. In addition, lowering the pH to 5.0, near the iso-electric point of the protein, resulted in a slightly lower retention of protein in spite of a higher degree of fouling (see Section 6.3.5), in keeping with a reduction in the electrostatic charge repulsion by the membrane.

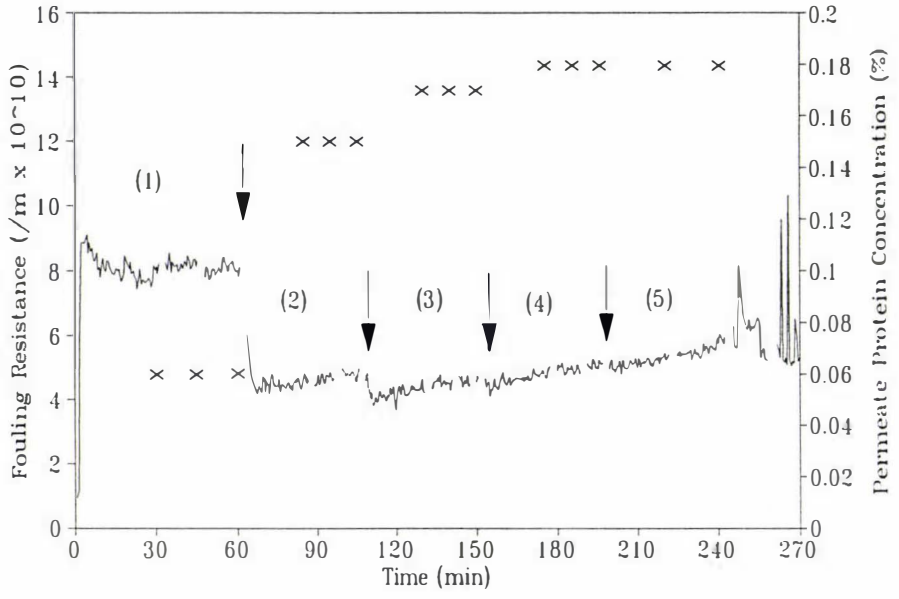

Figure 6.12. Effect of ionic strength (IS) on the fouling resistance (---) and the protein concentration in the permeate (x) as measured by spectrophotometer. Data shown is from trial 1: (1) IS 0.0009, pH 6.87; (2) IS 0.004, pH 6.71; (3) IS 0.0084, pH 6.64; (4) IS 0.0181, pH 6.56; (5) IS 0.0354, pH 6.48.

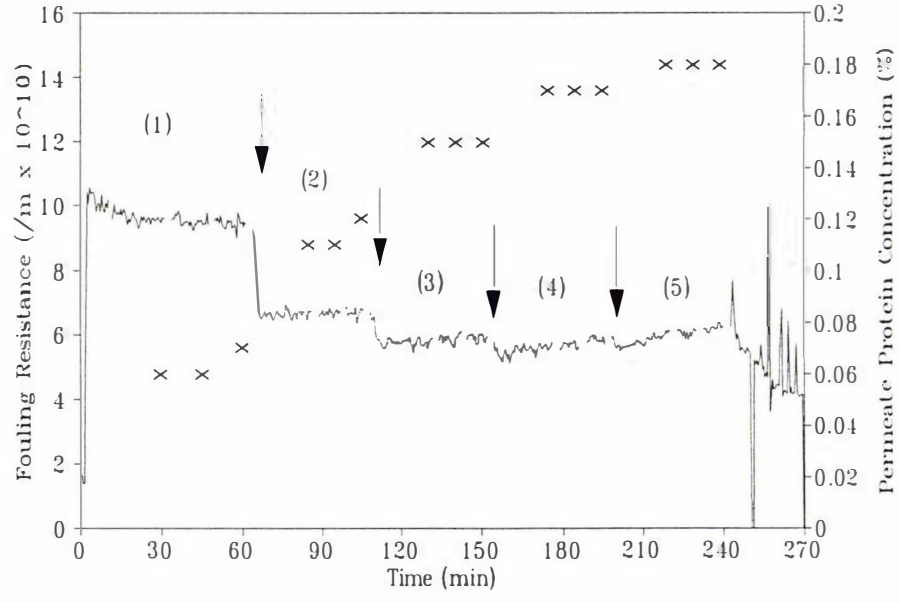

Figure 6.13. Effect of ionic strength (IS) on the fouling resistance (---) and the protein concentration in the permeate (x) as measured by spectrophotometer. Data shown is from trial 5: (1) IS 0.0009, pH 6.73; (2) IS 0.0021, pH 6.69; (3) IS 0.0042, pH 6.65; (4) IS 0.085, pH 6.58; (5) IS 0.0188, pH 6.49.

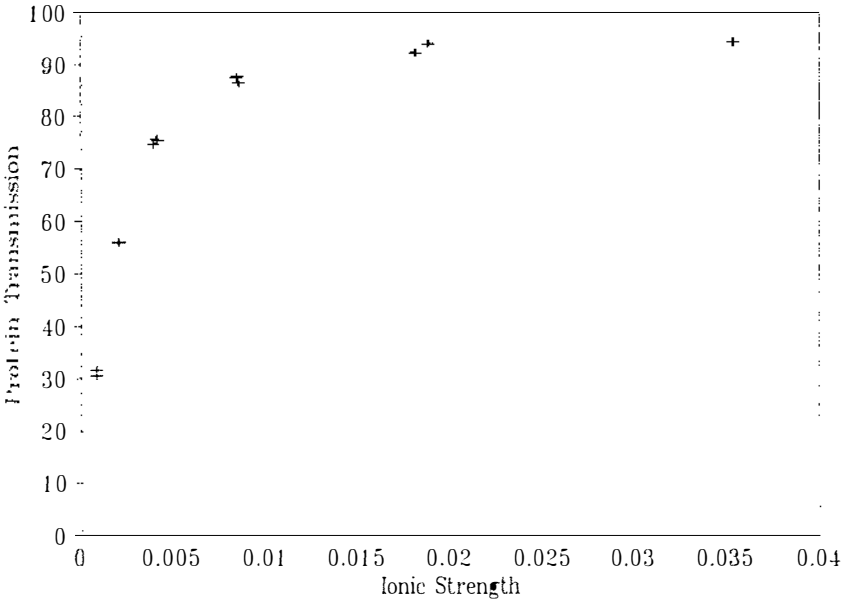

Figure 6.14. Effect of ionic strength (IS) on the protein transmission (+) of β-lactoglobulin on a 100 nm zirconium oxide membrane.

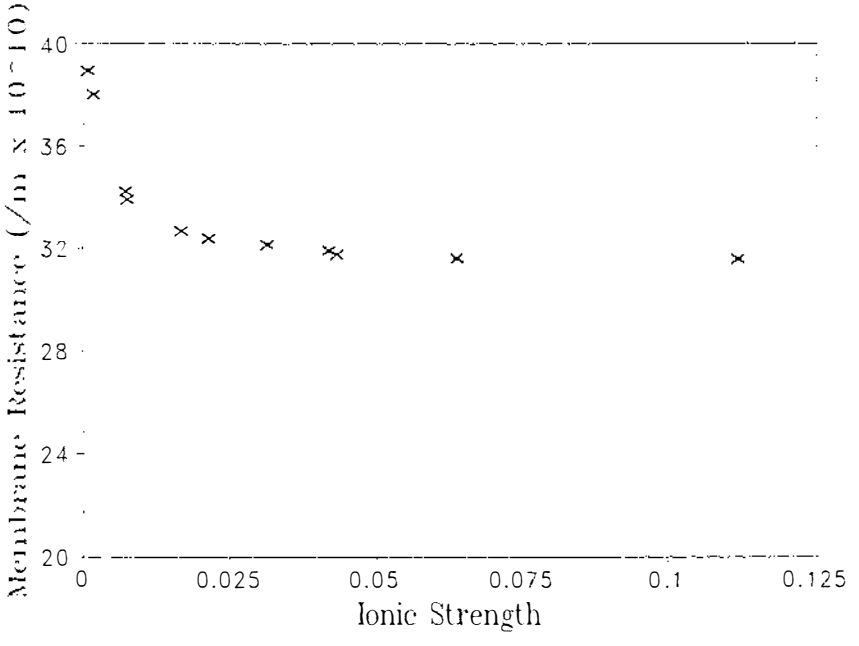

Figure 6.15. Effect of ionic strength (IS) on the clean membrane resistance of a 50 nm zirconium oxide membrane.

The equilibrium constants for zirconium oxide (ZrO_2) are $pK_1=4.8$ and $pK_2=10.4$ (Randon *et al.*, 1991; Dumon & Barnier, 1992). The distribution of surface charges depends upon the pH; the majority of the surface groups being:

$$\equiv ZrOH_2^+ \quad \text{at } pH<3.8$$
$$\equiv ZrOH \quad \text{at } 5.8<pH<9.4$$
$$\equiv ZrO^- \quad \text{at } pH>11.4$$

Thus at pH 6.2-6.7 the majority of the surface groups on the membrane will be neutral with a small number of positive groups leading to a slightly positive membrane charge: the opposite to the charge on the protein at this pH! At first glance this is contradictory to the concept of charge repulsion. However, the effect of protein monolayer adsorption must be considered. During the initial adsorption period negatively charged proteins bind to the slightly positive membrane surface, and after this the free proteins in solution would effectively see a negatively charged "protein surface" that was of similar charge to the free proteins.

Also of interest was the effect of ionic strength greater than 0.04 as this was the region where the majority of the experiments were performed. Increasing the ionic strength of the solution by the addition of NaCl in the range 0.047-0.12 had no obvious effect on the fouling resistance or the protein transmission of the membrane (Figs. 6.16&6.17).

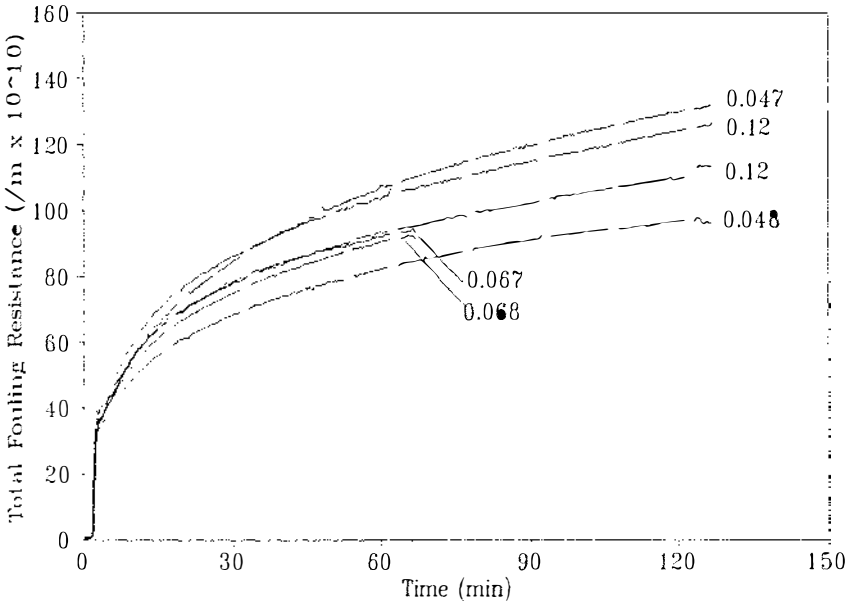

Figure 6.16. Effect of NaCl concentration (expressed as ionic strength) on the fouling resistance during MF of a 0.2% β-lactoglobulin solution at 200 L/m².h on a 50 nm membrane.

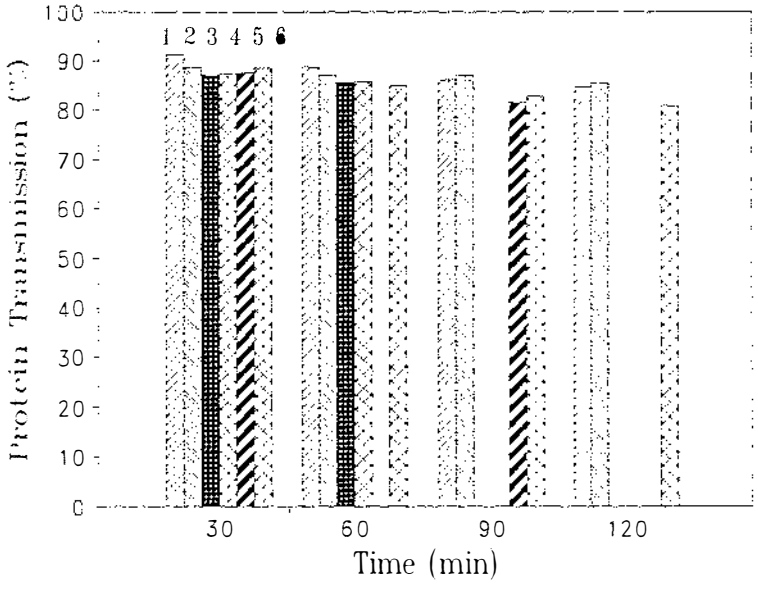

Figure 6.17. Effect of NaCl concentration on protein transmission during MF of a 0.2% β-lactoglobulin solution at 200 L/m².h on a 50 nm membrane. (1) & (2), IS 0.047-0.048; (3) & (4), IS 0.067-0.068; (5) & (6) IS 0.119-0.12.

6.3.5. Effect of pH

Two trials were performed on the 100 nm membrane at pH 5.0 near the iso-electric point of the protein. Reducing the pH increased the level of fouling although not sufficiently to decrease the protein transmission by the membrane (Fig. 6.18). In fact there is an indication that the protein transmission slightly increased with reduced pH in spite of the increased degree of fouling (Fig. 6.19). In these experiments the ionic strengths of the solutions were in the range 0.0086-0.0099. In this range electrostatic repulsion by the membrane may have a small effect on the transmission of protein. The increased transmission observed at pH 5.0 may be a result of the reduced protein charge minimising the effect of electrostatic repulsion.

The wild fluctuation in resistance in one of the trials at pH 5.0 was due to variations in the air supply pressure that affected the permeate control valve. The disturbance that resulted in short-term variations in the permeate flux both up and down did not affect the long-term time-resistance curve as evidenced by a comparison with the trial where no disturbance occurred.

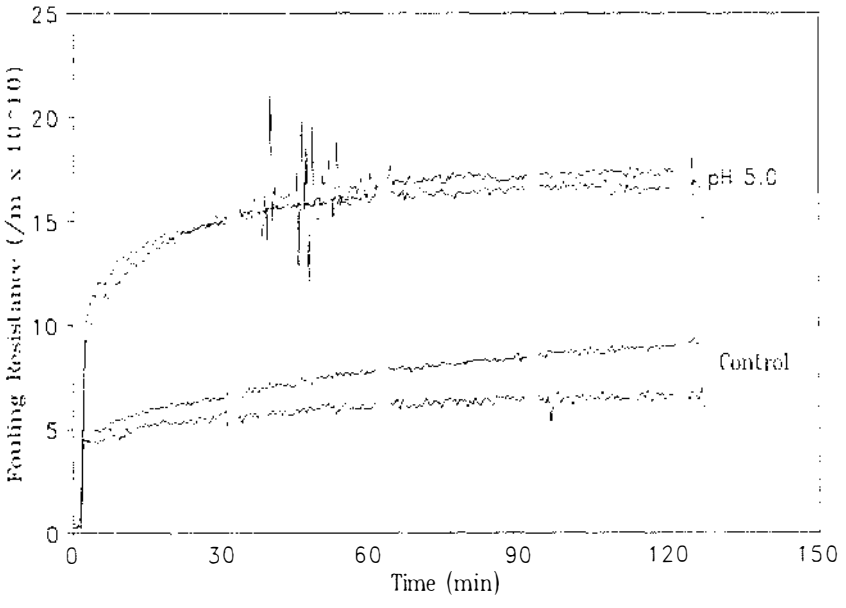

Figure 6.18. Effect of pH 5.0 on the fouling resistance during MF of a 0.2% β-lactoglobulin solution at 50 L/m².h on a 100 nm membrane. The ionic strength of the solutions were 0.0086 to 0.0099, and the pH of the controls 6.5 to 6.7.

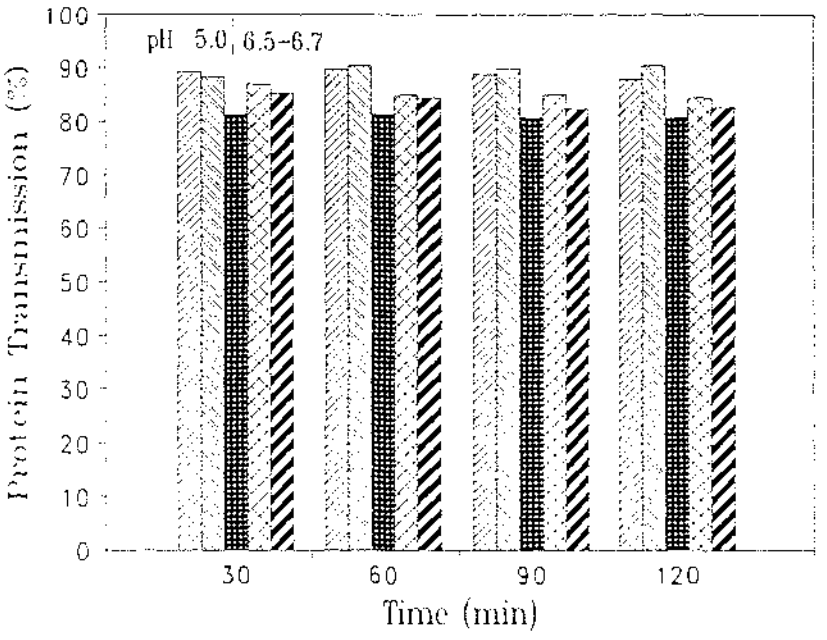

Figure 6.19. Effect of pH 5.0 on the protein transmission during MF of a 0.2% β-lactoglobulin solution at 50 L/m².h on a 100 nm membrane. The ionic strength of the solutions were 0.0086 to 0.0099.

6.3.6. Effect of the permeate flux

Trials were performed on the 100 and 50 nm membranes. With both membranes and in the absence of calcium the membrane resistance was higher at higher flux. The major difference occurred in the first hour of operation and had no significant effect on the protein transmission (Figs. 6.20-6.23). Indeed, the protein transmission appeared to be slightly higher at higher flux on the 100 nm membrane in spite of the increased fouling resistance, perhaps because of increased concentration polarisation. However, the effect is not so marked with the 50 nm membrane when trials were performed at a higher ionic strength suggesting perhaps that in some way the higher flux has influenced the electrostatic repulsion by the membrane.

In the presence of calcium quite different behaviour was observed. Starting first with the 50 nm membrane, fouling increased dramatically if the permeate flux was increased (Figs. 6.24&6.25). Furthermore the transmission of protein through the membrane diminished with higher permeate fluxes (Figs. 6.26&6.27). From these spectrophotometer data (Fig. 6.26) it can be seen that the protein transmission in runs at 50 $L/m^2.h$ did not decrease with time, whereas, the transmission decreased with time for all of the higher fluxes, more severely as the flux increased. Similar trends can be seen in data obtained from the UV-cell (Fig. 6.27). Initially the apparent transmission of protein was zero. Then it increased rapidly to a maximum value as the water initially in the permeate chamber was removed. Thereafter the transmission decreased as fouling increased. Similar data was obtained for the 100 nm membrane (Figs. 6.28&6.29).

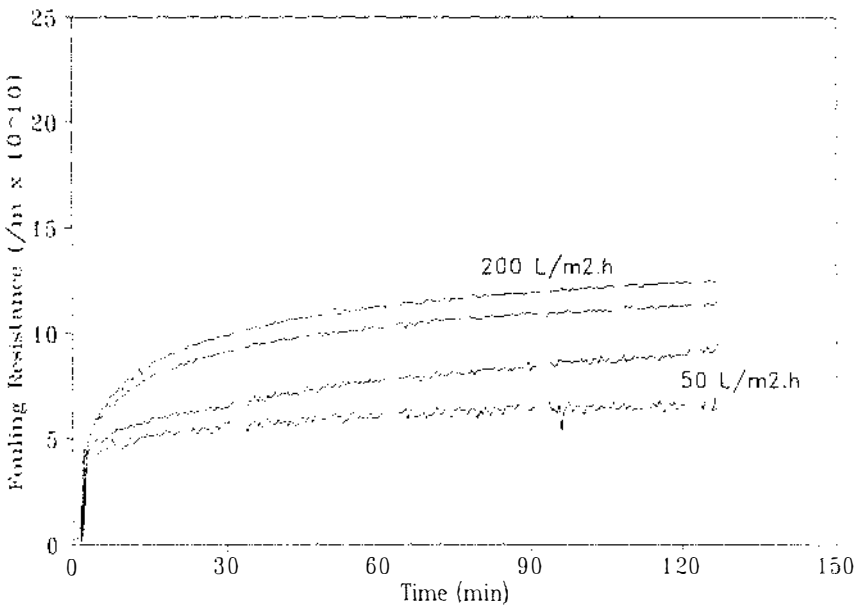

Figure 6.20. Effect of the permeate flux on the fouling resistance during MF of a 0.2% β-lactoglobulin solution in the absence of calcium on a 100 nm membrane. The ionic strength of the solutions was 0.0086 to 0.0099 and the pH from 6.5 to 6.7.

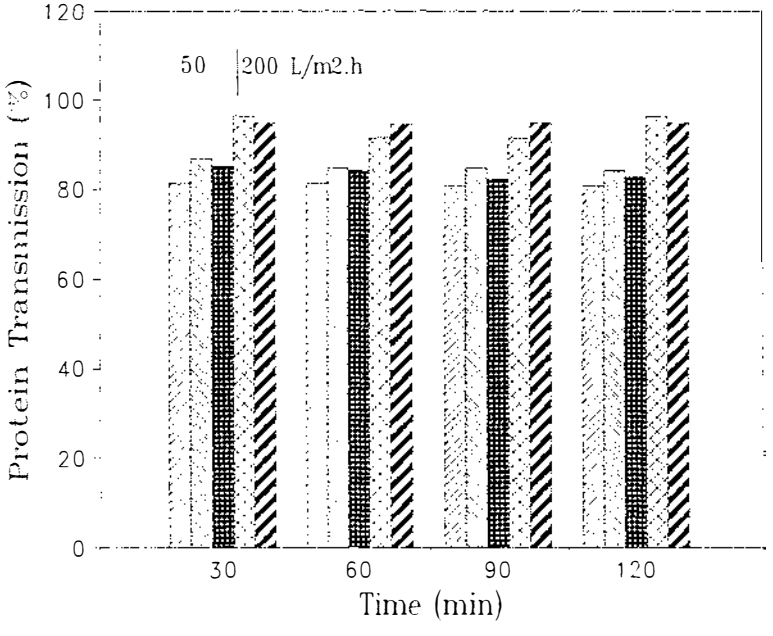

Figure 6.21. Effect of the permeate flux on the protein transmission during MF of a 0.2% β-lactoglobulin solution in the absence of calcium on a 100 nm membrane. The ionic strength of the solutions was 0.0086 to 0.0099 and the pH from 6.5 to 6.7.

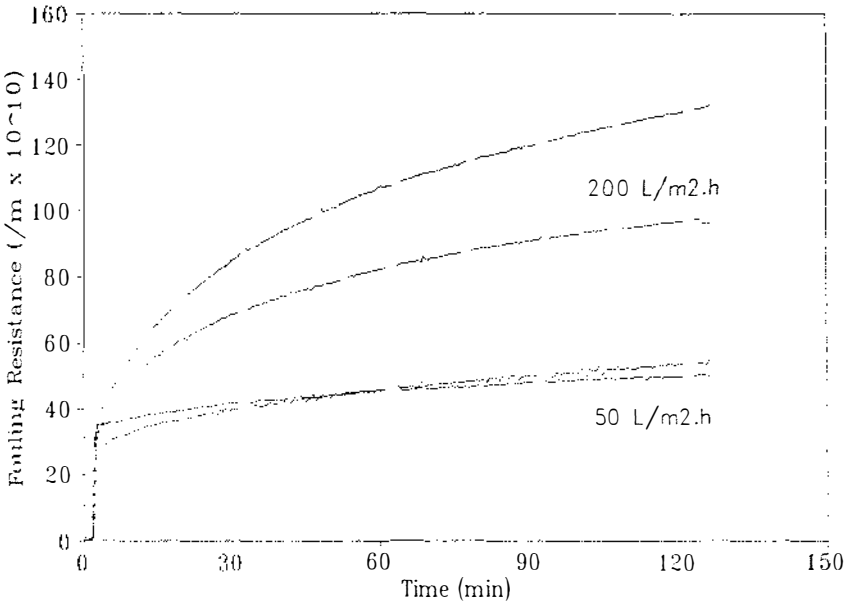

Figure 6.22. Effect of the permeate flux on the fouling resistance during MF of a 0.2% β-lactoglobulin solution in the absence of calcium on a 50 nm membrane. The ionic strength of the solutions was 0.047 to 0.048 and the pH from 6.3 to 6.5.

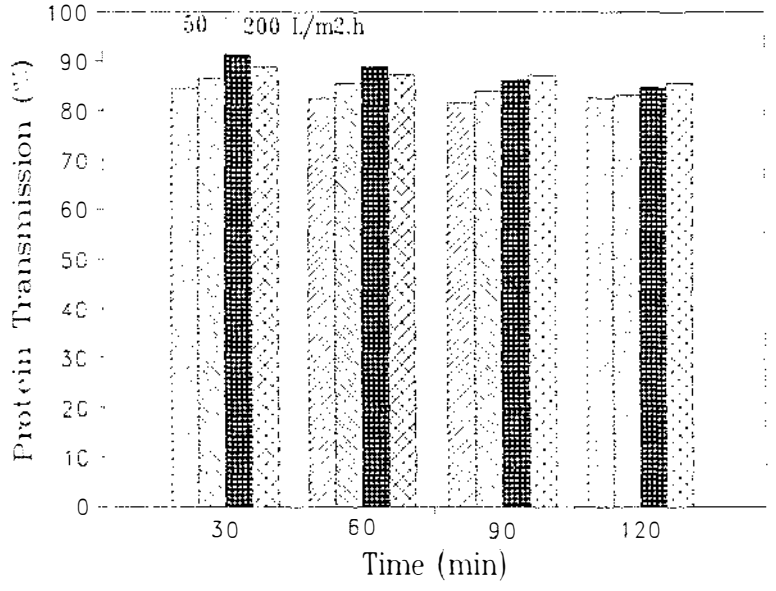

Figure 6.23. Effect of the permeate flux on the protein transmission during MF of a 0.2% β-lactoglobulin solution in the absence of calcium on a 50 nm membrane. The ionic strength of the solutions was 0.047 to 0.048 and the pH from 6.3 to 6.5.

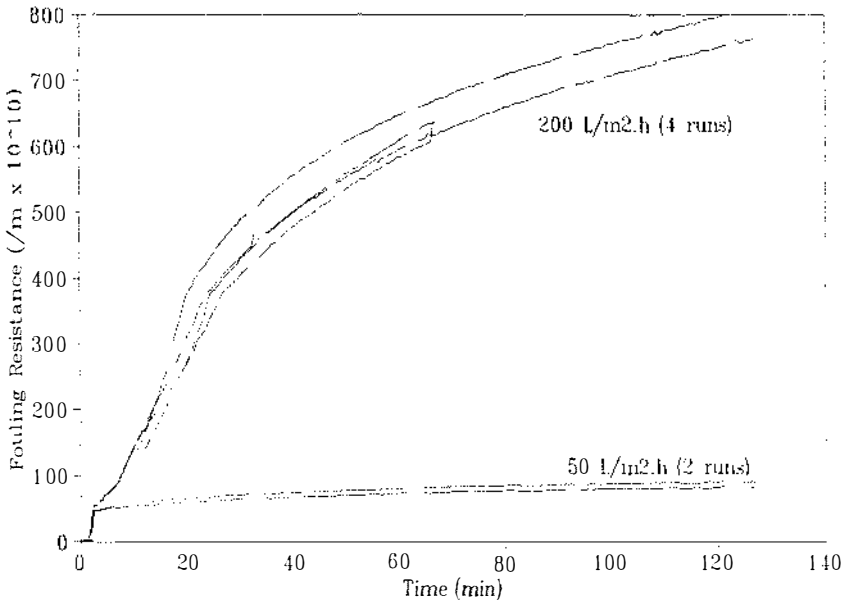

Figure 6.24. Effect of the permeate flux on the fouling resistance during MF of a 0.2% β-lactoglobulin solution in the presence of calcium on a 50 nm membrane. The ionic strength of the solutions was 0.0568 to 0.0575, the calcium content from 8.0-8.4 mmol/L and the pH from 6.2 to 6.4.

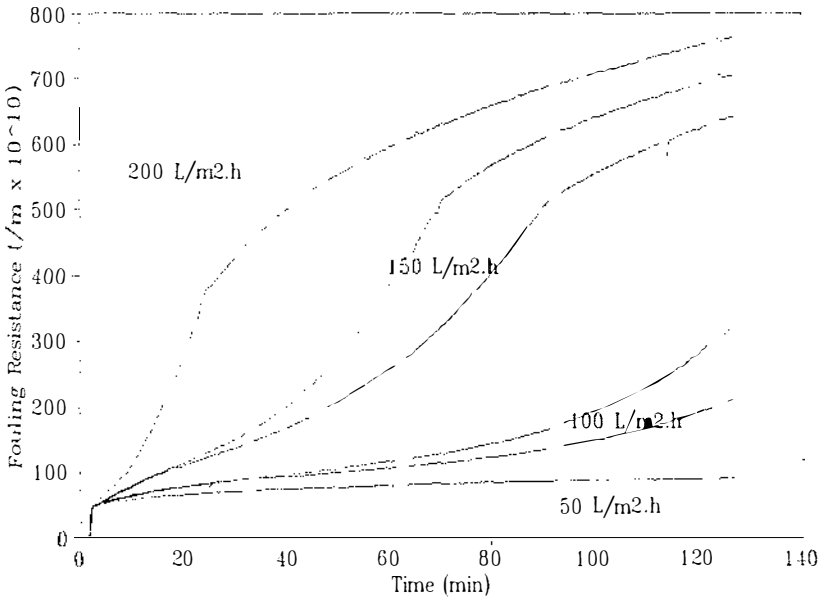

Figure 6.25. Effect of the permeate flux on the fouling resistance during MF of a 0.2% β-lactoglobulin solution in the presence of calcium on a 50 nm membrane. The trials at 50 and 200 L/m².h from Fig. 6.26 are shown for comparison. The ionic strength of the solutions was 0.0568 to 0.0577, the calcium content from 8.0-8.5 mmol/L and the pH from 6.2 to 6.4.

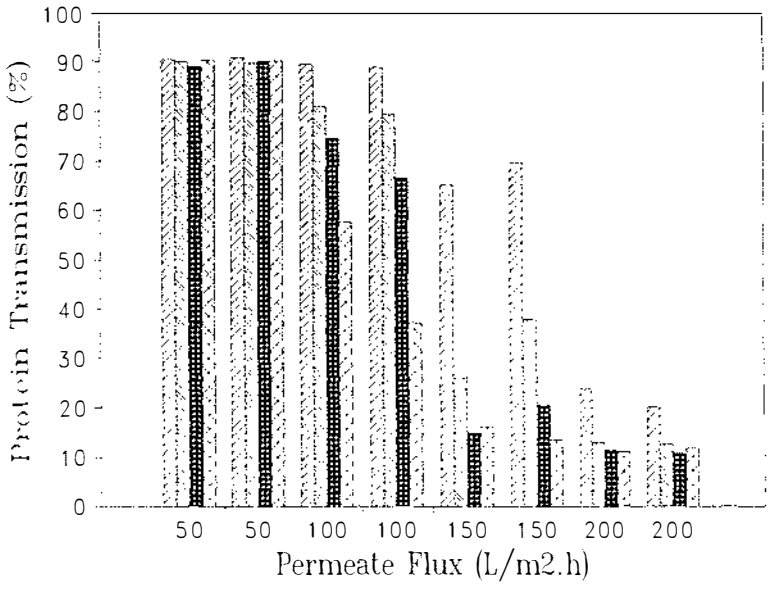

Figure 6.26. Effect of the permeate flux on protein transmission during MF of a 0.2% β-lactoglobulin solution in the presence of calcium on a 50 nm membrane. The ionic strength of the solutions was 0.0568 to 0.0577, the calcium content from 8.0-8.5 mmol/L and the pH from 6.2 to 6.4. For each permeate flux the 4 bars represent values measured at 30, 60, 90 and 120 min respectively.

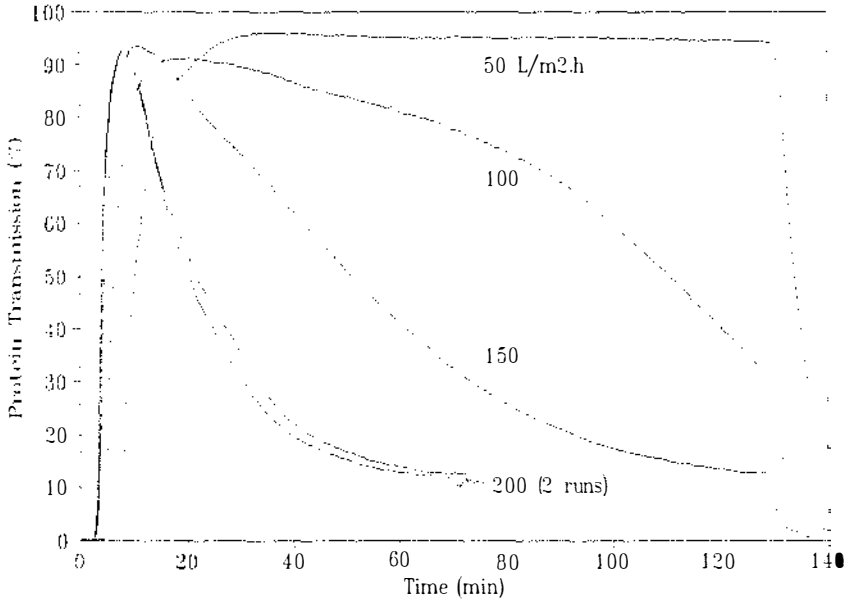

Figure 6.27. Effect of the permeate flux on the protein transmission (as measured by a UV-cell) during MF of a 0.2% β-lactoglobulin solution in the presence of calcium on a 50 nm membrane. The ionic strength of the solutions was 0.0568 to 0.0577, the calcium content from 8.0-8.5 mmol/L and the pH from 6.2 to 6.4.

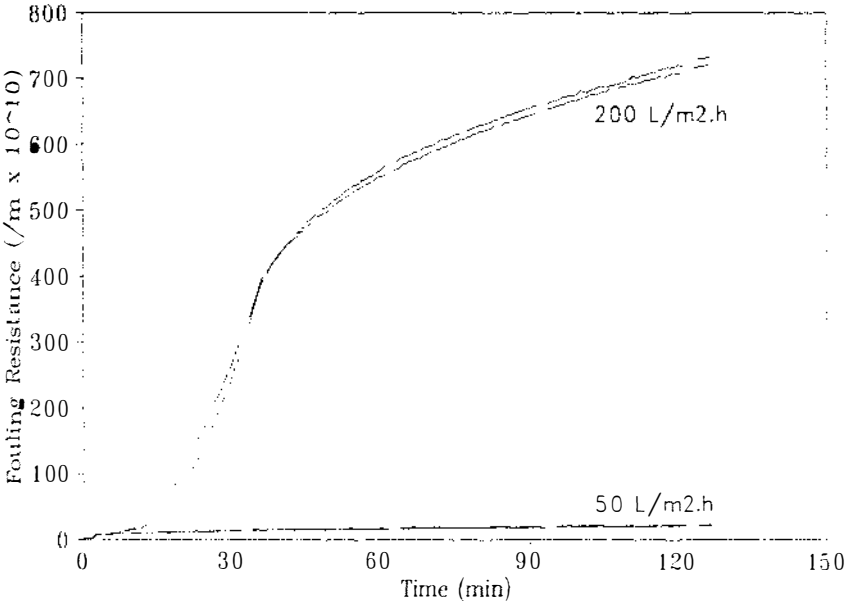

Figure 6.28. Effect of the permeate flux on the fouling resistance during MF of a 0.2% β-lactoglobulin solution in the presence of calcium on a 100 nm membrane. The ionic strength of the solutions was 0.0268-0.0278 for the runs at 50 L/m².h and 0.0567-0.0580 for the runs at 200 L/m².h, the calcium content from 7.6-8.6 mmol/L and the pH from 6.1 to 6.4.

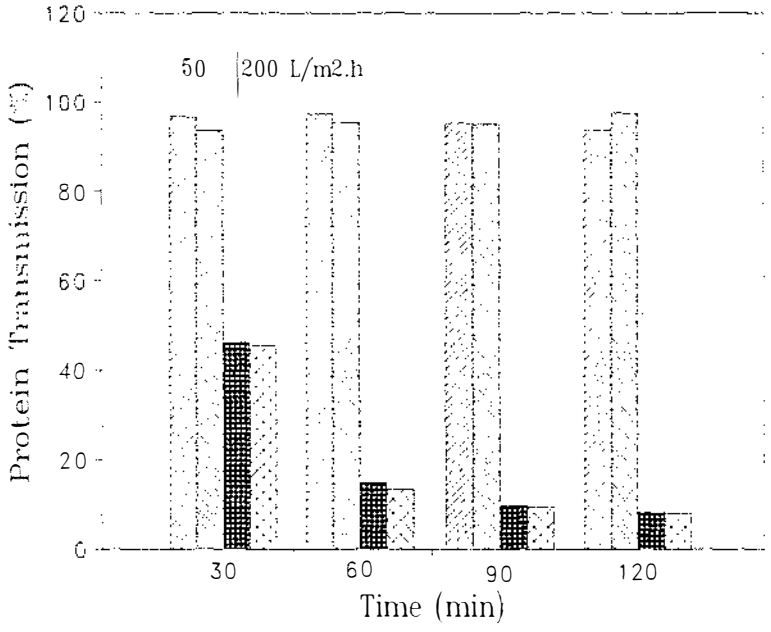

Figure 6.29. Effect of the permeate flux on the protein transmission during MF of a 0.2% β-lactoglobulin solution in the presence of calcium on a 100 nm membrane. The ionic strength of the solutions was 0.0268-0.0278 for the runs at 50 L/m².h and 0.0567-0.0580 for the runs at 200 L/m².h, the calcium content from 7.6-8.6 mmol/L and the pH from 6.1 to 6.4.

A comparison of the irreversible and reversible fouling showed that the majority of the increase in resistance seen with higher permeate fluxes was reversible (Fig. 6.30). See the previous discussion on the results at 200 L/m^2.h in Section 6.3.3. The irreversible resistance did not appear to change significantly with increasing flux up to 150 L/m^2.h. Furthermore the irreversible resistance was similar in magnitude to that observed in the absence of calcium (Fig. 6.31). In the absence of calcium reducing the flux decreased the irreversible resistance by a small amount.

If a pore narrowing model is assumed then the apparent reduction in pore diameter can be calculated from the irreversible resistance data (Zeman, 1983). Using this analysis the pore size reduction in the trials with calcium on the 50 nm membrane were generally around 13-14 nm for permeate fluxes in the range 50-150 L/m^2.h. Similar results were obtained in trials without calcium at 200 L/m^2.h on the 50 nm membrane. In trials without calcium at 50 L/m^2.h, on both the 50 and 100 nm membranes the pore size reduction was around 9-10 nm.

It is reasonable to expect that the protein transmission should decrease as the membrane fouling increases. To explore this relationship further, all of the transmission results (measured by spectrophotometer) from trials on the 50 nm membrane were plotted against the fouling resistance measured at an equivalent time in each of the trials (Fig. 6.32). For the trials without calcium the points accumulated in the top left hand corner of the graph because of the absence of serious fouling. For trials with calcium the points all fitted on or near a single curve that decreased rapidly for fouling resistances in the range 120-300 x 10^{10}/m and more slowly thereafter. Varying the permeate flux did not appear to affect the relationship between fouling and transmission; however, varying the cross-flow velocity or retentate recirculation rate did (see Section 6.3.8 for a discussion of cross-flow velocity). The significance of these relationships will be considered in more detail in the discussion (Section 6.4).

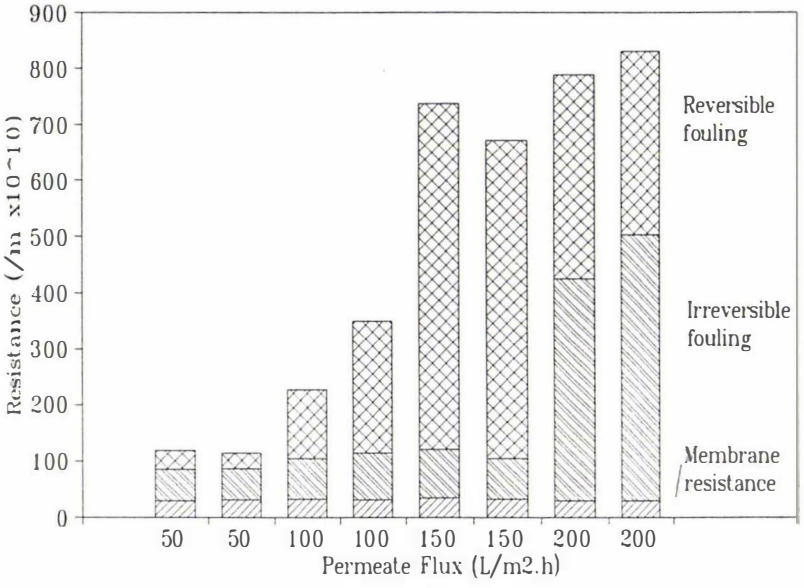

Figure 6.30. Effect of the permeate flux on the irreversible and reversible fouling during MF of a 0.2% β-lactoglobulin solution in the presence of calcium on a 50 nm membrane. The ionic strength of the solutions was 0.0568 to 0.0577, the calcium content from 8.0-8.5 mmol/L and the pH from 6.2 to 6.4.

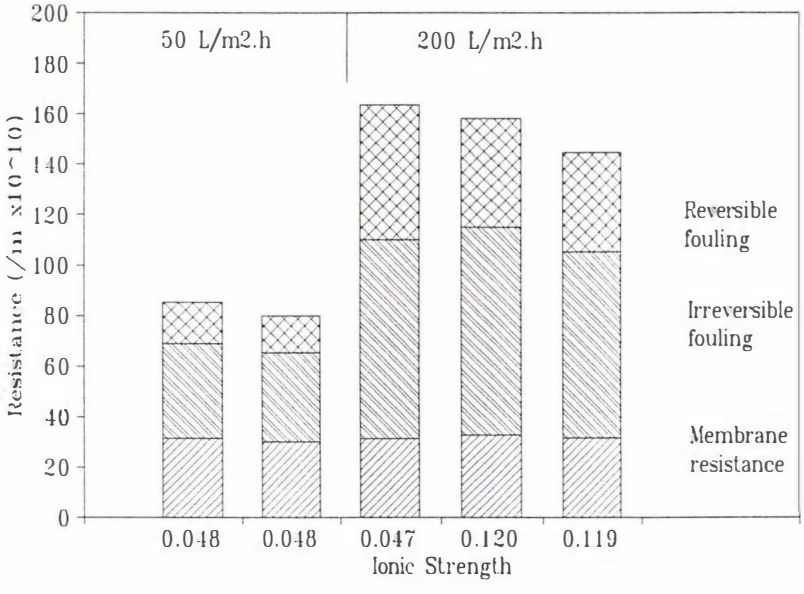

Figure 6.31. Effect of the permeate flux on the irreversible and reversible fouling during MF of a 0.2% β-lactoglobulin solution in the absence of calcium on a 50 nm membrane.

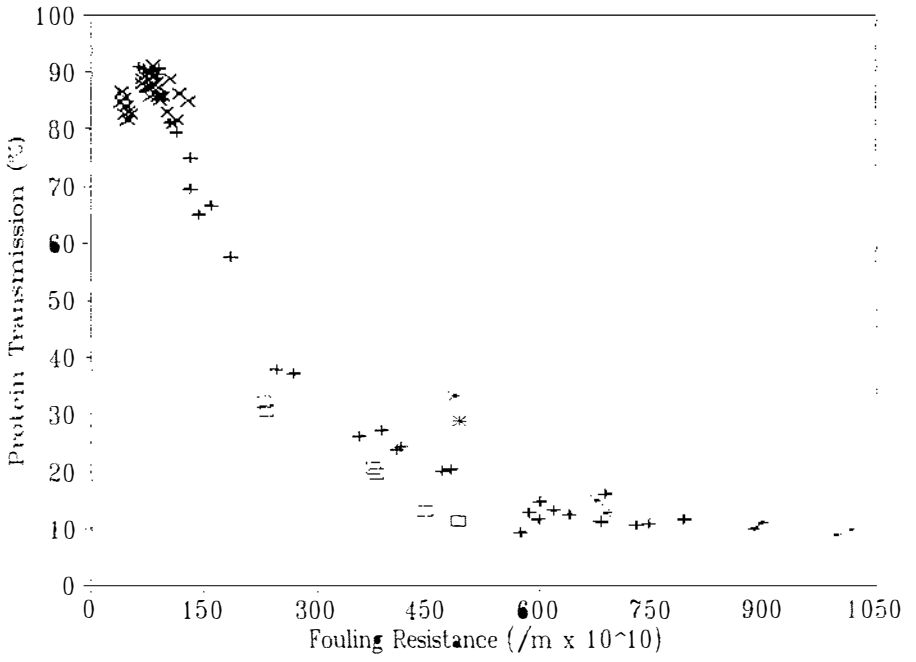

Figure 6.32. Protein transmission versus the fouling resistance for the 50 nm membrane: (x) data collected from trials without calcium; (+) trials with calcium (*) trials at a recirculation rate of 260 L/h; (□) trials at a recirculation rate of 540 L/h.

6.3.7. Effect of calcium

At 50 L/m^2.h on both the 50 and 100 nm membranes the presence of calcium increased the fouling resistance (Figs. 6.33&6.34). In spite of this, the transmission of protein through the membranes increased especially for the 100 nm membrane (Figs. 6.35&6.36). With the 100 nm membrane the ionic strength of the solution was increased significantly by the addition of calcium and the pH of the solution dropped; both effects would have reduced the electrostatic repulsion by the membrane thus giving rise to an increase in protein transmission. These effects were smaller with the 50 nm membrane as the overall ionic strength was higher and the pH shift smaller. The addition of calcium at 50 L/m^2.h did increase the apparent pore size reduction from 9-10 to 18-22 nm for the 100 nm membrane and from 9 to 11-12 nm for the 50 nm membrane.

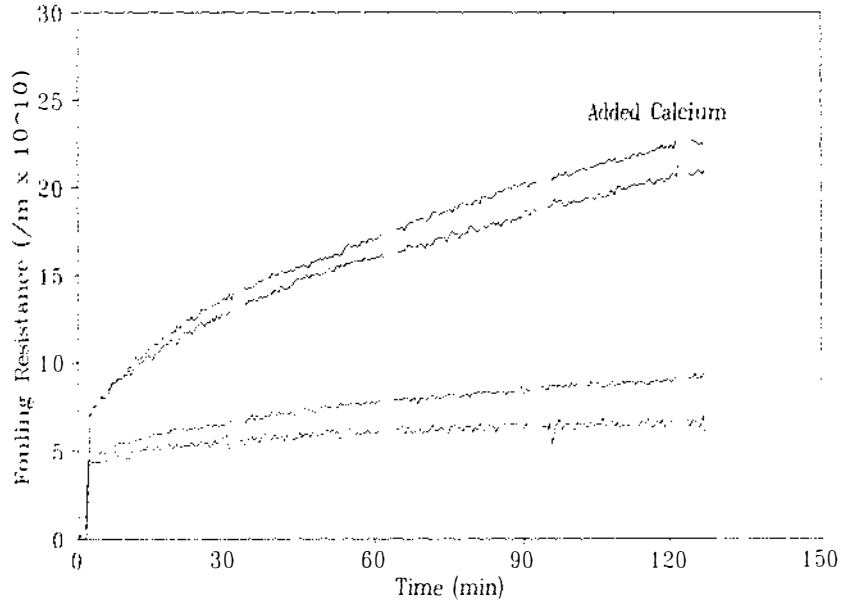

Figure 6.33. Effect of the addition of calcium on the fouling resistance during MF of a 0.2% β-lactoglobulin solution on a 100 nm membrane at 50 L/m².h. The ionic strength of the solutions was 0.0086 to 0.0099 and the pH 6.6 to 6.7 for the trials without calcium and 0.0268 to 0.0278 and pH 6.1 to 6.2 for the trials with calcium. The calcium content was 7.6-7.9 mmol/L.

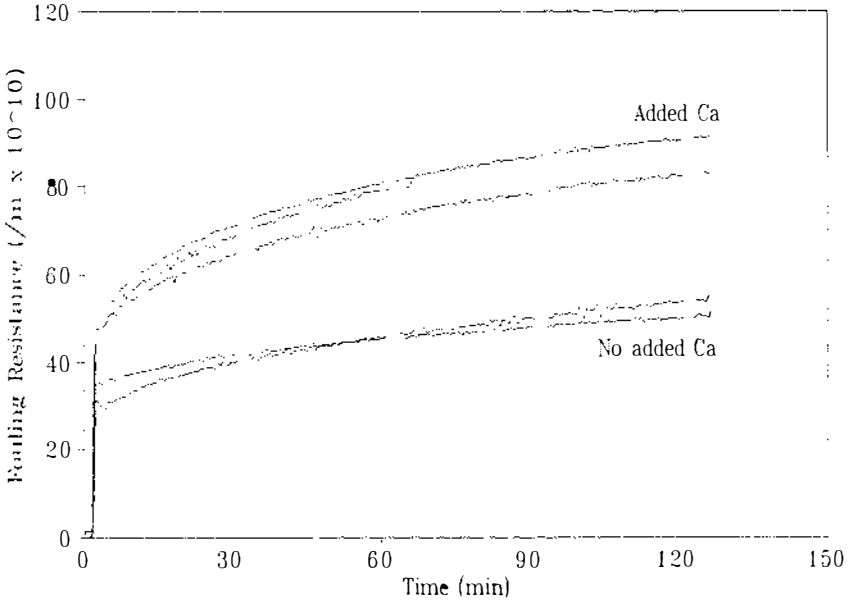

Figure 6.34. Effect of the addition of calcium on the fouling resistance during MF of a 0.2% β-lactoglobulin solution on a 50 nm membrane at 50 L/m².h. The ionic strength of the solutions was 0.0468 to 0.0469 and the pH 6.3 to 6.4 for the trials without calcium and 0.0569 to 0.0572 and pH 6.2 to 6.4 for the trials with calcium. The calcium content was 8.0-8.3 mmol/L.

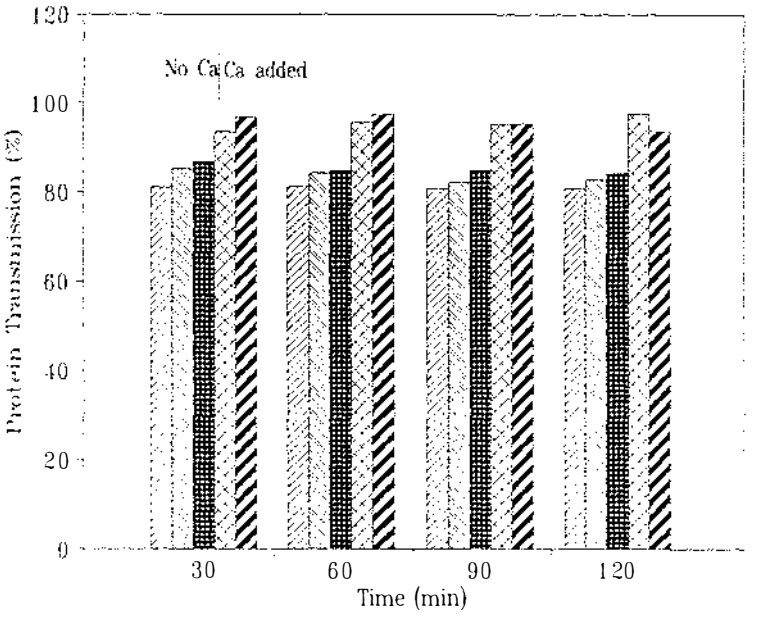

Figure 6.35. Effect of the addition of calcium on the protein transmission during MF of a 0.2% β-lactoglobulin solution on a 100 nm membrane at 50 L/m².h. The ionic strength of the solutions was 0.0086 to 0.0099 and the pH 6.6 to 6.7 for the trials without calcium and 0.0268 to 0.0278 and pH 6.1 to 6.2 for the trials with calcium. The calcium content was 7.6-7.9 mmol/L.

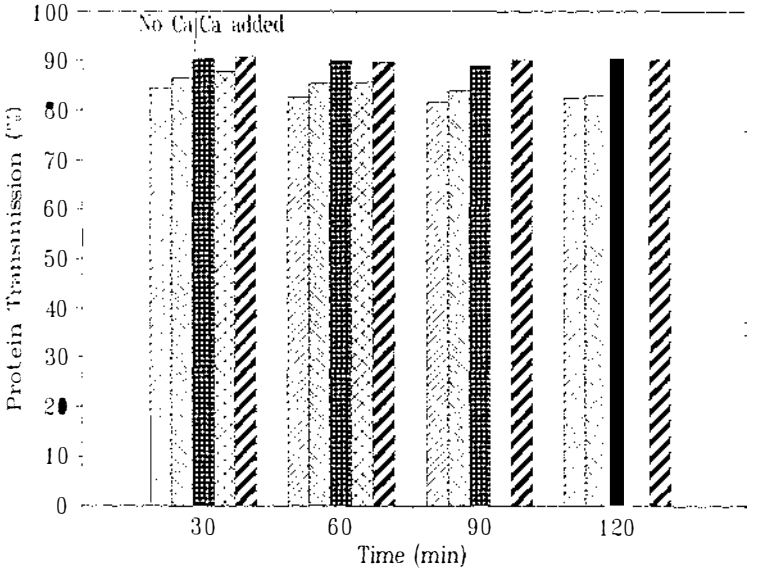

Figure 6.36. Effect of the addition of calcium on the protein transmission during MF of a 0.2% β-lactoglobulin solution on a 50 nm membrane at 50 L/m².h. The ionic strength of the solutions was 0.0468 to 0.0469 and the pH 6.3 to 6.4 for the trials without calcium and 0.0569 to 0.0572 and pH 6.2 to 6.4 for the trials with calcium. The calcium content was 8.0-8.3 mmol/L.

At 200 L/m^2.h, the addition of approximately 8 mmol/L calcium caused severe fouling on both the 100 and 50 nm membranes (Figs. 6.37&6.38) and had a major impact on the protein transmission (Figs. 6.39&6.40) indicating that the apparent pore size of the membrane has been significantly reduced. Two trials were performed on the 50 nm membrane with intermediate calcium concentrations. Fouling was not as severe as with higher calcium concentrations and the ionic strength appeared to interact with the calcium level as the trial with 4 mmol/L calcium (higher ionic strength) fouled less than the trial with 2 mmol/L. This area will be discussed more in Section 6.4.

Flushing the membrane with water at the completion of ß-lactoglobulin filtration removed the majority of the fouling (Fig. 6.11) with the irreversible fouling being reasonably constant regardless of the operating conditions used. This indicated that the additional fouling caused by the combination of high calcium and high flux was mostly reversible.

To further investigate the impact of calcium on fouling, trials were performed: (a) where calcium was added after 1 h operation without calcium; and (b) where after 1 h a protein solution without calcium was substituted in place of the original solution containing calcium. When calcium was added after 1 h, the rate of fouling increased due to the presence of calcium and the protein transmission decreased (Fig. 6.41). Interestingly, there was a brief increase in protein transmission immediately following the addition of calcium, further indicating that when fouling is light the presence of calcium in some way increases protein transmission. With increased fouling this benefit was lost. The rate of fouling increase was less than that in trials where calcium was present from the beginning (Figs. 6.38&6.42). This suggested that the state of the proteins initially bound to the membrane (adsorption) impact in some way on the further deposition of protein on the membrane. This will be discussed in more depth in Section 6.4.

The trials where a calcium-free protein solution was substituted for the initial protein solution containing calcium gave the opportunity to investigate the impact of removing calcium alone in contrast to the flushing data where both the protein and

calcium were removed. Upon the removal of calcium there was an immediate rapid reduction in the fouling resistance, and surprisingly a small drop in protein transmission, in spite of the drop in fouling and an increase in ionic strength. Again this suggested that calcium in some specific way improves the transmission of the protein through the membrane. The fouling resistance continued to drop to around $200x10^{10}$/m and the protein transmission increased to around 50-60%. A resistance of $200x10^{10}$/m is higher than the 120-140$x10^{10}$/m observed in trials without calcium but is considerably smaller than the resistance observed with calcium present for the entire run ($800x10^{10}$). These results show that the majority of the reversible fouling seen with high flux and calcium is stabilised by the presence of calcium and that, upon leaching of the calcium from the deposit, the deposit "redissolves" and the apparent pore size of the membrane increases.

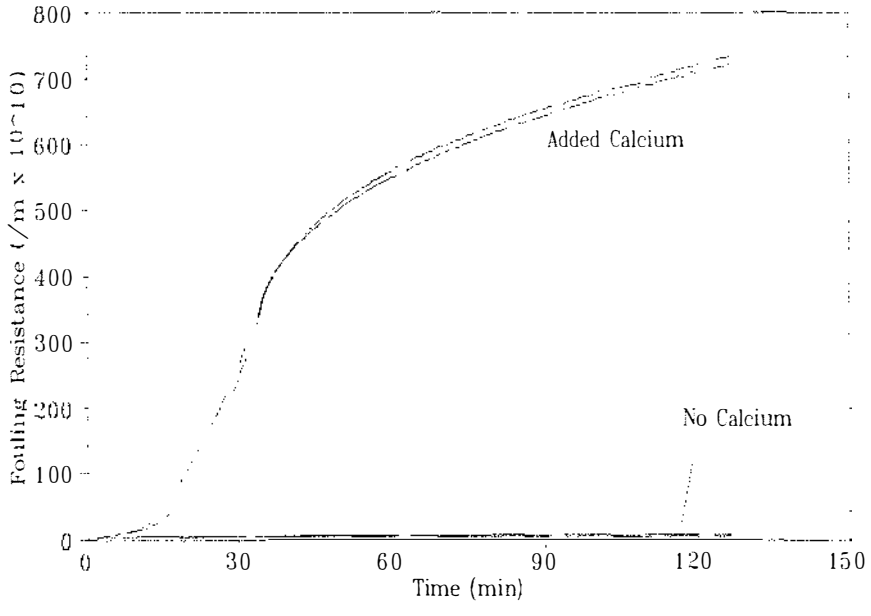

Figure 6.37. Effect of the addition of calcium on the fouling resistance during MF of a 0.2% β-lactoglobulin solution on a 100 nm membrane at 200 L/m².h. The ionic strength of the solutions was 0.0086 to 0.0099 and the pH 6.6 to 6.7 for the trials without calcium and 0.0567 to 0.0580 and pH 6.3 to 6.4 for the trials with calcium. The calcium content was 8.0-8.6 mmol/L.

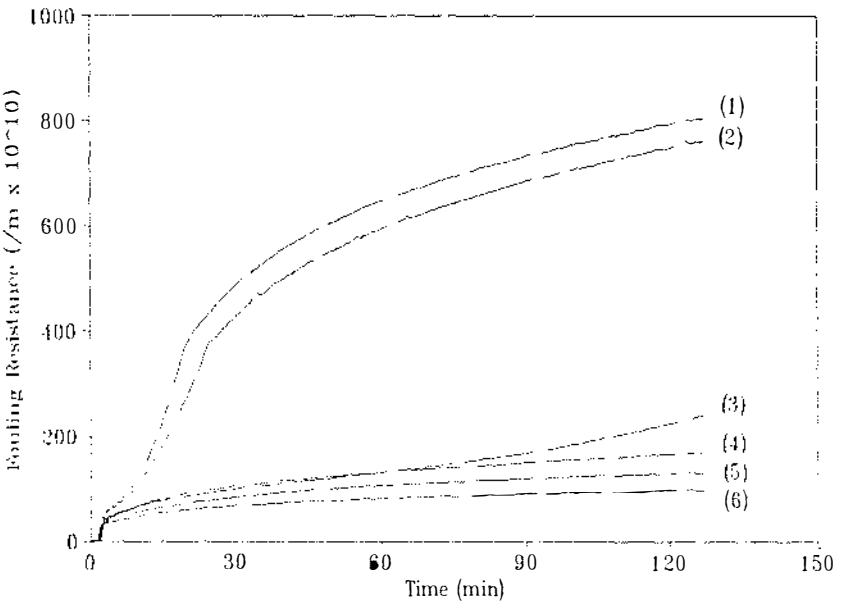

Figure 6.38. Effect of the addition of calcium on the fouling resistance during MF of a 0.2% β-lactoglobulin solution on a 50 nm membrane at 200 L/m².h: (1) & (2), 8.14-8.24 mmol/L calcium, I.S 0.0568-0.0570, pH 6.2; (3) 2.04 mmol/L calcium, I.S 0.0666, pH 6.4; (4) 4.12 mmol/L calcium, I.S 0.0822, pH 6.4; (5) & (6) no calcium, I.S 0.0465-0.0476, pH 6.4-6.6.

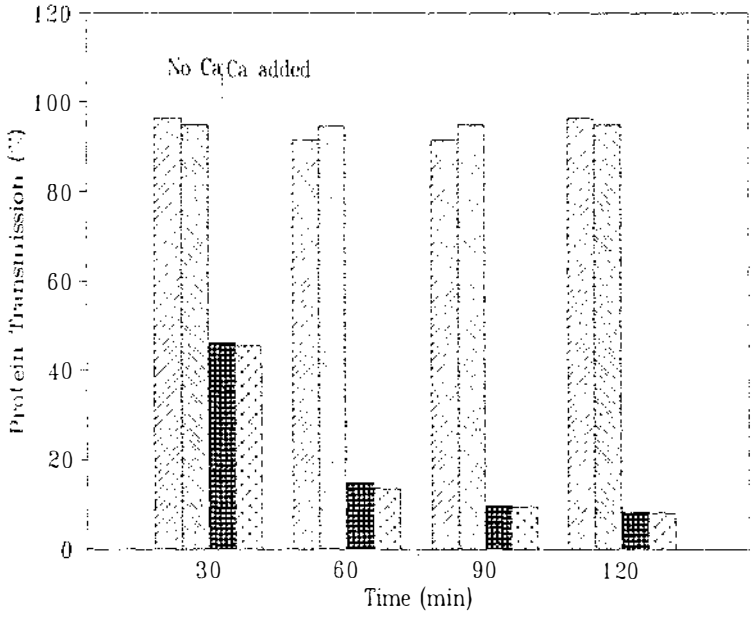

Figure 6.39. Effect of the addition of calcium on the protein transmission during MF of a 0.2% β-lactoglobulin solution on a 100 nm membrane at 200 L/m².h. The ionic strength of the solutions was 0.0086 to 0.0099 and the pH 6.6 to 6.7 for the trials without calcium and 0.0567 to 0.0580 and pH 6.3 to 6.4 for the trials with calcium. The calcium content was 8.0-8.6 mmol/L.

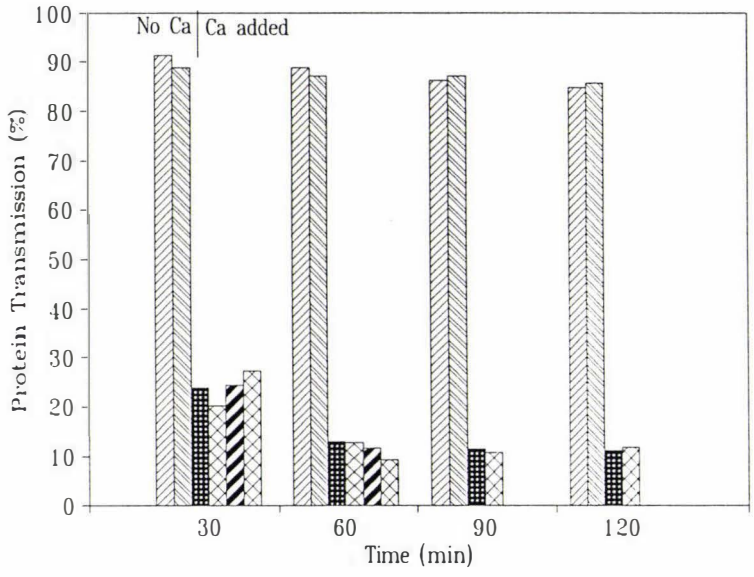

Figure 6.40. Effect of the addition of calcium on the protein transmission during MF of a 0.2% β-lactoglobulin solution on a 50 nm membrane at 200 L/m².h. In trials with calcium: 8.14-8.24 mmol/L calcium, I.S 0.0568-0.0570, pH 6.2-6.4; in trials without calcium, I.S 0.0465-0.0476, pH 6.4-6.6.

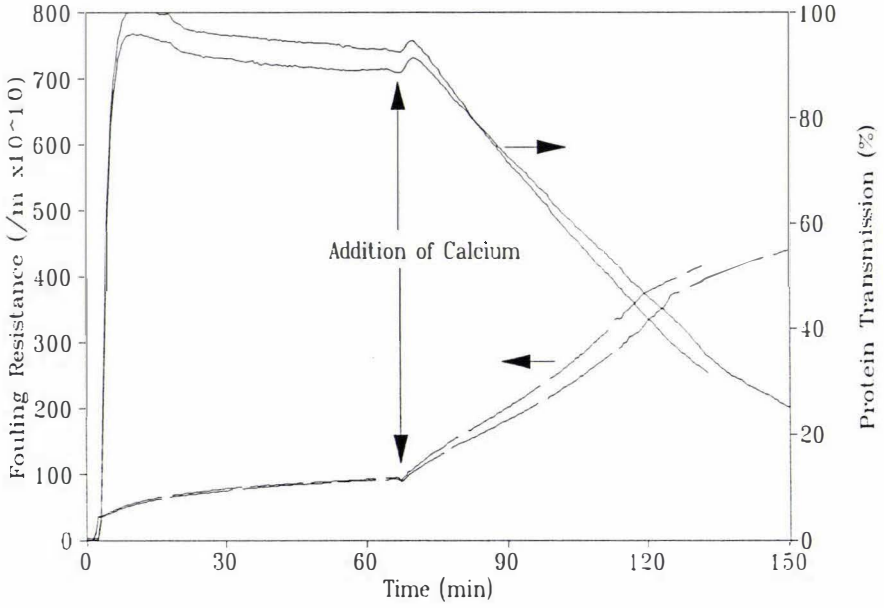

Figure 6.41. Effect of the addition of calcium after 1 h on the fouling resistance and protein transmission during MF of a 0.2% β-lactoglobulin solution on a 50 nm membrane at 200 L/m².h. Prior to the addition of calcium the ionic strength of the solutions was 0.0677 and the pH 6.4 to 6.5; after the addition of calcium the I.S. was 0.0918 to 0.0920 and the pH 6.3. The calcium content was 8.0 mmol/L.

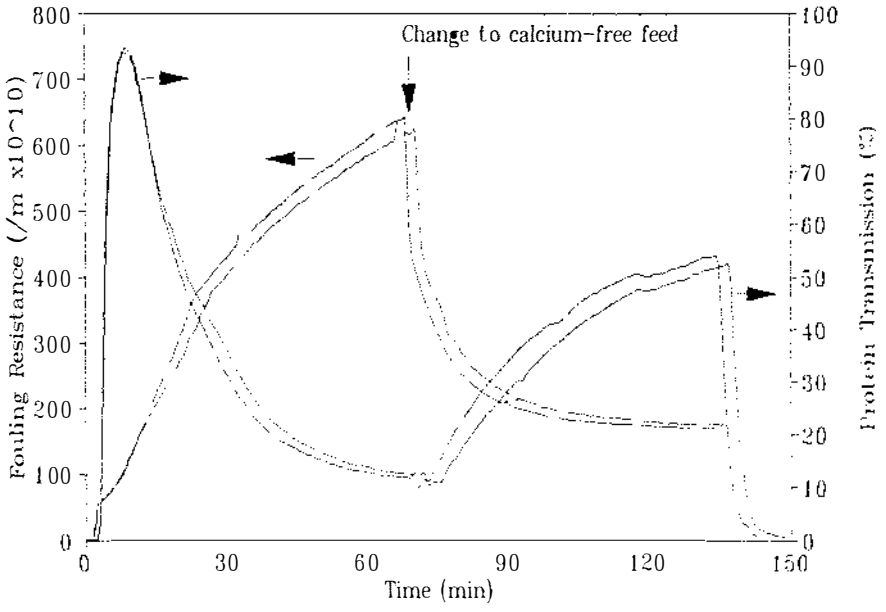

Figure 6.42. Effect of the removal of calcium after 1 h on the fouling resistance and protein transmission during MF of a 0.2% β-lactoglobulin solution on a 50 nm membrane at 200 L/m².h. Prior to the removal of calcium the ionic strength of the solutions was 0.0574, the pH 6.3 to 6.4 and the calcium content was 8.3-8.4 mmol/L; after the removal of calcium the I.S. was 0.0674 and the pH 6.3-6.4. Chemical analysis of samples indicated that the calcium content after calcium removal was 0-0.2 mmol/L.

The transmission data (measured by UV cell) were compared with the fouling resistance data (Fig. 6.43). The first hours data from the trial when calcium was present initially was the same as the data in Fig. 6.32 and showed the "standard relationship" between resistance and protein transmission. In the trial when there was no calcium initially the data collected in the top left hand corner of the graph in keeping with the lack of fouling under these conditions. Upon the addition of calcium after 1 h there was a jump in transmission, in keeping with the observation that the presence of calcium increases transmission, followed by a steady decline in transmission with time. The shape of the transmission-resistance curve for this period was similar to that for the standard conditions, indicating that although the rate of fouling was slower than in the cases where calcium was present from the start, the fouling mechanism appeared similar. When calcium was removed from the system

the resistance dropped quickly. The transmission-resistance relationship for this period of the run was different to that observed under standard conditions. For the same resistance transmission was lower. The change in resistance occurred very quickly in the drop from 700-300x10^{10}/m and the buffering effect of the liquid in the permeate chamber may be responsible in part for the slow apparent recovery of the protein transmission. It is also possible that deposited material, not crucial to the determination of the protein transmission is removed first. For example, the outside layers of the fouling layer might be removed first reducing the thickness of the fouling layer and reducing the fouling resistance. However, the protein transmission is determined by the minimum pore size of the layer not the layer depth and as long as a thin layer remains on the membrane protein transmission may not change significantly. Likewise, if the first material removed from the membrane is a surface layer and material from within the pores, that control the protein transmission, is not removed, then the resistance will fall but the protein transmission remain low.

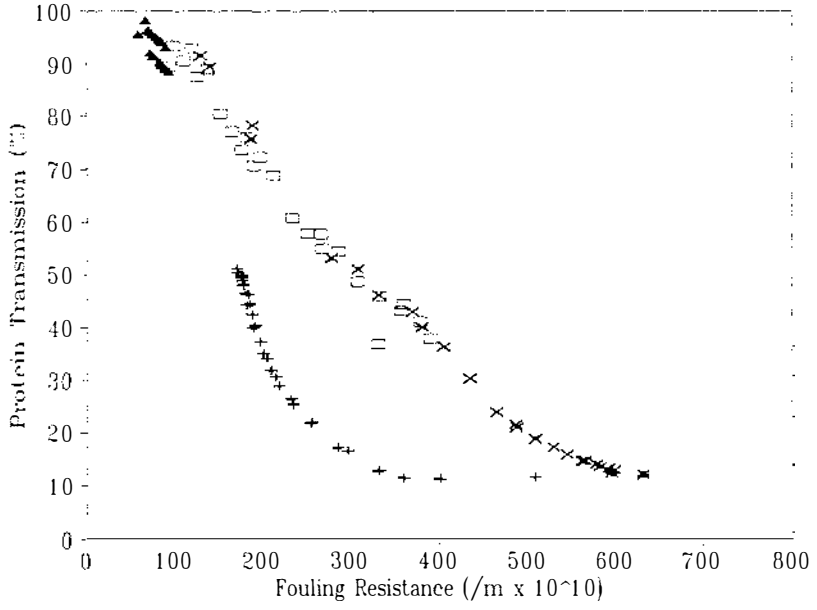

Figure 6.43. Effect of the addition and removal of calcium after 1 h on the relationship between fouling resistance and protein transmission during the MF of a 0.2% β-lactoglobulin solution on a 50 nm membrane at 200 L/m².h: (▲) 1st h, run with added calcium; (+) 2nd h run with added calcium; (x) 1st h run with removal of calcium; (□) 2nd h run with removal of calcium.

6.3.8. Effect of the cross-flow velocity

In UF, increasing the cross-flow velocity usually results in an improvement in the permeate flux. This is generally considered to be because of a reduction in concentration polarisation or a reduction in the thickness of the fouling layer on the membrane. However, changes in cross-flow velocity are not expected to have a major influence when the fouling is predominantly within the membrane pores (Bowen & Hughes, 1990). For this reason most of the trials reported here considered changes in the physico-chemical state of the protein and the permeate flux rather than the cross-flow velocity. One set of experiments was performed on the 50 nm membrane to consider the effect of the cross-flow velocity under conditions of high flux and in the presence of calcium. Under these conditions severe membrane fouling occurred.

The effects of the cross-flow velocity on the fouling resistance and the protein transmission are shown in Figs. 6.44-6.46. Increasing the cross-flow velocity reduced the rate of increase in the fouling resistance and the final level to which the fouling resistance climbed. However, increasing the recirculation rate to 540 L/h (4 m/s) after 2 h operation at 260 L/h (2 m/s) did not reduce the fouling resistance significantly indicating that concentration polarisation was not a major contributor to the differences in resistance. The fouling material, while considered reversible in that it was removed by flushing, was not removed by changes in the hydrodynamic conditions during operation on ß-lactoglobulin. Reducing the cross-flow velocity to 2 m/s (260 L/h) resulted in an increase in the fouling rate and an increase in the final fouling resistance. Furthermore, reducing the cross-flow velocity to 2 m/s (260 L/h) after 2 h operation at 4 m/s (540 L/h) saw an increase in the rate of fouling resistance. The run was terminated before pseudo-steady state was reached at this new recirculation rate so it was not possible to determine whether the fouling resistance would have approached the resistance observed when 2 m/s was used from the commencement of the trial. However, it is clear that reducing the cross-flow velocity during a trial resulted in an increase in fouling whereas increasing the cross-flow velocity has only a minimal effect on fouling already deposited on the membrane.

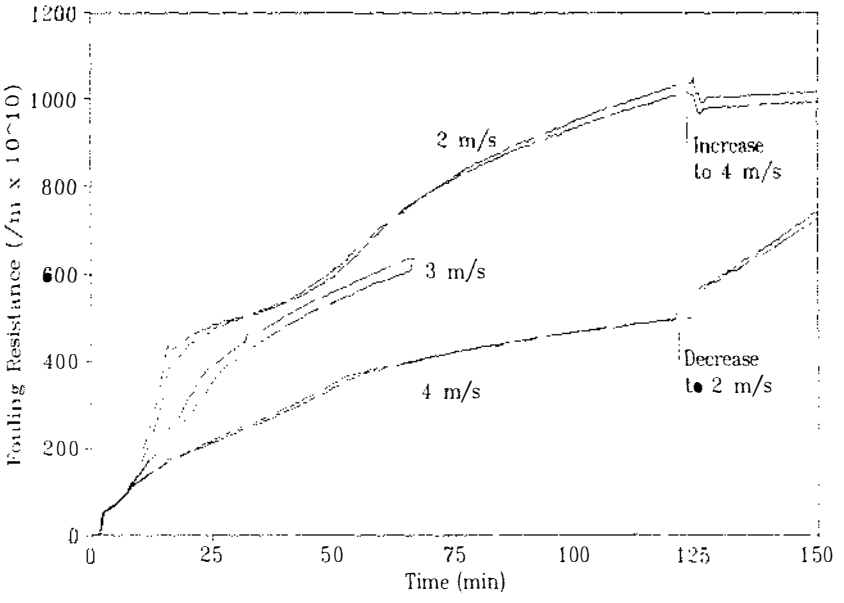

Figure 6.44. Effect of the cross-flow velocity on the fouling resistance during the MF of 0.2% β-lactoglobulin on a 50 nm membrane at an initial flux of 200 L/m².h. The ionic strength was 0.0557-0.0574, the pH 6.3-6.4 and the calcium concentration 7.6-8.4 mmol/L.

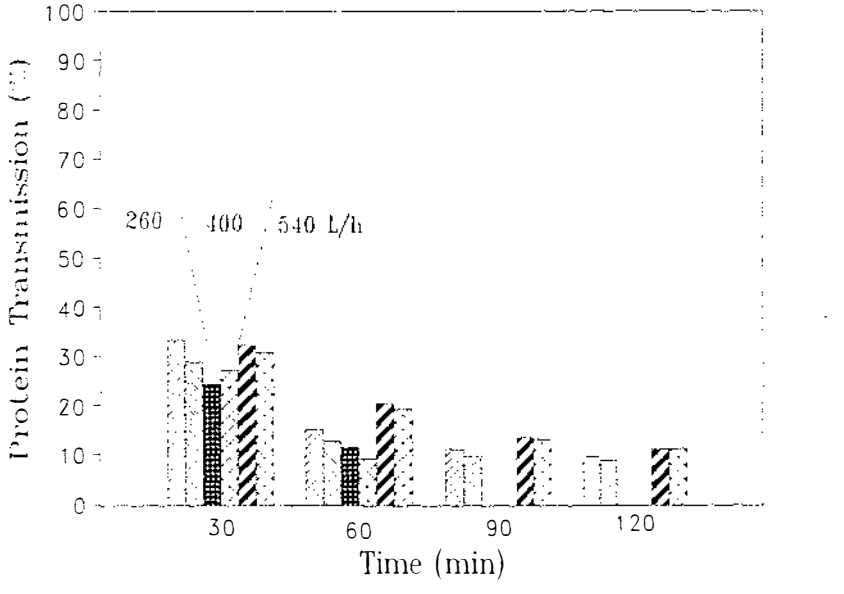

Figure 6.45. Effect of the cross-flow velocity on the protein transmission (spectrophotometer) during the MF of 0.2% β-lactoglobulin on a 50 nm membrane at an initial flux of 200 L/m².h. The ionic strength was 0.0557-0.0574, the pH 6.3-6.4 and the calcium concentration 7.6-8.4 mmol/L.

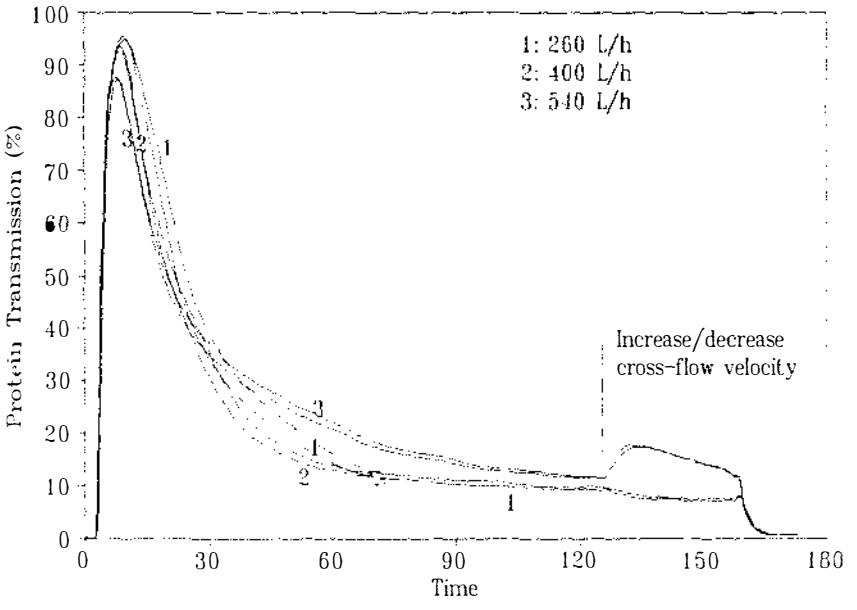

Figure 6.46. Effect of the cross-flow velocity on the protein transmission (UV cell) during the MF of 0.2% β-lactoglobulin on a 50 nm membrane at an initial flux of 200 L/m².h. The ionic strength was 0.0557-0.0574, the pH 6.3-6.4 and the calcium concentration 7.6-8.4 mmol/L.

Considering more closely the 2 m/s curve, it is possible to identify several separate phases of behaviour. Upon the introduction of product the resistance increased sharply, probably due to some form of dynamic resistance because of the presence of protein in the system. The resistance then increased exponentially for about 14 min. The initial increase in resistance and the first part of the exponential curve are similar for all three of the cross-flow velocities investigated suggesting that the cross-flow velocity had no impact on the initial deposition of fouling on the membrane. Thereafter, the curves diverge from each other with the fastest increase with the slowest recirculation rate. At the "break-point" in the curve at 14 min, control was changed from constant flux to constant pressure and the permeate flux decreased from this point. The break-point suggested that the rate of fouling was strongly related to the permeate flux as well as the cross-flow velocity. Break-points occurred with the higher cross-flow velocities, although they were not as pronounced, perhaps due to the slower decrease in the permeate flux once a transmembrane pressure of 200 kPa was reached and constant pressure control instigated. In the case of the trials

at 2 m/s, after the break-point, the rate of membrane fouling decreased reflecting the effect of the reducing permeate flux on fouling and almost appeared to approach a plateau level of fouling. However, at about 45 min, another contribution to fouling occurred leading to a further increase in fouling resistance. At this point the protein transmission had reduced to about 25% (Fig. 6.46) and it is suggested that the secondary effect is due to the formation of a surface layer brought about by an increase in concentration polarisation and thus, in the membrane wall concentration.

The protein transmission data from the spectrophotometer is shown in Fig. 6.45 and from the UV cell in Fig. 6.46. The UV data gives a better overall view of the behaviour. The initial low transmission was because of the water in the permeate chamber. The transmission increases as this water was removed until a "high point" where the dilution of water is balanced by the reduction in the protein transmission because of fouling. Interestingly, as the cross-flow velocity is decreased there is a small shift in the "high point" to a higher transmission and to a longer time after the addition of protein to the plant. The reasons for this are not clear. It may be because of increased concentration polarisation brought about by the lower cross-flow velocity, although with high protein transmissions this effect should be small. Following the "high point", the transmissions dropped rapidly and similarly for all of the cross-flow velocities in spite of differences in the fouling rates. The final level of transmission was higher with a cross-flow velocity of 4 m/s compared to a cross-flow velocity of 2 m/s. These results suggested that the drop in protein transmission in the first 30 min of the trial was not significantly affected by the cross-flow velocity. It appeared to be related to time but not directly to the fouling resistance. This is further shown in Fig. 6.47 where the protein transmission versus fouling resistance for the three different recirculation rates are shown. At a similar resistance the protein transmission is lower as the cross-flow velocity increased. It is suggested that the fouling deposits in two ways: one of which principally controls the protein transmission and is not significantly affected by the cross-flow velocity; and the second, that is affected by the cross-flow velocity, only has a secondary effect on protein transmission. This area will be discussed in more depth in Section 6.4.

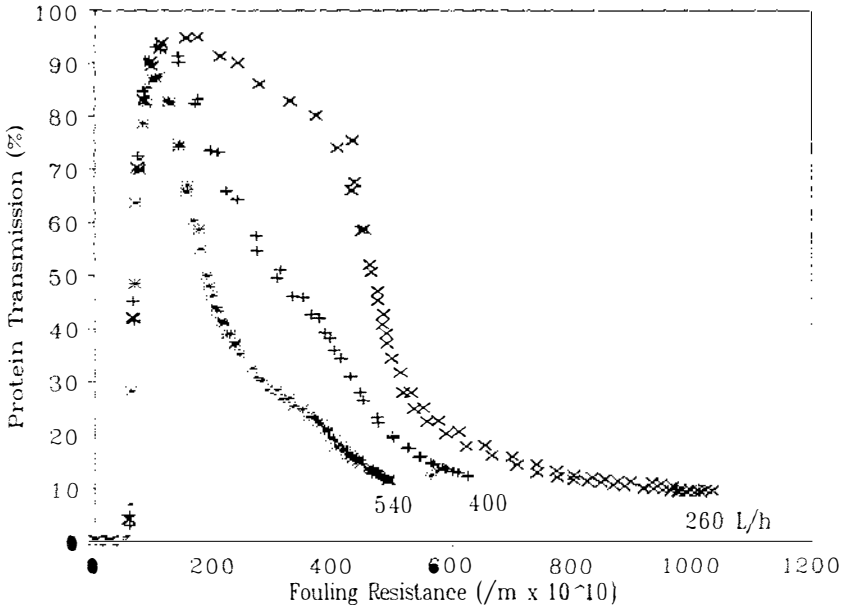

Figure 6.48. The effect of the cross-flow velocity (expressed as the recirculation rate) on the protein transmission versus the fouling resistance for the 50 nm membrane. (x) Data collected from trials at 260 L/h; (+) trials at 400 L/h; (∗) trials at 540 L/h.

At the point that fouling becomes established and the protein transmission reaches a pseudo-steady-state of around 10-15% (equivalent to an retention of 0.85-0.90) the transmission was higher with a higher cross-flow velocity (Fig. 6.46). If the velocity was reduced (at 2 h), the protein transmission initially increased, in spite of an increase in fouling, before declining as the impact of further fouling becomes more important. Increasing the cross-flow velocity saw a very small further reduction in the transmission even though the fouling resistance remained reasonably constant. Both these observations are in keeping with a concentration polarisation model where the protein transmission is affected by the membrane wall concentration. The fact that before changing the velocity the transmission was higher at high velocity (not what is expected from concentration polarisation theory if the intrinsic pore size is the same) suggested that the second fouling effect mentioned at the end of the previous paragraph does have some impact on protein transmission when higher retentions or lower transmissions are achieved.

6.3.9. Effect of the membrane pore size

Three membranes were used in the trials. In the absence of calcium and at low flux fouling was light and transmission high with the 50 and 100 nm membranes. However, the 20 nm membrane fouled severely and had a low protein transmission (Figs. 6.48&6.49). It appeared that the 20 nm membrane was sufficiently "tight" to act like a UF membrane. As a result protein transmission was low, the effect of concentration polarisation therefore high, and a surface layer formed on the membrane surface.

Further comparisons can be made between the 50 and 100 nm membranes. In the presence of calcium and at 50 $L/m^2.h$ fouling on both membranes was light and protein transmissions were high - slightly higher for the 100 nm membrane (Figs. 6.50&6.51). The differences in actual resistance values for the two membranes reflect the lower initial pore size of the 50 nm membrane and the impact of a similar pore size reduction on resistance. The high protein transmissions indicate that protein was able to pass relatively freely through the membranes.

At 200 $L/m^2.h$ with calcium present severe fouling occurred with both the 50 and 100 nm membranes (Fig. 6.52). The onset of severe fouling was delayed with the 100 nm membrane by about 15 min during which time the fouling resistance increased to near the clean resistance of the 50 nm membrane. Thereafter, the fouling resistance curves are identical in shape and trend, differing only by the 15 min delay seen with the 100 nm membrane. These results suggested that the fouling mechanism was similar for both membranes; taking longer to impact on the actual fouling resistance because of the larger initial pore size and lower clean membrane resistance of the 100 nm membrane.

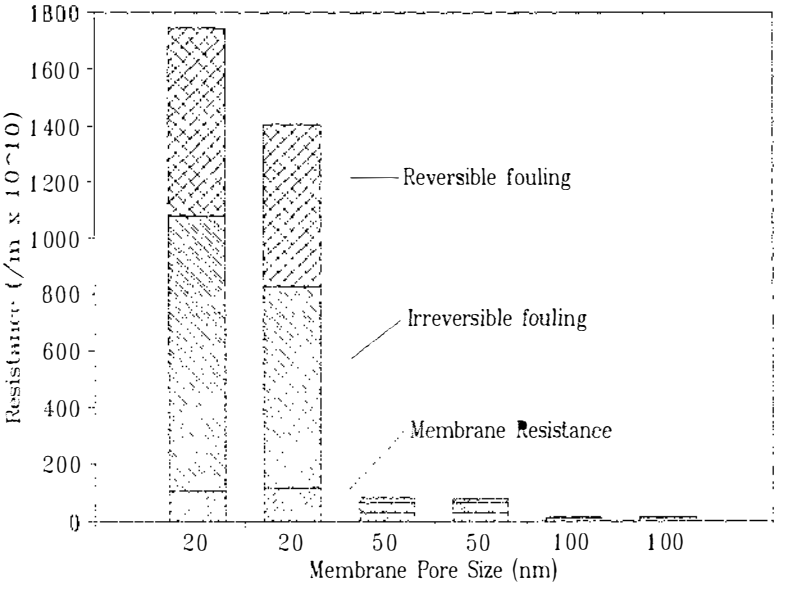

Figure 6.48. Effect of the pore size on the fouling resistance during the MF of 0.2% β-lactoglobulin at an initial flux of 50 L/m².h. No calcium was added in these trials. For the 20 nm membrane the ionic strength was 0.0481-0.0483 and the pH 6.4-6.5; for the 50 nm membrane the IS was 0.0477-0.0479 and the pH 6.3-6.4; for the 100 nm membrane the IS was 0.0188-0.0354 and the pH 6.5.

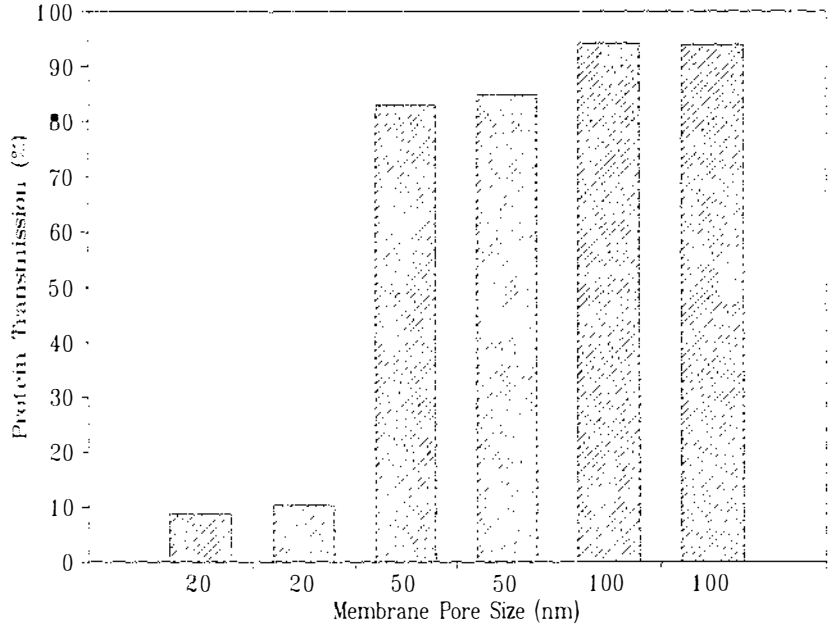

Figure 6.49. Effect of the pore size on the protein transmission during the MF of 0.2% β-lactoglobulin at an initial flux of 50 L/m².h. No calcium was added in these trials. For the 20 nm membrane the ionic strength was 0.0481-0.0483 and the pH 6.4-6.5; for the 50 nm membrane the IS was 0.0477-0.0479 and the pH 6.3-6.4; for the 100 nm membrane the IS was 0.0188-0.0354 and the pH 6.5.

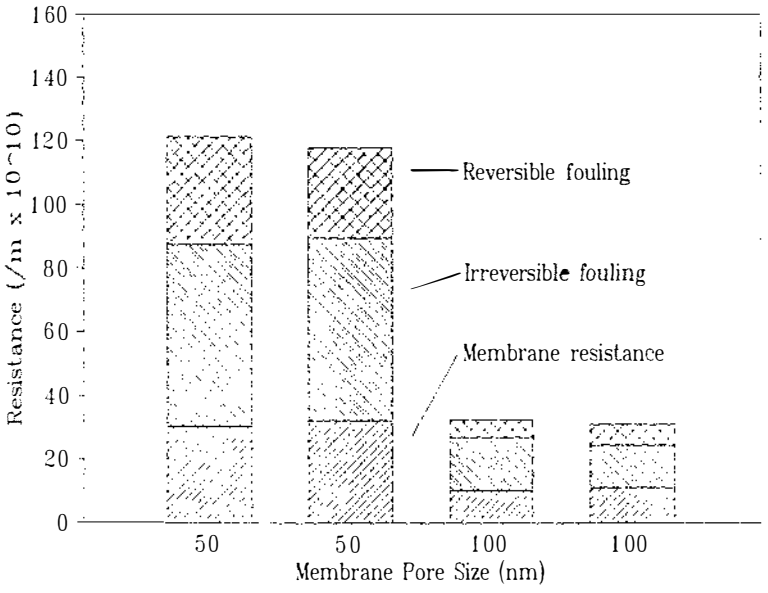

Figure 6.50. Effect of the pore size on the resistances during the MF of 0.2% β-lactoglobulin at an initial flux of 50 L/m².h. Calcium was added in these trials. For the 50 nm membrane the IS was 0.0569-0.0572, the pH 6.2-6.3 and the calcium concentration 8.0-8.3 mmol/L; for the 100 nm membrane the IS was 0.0268-0.0278, the pH 6.1-6.2 and the calcium concentration 7.6-7.9 mmol/L.

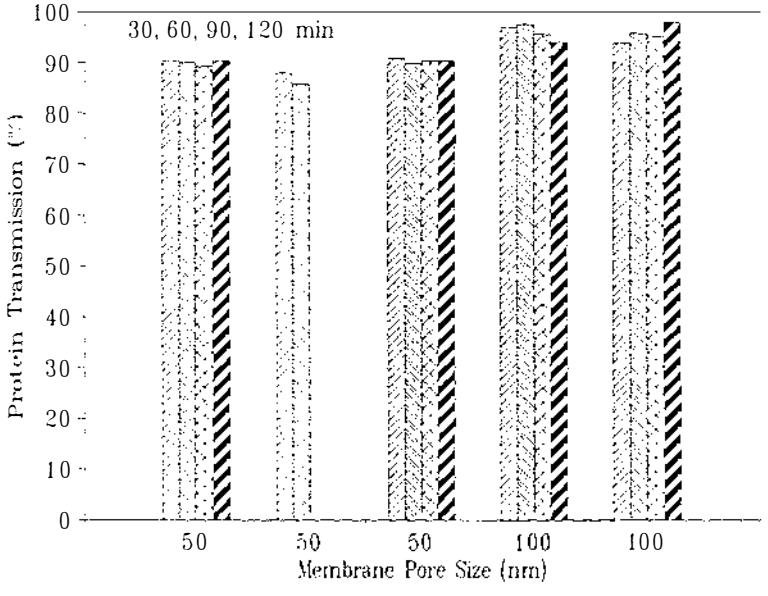

Figure 6.51. Effect of the pore size on the protein transmission during the MF of 0.2% β-lactoglobulin at an initial flux of 50 L/m².h. Calcium was added. For the 50 nm membrane the IS was 0.0569-0.0572, the pH 6.2-6.3 and the calcium concentration 8.0-8.3 mmol/L; for the 100 nm membrane the IS was 0.0268-0.0278, the pH 6.1-6.2 and the calcium concentration 7.6-7.9 mmol/L.

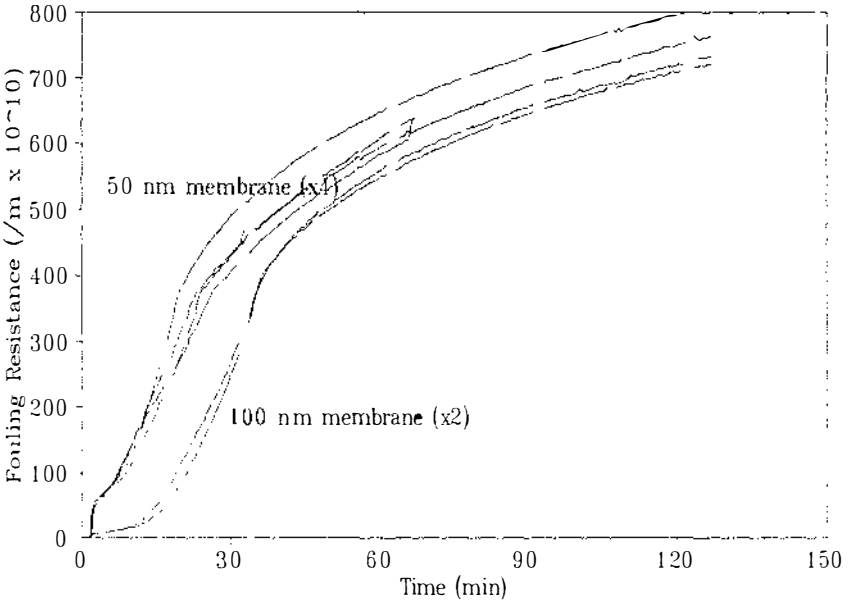

Figure 6.52. Effect of the pore size on the fouling resistance during the MF of 0.2% β-lactoglobulin at an initial flux of 200 L/m².h. For the 50 nm membrane the IS was 0.0568-0.0575, the pH 6.2-6.4 and the calcium concentration 8.1-8.4 mmol/L; for the 100 nm membrane the IS was 0.0567-0.0580, the pH 6.3-6.4 and the calcium concentration 8.0-8.6 mmol/L.

Looking at the transmission data for the two membranes the spectrophotometer data (Fig. 6.53) indicated that the 30 min protein transmission was higher for the 100 nm membrane reflecting the slower increase in fouling. The final protein transmissions were similar for both membranes, perhaps being slightly lower with the 100 nm membrane after 120 min, in spite of the slower initial decline of the protein transmission. Interestingly, the final protein transmissions of 8-11% were similar to the protein transmissions observed with the 20 nm membrane. The data collected via the UV cell shows similar behaviour (Fig. 6.54). After a few minutes the protein transmission through the 100 nm membrane was higher than the 50 nm membrane reflecting the larger initial pore size and the slower increase in membrane fouling. Thereafter, the protein transmission declined at a similar rate separated only by the 10-15 min delay in the onset of fouling for the 100 nm membrane. Again, the similar shape of the curves suggested that the fouling mechanism was similar. The final protein transmissions were similar for the two membranes. Unfortunately, UV data

was only available on the 50 nm membrane up until 1 h and it was not possible to verify whether the protein transmission of the 100 nm membrane was eventually lower than that of the 50 nm membrane.

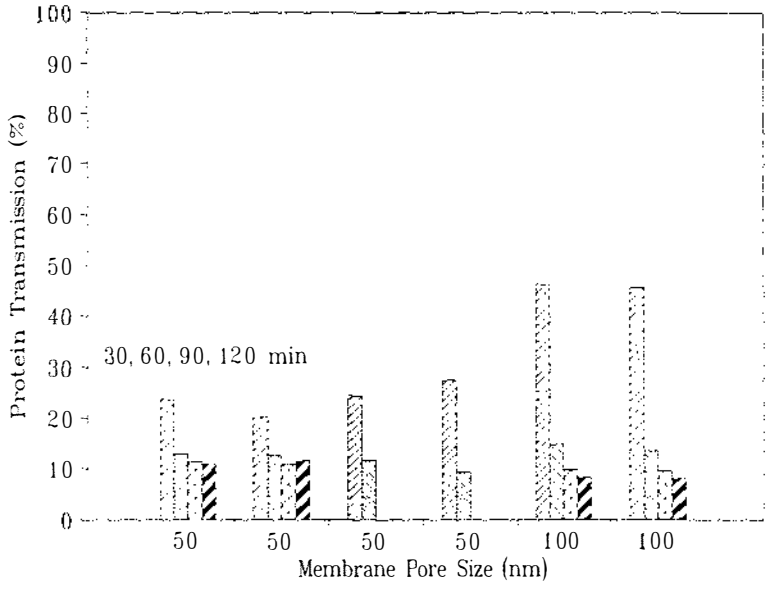

Figure 6.53. Effect of the pore size on the protein transmission during the MF of 0.2% β-lactoglobulin at an initial flux of 200 L/m².h. For the 50 nm membrane the IS was 0.0568-0.0575, the pH 6.2-6.4 and the calcium concentration 8.1-8.4 mmol/L; for the 100 nm membrane the IS was 0.0567-0.0580, the pH 6.3-6.4 and the calcium concentration 8.0-8.6 mmol/L.

A further comparison of these trials can be made by comparing the fouling resistance versus protein transmission data (Fig. 6.55). It is clear that the higher transmissions observed initially with the 100 nm membrane occur at resistances smaller than that possible with the 50 nm membrane. Once the fouling resistance had increased to a similar value to the 50 nm membrane the curves were similar. The higher transmission values for the 50 nm membrane in the resistance range 100-300x10^{10}/m are perhaps because values at these points occur after less than 15 min operation for this membrane compared to 20-30 min for the 100 nm membrane. For resistances above 300x10^{10}/m the resistance versus transmission curves are almost identical giving further support that the fouling mechanisms were similar.

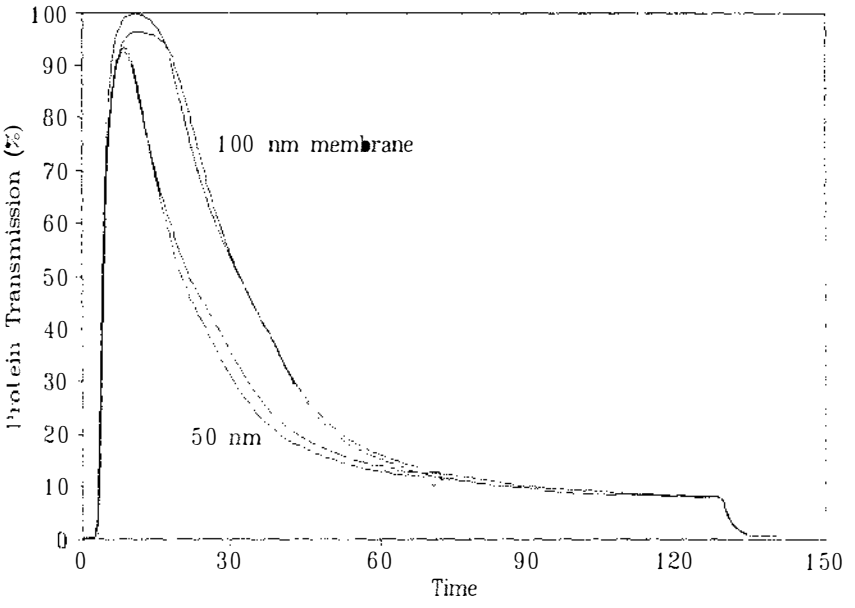

Figure 6.54. Effect of the pore size on the protein transmission during the MF of 0.2% β-lactoglobulin at an initial flux of 200 L/m².h. For the 50 nm membrane the IS was 0.0568-0.0575, the pH 6.2-6.4 and the calcium concentration 8.1-8.4 mmol/L; for the 100 nm membrane the IS was 0.0567-0.0580, the pH 6.3-6.4 and the calcium concentration 8.0-8.6 mmol/L.

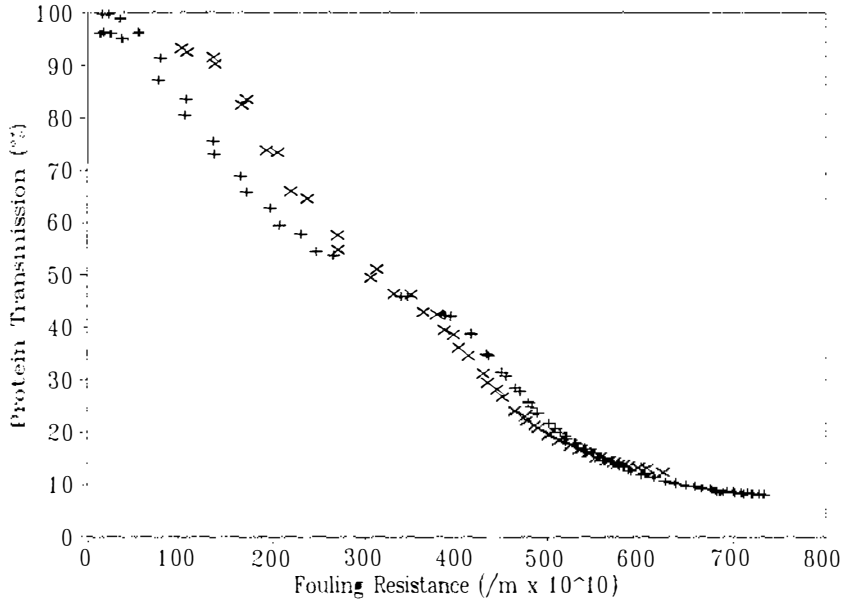

Figure 6.55. Effect of the pore size on the relationship between protein transmission and fouling resistance during the MF of 0.2% β-lactoglobulin at an initial flux of 200 L/m².h. For the 50 nm membrane (x) the IS was 0.0568-0.0575, the pH 6.2-6.4 and the calcium concentration 8.1-8.4 mmol/L; for the 100 nm membrane (+) the IS was 0.0567-0.0580, the pH 6.3-6.4 and the calcium concentration 8.0-8.6 mmol/L.

6.4 Discussion

6.4.1. Summary of fouling behaviour

It is useful at this point to summarise the fouling behaviour identified in these trials. With 50 and 100 nm membranes it was possible to prevent severe fouling and have consistent high transmission of protein through the membrane. However, with the 20 nm membrane, it was not possible, via control of the operating conditions, to prevent severe fouling occurring with ß-lactoglobulin. In effect, the 20 nm membrane behaved as a UF membrane and retained the bulk of the protein.

With the 50 and 100 nm membranes the fouling behaviour was highly dependent on the permeate flux and the concentration of calcium. Severe fouling, that reduced the protein transmission from around 90% to around 10%, occurred under conditions of high calcium concentration (8 mmol/L) and high permeate fluxes (100+ $L/m^2.h$). Severe fouling could be prevented either by reducing the permeate flux from the start of the run or by reducing the calcium content of the feed, preferably to zero. The effect of calcium was not solely due to ionic strength since trials with only sodium chloride and ionic strengths greater than the calcium trials did not invoke severe fouling. Calcium appeared to play a direct and specific role in severe fouling.

The severe fouling was predominantly reversible, that is, it could be removed by water. Furthermore, if calcium was removed from the feed solution (still leaving the membrane in contact with the protein) the majority of the resistance due to severe fouling was reversible and the protein transmission could be restored to at least 50%. The protein redissolved or desorbed if calcium was leached out of the deposit, again giving an indication that calcium played a direct specific role in the deposition on the membrane.

The trials with varying cross-flow velocity suggested that fouling occurred by at least two mechanisms: one of which principally controlled the protein transmission and was not affected by the cross-flow velocity; and the second, that was affected by the cross-flow velocity, but only had a secondary effect on protein transmission.

6.4.2. Proposed fouling mechanisms

It is proposed that there are three major contributors to fouling within this system: (1) protein adsorption to the membrane; (2) deposition of protein within the pores or at the pore entrance; and (3) the formation of a surface layer on the membrane.

Adsorption occurred in all experiments and was responsible for the increase in resistance at low flux and in the absence of calcium. With the 20 nm membrane protein adsorption alone was sufficient to reduce the apparent pore size of the membrane to a point where protein was retained. As a result a surface layer formed on the membrane that controlled the protein transmission.

With high flux and in the presence of calcium deposition within the membrane pores occurred. This was not affected by the cross-flow velocity (first fouling mechanism mentioned above in Section 6.3.8) and at least in the early stages of the run controlled the protein transmission.

Surface layer formation appeared to occur after pore narrowing and may be dependent upon the concentration of protein in the boundary layer. Protein retention will have a major impact on this. Again from the trials with the cross-flow velocity surface layer formation appeared to begin to make a contribution to the fouling resistance reasonably early in these trials although it did not initially affect the protein transmission. After severe fouling had occurred the surface layer appeared to enhance protein retention (reduce transmission).

6.4.3. Protein adsorption

It is well known that protein adsorbs on to membrane surfaces (see Section 2). The trials on the 50 and 100 nm membranes at 50 $L/m^2.h$ and in the absence of calcium resulted in the least fouling. A comparison of the resistances and the equivalent pore size reduction in these trials is shown in Table 6.1.

Table 6.1. Apparent pore size reduction in trials on the 100 and 50 nm membranes performed at 50 L/m².h and in the absence of calcium.

Run No.	Clean membrane resistance ($x10^{10}$/m)	Irreversible fouling resistance ($x10^{10}$/m)	Apparent reduction in pore size (nm)
50 nm membrane			
14	31.3	37.6	9
18	29.8	35.4	9
100 nm membrane			
3	12	5.3	9
11	10.7	5.5	10

ß-Lactoglobulin has a size of 4-5 nm (Hobman, 1992) and the pore size reduction of 9-10 nm (Table 6.1) observed is in keeping with the expectation that adsorption will cause a narrowing of the pores by the equivalent of 2 times the diameter of the protein.

With the 20 nm membrane the pore size reduction or pore entrance obstruction caused by adsorption was sufficient to retain protein and cause the formation of a surface layer on the membrane. UV cell data from trial 39 on the 20 nm membrane indicated that at no time did protein transmission exceed 10-15%. This suggested that the retention of protein by the membrane was initially high and surface layer formation may have been induced by the high boundary layer concentration. The high retention initially seen with this membrane is in contrast to the low retention initially observed with the 50 and 100 nm membranes in every experiment. When severe fouling occurred on the 50 and 100 nm membranes other fouling mechanisms, in addition to protein adsorption play an important part. Before moving on to discuss pore narrowing and the mechanisms of severe fouling it is useful to consider the results of the trials when severe fouling did not occur (in the absence of calcium or at low flux) in the light of a protein adsorption mechanism.

Reducing the pH to 5.0 resulted in an increase in the irreversible fouling from 5.3-5.5 to 13-16 x 10^{10}/m and an equivalent pore reduction of 19-20 nm compared to 9-10 nm. In UF, at the iso-electric point of the protein the quantity of strongly bound protein is lower than at higher pH even though the total quantity of protein deposited on the membrane is greater and the flux is lower (McDonough *et al.*, 1990). Furthermore, the quantity of deposit on the membrane appeared to be related to the solubility or stability of the protein in solution (lower at the IEP) rather than charge differences between the protein and the membrane or the degree of strongly bound adsorbed protein (Nyström, 1989). Thus, an increase in the "adsorbed" protein within the membrane pores is unlikely to be the explanation for the increased fouling observed at pH 5.0. The increased deposition of protein on the membrane surface at the IEP seen in UF is probably concentration induced, again something not expected within the pores of an MF membrane. Thus, the reasons for increased fouling in MF appear to be different to those observed in UF. At pH 5.0 protein aggregation, particularly of denatured or partially denatured protein, occurs to a greater extent than at pH 6.5. Furthermore, at pH 5 ß-lactoglobulin may form octamers. Thus the feed material may have contained a small quantity of larger or aggregated protein groups. It is suggested that the increase in resistance at pH 5.0 is because of pore plugging by a small number of aggregates: insufficient to cause severe fouling of the membrane.

Increasing the flux to 200 L/m^2.h on both the 50 and 100 nm membranes in the absence of calcium increased the fouling resistance but did not cause a reduction in protein transmission. The resistance data from these trials are summarised in Table 6.2. The apparent reduction in pore size was similar in both cases (13-14 nm) and was larger than that observed in trials at 50 L/m^2.h (9-10 nm). The reasons for the increase in irreversible fouling with higher flux is not clear. It is possible that the increased volume of permeate and therefore, an increased volume of a small feed fraction (*i.e.* aggregates) that fouls the membrane, caused the increase. However, most of the increase in fouling occurred in the first 30 min (Figs. 6.20&6.22) and thereafter the slope of the resistance/time curves were similar for both 50 and 200 L/m^2.h (especially for the 100 nm membrane; not so true for the 50 nm membrane). This suggests that the increase in fouling is related directly to the module

hydrodynamics and once established, the resistance remains reasonably constant. It is suggested that the higher flux caused a small increase in surface layer or dynamic layer formation, insufficient to affect the protein transmission, but sufficient to make a contribution to the fouling resistance.

Table 6.2. Fouling resistances and apparent pore size reduction in trials on the 100 and 50 nm membranes performed at 200 L/m^2.h and in the absence of calcium.

Run No.	Clean membrane resistance (x10^{10}/m)	Irreversible fouling resistance (x10^{10}/m)	Apparent reduction in pore size (nm)
50 nm membrane			
15	31.4	78.7	13
100 nm membrane			
4	10.3	8.4	14
7	10.5	8.8	14

When calcium was added to the feed severe fouling did not occur at 50 L/m^2.h, in contrast to the results at higher fluxes (mechanisms of severe fouling discussed in Section 6.4.4). In this section the effect of calcium on protein adsorption will be discussed. It is known that calcium affects the degree of protein deposition on the membrane but it is not clear by what mechanism or whether it is the protein multi-layer or protein adsorption that is affected (Marshall & Daufin, 1994). It is possible that charge neutralisation by salts (any type) and increased non-polar interaction may induce small conformational distortions or local unfolding of ß-lactoglobulin. In addition, calcium appears to have a more specific interaction with ß-lactoglobulin. One possible interaction is the formation of intramolecular ion bridges between the charged or carboxylic groups of ß-lactoglobulin and calcium (Jeyarajah & Allen, 1994). As a consequence calcium may further increase the unfolding and distortion of the protein. Thus the addition of calcium may change protein-protein interactions (discussed in Section 6.4.4) or the nature of the protein-membrane interactions, possibly changing the degree of protein adsorption or the nature of the deposited layer.

Further possible evidence that the properties of the adsorbed protein layer are affected by calcium can be found by comparing the results from the trials when calcium was added after 1 h and when calcium was added at the beginning of the trial (Figs. 6.41 & 6.42). In both cases severe fouling occurred and appeared to be by the same fouling mechanism (Fig. 6.43). However, in the trial when calcium was added after 1 h, the rate of fouling was much slower. It is suggested that the state of the protein in the adsorbed layer formed in the absence of calcium is different from that formed with calcium and in some way slows down the protein-protein interactions that lead to severe fouling.

6.4.4. Fouling in the pores

6.4.4.1. Location of fouling

It is proposed that internal deposition of protein within the membrane leading to pore narrowing is a major contributor to the fouling resistance and that surface layer formation only occurs after some reduction in the pore size (resulting in increased retention). Two questions arise as to the physical nature of the fouling: (1) can the internal fouling be described by any of the pore blocking laws; and (2) does the fouling occur throughout the membrane or only at or near the pore entrance.

In this analysis of the pore blocking laws only the constant flux portion of the resistance versus time curves of trials with calcium and varying flux (100-200 $L/m^2.h$) have been considered. In this way the blocking law equations derived for constant flow-rate can be utilised. These have been summarised by Grace (1956) and more recently by Hlavacek & Bouchet (1993). These models assume that the membrane pressure drop can be described by the Hagen-Poiseuille law; that is the pores consist of long straight circular ducts, all of the same size and shape. These assumptions are not necessarily valid for this membrane.

Three cases will be considered: (1) pore plugging (complete blocking law) where it is assumed that if particles lodge in a pore the pore is completely blocked; (2) pore narrowing (standard blocking law) where it is assumed that small particles

progressively deposit on the pore walls causing a reduction in the pore diameter; and (3) an intermediate blocking law (see Hermia (1982) for a physical description of the law). Plotting $\mathbf{R_0/R}$ versus time will give a straight line if the pore plugging mechanism is occurring (Equation (3.22)); plotting the square root of $\mathbf{R_0/R}$ versus time will be a straight line if pore narrowing is the mechanism (Equation (3.18)) and plotting the natural log of $\mathbf{R/R_0}$ versus time will be a straight line if the intermediate blocking law applies (Equation (3.27)). Each of these comparisons are shown in Figs. 6.56-6.58 for trials at 100, 150 and 200 L/m².h.

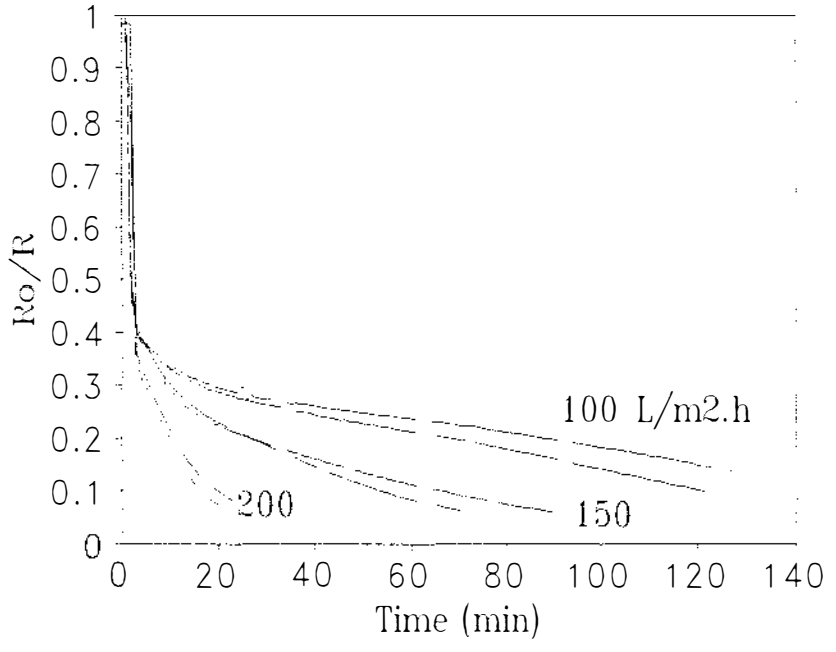

Figure 6.56. Investigation of pore plugging mechanism (complete blocking law) in the MF of ß-lactoglobulin on a 50 nm membrane.

None of the graphs showed straight lines in the first 20 min of operation. This probably reflects the establishment of a dynamic resistance due to the presence of the protein near the membrane and resistance due to the adsorption of protein. The data from the trials at 100 L/m².h perhaps fit a pore plugging mechanism for operating times beyond 20 min. But overall, pore plugging does not appear a reasonable mechanism as the protein transmission decreases quickly with increasing membrane resistance (Fig. 6.32) whereas if pore plugging was occurring (in its purest form) then the protein retention would not be affected. None of the models accurately predicted the behaviour of the fouling for all three fluxes examined and therefore cannot be considered to provide a complete picture of the fouling behaviour. This is

consistent with the observation that two fouling behaviours, one internal and one surface layer, are superimposed.

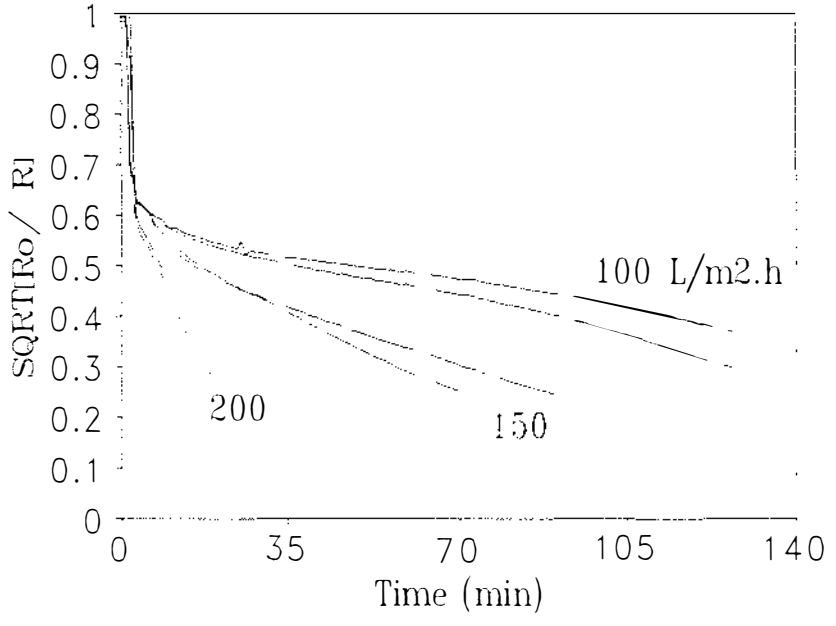

Figure 6.57. Investigation of pore narrowing mechanism (standard blocking law) in the MF of ß-lactoglobulin on a 50 nm membrane.

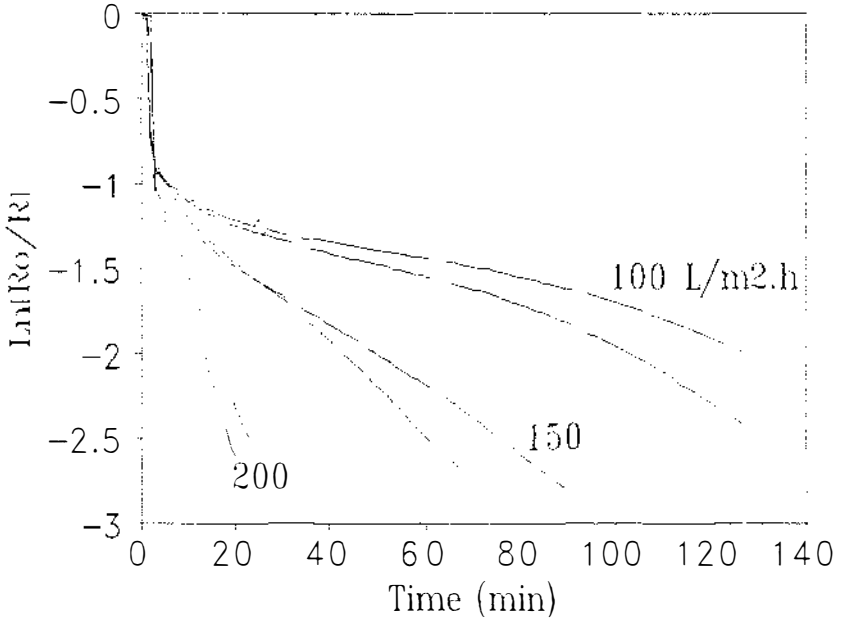

Figure 6.58. Investigation of intermediate blocking law in the MF of ß-lactoglobulin on a 50 nm membrane.

It is also possible to examine the fouling mechanisms by considering the relationship between the membrane resistance and the protein transmission (Fig. 6.32). The apparent pore size of the membrane can be determined from resistance data (Equation (3.36)). Based on the apparent pore size the protein transmission or retention can be calculated via the Ferry equation (Equation (3.34)).

Line (1) in Fig. 6.59 shows the predicted transmission/resistance relationship given an initial pore size of 50 nm, a protein size of 4.5 nm and assuming a pore narrowing mechanism. The data shown is taken from Fig. 6.32. Clearly, the model did not come anywhere near to predicting the observed behaviour. This equation is based on the pore narrowing model; this has already been shown to be inadequate for the purpose of describing the fouling behaviour and it is therefore not surprising that the model is not accurate. Line (2) in Fig. 6.59 represents the same equation but with an initial pore size of 33 nm. This pore size was chosen so that the protein transmissions at low resistances were predicted by the model. It is obvious that changing the initial pore size of the membrane does not improve the fit of the model very much.

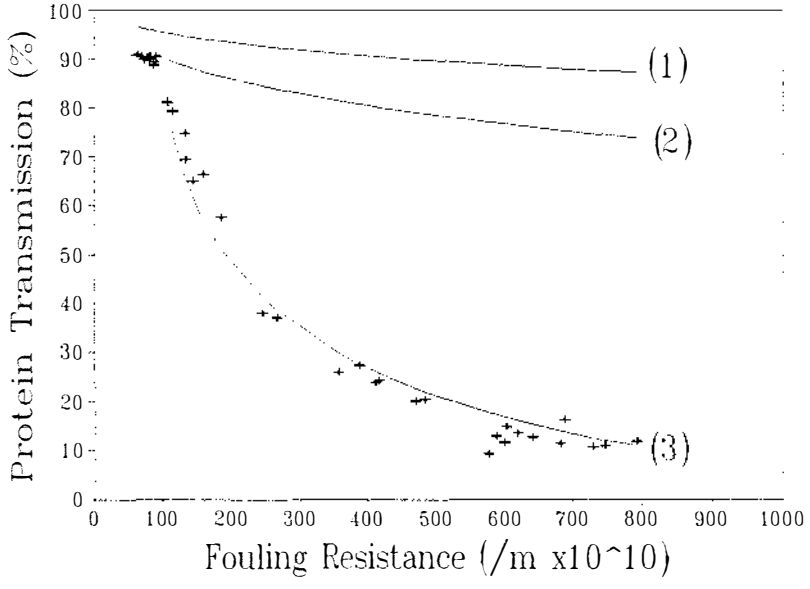

Figure 6.59. Comparison of pore narrowing models and protein transmission / fouling resistance data from MF runs on the 50 nm membrane with calcium. A description of the models is given in the text.

Upon the introduction of product to the plant there was an immediate increase in the membrane resistance; probably some form of dynamic resistance because of the presence of protein in the system. In the trials represented in Fig. 6.59 the initial jump in resistance was typically 50-55x10^{10}/m. This resistance can be considered as not contributing to pore blocking or narrowing. However, subtracting this value from the total resistance and recalculating Lines (1) and (2) in Fig. 6.59 did not significantly improve the prediction.

Having established that none of the pore blocking laws adequately describe the fouling behaviour observed, the possibility that fouling occurred at or near the pore entrance rather than throughout the length of the membrane pore was investigated.

Protein adsorption does occur over the entire pore length and this contribution must be considered in the model. In the trials at 200 L/m^2.h without calcium and at 50 L/m^2.h with calcium severe fouling did not occur and the average total fouling resistance was 100x10^{10}/m. This resistance includes the initial jump in resistance. Subtracting 52.5x10^{10}/m from this gives a resistance of 47.5x10^{10}/m caused by protein adsorption.

Conceptually, what is suggested is that, in addition to the effect of protein adsorption, there is a reduction in the pore size of a small section of the membrane pore adjacent to the pore entrance. To model this using a modification of Equation (3.36) requires isolation of the fouling resistance that contributes to the narrowing of the small section of membrane from the total fouling resistance. Consequently, the dynamic resistance due to the presence of protein and the resistance because of adsorption were subtracted from the total fouling resistance. The initial pore size of the membrane was also reduced by protein adsorption. For the 50 nm membrane this corresponded to 12 nm and hence, the pore size of the "adsorbed" membrane was considered to be 38 nm. The resistance of the adsorbed membrane equals the sum of the clean membrane resistance and the resistance due to adsorption.

If the resistance of the adsorbed membrane is constant over the length of the membrane pore then it is possible to consider the membrane as two sections of

membrane in series; section (1) being nearest the pore entrance. Thus assuming that the resistance of the adsorbed membrane section furthest from the pore entrance does not change then it is possible to calculate the reduction in pore diameter of membrane section (1). Mathematically the model looks like:

$$\frac{d_p}{38nm} = \left[\frac{R_{section\ 1}}{R_f + R_{section\ 1} - R_{dy+ad}}\right]^{0.25} \qquad (6.2)$$

where $\mathbf{R}_{section\ 1}$ is a percentage of the sum of the clean resistance and resistance because of adsorption. $\mathbf{R}_{section\ 1}$ was varied to fit the data in Fig. 6.59. The prediction of this model is shown by Line (3). The excellent fit of the data by a model with only one fitted variable demonstrates that the proposed fouling mechanism of protein deposition at or near the pore entrance is reasonable. From the fitted value of $\mathbf{R}_{section\ 1}$ it is then possible to calculated the respective length of the two membrane sections as the lengths will be proportional to the respective resistances. The clean membrane resistance was taken as $32x10^{10}$/m and the resistance due to adsorption as $47.5x10^{10}$/m. The value for the part membrane resistance corresponded to 0.47% of the total pore length or assuming a total pore length of 10 μm a fouling length of 47 nm. This is of the same order as the initial pore size of the membrane. Assumptions made in the above model with regard to pore shape and characteristics limit the model to a qualitative demonstration that this fouling mechanism is reasonable.

6.4.4.2. Protein-protein interactions and the role of calcium

Initially, the membrane pore size was reduced by monolayer adsorption of protein by 9-10 nm. Thus, further protein passing through a 50 nm membrane would essentially pass through a 40 nm pore with a surface covered by deposited protein. The nature of this protein cannot easily be determined as protein adsorption to a membrane is usually irreversible and can result in the disruption of the protein structure and denaturation of the protein (see Section 2). Thus, the surface may have a mixture of active groups and possible binding sites. One thing is clear, to block a 50 or 100 nm pore would require around 10-12 or 20-25 proteins respectively if they "stack" directly on top of each other. Clearly, the predominant interactions are protein-protein rather than protein-membrane and after protein adsorption has

occurred the membrane surface properties may have little impact on the fouling behaviour. Thus, it is appropriate to consider the protein-protein interactions of ß-lactoglobulin to see if there are analogies to the behaviour observed in membrane fouling. Papers that discuss the aggregation and gelation of ß-lactoglobulin or whey protein solutions have been reviewed.

The thermal behaviour of ß-lactoglobulin is complex, involving both molecular unfolding (denaturation) and subsequent intermolecular polymerisation (aggregation). Sawyer (1968) suggested the following pathway for ß-lactoglobulin. The first step of dissociation of the dimer to a monomer, the second step being molecular unfolding, the third a SH/SS aggregation and the last a non-specific secondary aggregation. He did recognise that it was possible to form aggregates from the unfolded molecule without SH/SS interactions. Morr & Josephson (1968) also suggested a similar mechanism: firstly, reversible denaturation of the whey proteins by breaking intramolecular hydrogen and hydrophobic bonds and irreversible denaturation by thiol-SH group reactions; secondly, the formation of intermediate sized aggregates, a step that was somewhat calcium dependent, but even more dependent upon thiol-sulphide interactions; and thirdly, gross aggregation, a step that was dependent upon calcium.

The protein's environment determines the susceptibility of the protein to denaturation. ß-Lactoglobulin denatures less readily in the presence of lactose and salts (de Wit, 1981); however, the aggregation of the denatured proteins is enhanced by the presence of salt (Gault & Fauquant, 1992). According to de Wit (1981), the susceptibility of the whey proteins to thermal denaturation is largely determined by the pH, increasing as the pH is raised, but the extent of aggregation seemed to be dependent upon the presence of calcium ions. Raising the pH also improves solubility of the protein, hence, reducing the tendency of the protein to aggregate (Xiong *et al.*, 1993).

Unfolding or denaturation of the protein changes the protein conformation to expose groups that were buried in the native protein structure, thus resulting in an increased activity of such groups and enabling interchange reactions, such as disulphide

interchange, to occur as part of aggregation. Sawyer (1968) found that if ß-lactoglobulin was heated at 97.5°C and at pH 7.0 the primary aggregation reaction arose from the formation of intermolecular disulphide bonds. Another reaction that was favoured at lower temperatures gave rise to a much heavier aggregate that was not the product of intermolecular disulphide bonds. Parris *et al.* (1993) stated "whey proteins can be destabilised to varying degrees by duration and temperature of the heat treatment, the pH and ionic strength and the ionic composition. Aggregate formation is aided by ionic calcium and the formation of intermolecular disulphide bonds". Kinsella & Whitehead (1989) indicated that the aggregation and precipitation of ß-lactoglobulin are influenced by pH and the presence of calcium ions. de Rham & Chanton (1984) suggest that calcium and a pH near the protein iso-electric point could produce precipitation during a heat treatment.

Whey protein aggregation is a multi-reaction process; the individual reactions may occur simultaneously or sequentially during heating. Disulphide interactions and interactions specifically with calcium appear to dominate the aggregation process although the exact mechanisms are complex and highly dependent upon the physico-chemical environment of the solutions and the time/temperature combination of the heat treatment. Disulphide interactions appear to dominate at higher temperatures whereas calcium interactions occur more often in the final stages of gross aggregation and precipitation. It also appears that the disulphide and calcium reactions inter-react and are dependent upon one another (de Wit, 1981). Hill (1988) also suggested that aggregations of ß-lactoglobulin are specific interactions of unfolded ß-lactoglobulin with itself or with denatured α-lactalbumin. Thus in a milk or whey preparation interactions with other components, especially the other proteins present, also impact on the aggregation phenomenon.

Looking more carefully at the role calcium plays in the aggregation or gelation process. The suppression of repulsion by counter ions, *i.e.* sodium or calcium, enhances protein-protein interaction and the formation of a more stable gel network (Matsudomi *et al.*, 1991). Calcium has a additional effect beyond charge neutralisation (Varunsatian *et al.,* 1983; Mulvihill & Kinsella, 1988; Kuhn & Foegeding, 1991; Foegeding *et al.*, 1992; Xiong, 1992; Xiong *et al.*, 1993) and

where sodium and calcium were mixed calcium dominated the behaviour (Kuhn & Foegeding, 1991). Increasing the ionic strength does reduce the interaction of calcium with the protein but does not prevent it (Baumy & Brule, 1988; Patocka & Jelen, 1991; Jeyarajah & Allen, 1994). At higher ionic strength there will be more competition of other cations with calcium for negative groups as well as for specific binding sites.

Mulvihill and Kinsella (1988) suggested that the primary effect of calcium is likely to involve electrostatic interactions with calcium acting to cross-link negatively charged partially unfolded protein molecules. Xiong (1992) suggested that being a divalent cation, calcium is capable of forming an ion-bridge between two adjacent carboxyl groups from different peptide chains, whereas sodium cannot. Likewise, Gault & Fauquant (1992) suggested that calcium was more efficient than sodium in inducing gelation because it was able to form intermolecular calcium bridges. Kinsella & Whitehead (1989) suggested that calcium interacted with the negatively charged carboxyl groups of the protein, reducing the net charge on the protein to zero and causing isoelectric precipitation (also see de Wit (1981)).

Rector *et al.* (1989) found that whey protein isolate that had been extensively dialysed formed reversible gels (solution gels at 8°C after a heat treatment but melts if reheated) under certain conditions (pH 6.5-8.0, 9-10.5% protein). Apparently polymers of ß-lactoglobulin form on heating, but do not form a continuous network. Weak cross-links form between these large aggregates on cooling to form a weak network. Gels were not reversible in the presence of calcium where strong divalent salt bridges existed between two negatively charged proteins and if the pH or concentration was raised SH/SS bonds form. Barbut & Foegeding (1993) looked at the formation of WPI gels after the addition of calcium at 25°C. Gels only formed if the WPI had been preheated to 70°C and cooled prior to calcium addition. Some turbidity of the solution was observed when the solution was heated above 64°C. They suggested that the preheat temperature made the protein susceptible to calcium gelation. If calcium was added prior to the heat treatment, turbidity was observed above 45°C, probably as a result of calcium mediated protein-protein interactions. The solution with calcium gelled at 66°C. For both calcium and thermally induced gelation, a certain degree of protein unfolding was required before gelation.

So in summary, protein aggregation appears to be dependent upon the protein first unfolding or denaturing. Thereafter a large number of mechanisms appear possible depending upon the physico-chemical state of the solution and the physical treatment (heat) given to the solution. Disulphide interactions may occur at high temperatures and pH and are essentially irreversible. Calcium can also induce gelation probably through an ion-bridge between two negatively charged protein groups. The results of Barbut & Foegeding (1993) suggested that once the protein is sufficiently denatured to be "conditioned" to gel, gelation was possible at temperatures as low as 25°C.

Moving back to the fouling behaviour observed, the strong relationship between the calcium level and fouling suggests that a calcium ion bridge is the most likely mechanism for the protein-protein interaction required to block the 50-100 nm pores. The reversibility of the fouling and the recovery of protein transmission strongly indicate that disulphide bridges are not present in the fouling deposit as such interactions are usually irreversible.

6.4.4.3. Protein unfolding and the effect of shear

The question that arises in the previous section is: how does the protein get to the "conditioned" or denatured form so that it is able to react with calcium and form a protein-protein bond? One possibility is that the shear stress exerted on the protein near the pore (adsorbed protein) wall as it enters the pore "stretches" or reversibly unfolds the proteins as has been suggested by Franken *et al.* (1990), Bowen and Gan (1991, 1992) and Jonsson *et al.* (1992). As the flux is increased, the shear stress in the pore is increased causing an increase in fouling as observed in the experimental data. Several studies have looked at the effect of shear on the gelation or viscosity behaviour of concentrated ß-lactoglobulin or whey protein solutions. Pradipasena & Rha (1977) studied the viscosity of 3-40% ß-lactoglobulin solutions for varying shear conditions. The rheopectic behaviour observed appeared to be a result of protein denaturation that was characterised by an increase in the size of the molecules and the exposure of hidden active groups. Behaviour appeared to be balanced between the formation of aggregates and the break up of the aggregates by shear. Ker &

Toledo (1992) stated: "mechanical stress on proteins has been implicated in denaturation reactions, particularly with pumped or vigorously stirred enzyme systems". In their own work they looked at the effect of shear on a 35% suspension of WPI. Increased shear (up to 5800 /s) resulted in an increase in the viscosity of the suspension and a tendency towards dilatancy. High shear also resulted in higher gel strengths although there was an interaction between the temperature of shear and the gel strength. They concluded that high mechanical shearing prior to heating accelerated protein-protein aggregation. Shearing appeared to accelerate the unfolding stage of the gelling/aggregation mechanism. Taylor and Fryer (1994) looked at the effect of shear on the gelation of whey protein concentrates. When shear was applied prior to gelation at pH 7.0, large protein aggregates formed and the initial gel strength after shear increased, suggesting that aggregation was enhanced by shear. Increased time of shearing had a secondary effect of breaking up the aggregates/network. Thus overall, shear appears to enhance protein-protein interactions at least in concentrated solutions.

Harris *et al.* (1989) looked at the effect of processing steps in the manufacture of a whey protein concentrate. They initially hypothesised that shear may cause the protein molecules to partly unfold, exposing hydrophobic domains that are normally shielded from water within the interior of the globular protein. This provides the potential for increased hydrophobic interactions that may be of advantage in food systems. However, excessive destabilizing forces such as elevated temperatures or extreme shear may cause further denaturation with an accompanying loss of functionality. In a review of previous work they found in most instances pumping alone did not change the properties of the protein. However, pressure regulating valves did cause some protein denaturation sufficient to reduce the whipping properties of egg white. In their own study they found that a centrifugal pump had no detrimental effect on the surface hydrophobicity of cheese whey (*i.e.* no denaturation). A plate and frame UF plant resulted in a slight enhancement of hydrophobicity indicating that there had been partial protein unfolding. A pressure regulating valve after the UF plant had a rapid deleterious effect on the hydrophobicity for pressure drops of 200-400 kPa. Plastic tubing provided a simple alternative method of pressure control that had no effect on the surface

hydrophobicity of the protein. The reason given for the deleterious effect of the ball valve compared to the plastic tubing is the magnitude of the shear developed. The valve produced the pressure drop over a very short distance (very high shear), whereas the plastic tubing dissipated the pressure over a considerable distance at much lower shear.

Shaking has also been found to denature ß-lactoglobulin (Reese & Robbins, 1981). The authors stated that while shear did have a minor role in the shaking inactivation of the protein, they believed that air-liquid surface effects played a major role. Proteins are adsorbed at the air-water interface, are unfolded and aggregate. Shaking removes the aggregates from the surface film allowing more protein to adsorb at the interface, denature and aggregate. Other workers have also found that protein can be denatured at an air-water interface (Narendranathan & Dunnill, 1982; Matthiasson, 1983; Andrews, 1991). Andrews (1991) worked with ß-lactoglobulin solutions.

Thus, shear has been found to enhance protein-protein interactions under some conditions; in particular, in pressure relief valves where a very high shear exists over a very short distance - a situation not too dissimilar to a MF membrane. So it seems reasonable that shear could be responsible for the observed behaviour with the permeate flux. Unfortunately, measurement or assessment of the actual shear at the pore entrance is difficult. Transmembrane pressure data was used to calculate an average shear rate over the thickness of the membrane (see Table 6.3). However, there is no guarantee that the pressure drop was even across the membrane thickness and in reality a much higher pressure drop might be expected at the pore entrance due to entrance effects and the asymmetric nature of the membrane. Furthermore, the work of Bowen & Gan (1993) found that the membrane pore structure and in particular the sharpness of the pore entrance has a major effect on protein fouling.

The average shear rates in the membrane pore calculated from data 3 min after the introduction of protein to the plant are reasonably high (Table 6.3) and may in fact be higher at the pore entrance. However, they are of the same order as the membrane wall shear rate because of the cross-flow velocity (the wall shear stress was typically 30 Pa (shear rate 34,000 /s)). This suggests that it is not the permeate

flux or shear rate alone that is responsible for fouling but that the shear or permeate flux interacts with the pore geometry and in particular the nature of the pore entrance to cause fouling as suggested by Bowen & Gan (1993).

Table 6.3. Estimation of shear rate in the membrane pores for varying permeate fluxes on the 50 nm membrane. The shear stress was calculated from Equation 3.39 using ΔP_{TM} data from 3 min. Shear rate was calculated assuming Newtoniun behaviour. A viscosity of 0.89×10^{-3} Pa.s and a membrane thickness of 10 μm were assumed.

Flux ($L/m^2.h$)	Run No	ΔP_{TM} (in) (kPa)	ΔP_{TM} (3 min) (kPa)	Shear Stress (Pa)	Shear Rate (/s)
50	16	3.8	10.1	12.6	14,190
	38	4.1	10.0	12.5	14,045
100	22	8.4	22.8	28.5	32,022
	24	7.9	20.7	25.9	29,073
150	21	12.8	33.8	42.3	47,472
	23	12.0	33.9	42.4	47,612
200	17	15.1	47.3	59.1	66,433
	19	14.8	49.9	62.4	70,084

The importance of the pore entrance in shear-related fouling suggests that deposition of protein will occur predominantly at the pore entrance. This is in total agreement with the conclusions drawn from mathematical modelling (see Section 6.4.4.1).

6.4.5. Surface layer formation

Under low fouling conditions when the protein transmission was high and constant there was little or no surface layer formation. However, the large impact of the cross-flow velocity on membrane resistance (Fig. 6.44) suggested that when fouling was more severe the formation of a surface or dynamic layer as a result of concentration polarisation occurred. In all trials there is an initial jump in membrane resistance upon the introduction of product to the plant. This resistance may be because of "inner pore" effects during the passage of protein through the membrane

or to surface layer effects. In the trials with cross-flow velocity the initial jump in resistance was similar for all of the velocities. Any surface or boundary layer effect is dependent upon the retention of protein by the membrane and this suggests that initially the retention of protein is close to zero in these trials. Once protein retention increased the cross-flow velocity did impact on the boundary layer reducing the boundary or surface layer effect as the cross-flow velocity increased. These observations are in keeping with a model where surface layer formation or boundary layer effects are dependent upon the concentration of protein at the membrane wall, and therefore with the 50 and 100 nm membranes, in the absence of pore narrowing, the surface layer does not impact on membrane behaviour as the protein retention remains low. Furthermore, the onset of surface layer formation would be more rapid at higher fluxes as was observed. For the 20 nm membrane protein retention was high initially and a surface layer formed on the membrane almost immediately.

It is interesting to compare the 2 h protein transmission of all three membranes after severe fouling had occurred (Table 6.4). For the 50 and 100 nm membranes calcium was present in the feed but not for the 20 nm membrane. For all three membranes the protein transmissions were similar (8-12%). This is in keeping with the formation of a surface layer on the membrane surface. Regardless of the initial pore size of the membrane the final selectivity of the membrane once heavily fouled was controlled by the porosity of the surface layer. The fact that the transmission does not reduce to zero indicates that the surface layer was not "100% complete" and a small quantity of protein still "leaks" through the membrane.

Table 6.4. Effect of the membrane pore size on the protein transmission (%) after severe fouling had occurred on the membrane.

Pore size (nm)	Run Nos	Protein Transmission (%)
20	12-39	8.6-10.2
50	17-19	11-11.7
100	40-41	8-8.2

6.5. Conclusions

Four phenomena contribute to membrane fouling during the MF of ß-lactoglobulin. Firstly, upon the introduction of protein to the system, there is a jump in resistance due to some form of dynamic fouling. This appears to be initially constant with respect to the flux and cross-flow velocity but may increase as the retention of protein increases. Secondly, protein adsorption to the membrane surface and throughout the membrane pores leads to a reduction in the pore diameter by twice the diameter of the protein.

Thirdly, under conditions of high flux and in the presence of calcium, a protein-protein interaction at the pore entrance leads to a narrowing of the pore entrance and the eventual retention of the protein by the membrane. The protein-protein interaction is strongly dependent upon calcium and it is suggested that the calcium forms an ion-bridge between negatively charged groups of the free protein and the protein already adsorbed or bound to the membrane. In order for this interaction to occur the protein must be reversibly or irreversibly denatured, that is, unfolded or with a distortion of conformation, and this occurs with high fluxes because of high localised shear rates at the pore entrance.

Finally, as the protein retention increases a surface layer of protein deposits on the membrane. It is not clear whether this protein layer is an extension of the dynamic fouling initially observed after the introduction of protein to the plant, or whether it is a separate behaviour induced by increased protein concentration at the membrane wall.

Once formed severe fouling was not easily removed by mild changes in the hydrodynamic conditions when operating on product but the removal of calcium from the system or flushing the plant with water removed most of the resistance fouling. In the presence of calcium the level of irreversible resistance remained reasonably constant regardless of the degree of severe fouling or the operating conditions used.

7. Recommendations for further study

7.1. MF of skim milk

The research presented in this thesis has demonstrated that casein micelles form a "gel layer" on the membrane surface if concentration polarisation results in a wall concentration above that critical for gel layer formation. Clearly the nature of this layer, especially its stability or "removability", and control of the membrane hydrodynamics are of critical importance.

Research is needed to identify the nature of the gel layer and the forces that "hold it" together. Rheological studies with concentrated casein or skim milk solutions could determine the actual concentration of casein required for "gel formation" or the occurrence of extremely high viscosities. The addition or removal of the whey proteins or minerals, *e.g.* calcium or phosphate, would give some indication of the role of these components in the stability of the layer.

Research is also needed to identify how the gel layer on the membrane can be disrupted. It has been shown that reducing the concentration driving force by reducing the flux or increasing the cross-flow velocity does not remove the gel layer from the membrane but the immediate flushing of the membrane with water after gel layer formation does. What effect would reducing the permeate flow to zero for a short period of time (leaving the membrane in contact with the skim milk), or a short "plug" of water in the retentate, or back-flushing have on the stability of the gel layer? Research is needed to identify whether process steps like these could be used to restore the membrane cleanliness and thus, offer a means of recovering plant performance without the cost and disruption of a full cleaning cycle.

The membrane module hydrodynamics are clearly important and more research is required in this area. Module designs that minimise concentration polarisation over all of the membrane area and operate in constant flux mode are required in order to increase the allowable permeate flux.

7.2. Fouling by ß-lactoglobulin or other smaller proteins

The influence of the permeate flux or shear in the pores has been demonstrated for several proteins, ß-lactoglobulin in this study, BSA and YADH in the studies of Bowen & Hughes (1990) and Bowen & Gan (1991, 1992, 1993).

In this thesis, by analogy to gelation and aggregation research on ß-lactoglobulin, a mechanism for the protein-protein interactions necessary to block a large pore has been suggested. Further research is required (separate from membrane studies) to confirm that shear forces are able to enhance protein-protein interactions in a ß-lactoglobulin solution.

Clearly calcium plays a pivotal role in the protein interaction and more studies are required with differing calcium, protein and other mineral concentrations to explore this mechanism. Also of interest in this study was the partial reversibility of the fouling. Experiments are needed to explore this area. Flushing with a calcium solution rather than water and further experiments where the active calcium content of the feed material is reduced after severe fouling has occurred could be performed.

7.3. General

Although the effect of shear on pore fouling has been demonstrated for BSA and YADH and the location of this fouling identified, no detailed mechanisms for the protein-protein interactions occurring have been presented. More research and emphasis on identifying protein interaction and deposition mechanisms is required. Furthermore, each protein has different properties and will behave differently during MF. Therefore, there is a great need in membrane research in this area to extend studies to other proteins apart from BSA.

Clearly, an understanding of the nature of the protein filtered and its physical interactions is crucial if the mechanisms of protein fouling are to be unravelled. Far more emphasis on protein behaviour and less on engineering modelling is required in future research.

8. Nomenclature

Symbol	Description	Units
A_i	Area of blocked membrane (Eq. 3.28)	m^2
A_m	Membrane area	m^2
A_o	Original membrane area (Eq. 3.28)	m^2
C	Concentration	%
C_b	Bulk or feed concentration	%
C_p	Permeate concentration	%
C_r	Retentate concentration	%
C_w	Membrane wall concentration	%
D	Diffusion coefficient	m^2/s
D_c	Diffusion coefficient at particular C	m^2/s
D_o	Diffusion coefficient from Stokes-Einstein relationship	m^2/s
d	Diameter	m
d_e	Equivalent diameter	m
d_p	Pore diameter	m
J	Permeate flux	$L/m^2.h$ or g/min
J_o	Original permeate flux	$L/m^2.h$ or g/min
J_{ss}	Steady state permeate flux (Eq. 3.13)	$L/m^2.h$
K_i	Constant in intermediate blocking law	
K_p	Constant in complete blocking law	
K_s	Constant in standard blocking law	
k	Mass transfer coefficient	
k_b	Boltzmann constant	
k_d	Rate constant	
L	Length	m
M	Molecular weight	
M_p	Mass of protein deposited (Eq. 3.23)	g
M_s	Mass of protein deposited (Eq. 3.15)	g

Symbol	Description	Units
N	Number of pores	
ΔP	Pressure difference	Pa
ΔP_e	Effective pressure	Pa
ΔP_L	Longitudinal pressure drop	kPa
ΔP_o	Original pressure difference	kPa
ΔP_{TM}	Transmembrane pressure	kPa
Q	Filtration rate (J x A_m)	m^3/s
Q_o	Original filtration rate	m^3/s
R	Resistance	/m x 10^{10}
R_f	Fouling resistance	/m x 10^{10}
R_f^*	Plateau fouling resistance (Eq. 3.7)	/m x 10^{10}
R_g	Gas constant	
R_{if}	Irreversible resistance	/m x 10^{10}
R_m	Clean membrane resistance	/m x 10^{10}
R_o	Original resistance	/m x 10^{10}
R_{rf}	Reversible resistance	/m x 10^{10}
r	Radius	m
r_o	Original radius	m
SD	Standard deviation	
SP	Set point	
T	Temperature	°C or K
T_r	Transmission	%
TMP	Transmembrane pressure	kPa
t	Time	s or min or h
u	cross-flow velocity	m/s
V	Volume	m^3
x	Distance	m
α_f	Specific cake resistance	

Symbol	Description	Units
ϵ	Porosity or void volume	
λ	Ratio of particle / pore diameter (Eq. 3.35)	
μ	Dynamic viscosity	Pa.s
μ_p	Permeate viscosity	Pa.s
μ_s	Solvent viscosity	Pa.s
$\Delta\Pi$	Osmotic pressure	kPa
ρ	Density	Kg/m^3
ρ_p	Permeate density	Kg/m^3
σ	Real retention coefficient	
σ_i	Intrinsic retention coefficient	
τ	Shear stress	Pa
ϕ	Volume fraction	
ψ	Interaction factor (Eq. 5.1)	

9. References

Abaticchio P, Bottino A, Camera Roda G, Capannelli G & Munari S (1990). Characterisation of ultrafiltration polymeric membranes. *Desalination*, **78**, 235-255.

Aimar P, Baklouti S & Sanchez V (1986). Membrane-solute interactions: influence on pure solvent transfer during ultrafiltration. *Journal of Membrane Science*, **29**, 207-224.

Aimar P, Taddei C, Lafaille J-P & Sanchez V (1988). Mass transfer limitations during ultrafiltration of cheese whey with inorganic membranes. *Journal of Membrane Science*, **38**, 203-221.

Andrews A T (1991). Partial denaturation and renaturation of ß-lactoglobulin at air-water interfaces. *Biochemical Society Transactions*, **19**, 272S.

Attia H, Bennasar M & Tarodo de la Fuente B (1988). Ultrafiltration sur membrane minérale de laits acidifiés à divers pH par voie biologique ou chimique et de coagulum lactique. *Le Lait*, **68**(1), 13-32.

Attia H, Bennasar M & Tarodo de la Fuente B (1991a). Study of the fouling of inorganic membranes by acidified milks using scanning electron microscopy and electrophoresis. I. Membrane with pore diameter 0.2 μm. *Journal of Dairy Research*, **58**, 39-50.

Attia H, Bennasar M & Tarodo de la Fuente B (1991b). Study of the fouling of inorganic membranes by acidified milks using scanning electron microscopy and electrophoresis. II. Membrane with pore diameter 0.8 μm. *Journal of Dairy Research*, **58**, 51-65.

Baker R J, Fane A G, Fell C J D & Yoo B H (1985). Factors affecting flux in crossflow filtration. *Desalination*, **53**, 81-93.

Barbut S & Foedeging E A (1993).
Ca^{2+}-induced gelation of pre-heated whey protein isolate. *Journal of Food Science*, **58**, 867-871.

Baumy J J & Brule G (1988).
Binding of bivalent cations to α-lactalbumin and ß-lactoglobulin: effect of pH and ionic strength. *Le Lait*, **68**(1), 33-48.

Bauser H, Chmiel H, Stroh N & Walitza E (1986).
Control of concentration polarisation and fouling of membranes in medical, food and biotechnical applications. *Journal of Membrane Science*, **27**, 195-202.

Bennasar M, Rouleau D, Mayer R & Tarodo de la Fuente B (1982).
Ultrafiltration of milk on mineral membranes: improved performance. *Journal of the Society of Dairy Technology*, **35**, 43-49.

Bentham A C, Ireton M J, Hoare M & Dunnill P (1988).
Protein precipitate recovery using microporous membranes. *Biotechnology and Bioengineering*, **31**, 984-994.

Bhattacharyya D, Jumawan A B, Grieves R B & Harris L R (1979).
Ultrafiltration characteristics of oil-detergent-water systems: membrane fouling mechanisms. *Separation Science and Technology*, **14**, 529-549.

Blatt W F, Dravid A, Michaels A S & Nelsen L (1970).
Solute polarisation and cake formation in membrane ultrafiltration: causes, consequences, and control techniques. In J E Flinn (Ed.), *Membrane Science and Technology*, Plenum Press, New York, 47-97.

Bottino A, Capannelli G, Imperato A & Munari S (1984).
Ultrafiltration of hydrosoluble polymers. Effect of operating conditions on the performance of the membrane. *Journal of Membrane Science*, **21**, 247-267.

Bowen W R & Hughes D T (1990).
Properties of microfiltration membranes. II. Adsorption of bovine serum albumin at aluminium oxide membranes. *Journal of Membrane Science*, **51**, 189-200.

Bowen W R & Gan Q (1991).
Properties of microfiltration membranes: flux loss during constant pressure permeation of bovine serum albumin. *Biotechnology and Bioengineering*, **38**, 688-696.

Bowen W R & Gan Q (1992).
Properties of microfiltration membranes: the effects of adsorption and shear on the recovery of an enzyme. *Biotechnology and Bioengineering*, **40**, 491-497.

Bowen W R & Gan Q (1993).
Microfiltration of protein solutions at thin film composite membranes. *Journal of Membrane Science*, **80**, 165-173.

Brink L E S & Romijn D J (1990).
Reducing the protein fouling of polysulphone surfaces and polysulphone ultrafiltration membranes: optimisation of the type of presorbed layer. *Desalination*, **78**, 209-233.

Capannelli G, Vigo F & Munari S (1983).
Ultrafiltration membranes-characterisation methods. *Journal of Membrane Science*, **15**, 289-313.

Casiraghi E M & Peri C (1983).
Performance of new membranes in milk and whey ultrafiltration. In: C Cantarelli & C Peri, *Progress in Food Engineering*, Forster-Verlag, Kusnacht, 349-356.

Chen V, Fane A G & Fell C J D (1992).
The use of anionic surfactants for reducing fouling of ultrafiltration membranes: their effects and optimisation. *Journal of Membrane Science*, **67**, 249-261.

Cheryan M (1986).
Ultrafiltration handbook. Technomic Publishing, Lancaster.

Cheryan M & Chiang B H (1984).
Performance and fouling behaviour of hollow fibre and spiral wound ultrafiltration modules processing skim milk. In: B M KcKenna (Ed.), *Engineering and Food*, **Vol 1**, Elvevier Applied Science Publishers, London, 191-197.

Chiang B H & Cheryan M (1987).
Modelling of hollow-fibre ultrafiltration of skimmilk under mass-transfer limiting conditions. *Journal of Food Engineering*, **6**, 241-255.

Chmiel H & McDonough R M (1989).
Membrane fouling due to unspecific interaction of proteins. In: H G Kessler & D B Lund (Eds.), *3rd International Conference on Fouling and Cleaning in Food Processing*, Technische Universitat, Munich, 313-322.

Chudacek M W & Fane A G (1984).
The dynamics of polarisation in unstirred and stirred ultrafiltration. *Journal of Membrane Science*, **21**, 145-160.

Chichocki B & Felderhof B U (1990).
Journal of Chemical Physics, **93**, 442.

Clark W M, Bansal A, Sontakke M & Ma Y H (1991).
Protein adsorption and fouling in ceramic ultrafiltration membranes. *Journal of Membrane Science*, **55**, 21-38.

Daufin G, Labbe J-P, Quemerais A, Michel F, Robert F & Fiaud C (1989).
Spectroscopic analysis of fouling layers of inorganic ultrafiltration membranes. In: H G Kessler & D B Lund (Eds.), *3rd International Conference on Fouling and Cleaning in Food Processing*, Technische Universitat, Munich, 207-215.

Daufin G, Labbe J-P, Quemerais A & Michel F (1991).
Fouling of an inorganic membrane during ultrafiltration of defatted whey protein concentrates. *Netherlands Milk and Dairy Journal*, **45**, 259-272.

Daufin G, Radenac J-F, Gesan G, Kerherve F-L, Le Berre O & Michel F (1993).
A novel rig design for ultra- and microfiltration experiments. *Separation Science and Technology*, **28**, 2635-2642.

de Balmann H & Nobrega R (1989).
The deformation of dextran molecules. Causes and consequences in ultrafiltration. *Journal of Membrane Science*, **40**, 311-327.

de Balmann H, Aimar P & Sanchez V (1990).
Membrane partition and mass transfer in ultrafiltration. *Separation Science and Technology*, **25**, 507-534.

Defrise D & Gekas V (1988).
Microfiltration membranes and the problem of microbial adhesion - A literature survey. *Process Biochemistry*, **23**, 105-116.

Dejmek P & Nilsson J L (1989).
Flux-based measures of adsorption to ultrafiltration membranes. *Journal of Membrane Science*, **40**, 189-197.

de Kruif C G (1992).
Casein micelles: diffusivity as a function of renneting time. *Langmuir*, **8**, 2932-2937.

Delaney R A M & Donnelly J K (1977).
Applications of reverse osmosis in the dairy industry. In: S Sourirajan (Ed.), *Reverse Osmosis and Synthetic Membranes: Theory - Technology - Engineering*, National Research Council Canada, 417-443.

de Rham O & Chanton S (1984).
Role of ionic environment in insolubilization of whey protein during heat treatment of whey proteins. *Journal of Dairy Science*, **67**, 939-949.

Devereux N & Hoare M (1986).
Membrane separation of protein precipitates: studies with cross flow in hollow fibres. *Biotechnology and Bioengineering*, **28**, 422-431.

de Wit J N (1981).
Structure and functional behaviour of whey proteins. *Netherlands Milk and Dairy Journal*, **35**, 47-64.

Dumon S & Barnier H (1992).
Ultrafiltration of protein solutions on ZrO_2 membranes. The influence of surface chemistry and solution chemistry on adsorption. *Journal of Membrane Science*, **74**, 289-302.

Elbers S J G & Brink L E S (1990).
Mechanism of the anti-fouling action of polymers presorbed on ultrafiltration membranes. *Membraantechnologie*, **5**, 68.

Fane A G (1983).
Factors affecting flux and rejection in ultrafiltration. *Journal of Separation Process Technology*, **4**(1), 15-23.

Fane A G & Fell C J D (1987).
A review of fouling and fouling control in ultrafiltration. *Desalination*, **62**, 117-136.

Fane A G, Fell C J D & Waters A G (1981).
The relationship between membrane surface pore characteristics and flux for ultrafiltration membranes. *Journal of Membrane Science*, **9**, 245-262.

Fane A G, Fell C J D & Waters A G (1983a).
Ultrafiltration of protein solutions through partially permeable membranes - the effect of adsorption and solution environment. *Journal of Membrane Science*, **16**, 211-224.

Fane A G, Fell C J D, McDonogh R M, Suki A & Waters A G (1983b).
The fouling of membranes. In: *Proceedings of the Eleventh Australian Conference on Chemical Engineering (Chemeca 83)*, Brisbane, 4-7 September 1983, 729-737.

Fane A G, Fell C J D & Suki A (1983c).
The effect of pH and ionic environment on the ultrafiltration of protein solutions with retentive membranes. *Journal of Membrane Science*, **16**, 195-210.

Fane A G, Fell C J D & Kim K J (1985).
The effect of surfactant pretreatment on the ultrafiltration of proteins. *Desalination*, **53**, 37-55.

Fauquant J, Maubois J-L & Pierre A (1988).
Microfiltration du lait sur membrane minerale. *Technique Laitiere*, **1028**, 21-23.

Ferry J D (1936).
Ultrafilter membranes and ultrafiltration. *Chemical Reviews*, **18**, 373-455.

Finnigan S M & Howell J A (1989).
The effect of pulsed flow on ultrafiltration fluxes in a baffled tubular membrane system. In: H G Kessler & D B Lund (Eds.), *3rd International Conference on Fouling and Cleaning in Food Processing*, Technische Universitat, Munich, 216-237.

Foegeding E A, Kuhn P R & Hardin C C (1992).
Specific divalent cation-induced changes during gelation of ß-lactoglobulin. *Journal of Agricultural and Food Chemistry*, **40**, 2092-2097.

Fontyn M, van't Riet K & Bijsterbosch B H (1989).
Adsorption mechanism of PPG on polysulfone membranes; chemical interaction and pore size distribution alteration. *Membraantechnologie*, **4**, 58.

Forman S M, DeBernardez E R, Feldberg R S & Swartz R W (1990).
Crossflow filtration for the separation of inclusion bodies from soluble proteins in recombinant *Escherichia coli* cell lysate. *Journal of Membrane Science*, **48**, 263-279.

Franken A C M, Sluys J T M, Chen V, Fane A G & Fell C J D (1990).
Role of protein conformation on membrane characteristics. In: Proceeding of Vth World Filtration Conference, Nice, 207-213.

Gatenholm P, Paterson S, Fane A G & Fell C J D (1988a).
Performance of synthetic membranes during cell harvesting of *E. Coli*. *Process Biochemistry*, **23**, 79-81.

Gatenholm P, Fell C J and Fane A G (1988b).
Influence of the membrane structure on the composition of the deposit-layer during processing of microbial suspensions. *Desalination*, **70**, 363-378.

Gault P & Fauquant J (1992).
Aptitude à la gélification thermique de la ß-lactoglobuline: influence du pH,de l'environment ionique et de la présence des autres protéines du lactosérum. *Lait*, **72**, 491-510.

Gekas V (1988).
Terminology for pressure-driven membrane operations. *Desalination*, **68**, 77-92.

Gekas V & Hallström B (1987).
Mass transfer in the membrane concentration polarisation layer under turbulent cross flow. I. Critical literature review and adaptation of existing sherwood correlations to membrane operations. *Journal of Membrane Science*, **30**, 153-170.

Gekas V & Hallström B (1990).
Microfiltration membranes, cross-flow transport mechanisms and fouling studies. *Desalination*, **77**, 195-218.

Gergen R, Gerner F J & Konstantin P (1989).
UF - membrane characterisation by gel permeation chromatography. Poster Presented at 6th International Symposium on Synthetic Membranes in Science and Industry, Tubingen, 4-8 September.

Glover F A (1985).
Modifications to the composition of milk. In: R K Robinson (Ed.), *Modern Dairy Technology - Advances in Milk Processing*, Volume 1, Elsevier Applied Science, London, 235-271.

Glover F A & Brooker B E (1974).
The structure of the deposit formed on the membrane during the concentration of milk by reverse osmosis. *Journal of Dairy Research*, **41**, 89-93.

Goldsmith R L (1971).
Macromolecular ultrafiltration with microporous membranes. *Industrial and Engineering Chemistry Fundamentals*, **10**(1), 113-120.

Grace H P (1956).
Structure and performance of filter media. *A.I.Ch.E. Journal*, **2**(3), 307-336.

Hallström M & Dejmek P (1988).
Rheological properties of ultrafiltered milk. II. Protein voluminosity. *Milchwissenschaft*, **43**, 95-97.

Hallström B, Trägårdh G & Nilsson J L (1989).
Membrane technology in the food industry. In: W E S Spiess & H Schubert (Eds.), *Engineering and Food, Volume 3 - Advanced Processes*, Elsevier Applied Science, London, 194-208.

Hanemaaijer J H (1985).
Microfiltration in whey processing. *Desalination*, **53**, 143-155.

Hanemaaijer J H, Robbertsen T, van den Boomgaard Th, Olieman C, Both P & Schmidt D G (1988).
Characterisation of clean and fouled ultrafiltration membranes. *Desalination*, **68**, 93-108.

Hanemaaijer J H, Robbertsen T, van den Boomgaard Th & Gunnick J W (1989).
Fouling of ultrafiltration membranes. The role of protein adsorption and salt precipitation. *Journal of Membrane Science*, **40**, 199-217.

Hansen R (1988).
Better market milk, better cheese milk and better low heat milk powder with Bactocatch treated milk. *North European Food and Dairy Journal*, **54**(1), 39-41.

Harris J L, Pecar M A & Pearce R J (1989).
Effects of the processing equipment on protein functionality in the concentration of cheese whey by ultrafiltration. *Australian Journal of Dairy Technology*, **44**, 78-81.

Hayes J F, Dunkerley J A, Muller L L & Griffin A T (1974).
Studies on whey processing by ultrafiltration. 2. Improving permeation rates by preventing fouling. *The Australian Journal of Dairy Technology*, **29**, 132-140.

Heinemann P, Howell J A & Bryan R A (1988).
Microfiltration of protein solutions: effect of fouling on rejection. *Desalination*, **68**, 243-250.

Hermia J (1982).
Constant pressure blocking laws-application to power-law non-newtonian fluids. *Transactions of the Institution of Chemical Engineers*, **60**, 183-187.

Hill A R (1988).
Thermal precipitation of whey proteins. *Milchwissenschaft*, **43**, 565-567.

Hlavacek M & Bouchet F (1993).
Constant flowrate blocking laws and an example of their application to dead-end microfiltration of protein solutions. *Journal of Membrane Science*, **82**, 285-295.

Hobman P G (1992).
Ultrafiltration and manufacture of whey protein concentrates. In J G Zadow (Ed.), *Whey and Lactose Processing*, Elsevier Applied Science, London, 195-230.

Hodgson P H & Fane A G (1991).
Crossflow microfiltration of biomass with inorganic membranes. The influence of membrane surface and fluid dynamics. Paper Presented at ICIM 91, Montpellier, 1-4 July 1991.

Horne D S (1986).
Steric stabilization and casein micelle stability. *Journal of Colloid and Interface Science*, **111**(1), 250-260.

Howell J A & Velicangil Ö (1980).
Protein ultrafiltration: theory of membrane fouling and its treatment with immobilised proteases. In: A R Cooper (Ed.), *Ultrafiltration Membranes and Applications*, Plenum Press, New York, 217-229.

Howell J A, Velicangil Ö, Le M S & Herrera Zeppelin A L (1981).
Ultrafiltration of protein solutions. *Annals of the New York Academy of Sciences*, **369**, 355-366.

Isaacson K, Duenas P, Ford C & Lysaght M (1980).
Determination of graetz solution constants in the *in-vitro* hemofiltration of albumin, plasma, and blood. In: A R Cooper (Ed.), *Ultrafiltration Membranes and Applications,* Plenum Press, New York, 507-522.

Jeyarajah S & Allen J C (1994).
Calcium binding and salt-induced structural changes of native and preheated ß-lactoglobulin. *Journal of Agricultural and Food Chemistry*, **42**, 80-85.

Jonsson G (1984).
Boundary layer phenomena during ultrafiltration of dextran and whey protein solutions. *Desalination*, **51**, 61-77.

Jonsson G (1985).
Molecular weight cut-off curves for ultrafiltration membranes of varying pore sizes. *Desalination*, **53**, 3-10.

Jonsson G (1986).
Transport phenomena in ultrafiltration: membrane selectivity and boundary layer phenomena. *Pure and Applied Chemistry*, **58**, 1647-1656.

Jonsson G & Christensen P M (1986).
Separation characteristics of ultrafiltration membranes. In: E Drioli & M Nakagaki (Eds.), *Membranes and Membrane Processes*, Plenum Press, New York, 179-190.

Jonsson G, Li W & Johansen P L (1992).
Fouling of UF/MF membranes by BSA: comparison between adsorption type and pore-blocking type of mechanisms. Paper Presented at Engineering of Membrane Processes, Garmish-Partenkirchen, 13-15 May 1992.

Kelly S T, Opong W S & Zydney A L (1993). The influence of protein aggregates on the fouling of microfiltration membranes during stirred cell filtration. *Journal of Membrane Science*, **80**, 175-187.

Kessler H G (1981).
Ultrafiltration - reverse osmosis - electrodialysis. *Food Engineering and Dairy Technology*, Verlag A Kessler, Freising, 82-118.

Ker Y C & Toledo R T (1992).
Influence of shear treatments on consistency and gelling properties of whey protein isolate suspensions. *Journal of Food Science*, **57**(1), 82-85, 90.

Kim K-J, Chen V & Fane A G (1993).
Ultrafiltration of colloidal silver particles: flux, rejection, and fouling. *Journal of Colloid and Interface Science*, **155**, 347-359.

Kim K-J, Fane A G & Fell C J D (1987).
The performance of ultrafiltration membranes modified by surface treatment. In: Proceedings of International Conference on Membranes and Membrane Processes (ICOM 87), Tokyo, 363-364.

Kim K-J, Fane A G & Fell C J D (1989). The effect of langmuir-blodgett layer pretreatment on the performance of ultrafiltration membranes. *Journal of Membrane Science*, **43**, 187-204.

Kim K-J, Fane A G, Fell C J D, Suzuki T & Dickson M R (1990).
Quantitative microscopic study of surface characteristics of ultrafiltration membranes. *Journal of Membrane Science*, **54**, 89-102.

Kim K-J, Fane A G, Fell C J D and Joy D C (1992).
Fouling mechanisms of membranes during protein ultrafiltration. *Journal of Membrane Science*, **68**, 79-91.

Kimura S & Nakao S-I (1975).
Fouling of cellulose acetate tubular reverse osmosis modules treating the industrial water in Tokyo. *Desalination*, **17**, 267-288.

Kinsella J E & Whitehead D M (1989).
Proteins in whey: chemical, physical, and functional properties. *Advances in Food and Nutrition Research*, **33**, 343-438.

Kroner K H, Nissinen V & Ziegler H (1987).
Improved dynamic filtration of microbial suspensions. *Bio/technology*, **5**, 921-926.

Kroner K H & Nissinen V (1988).
Dynamic filtration of microbial suspensions using an axially rotating filter. *Journal of Membrane Science*, **36**, 85-100.

Kuhn P R & Foegeding E A (1991).
Mineral salts effects on whey protein gelation. *Journal of Agricultural and Food Chemistry*, **39**, 1013-1016.

Labbe J-P, Quemerais A, Michel F & Daufin G (1990).
Fouling of inorganic membranes during whey ultrafiltration: analytical methodology. *Journal of Membrane Science*, **51**, 293-307.

Larsson K (1980).
Interfacial Phenomena - Bioadhesion and Biocompatibility. *Desalination*, **35**, 105-114.

Le M S & Howell J A (1983).
The fouling of ultrafiltration membranes and its pretreatment. In: C Cantarelli & C Peri (Eds.), *Progress in Food Engineering*, Forster-Verlag, Kusnacht, 321-326.

Le M S & Howell J A (1984).
Alternative model for ultrafiltration. *Chemical Engineering Research and Design*, **62**, 373-380.

Le M S, Spark L B & Ward P S (1984).
The separation of aryl acylamidase by crossflow microfiltration and the significance of enzyme/cell debris interaction. *Journal of Membrane Science*, **21**, 219-232.

Lee C K & Hong J (1988).
Characterisation of electric charges in microporous membranes. *Journal of Membrane Science*, **39**, 79-88.

Lee D N & Merson R L (1975).
Examination of cottage cheese whey proteins by scanning electron microscopy: relationship to membrane fouling during ultrafiltration. *Journal of Dairy Science*, **58**, 1423-1432.

Lee D N & Merson R L (1976).
Prefiltration of cottage cheese whey to reduce fouling of ultrafiltration membranes. *Journal of Food Science*, **41**, 403-410.

Lim T H, Dunkley W L & Merson R L (1971).
Role of protein in reverse osmosis of cottage cheese whey. *Journal of Dairy Science*, **54**, 306-311.

Lundström I (1985).
Models of protein adsorption on solid surfaces. *Progress in Colloid and Polymer Science*, **70**, 76-82.

McDonogh R M, Bauser H, Stroh N & Chmiel H (1990).
Concentration polarisation and adsorption effects in cross-flow ultrafiltration. *Desalination*, **79**, 217-231.

Madec M N, Mejean S & Maubois J-L (1992).
Retention of *Listeria* and *Salmonella* cells contaminating skim milk by tangential membrane microfiltration ("Bactocatch" process). *Lait*, **72**, 327-332.

Malmberg R & Holm S (1988).
Better market milk, better cheese milk and better low-heat milk powder with Bactocatch treated milk. *North European Food and Dairy Journal*, **1**, 1-7.

Marshall A D & Daufin G (1994).
Physico-chemical aspects of membrane fouling by dairy fluids. In: IDF Monograph, *Fouling and Cleaning in Pressure-driven Membrane Processes*, Accepted for Publication.

Matsudomi N, Rector D & Kinsella J E (1991).
Gelation of bovine serum albumin and ß-lactoglobulin; effects of pH, salts and thiol reagents. *Food Chemistry*, **40**, 55-69.

Matsumoto Y, Nakao S & Kimura S (1988).
Cross-flow filtration of solutions of polymers using ceramic microfiltration. *International Chemical Engineering*, **28**, 677-683.

Matthiasson E (1983).
The role of macromolecular adsorption in fouling of ultrafiltration membranes. *Journal of Membrane Science*, **16**, 23-26.

Matthiasson E (1984).
Macromolecular adsorption and fouling in ultrafiltration and their relationships to concentration polarisation. PhD Dissertation, University of Lund, Sweden.

Maubois J-L, Pierre A, Fauquant J & Piot M (1987).
Industrial fractionation of main whey proteins. *Bulletin of the International Dairy Federation*, **212**, 154-159.

Meireles M, Aimar P & Sanchez V (1991a).
Effects of protein fouling on the apparent pore size distribution of sieving membranes. *Journal of Membrane Science*, **56**, 13-28.

Meireles M, Aimar P & Sanchez V (1991b).
Albumin denaturation during ultrafiltration: effects of operating conditions and the consequences on membrane fouling. *Biotechnology and Bioengineering*, **38**, 528-534.

Merin U, Gordin S & Tanny G B (1983).
Microfiltration of sweet cheese whey. *New Zealand Journal of Dairy Science and Technology*, **18**, 153-160.

Michaels A S (1968).
New separation technique for the CPI. *Chemical Engineering Progress*, **54**, 31-43.

Mochizuki S, Opong W S & Zydney A L (1990).
Macromolecular sieving by protein deposits formed during ultrafiltration and microfiltration. In: Proceedings of the 1990 International Conference on Membranes (ICOM 90), Chicago, 1137-1139.

Morr C V & Josephson R V (1968).
Effect of calcium, N-ethylmaleimide and casein upon heat induced whey protein aggregation. *Journal of Dairy Science*, **51**, 1349-1355.

Muller L L, Hayes J F & Griffin A T (1973).
Studies on whey processing by ultrafiltration. I. Comparative performance of various ultrafiltration modules on whey from hydrochloric acid casein and cheddar cheese. *The Australian Journal of Dairy Technology*, **28**, 70-77.

Mulvihill D M & Kinsella J E (1988).
Gelation of ß-lactoglobulin: effect of sodium chloride and calcium chloride on the rheological and structural properties of gels. *Journal of Food Science*, **53**(1), 231-236.

Munari S, Bottino A, Capannelli G & Moretti P (1987).
Ultrafiltration membrane characterisation. In: *Proceedings of the International Conference on Membranes and Membrane Processes (ICOM 87)*, Tokyo, 299-300.

Nabetani H, Nakajima M, Watanabe A, Nakao S & Kimura S (1987).
Effect of ovalbumin adsorption on the performance of ultrafiltration membrane. In: *Proceedings of International Conference on Membranes and Membrane Processes (ICOM 87)*, Tokyo, 451-452.

Nakanishi K & Kessler H-G (1985).
Rinsing behaviour of deposited layers formed on membranes in ultrafiltration. *Journal of Food Science*, **50**, 1726-1731.

Nakao S-I, Nomura T & Kimura S (1979).
Characteristics of macromolecular gel layer formed on ultrafiltration tubular membrane. *AIChE Journal*, **25**, 615-622.

Nakao S, Osada H, Kurata H, Tsuru T & Kimura S (1988).
Separation of proteins by charged ultrafiltration membranes. *Desalination*, **70**, 191-205.

Narendranathan T J & Dunnill P (1982).
The effect of shear on globular proteins during ultrafiltration: studies of alcohol dehydrogenase. *Biotechnology and Bioengineering*, **24**, 2103-2107.

Nilsson J-L (1989).
A study of ultrafiltration membrane fouling. PhD Dissertation, Department of Food Engineering, University of Lund, Sweden.

Nobrega R, de Balmann H, Aimar P & Sanchez V (1989).
Transfer of dextran through ultrafiltration membranes: a study of rejection data analysed by gel permeation chromatography. *Journal of Membrane Science*, **45**, 17-36.

Nyström M (1989).
Fouling of unmodified and modified polysulphone ultrafiltration membranes by ovalbumin. *Journal of Membrane Science*, **44**, 183-196.

Nyström M & Lindström M (1988).
Optimal removal of chlorolignin by ultrafiltration achieved by pH control. *Desalination*, **70**, 145-156.

Oh S S, Ricomini M A, Richardson T & Tong P S (1989).
Use of radiolabeled whey proteins to study interactions of heat induced whey proteins and membrane fouling during ultrafiltration. In: California Dairy Foods Research Center, Annual Report 1988-1989, 34.

Olesen N & Jensen F (1989).
Microfiltration. The influence of operation parameters on the process. *Milchwissenschaft*, **44**, 476-479.

Olson W P, Bethel G & Parker C (1977).
Rapid delipidation of and particulate removal from human serum by membrane filtration in a tangential flow system. *Preparative Biochemistry*, **7**, 333-343.

Papamichael N & Kula M-R (1987).
A hydrodynamic study of the retention of polyethylene glycols by cellulose acetate membranes in the absence and presence of proteins. *Journal of Membrane Science*, **30**, 259-272.

Parris N, Anema S G, Singh H & Creamer L K (1993).
Aggregation of whey proteins in heated sweet whey. *Journal of Agricultural and Food Chemistry*, **41**, 460-464.

Patocka J & Jelen P (1987).
Calcium chelation and other pretreatments for flux improvement in ultrafiltration of cottage cheese whey. *Journal of Food Science*, **52**, 1241-1244.

Patocka G & Jelen P (1991).
Calcium association with isolated whey proteins. *Canadian Institute of Food Science and Technology Journal*, **24**, 218-223.

Persson K M, Capannelli G, Bottino A & Trägårdh G (1993).
Porosity and protein adsorption of four polymeric microfiltration membranes. *Journal of Membrane Science*, **76**, 61-71.

Pierre A, Fauquant J, Le Graet Y, Piot M & Maubois J-L (1992).
Préparation de phosphocaséinate natif par microfiltration sur membrane. *Lait*, **72**, 461-474.

Piot M, Maubois J-L, Schaegis P, Veyre R & Luccioni (1984).
Microfiltration en flux tangentiel des lactosérums de fromagerie. *Le Lait*, **64**, 102-120.

Piot M, Vachot J-C, Veaux M, Maubois J-L & Brinkman G-E (1986).
Ecrémage et épuration bactérienne du lait entier cru par microfiltration sur membrane en flux tangentiel. *Technique Laitiere*, **1016**, 42-46.

Porter M C (1988).
Membrane filtration. In: P Schweitzer (Ed.), *Handbook of Separation Techniques for Chemical Engineers, 2nd Edn.*, 2.3-2.103.

Pradipasena P & Rha C (1977).
Pseudoplastic and rheopectic properties of a globular protein (ß-lactoglobulin) solution. *Journal of Texture Studies*, **8**, 311-325.

Pritchard M (1990).
The influence of rheology upon mass transfer in cross-flow membrane filtration. PhD Dissertation, University of Bath, Great Britain.

Probstein R F, Chen J S & Leung W F (1978).
Ultrafiltration of macromolecular solutions at high polarisation in laminar flow. *Desalination*, **24**, 1-16.

Probstein R F, Chan K K, Cohen R & Rubenstein I (1981).
Model and preliminary experiments on membrane fouling in reverse osmosis. *ACS Symposium Series*, **153**, 131-145.

Pusch W & Walch A (1982).
Membrane structure and its correlation with membrane permeability. *Journal of Membrane Science*, **10**, 325-360.

Randon J, Larbot A, Julbe A, Guizard C & Cot L (1991).
Study of ZrO_2 membrane - aqueous solutions interface. *Key Engineering Materials*, **61** & **62**, 495-498.

Rector D J, Kella N K & Kinsella J E (1989).
Reversible gelation of whey proteins: melting, thermodynamics and viscoelastic behaviour. *Journal of Texture Studies*, **20**, 457-471.

Reese E T & Robbins F M (1981).
Denaturation of ß-lactoglobulin by shaking and its subsequent renaturation. *Journal of Colloid and Interface Science*, **83**, 393-400.

Reihanian H, Robertson C R & Michaels A S (1983).
Mechanisms of polarisation and fouling of ultrafiltration membranes by proteins. *Journal of Membrane Science*, **16**, 237-258.

Renner E & Abd El-Salam M H (1991).
Application of Ultrafiltration in the Dairy Industry, Elsevier Applied Science, London.

Rinn J-C, Morr C V, Seo A & Surak J G (1990).
Evaluation of nine semi-pilot scale whey pretreatment modifications for producing whey protein concentrate. *Journal of Food Science*, **55**, 510-515.

Robertson B C & Zydney A L (1990).
Protein adsorption in asymmetric ultrafiltration membranes with highly constricted pores. *Journal of Colloid and Interface Science*, **134**, 563-575.

Rolchigo P M, Raymond W A & Hildebrandt J R (1989).
Improved control of ultrafiltration using vorticular hydrodynamics and hydrophilic membranes. *Process Biochemistry*, **24**, Pro Bio Tech iii-vii.

Romero C A & Davis R H (1988).
Global model of crossflow microfiltration based on hydrodynamic particle diffusion. *Journal of Membrane Science*, **39**, 157-185.

Saksena S & Zydney A L (1994).
Effect of solution pH and ionic strength on the separation of albumin from immunoglobulins (IgG) by selective filtration. *Biotechnology and Bioengineering*, **43**, 960-968.

Sandblom R M (1978).
Filtering process. *US patent*, **4,105,547**.

Sawyer W H (1968).
Heat denaturation of bovine ß-lactoglobulin and relevance to disulfide aggregation. *Journal of Dairy Science*, **51**, 323-329.

Schmidt D G & Payens T A J (1976).
Micellar aspects of casein. In: E Matijevic (Ed.), *Surface and Colloid Science*, **Vol 9**, John Wiley & Sons, New York, 165-229.

Scott J A (1988).
Application of cross-flow filtration to cider fermentations. *Process Biochemistry*, **23**, 146-148.

Sheldon J M, Reed I M & Hawes C R (1991).
The fine-structure of ultrafiltration membranes. II. Protein fouled membranes. *Journal of Membrane Science*, **62**, 87-102.

Shoji T, Nakajima M, Nabetani H, Ohtani T & Watanabe A (1988).
Effect of pore size of ceramic support on the self-rejection characteristics of the dynamic membrane formed with water soluble proteins in waste water. *Journal of the Agricultural Chemical Society of Japan*, **62**, 1055-1060.

Snoeren T H M, Damman A J & Klok H J (1982).
The viscosity of skim-milk concentrates. *Netherlands Milk and Dairy Journal*, **36**, 305-316.

Stengaard F F (1988).
Characteristics and performance on new types of ultrafiltration membranes with chemically modified surfaces. *Desalination*, **70**, 207-224.

Suki A, Fane A G & Fell C J D (1984).
Flux decline in protein ultrafiltration. *Journal of Membrane Science*, **21**, 269-283.

Sun P S & Ouyang C (1988).
The fouling of ultrafiltration membranes by proteins. Paper Presented at International Membrane Technology Conference (IMTEC 88), Sydney, G79-G82.

Taddei C, Aimar P, Daufin G & Sanchez V (1986).
Etude du transfert de matière lors de l'ultrafiltration de lactosérum doux sur membrane minérale. *Le Lait*, **66**, 371-390.

Taddei C, Aimar P, Daufin G & Sanchez V (1988).
Factors affecting fouling of an inorganic membrane during sweet whey ultrafiltration. *Le Lait*, **68**, 157-176.

Tam C M & Tremblay A Y (1991).
Membrane pore characterisation-comparison between single and multicomponent solute probe techniques. *Journal of Membrane Science*, **57**, 271-287.

Tanny G B, Hauk D & Merin U (1982).
Biotechnical applications of a pleated crossflow microfiltration module. *Desalination*, **41**, 299-312.

Taylor S M & Fryer P J (1994).
The effect of temperature/shear history on the thermal gelation of whey protein concentrates. *Food Hydrocolloids*, **8**(1), 45-61.

Trouvé E, Maubois J-L, Piot M, Madec M N, Fauquant J, Rouault A, Tabard T & Brinkman G (1991).
Retention of various microbial species during milk purification by cross-flow microfiltration. *Lait*, **71**(1), 1-13.

Turker M & Hubble J (1987).
Membrane fouling in a constant-flux ultrafiltration cell. *Journal of Membrane Science*, **34**, 267-281.

Tutunjian R S (1984).
Cell separations with hollow fiber membranes. *Developments in Industrial Microbiology*, **2**, 415-435.

Tweddle T A, Striez C, Tam C M & Hazlett J D (1992).
Polysulphone membranes. I. Performance comparison of commercially available ultrafiltration membranes. *Desalination*, **86**, 27-41.

van Boxtel A J B, Otten Z E H & van der Linden H J L J (1991).
Evaluation of process models for fouling control of reverse osmosis of cheese whey. *Journal of Membrane Science*, **58**, 89-111.

van der Horst H C & Hanemaaijer J H (1990).
Cross-flow microfiltration in the food industry. State of the Art. *Desalination*, **77**, 235-258.

van der Waal M J & Racz I G (1987).
Mass transfer in corrugated plate membrane modules. *Membraantechnologie*, **2**, 13.

van der Waal M J & Racz I G (1988).
Flux enhancement in corrugated plate membrane modules - microfiltration. *Membraantechnologie*, **3**, 29.

van Gassel T J & Ripperger S (1985).
Crossflow microfiltration in the process industry. *Desalination*, **53**, 373-387.

Varunsatian S, Watanabe K, Hayakawa S & Nakamura R (1983).
Effects of Ca^{++}, Mg^{++} and Na^{+} on heat aggregation of whey protein concentrates. *Journal of Food Science*, **48**, 42-46, 70.

Vetier C, Bennasar M, Tarodo de la Fuente B & Nabias G (1986).
Etude des interactions dentre constituants du lait et membranes minérales de microfiltration. *Le Lait,* **66**,, 269-287.

Vetier C, Bennasar M & Tarodo de la Fuente B (1988).
Study of the fouling of a mineral microfiltration membrane using scanning electron microscopy and physicochemical analyses in the processing of milk. *Journal of Dairy Research*, **55**, 381-400.

Vilker V L, Colton C K & Smith K A (1981).
The osmotic pressure of concentrated protein solutions: effect of concentration and pH in saline solutions of bovine serum albumin. *Journal of Colloidal and Interface Science*, **79**, 548-566.

Vilker V L, Colton C K, Smith K A & Green D L (1984).
The osmotic pressure of concentrated protein and lipoprotein solutions and its significance to ultrafiltration. *Journal of Membrane Science*, **20**, 63-77.

Visvanathan C & Ben Aim R (1989).
Studies on colloidal membrane fouling mechanisms in crossflow microfiltration. *Journal of Membrane Science*, **45**, 3-15.

Wahlgren M & Arnebrant T (1989).
Protein adsorption onto polysulphone surfaces and some aspects on fouling of membranes. In: H G Kessler & D B Lund (Eds.), *3rd International Conference on Fouling and Cleaning in Food Processing*, Technische Universitat, Munich, 200-206.

Walstra P (1979)
The voluminosity of bovine casein micelles and some of its implications. *Journal of Dairy Research*, **46**, 317-323.

Weldring J A G & van't Riet K (1988).
Physical properties of sodium carboxymethyl cellulose molecules adsorbed on a polyacrylonitrile ultrafiltration membrane. *Journal of Membrane Science*, **38**, 127-145.

Wijmans J G, Nakao S & Smolders C A (1984).
Flux limitation in ultrafiltration: osmotic pressure model and gel layer model. *Journal of Membrane Science*, **20**, 115-124.

Wyatt J M, Knowles C J & Bellhouse B J (1987).
A novel membrane module for use in biotechnology that has high transmembrane flux rates and low fouling. In: *Proceedings of International Conference on Bioreactors and Biotransformations*, Gleneagles, 166-172.

Xiong Y L (1992).
Influence of pH and ionic environment on thermal aggregation of whey proteins. *Journal of Agricultural and Food Chemistry*, **40**, 380-384.

Xiong Y L, Dawson K A & Wan L (1993).
Thermal aggregation of ß-lactoglobulin: effect of pH, ionic environment, and thiol reagent. *Journal of Dairy Science*, **76**, 70-77.

Zeman L J (1983).
Adsorption effects in rejection of macromolecules by ultrafiltration membranes. *Journal of Membrane Science*, **15**, 213-230.

Appendix 1. Component list of membrane test rig

Component	Code (Fig 4.1)	Make / Model
Hardware		
Feed Pump	P1	Johnson OL1-0004-15 Rotary lobe pump with direct coupled 1.1 kW 8-pole electric motor.
Pump speed controller	MD1	PDL μ-Drive 3
Balance tanks		Jacketed 5L tanks, 150 mm diameter
Temperature controller	TC1	Varied (see Section 4)
Water Filter	WF1	Sartorius 5 μm woven filter
Membrane modules		see Section 4 for description
Permeate balance		Mettler PM2500
Valves		
Feed tank shut-off (x2)	V01& V02	1 inch Butterfly valves
Pressure relief valve	V03	Nupro RL3 series
Permeate control valve	V04	Badger Meter type 807
Baseline pressure manual control valve	V05	Saunders 15 mm diagphram
Manual control valves	V06 - V08	Saunders 15 mm diagphram
Instruments - control and monitoring		
Membrane constant pressure controller	PC1	Taylor μScan 200
Magnetic flow meter	F1	Honeywell MagNeW 3000
Temperature probe	TI1	PT100, Analog Services
Feed pressure transmitter	PI1	Foxboro 841GM
ΔP_L pressure indicator	PD1	Rosemont 3051B (0-62 kPa)
ΔP_{TM} pressure indicator	PD2	Rosemont 3051C (0-248 kPa)
UV cell	UV1	Pharmacia UV1 with industrial flow through cell

Appendix 1 cont. Component list of membrane test rig

Component	Code (Fig 4.1)	Make / Model
Instruments - Computer and Data Logger		
Computer		Zenith 386 SX
Datalogger I/O rack		Opto 22 PB16AH / B2
Balance - computer connection		RS232 / 422 Converter - Opto AC7B
Instruments - Miscellaneous		
Feed flow display		Analogic measuremeter II
Feed pressure display		Analogic measuremeter II
Set speed display		Precision Digital PD610
5V, 15V power supply		PSR-ME30-DI-AC200
24V Power supply		Modicon PE0001-000
Permeate valve I/P		Bellofram type 1000

Appendix 2. Run data from trials on ß-lactoglobulin

A: Summary of Trials

Run No.	Run Date	Membrane Pore, nm	Permeate flux L/m².h	Comments/Purpose
Trials in Lund				
1	25/10/93	100	50	Ionic Strength
2	26/10/93	100	50	Low pH
3	1/11/93	100	50	No Calcium
4	2/11/93	100	200	No Calcium
5	3/11/93	100	50	Ionic Strength
6	4/11/93	100	50	pH
7	8/11/93	100	200	No Calcium
8	9/11/93	100	50	
9	10/11/93	100	50	No Ca / not logged
10	11/11/93	100	50	
11	15/11/93	100	50	No Calcium
12	16/11/93	20	50	No Calcium
13	17/11/93	20	20	Low flux / ΔP_{TM}
14	19/11/93	50	50	No Calcium
15	22/11/93	50	200	No Calcium
16	23/11/93	50	50	
17	24/11/93	50	200	
18	25/11/93	50	50	No Calcium
19	26/11/93	50	200	

A cont: Summary of Trials

Run No.	Run Date	Membrane Pore, nm	Permeate flux L/m².h	Comments/Purpose
Trials in New Zealand				
20	8/2/94	50	50	B powder/changed flux
21	10/2/94	50	150	
22	15/2/94	50	100	
23	16/2/94	50	150	
24	17/2/94	50	100	
25	1/3/94	50	200	No Ca / Ionic strength
26	2/3/94	50	200	Added Ca after 1h
27	3/3/94	50	200	B powder / Ca removed 1h
28	9/3/94	50	200	Low Ca
29	10/3/94	50	200	B powder / Ca removed 1h
30	11/3/94	50	200	Low Ca
31	14/3/94	50	200	High ionic strength
32	16/3/94	50	200	Added Ca after 1h
33	21/3/94	50	200	B Powder / Cross-flow V
34	22/3/94	50	200	B Powder / Cross-flow V
35	23/3/94	50	200	B Powder / Cross-flow V
36	24/3/94	50	200	B Powder / Cross-flow V
37	25/3/94	50	200	High ionic strength
38	28/3/94	50	50	
39	29/3/94	20	50	No Calcium
40	30/3/94	100	200	
41	31/3/94	100	200	

B: Feed Properties

Run No	Dilution	Protein %	pH	Ion Conc. (mmol/L) Ca	Na	Cl	IS
Trials in Lund							
1	0.83	0.19-0.20	varied	-	varied	varied	varied
2	na	0.21	5.02	-	8.78	8.78	0.0088
3	0.81	0.20	6.67	-	8.61	8.61	0.0086
4	0.85	0.20-0.21	6.66	-	9.03	9.03	0.0090
5	0.82	0.20-0.21	varied	-	varied	varied	varied
6	0.85	0.19	4.98	-	8.99	8.99	0.0090
7	0.80	0.19-0.20	6.57	-	9.24	9.24	0.0092
8	0.79	0.19-0.20	6.05	7.85	8.40	24.1	0.0278
9	0.81	0.2	6.49	-	8.91	8.91	0.0089
10	0.76	0.19-0.2	6.2	7.55	8.40	23.5	0.0268
11	0.81	0.19-0.20	6.55	-	9.92	9.92	0.0099
12	0.82	0.21	6.36	-	48.2	48.2	0.0482
13	0.83	0.20-0.21	6.2	-	47.8	47.8	0.0478
14	0.83	0.19-0.20	6.33	-	48.0	48.0	0.0479
15	0.78	0.20	6.39	-	47.3	47.3	0.0473
16	0.84	0.2-0.21	6.15	8.34	32.2	48.9	0.0572
17	0.82	0.21	6.21	8.14	32.4	48.6	0.0568
18	0.82	0.20-0.21	6.36	-	47.7	47.7	0.0477
19	0.83	0.21-0.22	6.19	8.24	32.3	48.8	0.0570

B cont: Feed Properties

Run No	Dilution	Protein %	pH	Ion Conc. (mmol/L) Ca	Na	Cl	IS
Trials in Lund							
20	0.84	0.22-0.23	6.36	8.34	32.2	48.9	0.0572
21	0.85	0.21-0.22	6.34	8.44	32.3	49.1	0.0576
22	0.86	0.2-0.21	6.27	8.54	32.1	49.2	0.0577
23	0.83	0.2	6.29	8.24	32.3	48.8	0.0571
24	0.83	0.2-0.21	6.25	8.24	32.3	48.8	0.0570
25	0.83	0.18-0.20	varied	-	varied	varied	varied
26	0.81	0.19	6.42	-	67.7	67.7	0.0677
27	0.84	0.21	6.26	8.34	32.3	49.0	0.0573
28	0.83	0.19	6.41	2.06	60.4	64.5	0.0666
29	0.85	0.20-0.21	6.43	8.44	32.2	49.1	0.0575
30	0.83	0.19	6.38	4.12	69.9	78.1	0.0822
31	0.84	0.19	6.36	-	119.6	119.6	0.1196
32	0.81	0.19	6.46	-	67.8	67.8	0.0678
33	0.81	0.20-0.21	6.33	8.04	32.8	48.8	0.0569
34	0.82	0.20-0.21	6.34	8.14	32.7	48.9	0.0571
35	na	0.20-0.21	6.31	na	na	na	na
36	0.76	0.2	6.32	7.55	33.1	48.2	0.0557
37	0.83	0.19-0.2	6.42	-	119.1	119.1	0.1191
38	0.83	0.19	6.33	8.04	32.8	48.9	0.0569
39	0.81	0.19	6.46	-	48.1	48.1	0.0481
40	0.83	0.19-0.20	6.35	8.04	32.6	48.7	0.0567
41	0.87	0.19-0.20	6.34	8.64	32.1	49.4	0.0580

C: Operating Conditions

Run No	Temp °C	Ret Flow rate L/h	Shear Pa	Flux $L/m^2.h$	Time to 200 kPa min	ΔP_{TM} kPa
Trials in Lund						
1	24.8	400	31	50.0	-	-
2	24.8	400	31.1	49.9	-	-
3	24.8	400	31.2	50.0	-	-
4	24.9	400	30.9	200	-	-
5	25.0	400	31.1	50.0	-	-
6	24.6	400	31.2	49.9	-	-
7	24.9	400	30.9	200	-	-
8	25.0	400	31.1	50.0	-	-
9	Did not log to disk.					
10	25.0	400	31.1	50.0	-	-
11	25.1	400	31.0	50.0	-	-
12	25.0	400	36.5	49.4	27	196.7
13	24.9	400	36.5	20.1	0.5	16.5
14	25.0	400	30.2	50.0	-	-
15	25.0	400	29.8	199.8	-	-
16	25.0	400	30.4	50.0	-	-
17	25.0	400	30.3	198.7	22	197.5
18	25.0	400	30.5	50.0	-	-
19	25.0	400	30.3	198.4	18	197.4

C cont: Operating Conditions

Run No	Temp °C	Ret Flow rate L/h	Shear Pa	Flux L/m².h	Time to 200 kPa min	ΔP_{TM} kPa
Trials in New Zealand						
20	25.2	400	29.5	50.0	-	-
21	25.0	400	29.5	149.6	68	197.6
22	24.8	400	29.5	99.9	-	-
23	24.9	400	29.3	149.6	89	197.5
24	25.1	400	29.6	99.9	-	-
25	24.9	400	29.5	199.9	-	-
26	24.9	400	29.6	199.7	-	-
27	25.1	400	29.6	198.3	21	197.5
28	25.0	400	29.5	199.7	-	-
29	25.0	400	29.6	198.7	25	197.4
30	25.0	400	29.7	199.8	-	-
31	24.8	400	29.7	199.8	-	-
32	24.9	400	29.7	199.7	-	-
33	25.0	260 then 540	13.6 50.9	197.7	15	199.0
34	25.0	540 then 260	50.7 13.6	199.2	53	195.4
35	25.0	540 then 260	50.9 13.7	199.2	51	195.4
36	25.0	260 then 540	13.7 51.1	197.5	14	199.0
37	24.9	400	29.7	199.8	-	-
38	24.9	400	29.7	50.0	-	-
39	25.0	400	33.9	49.9	-	-
40	25.0	400	30.1	198.9	34	197.3
41	25.1	400	30.3	199.6	34	197.3